STUDY OF THE INFLUENCE OF SUPPLEMENTARY CEMENTITIOUS MATERIALS ON SELECTED DURABILITY PARAMETERS OF CONCRETE

A THESIS

submitted by

DHANYA B. S.

for the award of the degree

of

DOCTOR OF PHILOSOPHY

BUILDING TECHNOLOGY AND CONSTRUCTION MANAGEMENT
DEPARTMENT OF CIVIL ENGINEERING
INDIAN INSTITUTE OF TECHNOLOGY MADRAS
CHENNAI, INDIA

SEPTEMBER 2015

THESIS CERTIFICATE

This is to certify that the thesis titled "**STUDY OF THE INFLUENCE OF SUPPLEMENTARY CEMENTITIOUS MATERIALS ON SELECTED DURABILITY PARAMETERS OF CONCRETE"**, submitted by **Dhanya B. S.**, to the Indian Institute of Technology Madras, Chennai for the award of the degree of **Doctor of Philosophy**, is a bona fide record of the research work done by her under my supervision. The contents of this thesis, in full or in parts, have not been submitted to any other Institute or University for the award of any degree or diploma.

Dr. Manu Santhanam
Research Guide
Professor
Dept. of Civil Engineering
IIT Madras, 600 036

Place: Chennai
Date: 28th September 2015

ACKNOWLEDGEMENTS

I thank GOD, the Almighty for giving me an opportunity to do my research at IIT Madras and for the strength and peace of mind to do this work.

I am very much thankful to my research guide Prof. Manu Santhanam, Professor, Department of Civil Engineering for accepting me as his student. This work is materialized only because his constant support, valuable guidance, timely and thoughtful feedback, and encouragement. His advices on both research and my career is priceless. He will be a constant source of inspiration to me throughout my life.

I am extremely grateful to Prof. Ravindra Gettu, Professor, Department of Civil Engineering for his critical comments, suggestions and all the supports given to me during my research journey. I am also greatly indebted to Dr. Radhakrishna G. Pillai, Asst. Professor, Department of Civil Engineering for all his support and suggestions throughout my research work. His vibrant nature will be a source of inspiration to me in my teaching and research career.

I express my sincere thanks to other doctoral committee members Prof. B.S. Murthy, Professor, Department of Metallurgical and Materials Engineering and Prof. Krishnan Balasubramanian, Professor, Department of Mechanical Engineering for their suggestions regarding various aspects of my research work.

My sincere thanks to Prof. Meher Prasad, Head of the Department of Civil Engineering and to Prof. S.R. Gandhi, Former Head of the Department of Civil Engineering for providing excellent facilities in the department.

I would like to thank all the faculty members of the Department of Civil Engineering, especially in the Building Technology and Construction Management Division for their support and suggestions given especially during my seminars. Thanks a lot to Dr. Amalan K. Sen Gupta, Dr. Srinivasan Chandrasekharan and Dr. M.S. Sivakumar who were the committee members of my comprehensive viva and thesis proposal evaluation for their valuable comments and suggestions.

My sincere thanks to Prof. Mark Alexander, Professor, University of Cape Town, South Africa and Prof. Surendra P. Shah, Professor of Emeritus, North Western University, U.S.A and Visiting Professor, IIT Madras and Dr. J.H.M. Visser, T N O, The Netherlands for all their valuable suggestions and criticisms given to me during their stay at IIT Madras. I would also like to thank Dr. Roberto Torrent, Prof. Yunus Ballim, Prof. Basheer for their valuable inputs given during their visit to IIT Madras.

Most of the work has carried out in the IITM – Lafarge Laboratory for Durability and Long-Term Behaviour of Concrete. My deepest sense of gratitude to all the supporting staff in the BTCM laboratory, especially Ms. A. Malarvizhi, Mr. M. Soundarapandian, Mr.D. Murthy, Mr. G.Subrahmanian, Mr. B. Krishnan for their constant support given to me for the successful completion of my experimental work. I would also thank Mr. Surya, Mr. Krishnan, Mr. Kanagadri, Mr. Hari, Mr. Chinnaiah and Mr. Praveen for all their help during casting and testing. I thank Mr. R. Murali, Civil Engineering Department Workshop facility for his help rendered in fabrication of moulds. Thanks a lot to Mr. Balaganeshan and Mr. Mani of the Central workshop facility for helping in profiling. I am thankful to the supporting staff of the MME and Chemistry departments of IIT Mr. Raghavendra, Ms. Meena, Mr.Chari, Mr.Karthik for their help and support.

I thank the Science and Engineering Research Council, Department of Science and Technology, Govt. of India for supporting this work. Partial financial support from the Lafarge Center de Reserche, France is also appreciated. Partial financial assistance from the alumni association to attend the international conference is also greatly appreciated.

I would like to thank the Department of Technical Education, Government of Kerala for sponsoring me under the QIP scheme to do Ph. D. at IIT Madras. Support from all my colleagues at my parent institution, Rajiv Gandhi Institute of Technology, Govt. Engineering College, Kottayam especially Dr. Bino I. Koshy, Dr. Bindhu B. K. and Ms. Bindumol Varghese are greatly appreciated.

My sincere thanks to all my friends and fellow researchers at IIT Madras, Sunitha K. Nayar, K. Jayachandran, Dr. Mohammed Haneefa, K., Dr. A. Bahurudeen, T. Sakthivel, B. Karmugil, N. Srinivasan, Deepa Rani. R., Manju G. Nair, Siva. M., Hemalatha M. S., Sujatha Jose, Reesha Bharat, Dr. Elson John, Dr.Ganesh, Sanish K. B., Muthu Kumar E., Murugan M., Jeevan Jacob, Aneetha Murugan, Pinky Devi L., Dr.Venkata, Sobha, Vinay, Praveen, Chinchu, V.G. Ram, C. P. Nair, Stephie J. Stephen, Santhosh, Divya Rani, Mogul Sirajudin, Sathya Narayanan, Prabha, M., Ranjitha, R., Dr. Priya Nair, Fathima Suma, Sheetal Surana, Ranjith K. Soman, Sivakumar, Kalyani, Vasanth, Amman, ….for this suggestions, discussions and help rendered

during different stages of my research work. My deep sense of gratitude to all the project associates who worked with me especially Abul Khalid, Naga Pavan, Suresh, Pushpakaran and Anila. Thanks a lot to all the internship students who worked in the BTCM lab during 2011 to 2014 who had helped me in one way or the other. Special thanks to the M Tech students Santhosh George Cherian for helping me during the initial stages of my research and Nithish, Ariffulla and Dinesh for their help rendered for the analysis of data.

I would like to thank the BTCM office staff Ms. Ezhil Arasi, Ms. Sushma and Mr. Obaiah for all their help. Support from Civil Engg. Department office especially, Ms. Rani, Ms. Geetha. Mr. Subramani, Ms. Padmini, Mr. Ramaswamy are gratefully acknowledged. The support from the Chairman and office staff of the Centre for Continuing Education, IIT Madras are also acknowledged gratefully. All the valuable suggestions from the members of the ICI Technical Committee on Concrete Durability are greatly appreciated, which made my work more practically significant. Thanks a lot to the Chairman Mr. Vijay Kulkarni for all his critical comments.

Thanks a lot to the teachers of Kendriya Vidyalaya, IIT Madras and Vanavani Matriculation Higher Secondary School, IIT Madras for opening the world of knowledge to my kids and for all the help rendered.

This work is dedicated to my family. Without the support of my husband Mr. Vinod Kumar A., father Mr. N. Balakrishnan, mother Mrs. A.K. Santhamma and my kids Eesha Vinod and Deva Vinod, my dream of doing Ph.D. at IIT Madras would not have been materialized. They have sacrificed a lot for me during this period. I am also thankful to my in-laws Mr. V. Appukuttan and Mrs.C. Valsa for their support.

I am very much obliged to each and every person who helped me one way or the other in my research journey. Thanks a lot to all of them who made my stay in IIT Madras the most pleasant and memorable period in my life.

DHANYA B. S.

ABSTRACT

KEYWORDS: Durability parameters; Supplementary Cementitious Materials (SCMs); Corrosion; Carbonation; Microstructure; Transport Mechanisms

There is an increase in concern about concrete durability as numerous cases of premature deterioration of concrete are reported in recent years. The three major factors controlling the deterioration of a reinforced concrete structure are the aggressiveness of the environment, the materials used for construction, and the near-surface quality of the concrete obtained at site. The present work concentrates on the second aspect, i.e. the materials used for construction, particularly the binder. Supplementary Cementitious Materials (SCMs) are well known for their capability to enhance concrete durability in general; however, controversies exist regarding their performance in environments where carbonation is predominant.

The present work deals with the creation of a database of durability parameters using locally available SCMs. The influence of SCMs on the durability parameters corresponding to chloride ingress and carbonation is assessed, along with micro-analytical investigations to understand the microstructural alterations occurring in the concrete. Further, attempts are made to link transport mechanisms with deterioration mechanisms and to assess the suitability of using combinations of durability parameters in various service environments.

In order to achieve these objectives, forty one concrete mixes with different proportions of SCMs, binder content and water to binder ratio were designed and produced. Different durability tests and compression test were performed on specimens prepared from the mixes. The durability tests are grouped into three categories - related to chloride, gas and water penetrability. The test results were analysed to get the relevant durability parameters, which resulted in a database of durability parameters with different binder combinations. Further, the effects of SCMs on durability were quantified with the help of existing service life prediction models. Micro-analytical studies were conducted to understand the behaviour of mixes with different SCMs during the durability investigations.

Based on the database, a qualitative ranking system for different SCMs was developed. A new concept of "Strength grade classification" was developed, which gives the durability enhancement potential of different SCMs for concretes at the same strength level. The qualitative ranking system and strength grade classification system can act as a tool for the practicing engineers for better material selection. The strength grade classification results show that the options available to make concrete at a particular strength level can result in different levels of durability. Even with mixes having high w/b and low binder content, with the use of SCMs, high level of durability is achievable. Depending on the requirement of the service environment, the mixture can be tailor-made.

The test results indicate that in the case of test methods where the specimens are fully saturated, the performance of SCM mixes is well ahead of OPC mixes, whereas in those tests where drying is performed, the performance of OPC and SCM mixes are close. Slag and Class F fly ash at higher dosages are found to be better choices in a chloride laden environment. Resistance against carbonation is less for SCM mixes.

The data from the durability tests were compared and the correlations between different durability parameters pointing towards a particular deterioration mechanism of concrete were evaluated. By taking necessary inputs from the correlation study, a combined classification system was developed for both chloride and carbonation induced corrosion environments. This system involves a combination of test parameters addressing different transport mechanisms and gives a more realistic estimate of durability performance. Using this approach, the concrete mixtures tested in the current project work were analysed for their suitability in these service environments.

Micro-analytical studies performed in this research project were helpful to establish the link between microstructure and performance. The consumption of calcium hydroxide by the SCMs was detected by thermo gravimetric analysis (TGA). Evidence of chloride binding was obtained in mixes having higher replacement levels of SCMs from scanning electron microscopy (SEM) and X – ray diffraction (XRD). Further, the chemical and phase changes due to carbonation were studied by TGA and XRD.

The influence of several testing-related factors affecting the durability parameters was also evaluated to give a more meaningful interpretation to the effects of the SCMs. This helped in a critical evaluation of their influence on concrete durability characteristics.

The study resulted in a database of durability parameters for concretes used for common construction having different SCMs. The qualitative ranking system and the strength grade concept developed based on the database can act as a guideline for material selection. The combined classification criteria developed was able to link the deterioration mechanisms with transport mechanisms. Based on the present study, a quality framework was developed, incorporating the concepts of strength grade classification and combined classification system. This framework is expected to pave the way for practicing engineers towards adopting more relevant performance-based specifications for concrete construction.

Table of Contents

CHAPTER 1

CHAPTER 2

CHAPTER 9

CHAPTER 10

LIST OF TABLES

LIST OF FIGURES

ABBREVIATIONS

A	Aragonite
AF_m	Monosulphate
AF_t	Ettringite
BSE	Back Scattered Electron
C	Calcite
CCT	Chloride Conductivity Test
CH	Calcium Hydroxide
CSH	Calcium Silicate Hydrate
DI	Durability Index
DP	Durability Parameter
EDS	Energy Dispersive X – Ray analysis
OPC	Ordinary Portland Cement
OPI	Oxygen Permeability Index
RCPT	Rapid Chloride Permeability Test
RMT	Rapid Migration Test
RH	Relative Humidity
SCM	Supplementary Cementitious Material
SEM	Scanning Electron Microscopy
SH	Silicate Hydrate
SI	Sorptivity Index
SLM	Service Life Modelling
SP	Super Plasticizer
SR	Surface Resistivity
TG/DSC	Thermo Gravimetric/Differential Scanning Caloriemetry
TGA	Thermo Gravimetric Analysis
V	Vaterite
w/b	Water binder ratio
w/c	Water cement ratio
XRD	X – Ray Diffraction
F	Friedel’s Salt

NOTATIONS

D	Diffusion coefficient
D_{nssm}	Non steady state migration coefficient
I	Current
K	Coefficient of permeability
Q	Charge passed
S	Sorptivity
ti	Time for corrosion initiation
tp	Time for corrosion propagation
V	Voltage
ρ	Resistivity

CHAPTER 1

INTRODUCTION

1.1 PROBLEM STATEMENT

Concrete is normally designed to meet workability and strength criteria. Since numerous cases of premature deterioration of concrete are reported in recent years, there is an increasing concern about concrete durability. Out of the different deterioration mechanisms, corrosion of the reinforcement due to chloride ingress and carbonation draw special attention owing to its huge economic impact. The annual cost of corrosion across the world is estimated to exceed 1.8 trillion U. S. Dollar (USD) i.e., about 3 to 4 % of the Gross Domestic Product (GDP) of the industrialised countries (Schmitt, 2009).

The three major factors controlling the deterioration of a reinforced concrete structure are the aggressiveness of the environment, materials used for construction, and the near-surface quality of the concrete obtained at site (Alexander et al., 2008). The near surface quality of the as-built concrete is a reflection of the construction practices such as the level of compaction, the extent of curing etc.

Supplementary Cementitious Materials (SCMs) or mineral admixtures are well known for their capability to enhance concrete durability in general (Thomas et al., 2012). However, controversies exist regarding the effect of SCMs on carbonation (Sulapha et al., 2003). Even though SCMs are specified in many of the construction projects in India, the specification is random and not based on any solid experimental database (Dhanya and Santhanam, 2013). A database of the durability parameters with the commonly used SCMs is required, so that the potential of the SCMs for ensuring durability can be reaffirmed and the database can act as a guideline for the material selection for a particular service environment. Further, in order to have a better clarity on the performance of SCMs, there is a need to establish the link between microstructure and performance through micro-analytical studies.

There are many approaches to durability design of concrete such as avoidance of deterioration, prescriptive, semi-probabilistic and probabilistic (Andrade et al., 2013). In order to accomplish durability design of concrete, numerous challenges need to be overcome. First of all, a clear understanding of the deterioration mechanisms in a particular service environment is needed. Secondly, the environmental classification system should be based on the deterioration mechanism. The third issue is regarding the durability parameters. There are a number of test methods available which deal with different parameters pointing towards durability. These are well-compiled by various authors and agencies (Bjegović et al., 2015, Bickley et al., 2006, Stanish et al., 1997). A deep scientific understanding of the test methods and the underlying transport mechanisms along with the parameters obtained is required. The test methods generally deal with a single transport mechanism. However, in the field, combinations of transport mechanisms lead to the processes that cause deterioration of structures. Efforts are needed to identify the relevant transport mechanisms involved in each service environment and the combination of durability parameters addressing the same. The influence of SCMs on the durability parameters needs to be assessed and quantified for better assessment of the service life in each service environment.

The present work deals with the creation of a database of durability parameters using locally available SCMs. The influence of SCMs on the durability parameters corresponding to chloride ingress and carbonation is assessed, along with micro-analytical investigations to understand the microstructural alterations occurring in the concrete. Further, attempts are made to link transport mechanisms with deterioration mechanisms and to assess the suitability of using combinations of durability parameters in various service environments.

1.2 OBJECTIVES

The objectives of the present study are as follows.

1. To create a database of durability parameters for concretes made using locally available materials, covering a range of binder combinations
2. To evaluate the suitability of different durability parameters and their combinations for various service environments
3. To understand the alterations in the microstructure of concretes having supplementary cementitious materials caused by chloride ingress and carbonation

1.3 SCOPE

The scope of the study is limited to concrete mixes having a mean compressive strength range from 20 to 60 MPa. The tests conducted are related to gas, water and chloride penetration in concrete. Materials in the study are restricted to one cement (OPC 53 grade), two slags (from two different sources in India) and two fly ashes (Class F and Class C). All the specimens were cured by moist room curing. The durability tests selected for the study are related to chloride induced corrosion and carbonation induced corrosion. In the case of service life models, the initiation of corrosion is assumed as the end of service life. The scope of the present work is to assess the material potential alone with regard to durability.

1.4 METHODOLOGY

The key steps involved to achieve the objectives are described. The complete methodology is represented pictorially in Figure 1.1.

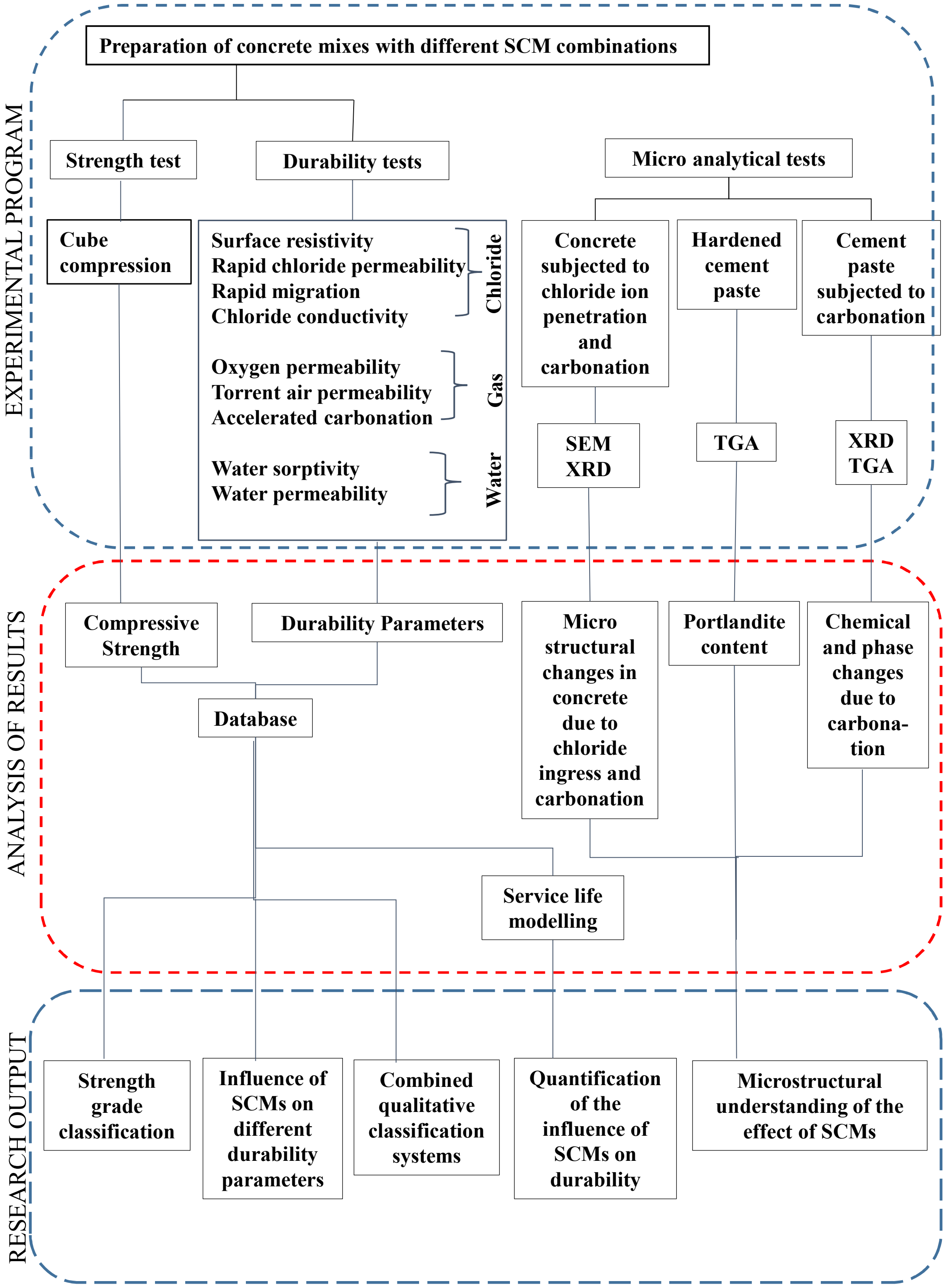

Figure 1.1 Methodology of the research study

1.4.1 Preparation of concrete mixes

Forty one concrete mixes with different proportions of SCMs, binder content and water to binder ratio were designed and produced. The mixes were divided into two categories namely, commonly used design mixes and mixes having limiting prescriptive values. The mean compressive strengths of the selected mixes ranged between 20 and 60 MPa, which is the usual range of compressive strength for the mixes that are used in common construction.

1.4.2 Tests on concrete

Different durability tests and compression test were performed on specimens prepared from the mixes cast as mentioned in section 1.4.1. The durability tests belong to three categories - test methods to assess chloride penetrability, gas penetrability and water penetrability. The durability test methods used were Surface resistivity test (Wenner 4-probe method), Rapid chloride permeability test (ASTM C1202, 2010), Rapid migration test (NT BUILD 492), Chloride conductivity test (Durability index testing procedure manual, South Africa), Oxygen permeability index test (Durability index testing procedure manual, South Africa, 2009), Torrent air permeability test (SIA 262/1, 2003), Accelerated carbonation test (at 1% CO_2, 25°C, 65% RH), Water sorptivity test (Durability index testing procedure manual, South Africa), and Water permeability test (DIN 1048 Part 5).

1.4.3 Analysis of durability parameters

The test results were analysed to get the relevant durability parameters. The influence of SCMs on different durability parameters were assessed in this step. The existing classification systems were used to classify the concrete. This step resulted in a database of durability parameters with different binder combinations. This database can act as a useful tool for concrete mixture design. Based on the results of this step, a qualitative ranking system for different SCMs was developed. A new concept of "Strength grade classification" was developed at the end of this step, which gives the durability enhancement potential of different SCMs for concretes at the same strength level. This is a useful tool for practicing engineers to make a better material selection. Moreover, the influence of different variables such as temperature, specimen conditioning etc. on selected durability parameters was also assessed.

1.4.4 Correlations between durability parameters

The data from the durability tests were compared and the correlation between different durability parameters pointing towards same deterioration mechanism of concrete were evaluated. This correlation was useful to judge whether one test can be used instead of the other. Since many laboratories do not have all the durability testing facilities, the correlation is expected to estimate different parameters by any one of the tests.

1.4.5 Combined qualitative classification systems for different service environments

In this step, a combined classification system based on more than one durability parameter was developed for different service environments. For this, necessary inputs were also taken from the correlation study. This kind of combined classification system was considered necessary owing to the fact that in each exposure condition, different transport mechanisms act together. Thus, a combination of test parameters addressing different transport mechanisms gives a more realistic estimate of durability performance. Further, this step gives a qualitative estimation of the enhancement of durability due to addition of SCMs. The effect of the percentage replacement of SCMs and the curing is well understood from this step. The suitability of using combination of durability parameters and their limiting values for assessing the performance of concrete in different service environments with respect to chloride induced and carbonation induced corrosion was also assessed.

1.4.6 Quantification of the effect of SCMs

The effect of SCMs on durability were quantified with the help of existing service life prediction models. For carbonation induced corrosion category, two existing service life models such as square root of time and DuraCrete models were used to do the prediction. In the case of chloride induced corrosion, DuraCrete model was used for service life prediction. The service life prediction helped to get the quantification of the pattern of results obtained in the previous sections.

1.4.7 Micro-analytical studies

Micro-analytical studies were conducted to understand the behavior of mixes with different SCMs during the durability investigations. These studies were performed on the mixes having a total binder content of 310 kg/m^3 and w/b 0.5. Mainly three sets of studies were carried out under this category.

In the first set of studies, micro structural changes in concretes due to chloride ingress and carbonation on concretes with different SCMs were investigated. The samples were prepared from carbon dioxide and chloride exposed concrete specimens (from accelerated carbonation test and from specimens immersed in 3% sodium chloride solution respectively). Backscattered electron (BSE) imaging in scanning electron microscopy (SEM) was carried out on epoxy impregnated polished concrete surfaces. The powder resulting from chloride profiling was subjected to X–ray diffraction (XRD) to identify the crystalline phases formed.

In the second set, thermo gravimetric analysis (TGA) was performed on paste samples cured in lime water at two ages (28 days and 90 days) to determine the portlandite content, which is an indicator of the degree of hydration in general and the degree of pozzolanic reaction in the case of SCM mixes.

The third set deals with study of the chemical and phase changes due to carbonation. These tests were conducted on paste samples (9 mm diameter and 30 mm height) which were subjected to complete carbonation at 3% CO_2 concentration. The samples were analysed using XRD (to identify the crystalline phases) and TGA (to find the degree of carbonation).

1.5 OUTLINE OF THESIS

There are ten chapters in this thesis. The present chapter discussed the problem in general followed by the objectives, scope and methodology of the research study. The second chapter gives a detailed review of the literature covering different aspects of durability pertaining to this study. The need for present research is also described in the second chapter. The details of the experimental program which include description of the materials, experimental design and test procedures are explained in the third chapter. The database of the durability parameters and the strength grade classification is presented in the fourth chapter. The fifth chapter deals with the evaluation of the influence of different test related factors on the durability parameters. The sixth chapter describes the assessment of the influence of SCMs on different durability parameters of concrete. The results are presented both qualitatively and quantitatively. Chapter 7 deals with the results of the micro-analytical studies, which help in explaining the trends obtained in the sixth chapter. Chapter 8 presents a proposal for combined qualitative classification system for different exposure conditions in terms of both chloride and carbonation induced corrosion. Chapter 9 is a general discussion chapter on the practical significance of the findings from the current thesis work. A quality framework for concrete construction is developed, which is rooted in the performance based durability design approach. The concluding remarks followed by specific conclusions and scope for further research are presented in Chapter 10.

CHAPTER 2

LITERATURE REVIEW

2.1 DURABILITY OF CONCRETE

Durability of concrete is its resistance against any form of deterioration. Durable concrete will retain its original form, quality and serviceability when exposed to its intended service environment (ACI 201 - 2R, 2008). Durable concrete structures are assets of the nation. Practices in the concrete industry have significant global effects, because of the volumes of concrete involved. The implications of durability of concrete are three-fold, namely social, economic and ecological. These three factors are the key aspects of sustainable development (Bilodeau and Malhotra, 1998). The socio-economic aspects include increased repair and replacement costs, which can hike the overall construction budget up to 40% (Mehta and Monteiro, 2006). Considering the ecological aspects, deterioration of the structure will have double impact on the environment. Firstly, all the debris go directly into the environment in one form or another and secondly, natural resources get depleted for new construction.

The challenge before the engineering community is to achieve durable concrete having adequate strength, which is cost effective, environment friendly and thus sustainable (Richardson, 2002). The simple way towards this goal is by specifying the concrete accurately for its intended purpose. The specification should address different aspects such as service life, serviceability requirement, quantifiable description regarding serviceability and failure, acceptable level of risk and possible extent of maintenance (Richardson, 2002).

2.1.1 Reasons for concrete durability problems

Deterioration of concrete happens mainly due to the heterogeneity and porosity of concrete. Concrete mainly has three phases at the microscopic level - the Hydrated Cement Phase (HCP), the aggregate phase and the Interstitial Transition Zone (ITZ). The hydrated cement phase consists of Calcium Silicate Hydrate (CSH), Calcium Hydroxide (CH), and calcium sulphoaluminates such as ettringite and monosulphate. The structure of CSH consists of randomly oriented sheets of CSH, with water adsorbed on the surface of the sheets (adsorbed water), in between the layers (interlayer water), and in the spaces inside (capillary water).

Regarding porosity, there are mainly three kinds of pores in hardened cement paste - interlayer space in calcium silicate hydrate (gel pores), capillary pores, and air voids. The transport of fluids through concrete occurs due to the porous nature of the hydrated cement paste and due to the existence of ITZ. In this aspect, two parameters are of utmost importance. They are open porosity and pore size distribution. Open porosity indicates interconnectivity of pores through which transport of liquids, gases or ions takes place. Pore size distribution influences the rate of transport. In particular, capillary porosity is more relevant with respect to durability (Ramachandran and Beaudoin, 2001).

Further, the tensile strength of concrete is very low compared to its compressive strength. As a result, it is susceptible to cracking easily. Concrete can crack due to thermal shocks, shrinkage or due to stress concentration. Cracking reduces the service life of structures as cracks form direct pathways for the ingress of aggressive agents.

2.1.2 Challenges to achieve durability in concrete construction

In order to achieve the goal of durability in concrete construction, several challenges need to be overcome. First of all, there should be a clear understanding of the actual deterioration mechanisms of concrete in a particular service environment. The deterioration mechanisms should be linked to transport mechanism(s) by which the aggressive species are entering into concrete. Accordingly, the environmental exposure classification system should be defined or redefined. Next, the durability parameter(s) relevant to a particular service environment need to be identified along with their limiting values. This requires deep scientific understanding of the durability test methods and the parameters generated. The limiting values for the durability parameters should be developed for different binders so that the potential of SCMs, which are known to influence the concrete durability, can be explored more scientifically. Further, this effect should be quantified with the help of service life prediction models. Finally, steps should be taken to achieve durable concrete on site through good construction practices and reliable monitoring techniques. Test methods to check the as-built concrete quality should be identified and the acceptance criteria for these test parameters should be developed.

The following sections explore the available literature in the first two aspects mentioned in Section 2.1.2 in detail. The third aspect is out of the scope of the present study.

2.2 DETERIORATION OF CONCRETE STRUCTURES

Causes of deterioration either originate from the concrete system itself or due to the ingress of aggressive agents from the exterior. Chemical deterioration of concrete and corrosion of rebar occur due to the ingress of external elements such as chlorides, carbon dioxide, sulphates, moisture etc. from the surrounding atmosphere into concrete. Thus, the quality of cover concrete is the most important factor determining the durability of concrete structures.

Damage of reinforced concrete structures can occur either due to the deterioration of concrete or due to corrosion of reinforcement. The causes of concrete deterioration can be of two types, viz., physical and chemical. Fire, freeze and thaw, crystallisation of salts, abrasion, erosion, and cavitation are the major causes of physical degradation of concrete. The major chemical deterioration mechanisms are leaching due to soft water exposure, sulphate and other specific chemical attack, alkali silica reaction, alkali carbonate reaction, carbonation etc. Corrosion of reinforcement can be classified into two, viz., chloride induced corrosion and carbonation induced corrosion. The deterioration of concrete leads to loss of strength, rigidity and integrity of the concrete matrix, which are reflected primarily by an increase in porosity and permeability, loss of alkalinity, loss of mass, cracking and spalling, excessive deformation etc.

The following section gives a detailed description of corrosion of rebar in RC structures due to chloride ingress and carbonation, which are the topics of interest in this research work.

2.2.1 Corrosion of rebar in reinforced concrete structures

The corrosion of reinforcement in reinforced concrete structures is a major durability problem. The annual cost of corrosion across the world is assessed to be over 1.8 trillion USD. This is about 3 to 4 % of the GDP of the industrialised countries (Schmitt, 2009). The resultant damage to the infrastructure not only demands costly repair, but also creates many socio-economic issues like traffic jams, loss of time, pollution etc. (Aitcin, 2000).

When steel is embedded in concrete, a thin invisible stable passive layer is formed on the steel surface due to the high pH of the pore solution. The passive layer gives protection to the steel from corrosion. However, the passive layer becomes unstable in the presence of chloride ions or when the pH of the system is reduced due to carbonation. Once the steel gets depassivated, corrosion can happen when there is sufficient availability of oxygen and moisture.

Fundamentally, corrosion is an electro-chemical process. The essential parts of a corrosion cell include cathode, anode, ionic conductor and electron conductor. The current flow during the corrosion process in an RC structure is represented pictorially in Figure 2.1.

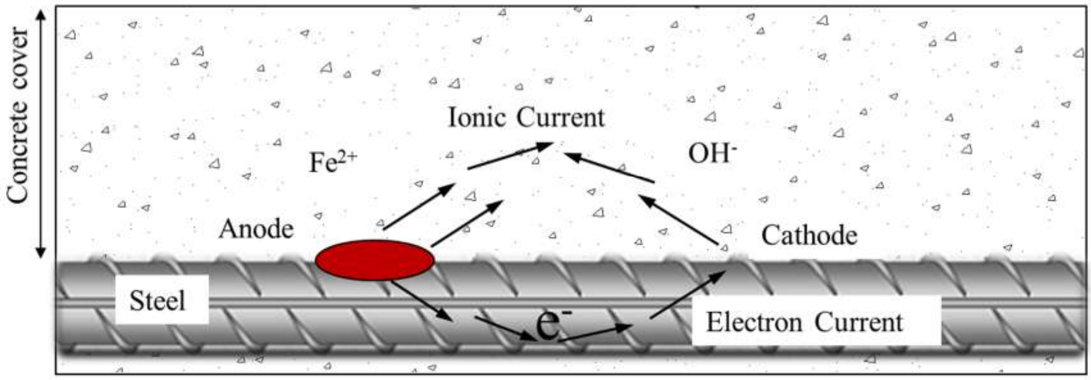

Figure 2.1 Current flow during corrosion process

In a typical RC structure, the cathode and anode are located in different locations of the same steel. At the anode, the iron gets oxidized to ferrous ions whereas at the cathode, water and oxygen get reduced to hydroxyl ions. Steel acts as the electron conductor whereas the ionic conductor is the pore solution.

The anodic half-cell reaction is represented by

$$2\,Fe \rightarrow 2\,Fe^{2+} + 2\,\bar{e} \qquad (2.1)$$

The cathodic half-cell reaction is represented by

$$O_2 + 2\,H_2O + 4\,\bar{e} \rightarrow 4\,OH^- \qquad (2.2)$$

The ferrous and hydroxyl ions combine to form rust products.

$$2\,Fe^{2+} + 4\,OH^- \rightarrow 2\,Fe(OH)_2 \qquad (2.3)$$

The first corrosion product, ferrous hydroxide ($Fe(OH)_2$) upon further oxidation produces other oxides of iron such as Fe_2O_3, Fe_3O_4 etc.

According to Tuutti (1982), the service life of a concrete structure can be divided into two – initiation stage and propagation stage, as shown in Figure 2.2.

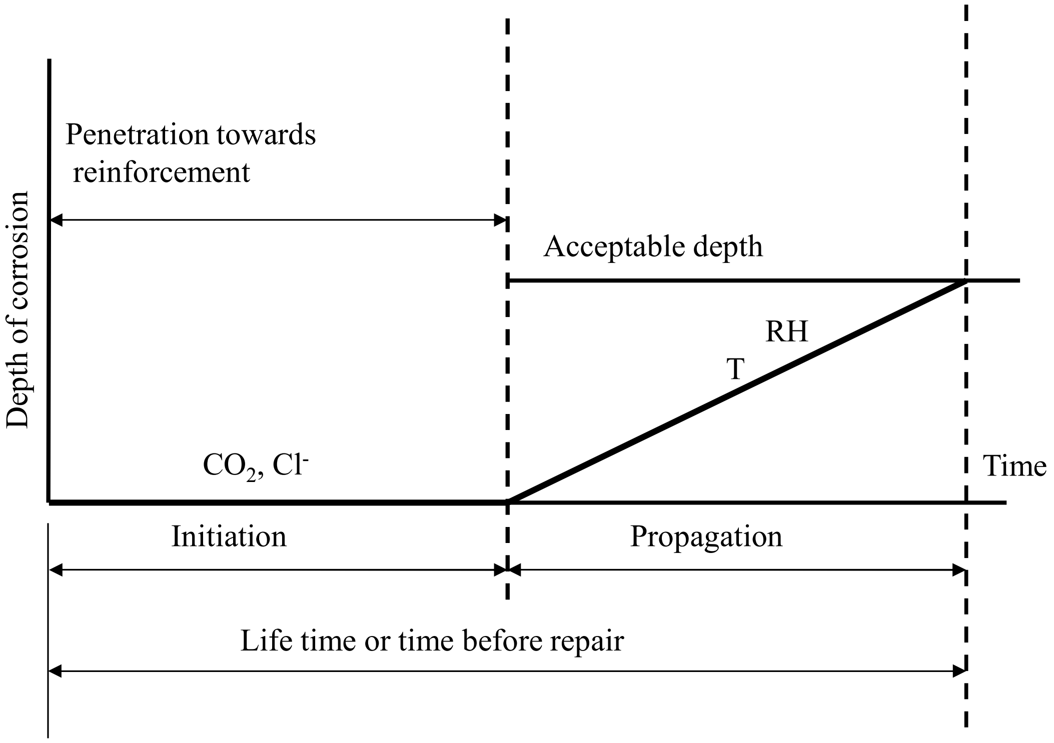

Figure 2.2 Steel corrosion sequence in concrete (Tuutti, 1982)

In many service life prediction models, initiation of corrosion is considered as the end of service life. The initiation period is influenced by the following factors - concentration of the aggressive chemical, transport distance (thickness of concrete cover), permeability of concrete, capacity of concrete to bind the aggressive species, and the threshold value required to initiate the corrosion process. The factors deciding the length of the propagation stage, which is controlled by the rate of corrosion, are the moisture condition (relative humidity of the pore system), temperature, chemical composition of the pore solution, porosity of concrete, thickness of concrete cover, and environmental variations along the metal etc. (Tuutti, 1982).

2.2.1.1 Chloride induced corrosion

Chloride induced corrosion is of non-uniform or pitting type, which can happen in marine environments and in structures subjected to de-icing salts. When Cl^- ions reach the passive layer, they replace some of the oxygen in the passive film. Because of that, the solubility, permeability and conductivity of the passive film increases. As a result, the film loses its protective nature eventually. Figure 2.3 indicates a schematic diagram of chloride induced corrosion (Adapted from http://www.cement.org/for-concrete-books-learning/concrete-technology/durability/corrosion-of-embedded-materials).

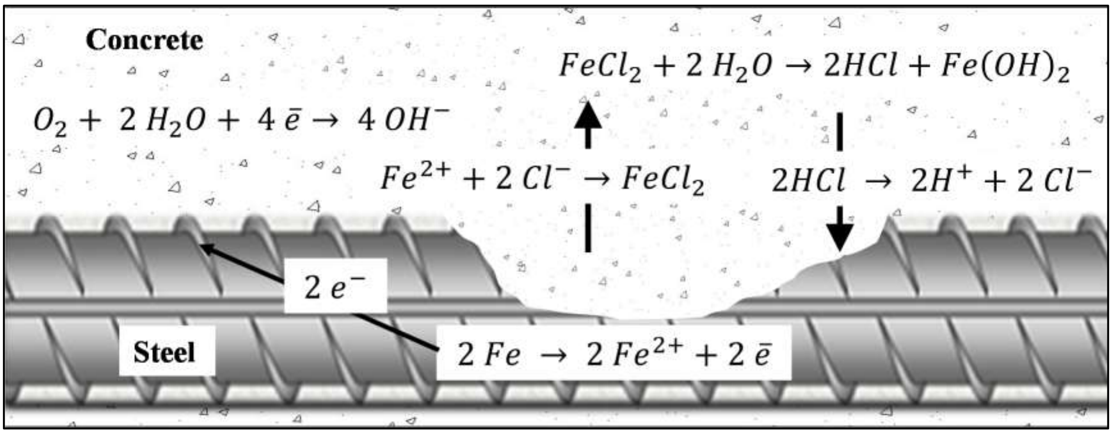

Figure 2.3 Schematic of chloride induced corrosion

The following are the reactions happening in chloride induced corrosion, where there is high pH and where oxygen is available.

The anodic and cathodic half-cell reactions are already presented in Equations 2.1 and 2.2. Presence of Cl^- can lead to additional reactions as shown in Equations 2.4 to 2.6.

$$Fe^{2+} + 2\,Cl^- \rightarrow FeCl_2 \tag{2.4}$$

$$FeCl_2 + 2\,H_2O \rightarrow 2HCl + Fe(OH)_2 \tag{2.5}$$

$$2HCl \rightarrow 2H^+ + 2\,Cl^- \tag{2.6}$$

When pH and O_2 concentration are high, the $FeCl_2$ breaks down, $Fe(OH)_2$ precipitates and the Cl^- and H^+ return to the anode. In this process, the corrosion continues at local anodes and deep pits are formed instead of spreading along the bar and thus it is called as pitting corrosion.

The major factors affecting the chloride resistance of concrete include initial curing, type of binder used, severity of exposure condition, maturity of concrete etc. When the initial curing duration increases, the capillary porosity and thus the chances of corrosion decreases. The use of SCMs can reduce the chances of corrosion owing to their ability to reduce capillary porosity and binding of chloride ions. These effects will be discussed in detail in the subsequent sections. The severity of corrosion varies with the type of exposure condition. For example, the effect of corrosion will be more in the zones where alternate wetting and drying happen compared to the fully immersed zone or atmospheric zone.

2.2.1.2 Carbonation induced corrosion

Carbonation induced corrosion is a major form of deterioration in inland environments, particularly in industrially polluted areas that have higher levels of CO_2. Unlike chloride induced corrosion, the corrosion induced due to carbonation produces a more uniform damage. The reactivity of CO_2 mainly depends on the type and content of binder, and degree of hydration. The diffusivity of CO_2 depends on the pore structure of concrete and the atmospheric conditions such as CO_2 concentration, relative humidity, temperature etc. (Bertos et al., 2004). Carbonation reaction is maximum when the RH is between 40 to 80%. This is because at low RH, the diffusion of CO_2 into concrete is high whereas there is not enough moisture for carbonation reaction to occur. When the RH is high, the gaseous diffusion of CO_2 becomes difficult, which in effect reduces the carbonation rate (Papadakis et al., 1991, Papadakis et al., 1992, Lagerblad, 2005). Figure 2.4 shows a schematic diagram of carbonation of concrete (adapted from http://www.cement.org/for-concrete-books-learning/concrete-technology/durability/corrosion-of-embedded-materials).

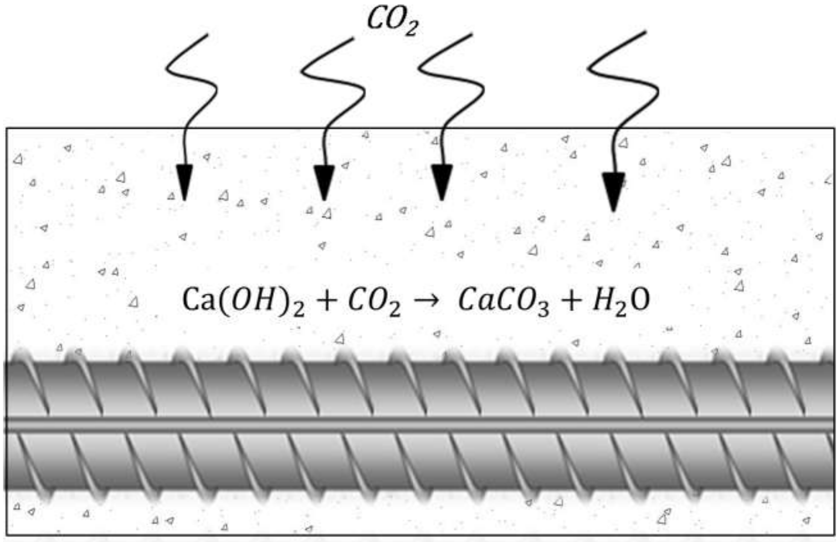

Figure 2.4 Schematic of concrete carbonation

Carbonation reaction can lead to some variation in properties of concrete such as decrease in permeability, increase in compressive strength, modification of the pore structure due to decrease in porosity and pore size, increase in pore tortuosity etc. These changes take place due to the deposition of the reaction product ($CaCO_3$) in the pores. Thus, the effect of carbonation is beneficial in the case of plain concrete. On the other hand, carbonation leads to decrease in pH and thus can lead to carbonation induced corrosion of steel in reinforced concrete structures.

Figure 2.5 indicates the influence of carbonation on the pore size distribution in fully hydrated hardened cement paste or mortar (Papadakis et al., 1991). It can be seen that due to carbonation, the curve from mercury intrusion porosimetry (MIP) gets shifted to the left side, indicating an improvement in the pore size distribution.

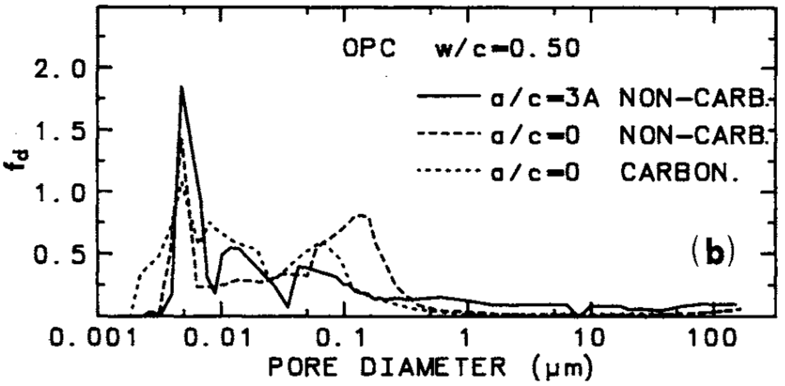

Figure 2.5 Effect of carbonation on the pore size distribution in fully hydrated hardened cement paste or mortar (Papadakis, 1991b)

The reactions that happen in a carbonation process are described below (Lagerblad, 2005).

CO_2 in gaseous form cannot react with cement hydrates. Accordingly, CO_2 gas gets dissolved in water and forms carbonate ions. The type of carbonate ion formed depends on the pH of water. When CO_2 dissolves in pore water, bicarbonates are formed initially. Due to the high pH of pore solution, these bicarbonates get dissociated and form carbonate ions. The carbonate ions react with Ca^{2+} ions in the pore solution and/or from $Ca(OH)_2$ (i.e., CH) dissolution forming $CaCO_3$ (i.e., CC).

As the Ca^{2+} ion concentration in the pore solution decreases, initially the dissolution of $Ca(OH)_2$ occurs. When $Ca(OH)_2$ gets fully consumed and the pH of the pore solution drops, more Ca^{2+} ions get released from the CSH and from the other Ca bearing phases. The dissolution changes the Ca/Si of the CSH. When the pH is around 10, the CSH gets converted to a silica gel. Due to carbonation, most of the Ca present in the CSH gets converted to $CaCO_3$ and very little remains in the silica gel.

When the pH is around 11.6, monosulphates decompose into ettringite and aluminate compounds. Further, at a pH around 10.5, ettringite gets decomposed to sulphate and aluminium hydroxide ions. At a pH below 9.2, none of the original Ca bearing phases exist. Table 2.1 shows the phase changes in carbonation process (Chen et al., 2004).

Table 2.1 Phase changes in carbonation process (Chen et al., 2004).

Intact concrete	First stage	Second stage	Third stage	Carbonated
CH	---	---	---	---
CSH (1)	CSH (1)	CSH (2)	CSH (3)	SH (with some CaO)
	CC	CC	CC	CC
AF_m	AF_m	$AF_t/Al(OH)_3$	$Al(OH)_3$	$Al(OH)_3$
AF_t	AF_t	AF_t	$Fe(OH)_3$	$Fe(OH)_3$
pH>12.5	pH<12.5	pH<11.6	pH<10.5	pH<10
Notations: CH – Calcium Hydroxide ; CSH – Calcium Silicate Hydrate; CC – Calcium Carbonate; AF_m – Monosulfates; AF_t - Ettringite				

The chemical equations involved in carbonation process are given below.

$$CO_2\,(g) + H_2O \rightarrow HCO_3^- + H^+ \tag{2.7}$$

$$HCO_3^- \rightarrow CO_3^{2-} + H^+ \tag{2.8}$$

$$Ca^{2+} + CO_3^{2-} \rightarrow CaCO_3 \tag{2.9}$$

Generally, three polymorphs of $CaCO_3$ are formed due to carbonation reaction. They are calcite, aragonite and vaterite. Calcium hydroxide gets converted to calcite, and this reaction leads to a volume expansion. According to Black et al. (2007) as cited by Morandeau et al. (2014), vaterite and aragonite are formed by the reaction between CSH having low C/S ratio and CO_2. Vaterite and aragonite are the metastable phases which eventually get converted to calcite. This conversion leads to volume reduction. As volume reduction happens, porosity increases, more ingress of CO_2 happens and the carbonation reaction proceeds at a faster rate. Further, the densities of CH, calcite, argonite and vaterite are 2.21, 2.71, 2.94 and 2.56 g/cm^3 respectively. Thus, formation of more dense products like aragonite can lead to reduction in the volume occupied, and thus an increase in porosity (Wowra et al., 2002). The impact of carbonation on the volume of reaction products is pictorially represented in Figure 2.6 (Wowra, 2002).

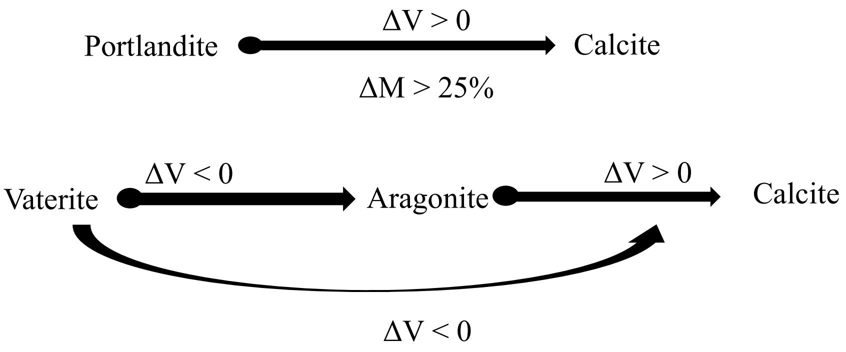

Figure 2.6 Impact of carbonation of the volume of reaction products (Wowra, 2002)

The study by Morandeau et al. (2014) confirms the formation of calcite, aragonite and vaterite in carbonated samples. Figure 2.7 shows the XRD patterns of non-carbonated, naturally carbonated and accelerated (10% CO_2) carbonated paste samples. The peaks corresponding to aragonite, vaterite, calcite and portlandite are marked as A, V, C and P respectively. The thermal analysis data of non-carbonated, naturally carbonated and accelerated carbonated (at 10% CO_2 concentration) paste samples (Morandeau et al., 2014) is presented in Figure 2.8.

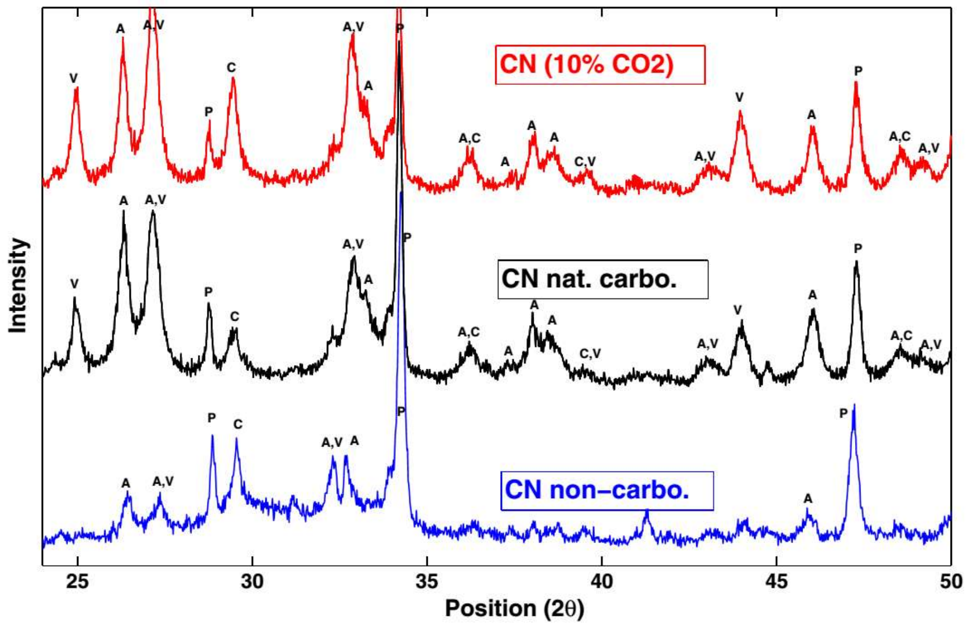

Figure 2.7 Comparison of XRD patterns for non-carbonated and carbonated CN samples (Morandeau et al., 2014)

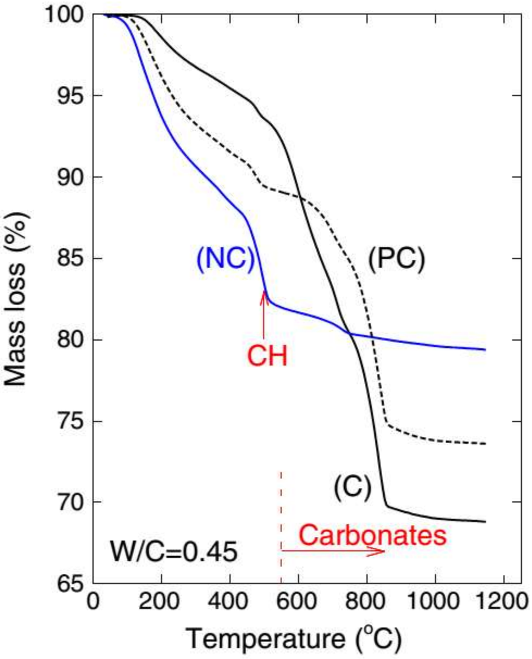

Figure 2.8 Mass loss during TGA on fully carbonated (C), partially carbonated (PC) and non-carbonated (NC) samples (Morandeau et al., 2014)

The peak between (750°C and 900°C) corresponds to the decomposition of calcite. According to Sauman (1971), other polymorphs of $CaCO_3$ such as vaterite and aragonite turn into calcite at 500°C during heating and decompose at a lower temperature range (650°C–900°C).

2.3 TRANSPORT MECHANISMS IN CONCRETE

The aggressive agents are transported or transferred into the concrete by means of certain transport or transference mechanisms. For analytical treatment, the transport properties of the materials are expressed in terms of material characteristics or intrinsic values. This is done using many assumptions and simplifications.

2.3.1 Diffusion

Diffusion is the process by which material transport occurs due to concentration difference. The amount of material moving across a unit area of a plane in unit time is known as diffusion flux (J) (Higgins, 1994, Andrade, 1993). Thus,

$$dJ = \frac{dm}{dt}\frac{1}{A} \tag{2.10}$$

where,

J	Diffusion flux (g/m^2.s)
m	Mass of the substance flowing (g)
t	Time (s)
A	Area (m^2)

Diffusion can happen in different material form such as ionic, gaseous and molecular. For ionic diffusion to occur, the existence of a continuous liquid phase concentration gradient are essential (Stanish et al., 1997). That is, ionic diffusion occurs in fully saturated concrete due to the random movement of ions in the pore solution from higher concentration region to the lower concentration region. In a marine structure, ionic diffusion happen in the submerged zones. When the RH is below 45%, molecular diffusion of water occurs, which is known as water vapour diffusion. Here, the humidity gradient works as the driving force (Alexander et al., 2011). Gaseous diffusion occurs in the case of fully or partially dried concrete. Here, the driving force is the concentration of gas molecules inside and outside the concrete. Examples of gaseous diffusion include diffusion of carbon dioxide and oxygen, which can lead to carbonation induced corrosion. Figure 2.9 shows the schematic depiction of the diffusion process.

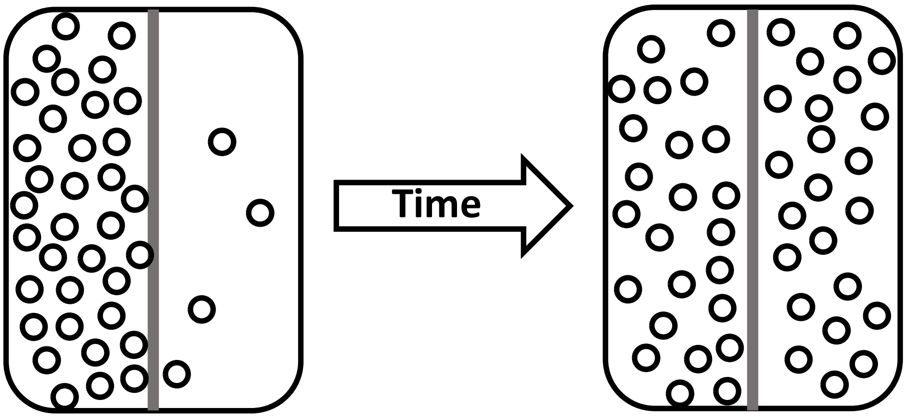

Figure 2.9 Schematic depiction of diffusion process

2.3.1.1 Fick’s laws of diffusion

In the case of steady state diffusion, the flux does not vary with time. This is explained by Fick’s first law of diffusion. By Fick’s first law of diffusion, the diffusion flux is proportional to the concentration gradient ($\frac{\partial C}{\partial x}$) normal to the section at the same instant. That is,

$$J = -D\frac{\partial C}{\partial x} \tag{2.11}$$

The proportionality constant D is the diffusion coefficient and x axis is in the direction of diffusion. D is expressed in m^2/s. The negative sign indicates that diffusion is in the direction opposite to that of increasing concentration. The diffusion coefficient is a material property, which describes the transferability of the given ionic species.

Effective diffusion coefficient represents steady state diffusion in which the chloride flux through the specimen to external solution is constant and the chloride binding does not contribute to any time dependent retardation effect. Effective diffusivity is the rate of movement of a particular ionic species within the pore solution in a porous medium (Andrade et al., 2002).

In the case of non-steady state diffusion, the diffusion flux and the concentration gradient at some particular point vary with time. That is, when diffusion happens, there is a change in the chloride concentration occurring at any time ‘t’ at every point ‘x’ (of the concrete). **Fick’s second law of diffusion** states that the change in chloride content per unit time is equal to the change of flux per unit length. That is,

$$\frac{\partial C}{\partial t} = \frac{\partial}{\partial x}(-D\frac{\partial C}{\partial x}) \tag{2.12}$$

If the diffusion coefficient D is independent of the composition, the Equation 2.12 can be simplified to

$$\frac{\partial C}{\partial t} = -D\frac{\partial^2 C}{\partial x^2}. \tag{2.13}$$

This is known as Fick’s second law of diffusion. As the microstructure in concrete is continuously evolving with respect to time, the transport processes in concrete are dependent on time. Thus, Fick's second law of diffusion is more appropriate for modelling the diffusion happening in concrete.

A solution to Equation 2.13 is obtained under the following assumptions and conditions (Paulson and Mejlbro, 2005).

- The concrete is cast at time $t = t_{ex}$ and is exposed to chloride at $t = 0$. The chloride profile is determined at time $t = t_{in}$ and the chloride environment around the concrete is assumed to be constant.
- The chloride diffusion coefficient ($x \geq 0$) is a constant ($D = D_0$)
- The chloride content of the concrete surface ($x = 0$) is constant (C_s=C_0) (boundary condition)
- The initial chloride content of the concrete C_s is assumed to be equally distributed throughout the concrete (initial boundary condition)

These conditions can be mathematically expressed as

$$D = D_0 \qquad \text{for } x \geq 0 \text{ and } t \geq 0 \tag{2.14}$$

$$C(x,t) = C_t \qquad \text{for } x \geq 0 \text{ and } t = 0 \tag{2.15}$$

$$C(x,t) = C_0 \qquad \text{for } x = 0 \text{ and } t \geq 0 \tag{2.16}$$

The solution of the Fick's second law of diffusion (Equation 2.13) under these conditions is

$$C(x, t_{in}) = C_i + (C_0 - C_i) erf\left[\frac{0.5x}{\sqrt{t_{in} D_0}}\right] \tag{2.17}$$

The slope of the chloride profile at the point (x,C) at the time of inspection t_{in} is the partial derivative of the above equation. The slope of the tangent at the point of the chloride profile (x,C) = (0,C_0) is given by

$$\left[\frac{\partial C}{\partial x}\right]_{x=0} = -\left[\frac{C_0 - C_i}{\sqrt{\pi t_{in} C_0}} exp\left(-\frac{x^2}{4 t_{in} D_0}\right)\right]_{x=0} \tag{2.18}$$

which works to

$$\left[\frac{\partial C}{\partial x}\right]_{x=0} = -\frac{C_0 - C_i}{\sqrt{\pi t_{in} C_0}} \tag{2.19}$$

Thus, the tangent of the chloride profile at the point (0, C_0) determines a line segment a of the asymptote from the ordinate axis to the intersection between the tangent and the asymptote. The length of a is

$$a = \sqrt{\pi t_{in} D_0} \tag{2.20}$$

The chloride profile can then be expressed as

$$\frac{C - C_i}{C - C_i} = erfc\left(\frac{x\sqrt{\pi}}{2a}\right) \tag{2.21}$$

Method of Surface tangents

From the equation 2.20, the chloride diffusion coefficient D_0 is expressed as

$$D_0 = \frac{a^2}{\pi t_{in}} \tag{2.22}$$

A typical chloride profile is presented in Figure 2.10 (Bjegović et al., 2015).

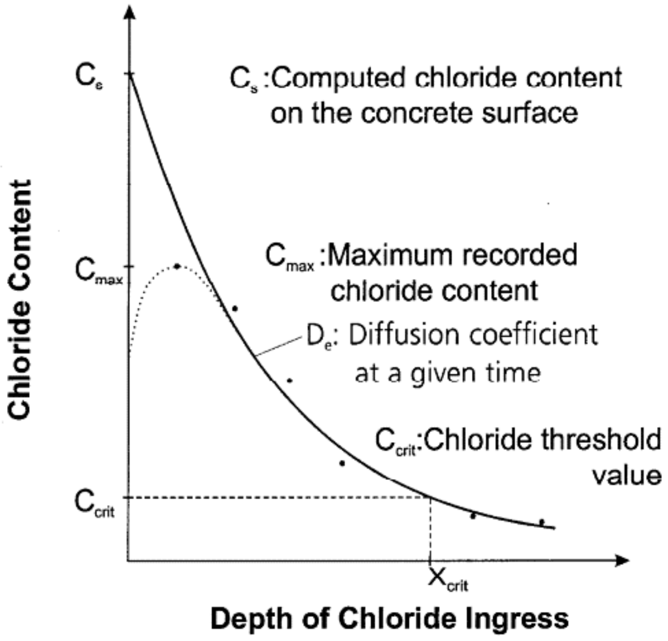

Figure 2.10 Typical chloride profile (Bjegović et al., 2015)

From the graph of the chloride profile, the asymptote C_i is estimated. The tangent to the chloride profile at the point (0, C_s) is drawn and the distance 'a' of the asymptote from the ordinate axis to the intersection between the tangent and the asymptote is measured. Then, using Equation 2.22, the chloride diffusion coefficient is calculated.

Apparent diffusion coefficient (D_a) is applicable in the case of non-steady state diffusion process, for which the flux through a particular element of the specimen evolves with time as chloride accumulation occurs within the element and chloride binding with cement contributes a time dependent retardation effect. As per ASTM C1556 (2003), apparent chloride diffusion coefficient, D_a is a chloride transport parameter calculated from acid-soluble chloride profile data obtained from saturated specimens exposed to chloride solutions, without correction for chloride binding, which provides an indication of the ease of chloride penetration into cementitious mixtures.

2.3.2 Permeation

Permeability is the process where external agents are transported into concrete with hydraulic pressure (pressure differential) as driving force. Both gases and water penetrate into concrete due to pressure difference. Permeation is governed by d'Arcy's law for laminar flow.

2.3.2.1 d'Arcy's law

d'Arcy's law states that the steady state rate of flow is directly proportional to the hydraulic gradient.

$$v = \frac{Q}{A} = -K\frac{dh}{dL} \tag{2.23}$$

where

v	Apparent velocity of flow
Q	Flow rate
A	Cross-sectional area of flow
dh	Head loss over a flow path of length dL

K	Coefficient of permeability, which is particular to the combination of the fluid as well as the material through which the fluid flows

To make the coefficient of permeability independent of the fluid properties, the concept of intrinsic permeability is introduced. The Equation 2.23 can be modified as

$$Q = \frac{KA\Delta P}{L} \tag{2.24}$$

In order to find the intrinsic permeability, the following simplifications can be made as described by Hubbert in 1956 (http://people.hofstra.edu/j_b_bennington/121notes/pdfs/Porosity_Perm_Darcy.pdf).

- Flow is proportional to the specific weight of the fluid γ which is the product of density ρ and acceleration due to gravity g.
- Flow is inversely proportional to the dynamic viscosity of the fluid μ.
- Flow is proportional to the square of the diameter of the particles d.

Thus,

$$K = \frac{-k\rho g}{\mu} \tag{2.25}$$

where k is the intrinsic permeability

In other words,

$$k = \frac{K\mu}{\rho g} \tag{2.26}$$

where

μ	Viscosity
ρ	Density of the solution

2.3.2.2 Hagen–Poiseuille equation

Gas permeability can be assessed by Hagen–Poiseuille equation. This law is applicable to pressure drop in a fluid flowing through long cylindrical pipe and the fluid is assumed to be in the laminar regime (Kropp and Alexander, 2007). According to this law,

$$k = \eta \frac{Q}{t}\frac{L}{A}\frac{2p}{(p_1 - p_2)(p_1 + p_2)} \tag{2.27}$$

where

k	Coefficient of gas permeability (m^2)
Q	Volume of gas flowing (m^3)
η	Viscosity of gas (N.s/m^2)
L	Thickness of permeated section (m)
A	Permeated area (m^2)
p	Pressure at which volume Q is measured (N/m^2)
p_1	Pressure at entry of gas (N/m^2)
p_2	Pressure at exit of gas (N/m^2)
t	Time (s)

This law forms the basis for the Torrent air permeability test (Permea – TORR user manual, 2000). However, additional effects such as non-Newtonian fluid characteristics, inertia effects causing turbulent flow patterns and slip flow can happen in gas permeability tests in concrete (Abbas et al., 1999, 2000). Many proposals are available to correct the coefficient of permeability to yield intrinsic coefficient of permeability. The gas permeability is not only affected by the pore structure and fluid characteristics, but also by the moisture condition of the specimen. Hence, for most of the gas permeation tests, dried samples are tested. However, the problem with this procedure is that it may lead to micro cracking, which can lead to erroneous results.

2.3.3 Capillary suction (Sorption)

Capillary suction or sorption denotes the transport of ions or liquids happening because of the action of capillary forces. Connected porosity is responsible for this kind of mechanism. This phenomenon is represented by Laplace equation. Figure 2.11 shows the schematic diagram of capillary suction.

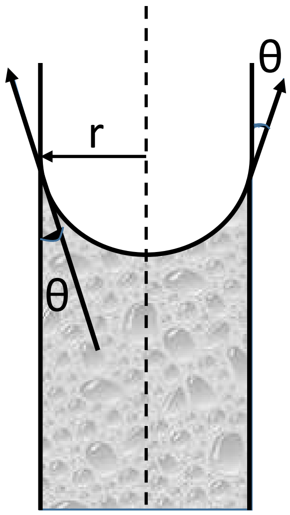

Figure 2.11 Schematic of capillary suction (Kropp and Alexander, 2007)

2.3.3.1 Laplace equation

By Laplace equation,

$$P_{cap} = P_l - P_g = \frac{2\sigma cos\theta}{r} \tag{2.28}$$

where

P_{cap}	Capillary pressure (N/m^2)
P_l	Pressure in liquid (N/m^2)
P_g	Pressure in gaseous phase above liquid column (N/m^2)
σ	Surface tension (N/m)
θ	Wetting angle
r	Radius of capillary (m)

According to Brauer (2002), as referred by Kropp and Alexander (2007), for a porous section in contact with a liquid,

$$z = \sqrt{\left(\frac{2\sigma cos\theta}{r} + P_a\right) \cdot \sqrt{\frac{r^2}{4\eta}}} \cdot \sqrt{t} \tag{2.29}$$

where

z	Capillary rise
σ	Surface tension
θ	Wetting angle
r	Radius of capillary
P_a	An external pressure for liquid, given by the density and the height of the liquid level
η	Viscosity of the liquid
t	Time in which the suction occurs

This equation is derived by considering the external and internal forces such as force induced by the mass of liquid column, force caused by friction at pore wall, inertia force, capillary force etc. acting in the capillaries. The derivation of the above equation can be found in Kropp and Alexander (2007). From the Equation 2.29, it can be found that there exists a square root of time relationship with the capillary rise. Thus, the Equation 2.29 can be written as

$$z(t) = B\sqrt{t} \tag{2.30}$$

where

$z(t)$	Capillary rise at time t in mm
B	Penetration coefficient in mm/√s

In other words,

$$M_l(t) = C\sqrt{t} \tag{2.31}$$

where

$M_l(t)$	Mass of liquid absorbed at time t per unit area of surface exposed to liquid in g/m^2
C	Absorption rate in g/m^2.√s

If the liquid is water, it has been suggested that (Kropp and Alexander, 2007, Kropp, 1999, Hall, 1989), the square root of time relationship is not strictly valid. Thus, a corrected equation as given below is suggested for the same.

$$M_l(t) = D + C\sqrt{t} \tag{2.32}$$

or

$$M_l(t) = D + Ct^n, \text{n} < 0.5 \tag{2.33}$$

where D is the initial absorption in g/m^2.

According to Hall et al. (1995), this behaviour of water is due to many effects such as chemical-mechanical interactions of water with the cement paste which lead to microstructural changes in the paste, on-going hydration of cement particles leading to changes in the pore structure, swelling of the paste etc. Due to these changes, the connectivity of capillaries gets affected, thus leading to this kind of behaviour. According to Martys (1995), for high w/c concrete, the total amount of water absorbed follows square root of time law. Nevertheless, for high performance concrete and for low w/b mixes, the exponent can be lowered by 1/5 to 1/3.

In addition to the factors mentioned above, Martys (1995) pointed out the morphology of the invading liquid as one of the reasons for this anomaly. Further, the constant D is associated with the initial water content of the specimen under consideration. This mechanism is in action when concrete is in contact with water on one surface and is dry at the other surface such as a slab in contact with ground water below (Alexander et al., 2011).

2.3.4 Migration

Migration is the movement of ions through a porous medium due to the difference in electrical potential. The basic equation used to describe migration is the Nernst-Plank equation. This equation deals not only with migration, but also with other mechanisms such as diffusion and convection (Andrade, 2003, Kropp and Alexander, 2007). Figure 2.12 indicates the schematic diagram of migration adapted from Andrade (1993).

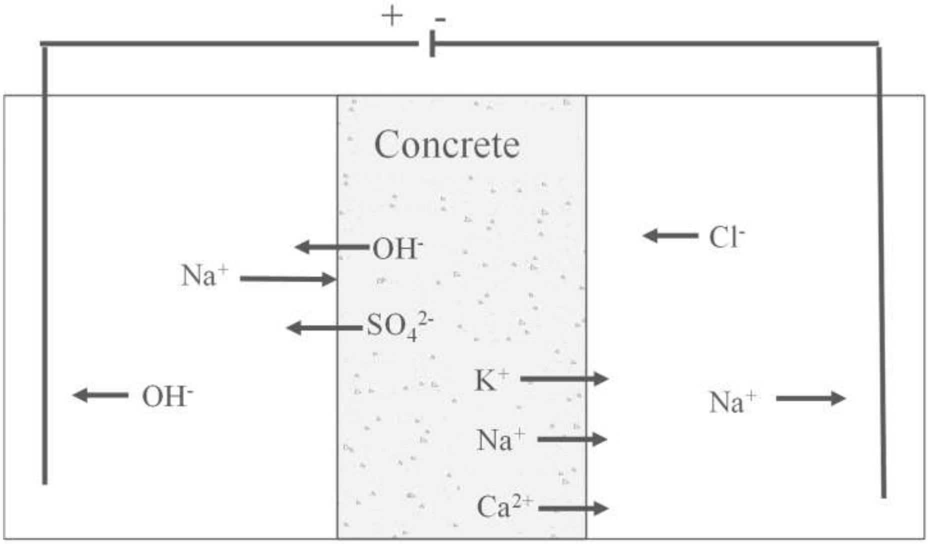

Figure 2.12 Schematic of Migration (Adapted from Andrade, 1993)

2.3.4.1 Nernst Plank equation

By Nernst Plank equation,

$$-J_j(x) = D_j \frac{\partial C_j(x)}{\partial x} + \frac{z_j F}{RT} D_j C_j \frac{\partial E(x)}{\partial (x)} + C_j V(x) \tag{2.34}$$

Where

$J_j(x)$	Uni-directional flux of jth species (mol/cm^2.s)
D_j	Diffusion coefficient of jth species (cm^2/s)
∂C	Variation of concentration (mol/cm^3)
∂x	Variation of distance (cm)
z_j	Electrical charge of jth species
F	Faraday's number (Coulomb/eq)
R	Gas constant (cal/mol/°C)
T	Absolute temperature (K)
C_j	Bulk concentration of the species j (mol/cm^3)

∂E	Variation of potential (V)
V	Artificial or forced velocity of ion (cm/s)

The Equation 2.34 can be translated as

$$\text{Flux} = \text{Diffusion} + \text{Migration} + \text{Convection} \tag{2.35}$$

Hence, the term $\frac{z_jF}{RT}\, D_jC_j\, \frac{\partial E(x)}{\partial(x)}$ accounts for migration.

The evaluation of the material transport parameters should be based on Nernst-Planck equation in the case of accelerated test methods. The convection term will not be there if completely saturated specimens are used.

2.3.4.2 Nernst- Einstein equation

Nernst-Einstein equation indicates the relationship between ion diffusivity and electrical resistivity for all porous materials (Sengul and Gjorv, 2008).

This equation is represented as

$$D_i = \frac{R.T}{Z^2.F^2}\frac{t_i}{\gamma_{i.}C_i\,\rho} \tag{2.36}$$

where

D_i	Diffusivity for i^{th} ion
R	Gas constant
T	Absolute temperature
Z	Ionic valence
F	Faraday constant
t_i	Transference number of i^{th} ion
$\gamma_{i.}$	Activity coefficient for i^{th} ion
C_i	Concentration of i^{th} ion in the pore water
ρ	Electrical resistivity

For a given type of concrete at a particular temperature and moisture condition, Equation 2.36 becomes

$$D = k.\frac{1}{\rho} \tag{2.37}$$

where, k is a constant equivalent to the slope of the linear correlation curve between the diffusivity and the conductivity.

2.3.4.3 Transference number

In the concrete pore solution, many ionic species such as OH^-, K^+, and Na^+ exist. In most of the accelerated chloride test methods, which involve the application of electrical potential, more than one ionic species (eg:- Cl^-, OH^- etc.) take part in the process of carrying the charge. In these situations, the term transference number needs to be understood.

The transference number of an ion moving under the action of an external electrical field is defined by the "proportion of the current carried by this ion in relation to the current carried by the rest of the ions”. Transference number is a function of the ionic mobility or the equivalent conductivity (Andrade et al., 2003). Transference number can be expressed as given in Equation 2.38.

$$t_j = \frac{i_j}{i} = \frac{z_j c_j \lambda_j}{\Sigma z c \lambda} = \frac{\lambda_j}{\lambda} \tag{2.38}$$

where

t_j	Transference number of j^{th} species
c_j	Concentration of j^{th} species
λ_j	Equivalent conductivity of j^{th} species
z_j	Electrical charge of j^{th} species

In migration tests, the hydroxides behave as a supporting electrolytes as the major proportion of the current is carried by the OH^- ions, rather than Cl^- ions. Thus, in order to find the specific contribution of chloride ions in current carrying ability, the transference number need to be calculated (Andrade et al., 1993).

2.3.5 Absorption

Absorption is the process by which a liquid is drawn into and tends to fill permeable pores in a porous solid body; also, it refers to the increase in mass of a porous solid body resulting from the penetration of a liquid into its permeable pores (ASTM C125, 2003). Absorption depends on pore structure as well as the moisture condition of the sample (Basheer et al., 2001.) It generally occurs in unsaturated or partially saturated concrete. Different methods like cold water saturation, boiling water saturation, vacuum saturation etc. are available to measure absorption of concrete (Safiuddin and Hearn, 2005). Out of the different methods, vacuum saturation method is considered to be comparatively better. Absorption depends on total porosity of the sample.

2.3.6 Adsorption

Adsorption is the process in which molecules of a liquid or gas adhere to the solid. The higher energy of the solid surface leads to the attraction of foreign atoms or molecules that have a slight affinity for the surface material. If the molecules adhere to the surface only because of physical forces such as van der Waals' bonding, it is known as physical adsorption. In the case of chemisorption, the molecules react chemically with the surface, leading to much stronger bonds. In the context of concrete, at low RH, water molecules get adsorbed onto the pore walls of concrete.

2.3.7 Wick action

Wick action is the transport of liquid through a porous element from a face in contact with water to a drying face (Buenfeld et al., 1995). If the liquid contains some dissolved ions, when the liquid evaporates, the ions are precipitated as salts in the pores or on the surface of the medium (Alexander et al., 2011). Transport mechanism due to wick action is a combination of capillary absorption, water vapour diffusion and evaporation. The wick action causes rapid penetration of deleterious substances such as chlorides and sulphates. Further, it leads to transmission of an unacceptable amount of water vapour into a dry space (Buenfeld et al., 1995). Figure 2.13 represents the schematic of wick action (adapted from Buenfeld et al., 1995).

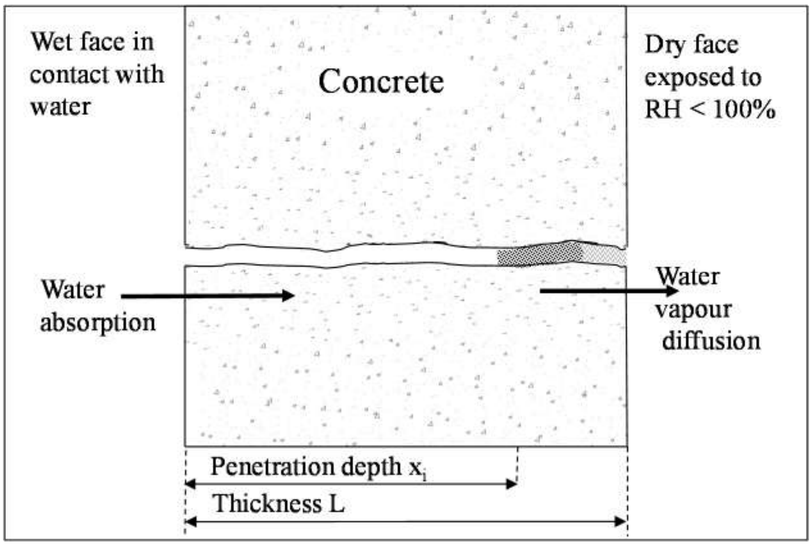

Figure 2.13 Schematic of Wick action (Adapted from Buenfeld et al., 1995)

Buenfeld et al. (1995), based on their experimental and analytical work proposed a partial differential equation to model water motion due to wick action.

$$\frac{\delta C}{\delta t} = \frac{\delta}{\delta x}\left(D(c)\frac{\delta C}{\delta x}\right) - \frac{S^2}{2x_1}\frac{\delta C}{\delta x} \tag{2.39}$$

where

$D(c)$	Water vapour diffusivity function (m^2/s)
C	Water content (kg/m^3)
x	Depth from the wet face (m)
x_1	Depth of the wet/dry interface from the wet face (m)
S	Sorptivity (m/√s)

Equations 2.40 and 2.41 provide the solutions developed.

$$X_1 = \frac{L}{1 - \frac{2D_w}{S^2} \ln \frac{(\rho - C_x)}{(\rho - C_L)}} \tag{2.40}$$

$$Q = \frac{\rho P}{L} \left[\frac{S^2}{2} - D_w \ln \left(\frac{\rho - C_x}{\rho - C_L} \right) \right] \tag{2.41}$$

where

S	Thickness of element or specimen (m)
D_w	Water vapour diffusion coefficient (m^2/s)
ρ	Density of liquid (water) (1000 kg/m^3)
C_x	Concentration of saturated vapour (kg/m^3)
C_L	Concentration of vapour at dry face (kg/m^3)
P	Porosity involved in sorption (< 1, dimensionless)
Q	Water leaving dry face (kg/sm^2)

2.3.8 Linking transport mechanisms to deterioration mechanisms

There are two approaches for specifying the general environments to which a concrete structure will get exposed to in its service life. In a very basic approach as given in IS 456: 2000, the code of practice for plain and reinforced concrete in India. In this, the service environments are classified arbitrarily such as mild, moderate, severe, very severe and extreme. In the second, more progressive approach, the exposure classes are based on the actual deterioration mechanisms, as presented in standards such as EN 206 - 1: 2000 and BS 8500 – 1: 2006. As BS 8500 is the complementary British standard to EN 206, the classifications are same in both standards, with the addition of more practical examples of structures or structural parts coming in each category in BS 8500. Further, there are prescriptive requirements specified for various material parameters for making concrete durable when exposed to each specified environment.

Table 2.2 shows the environmental exposure classification system as given in BS 8500. The practical examples given in the code are not incorporated in Table 2.2.

Table 2.2 Environmental exposure classification system (BS 8500 – 1: 2006)

Class designation	Class description
No risk of corrosion or attack (X0 Class)	
X0	For concrete without reinforcement or embedded metal: all exposures except where there is freeze-thaw, abrasion or chemical attack For concrete with reinforcement or embedded metal: very dry
Corrosion induced by carbonation (XC Class) (where concrete containing reinforcement or other embedded metal is exposed to air and moisture)	
XC1	Dry or permanently wet
XC2	Wet, rarely dry
XC3 & XC4	Moderate humidity or cyclic wet and dry
Corrosion induced by chlorides other than sea water (XD Classes) (where concrete containing reinforcement or other embedded metal is subject to contact with water containing chlorides, including de-icing salts from sources other than from sea water)	
XD1	Moderate humidity.
XD2	Wet, rarely dry.
XD3	Cyclic wet and dry.
Corrosion induced by chlorides from sea water (XS Classes) (where concrete containing reinforcement or other embedded metal is subject to contact with chlorides from sea water or air carrying salt originating from sea water)	
XS1	Exposed to airborne salt but not in direct contact with sea water
XS2	Permanently submerged
XS3	Tidal / splash and spray zones
Freeze-thaw attack (XF Classes) (where concrete is exposed to significant attack from freeze-thaw cycles whilst wet)	
XF1	Moderate water saturation without de-icing agent
XF2	Moderate water saturation with de-icing agent
XF3	High water saturation without de-icing agent
XF4	High water saturation with de-icing agent or sea water.

In order to link transport mechanisms to the deterioration mechanisms, practical examples are considered in two different service environments. The examples chosen are a bridge pier in a marine environment and a bridge pier in a city area. In these examples, only mechanisms relevant to a tropical climatic region such as India are considered. Deterioration due to specific effects such as freeze and thaw, cavitation, fire etc. is not considered. Further, material specific deterioration mechanisms such as alkali silica reaction and alkali carbonate reaction are not considered.

2.3.8.1 Bridge pier in a marine environment

There are mainly three possible exposure conditions for a reinforced concrete structure in a marine environment. They are (i) atmospheric zone, (ii) tidal zone or the splash zone, and (iii) submerged zone.

In the case of the atmospheric zone, the structure is exposed to air borne chlorides. Thus, chloride induced corrosion of the re-bars can be a deterioration mechanism in this sector. Further, the structure can be subjected to carbonation induced corrosion depending on other factors such as relative humidity, temperature etc. However, compared to carbonation induced corrosion, chloride induced corrosion will be the dominant deterioration mechanism. With regard to the transport mechanisms, both gaseous as well as water vapour diffusion can take place in this exposure condition. In addition to diffusion, sorption is another deciding mechanism as alternate wetting and drying can happen due to rain. Further, physical degradation of the structure can happen due to salt crystallization.

Concrete exposed to splash or tidal zone is in the worst condition of all the categories specified. All the mechanisms such as diffusion, sorption, wick action and permeation perform significant role in the transport of aggressive species. Moreover, in this zone, mechanical action of waves can lead to physical means of deterioration such as abrasion, erosion and salt crystallisation. Thus, in this condition, both strength and impermeability are important. Deterioration can happen because of chloride induced corrosion and other chemical deterioration processes such as sulphate attack.

Regarding concrete fully immersed in the sea, there is no effect of sorption, on the other hand, effect of permeation will be more. In addition, diffusion will also play a major role. Thus, impermeability will be more crucial than strength. Concrete can deteriorate because of chemical deterioration processes such as sulphate attack, leaching etc. and due to chloride induced corrosion.

In a similar way, transport mechanisms in different micro climatic conditions are described in BS 6349 – 1 (2000). This is shown pictorially in Figure 2.14.

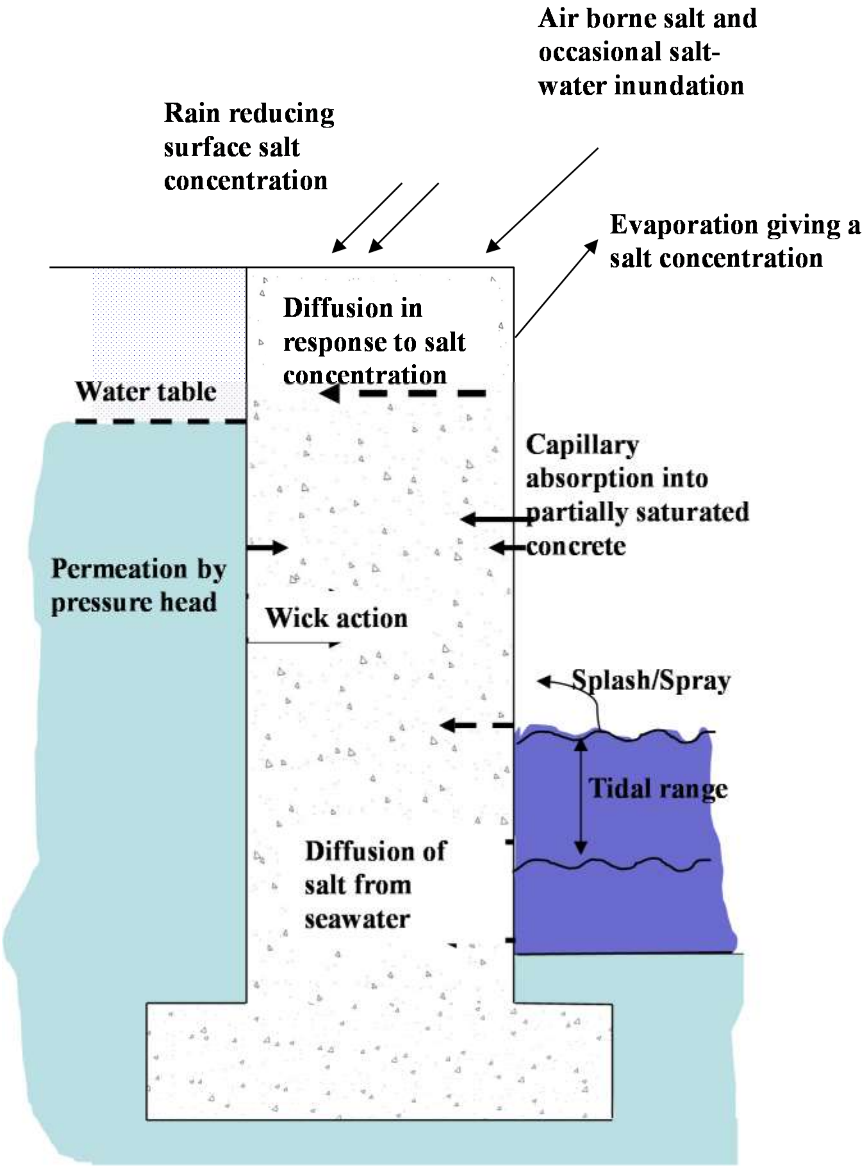

Figure 2.14 Chloride transport process in a maritime structure
(Adapted from BS 6349 -1, 2000)

2.3.8.2 Bridge pier in a city area

In the case of a reinforced concrete structure such as a bridge pier in a city area, there can be three exposure conditions viz., (i) atmospheric zone, (ii) zone below the ground level; but above the ground water table and (iii) zone below the ground water table.

In the case of atmospheric zone, corrosion of rebar induced by carbonation will be the most critical one. In addition to gaseous as well as water vapour diffusion, sorption is the other possible transport mechanism due to the likelihood of rain. Wick action and sorption are the possible transport mechanisms by which aggressive chemicals can enter into concrete in the case of the zone below ground level but above the ground water table. This can be due to the fluctuations of the ground water table. Concrete degradation can happen because of the chemical attack. The zone below the ground water table is subjected to permeation and diffusion. The deterioration can happen because of chemical degradation processes such as sulphate attack, leaching etc.

2.3.9 Interim summary

The Section 2.3 dealt with details of the mechanisms by which aggressive agents are transferred into concrete. In addition to description of each mechanisms, the governing laws/equations are dealt in detail. Two practical examples such as bridge pier in a marine environment and in a city area are considered for the purpose of linking transport mechanisms to deterioration mechanisms.

2.4 DURABILITY TEST METHODS

Numerous test methods have been developed, especially within the last thirty years, to assess concrete durability. These test methods evaluate some parameters of concretes that represent durability directly or indirectly. Many authors have attempted to classify these test methods based on different aspects. For example, Basheer (2001) classified the test methods to assess permeation properties of concrete as adsorption tests, diffusion tests, absorption tests and permeability tests. Stanish et al. (1997), classified the tests to find the chloride penetration resistance of concrete as long term tests, short term tests and other test methods. There is another classification by Yuan and Santhanam (2013) for the test methods for chloride transport in concrete, where the criterion is the theoretical basis of the test methods. Moreover, different technical groups such as RILEM, ACI, NRMCA (e.g:- RILEM TC 189 NEC, 2007, RILEM TC 230 PSC (Draft), 2015, RILEM TC 116 PCD, 1999, NRMCA P2P manual, 2006, ACI 222R, 2001) have published state-of-the art reports for durability, which also tried to classify and compile the existing knowledge about test methods on durability. Details of these classifications are given as Table A-1 in Appendix A.

In a broad sense, the test methods are classified into three groups such as (i) test methods used to assess chloride penetrability, (ii) test methods used to assess gas penetrability, and (iii) test methods used to assess water penetrability. The details of each test methods are consolidated in Tables A-2 to A-7 in Appendix A. The term penetrability is used such that it encompasses all the transport mechanisms leading to the penetration of the particular kind of aggressive species into concrete.

Based on the literature review, a set of test methods were chosen for the present study. The basis of the selection is as follows.

- Recommendations from different RILEM TCs (TC 116 PCD, 1999, TC 189 NEC, 2007, TC 211 PAE, 2013)
- Addressing the major transport mechanisms that lead to chloride induced corrosion and carbonation induced corrosion of RC structures
- Most widely specified test methods in major construction projects in India (Dhanya and Santhanam, 2013). More test methods related to chloride penetrability are selected as India has a large coast line and chloride induced corrosion is the major deterioration mechanism in reinforced concrete.
- All the durability index tests developed in South Africa are included in the study as these tests are in practice in that country. In South Africa, the projects under South Africa National Road Agency (SANRAL) use the durability index parameters in three stages such as in design, in specification and for quality control on site (Nanga, 2011).

Table 2.3 shows the test methods selected in each category along with the parameter obtained and the transport mechanism(s) addressed. The governing law or equations are also presented in the table.

Table 2.3 Selected durability test methods, parameters, transport mechanism(s) and governing law/equation

Category	**Test method**	**Parameter**	**Transport mechanism(s)**	**Governing law/equation**
Chloride penetrability	Rapid chloride permeability	Charge passed	Diffusion, Migration	Charge passed is calculated from current and time, based on trapezoidal rule
	Rapid migration	Non-steady state migration coefficient	Diffusion, Migration	Nernst Planck equation
	Chloride conductivity	Conductivity	Migration	Conductivity is calculated based on electro chemical theory
	Wenner 4 - probe surface resistivity	Surface resistivity	Migration	Resistivity is calculated from resistance which is the ratio of the potential difference to current
Gas penetrability	Oxygen permeability index	Oxygen permeability index	Permeation	d'Arcy's law
	Torrent air permeability	Coefficient of air permeability	Permeation	Hagen-Poiseuille equation
	Accelerated carbonation	Carbonation depth	Diffusion	Square root of time law
Water penetrability	Water sorptivity	Sorptivity index	Sorption, Absorption, Wick action	Laplace's Equation
	Water permeability	Water penetration depth	Permeation	

The following sections give a brief review of all the test methods selected for this study.

2.4.1 Wenner 4 – probe surface resistivity test

This method is standardized for the measurement of soil resistivity as ASTM G57 (2012), whereas for concrete application it is not yet standardized. However, many researchers (Andrade, 1993, Andrade and Alonso, 1996) favour surface resistivity as a good method for assessing concrete durability.

In this method, four equally spaced point electrodes are pressed on the concrete surface. The two outer electrodes induce current flow, whereas the two inner electrodes measure the potential drop. Resistivity of concrete ρ is calculated from the resistance which is the ratio of the potential difference to current, as given in Equation 2.42.

$$\rho = 2\pi a R \tag{2.42}$$

where

ρ	Resistivity of concrete
a	Spacing between the electrodes
R	Resistance (ratio of potential difference to current)

Figure 2.15 shows the line diagram of the Wenner 4 - probe resistivity test set up.

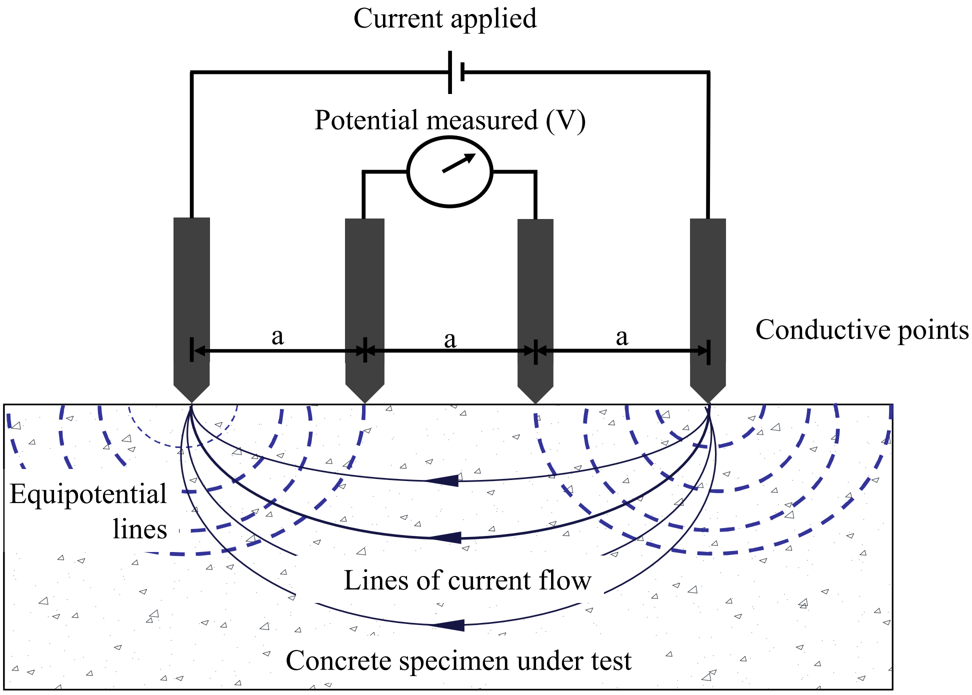

Figure 2.15 Line diagram of Wenner 4-probe resistivity test set up
(Adapted from Bjegović et al., 2015)

In terms of resistivity, many classification criteria for concrete quality have been proposed by different researchers. Some researchers relate resistivity and concrete quality (Bjegovic et al., 2015) whereas some others have tried to link resistivity and corrosion risk (Andrade et al., 2004, Andrade and Alonso, 1996). Table 2.4 shows the classification criteria proposed in the recommendations by RILEM TC 154 EMC, 2004.

Table 2.4 Concrete quality classification based on resistivity
(RILEM TC 154-EMC, 2004)

Resistivity (kΩ.cm)	Concrete Quality
>100	Good
50 - 100	Normal
10 - 50	Poor
< 10	Very poor

Table 2.5 shows the classification system relating resistivity and corrosion rate. This classification criterion has been given in ACI Committee report 222R (2001) on Protection of Metals in Concrete against Corrosion. Even though resistivity alone is not the only indicator of corrosion, it is a good parameter that reflects the material capability to resist corrosion propagation, as agreed by many of the researchers.

Table 2.5 Classification of corrosion rate based on resistivity
(ACI 222R, 2001)

Resistivity(kΩ.cm)	Corrosion rate
> 20	Low
10 to 20	Low to moderate
5 to 10	High
< 5	Very high

Resistivity ρ is dependent on the quantity and conductivity of the pore solution and the size, interconnectivity and tortuosity of pores (Andrade et al., 2007). According to Andrade et al. (2013), the major factors affecting the resistivity of concrete are age, water saturation level and temperature of concrete. As the age increases, resistivity improves because of the refinement of pore structure. This effect is more dominent in concrete having SCMs. As water saturation level increases, the resistivity decreases. The influence of temperature can be two fold. As temperature increases, ionic diffusivity increases and thus the resistivity decreases. On the contrary, as temperature increases, evaporation occurs, which can lead to an increase in resistivity. The work by Sengul and Gjorv (2008) also agrees with these observations. Further, they also studied the influence of some other factors on resistivity such as spacing of the probes, specimen geometry, testing location and direction etc. From their study, it is observed that as the probe spacing increases, resistivity increases, the effect of which is nullified in the case of Wenner 4 – probe testing method, as the probes are at constant spacing in this test. Moreover, they studied the influence of specimen geometry on resistivity by comparing the results obtained from cube, cylinder and block specimens. The study depicted that the resistivity obtained for the block specimens was relatively lower owing to the larger volume of concrete. They also concluded that the testing direction had no influence on the resistivity of concrete. However, the resistivity was found to be increased with decreasing distance from the edge to the testing location. Further, the resistivity obtained by Wenner 4 – probe test method was higher compared to that obtained from the two electrode method owing to the effect of surface conditions. However, for a given probe spacing and specimen type, the ratio between resistivity obtained by both methods is constant. Thus, Wenner method is recommended as a good method for quality control of concrete construction, provided all measurements are made on same type of concrete specimens in the same testing conditions, following the same testing procedure.

The following are the merits and demerits of this method.

Merits

- Quick method
- Resistivity is used to calculate the corrosion rates in concretes
- No heating
- Very low voltage (10V or lower) is applied for a short time

Demerits

- Depends on pore solution conductivity and moisture condition of the specimen
- Inclusion of conductive materials such as rebar affects the results
- Depends on temperature of the specimen

- Depends on specimen geometry

Service life prediction models are also proposed based on this non-destructive method. For example, Andrade et al. (2013) proposed a service life prediction model based on concrete resistivity. This model is based on the Nernst Einstein equation, which was discussed in section 2.3.4.2. The service life is divided into two periods namely the time of initiation of corrosion and time of corrosion propagation. For the determination of corrosion initiation time, resistivity is incorporated as a rate determining parameter, as a function of time. For the determination of corrosion propagation time, the loss in rebar diameter or pit depth is considered as the limit of corrosion attack. The model also takes into account the interaction between aggressive species and cement solid phases in terms of the reaction or binder factor, the environmental factor related to the exposure condition, effect of aging etc. The expression for calculating the service life is given in Equation 2.43, and the full solution of the same can be found in Andrade et al., 2013.

$$t_l = t_i + t_p = \frac{X^2 \rho_e \left(\frac{t_e}{t_0}\right)^q \cdot \gamma_{cl,co2}}{F_{Cl,CO2}} + \frac{P_x \rho_e \left(\frac{t_e}{t_0}\right)^q}{k_{crr}} \qquad (2.43)$$

Where

t_l	Service life of the structure
t_i	Time for corrosion initiation
t_p	Time for corrosion propagation
X	Depth of penetration of aggressive front = cover depth
ρ_e	Concrete resistivity under saturated condition
t_e	Age of concrete at which full hydration is assumed (usually 10 years)
t_0	Age of concrete at which resistivity is measured (usually 28 days)
q	Age factor

$\gamma_{cl,co2}$	Reaction factor or binding factor
$F_{Cl,CO2}$	Environmental factor
P_x	Pit depth
k_{crr}	A constant to find the corrosion rate = 3×10^4 µA/cm^2 kΩ.cm

2.4.2 Rapid chloride permeability test

Rapid chloride permeability test (RCPT) is the most popular and most widely criticized durability test method. This method was originally proposed by Whiting in 1981 and is standardized by ASTM (ASTM C1202, 2010) and AASHTO (AASHTO T277 – 07, 2008). The test involves the application of a potential of 60 Volts on a vacuum saturated cylindrical concrete specimen. One side of the specimen is exposed to 3% NaCl solution and the opposite side to 0.3 M NaOH solution. The resulting current is measured at an interval of 30 minutes for a total period of 6 hours. From the current measurements, the total charge passed (in Coulombs) is calculated using Equation 2.44, which is based on the trapezoidal rule. This ‘charge passed’ is used to categorize the concrete into different classes.

$$Q = 900\,(I_0 + 2\,I_{30} + 2\,I_{60} + \cdots. + 2\,I_{330} + I_{360}) \tag{2.44}$$

where

Q	Charge passed (Coulombs)
I_0	Current immediately after voltage is applied (Amperes)
I_{t}	Current at ‘t ‘minutes after voltage is applied (Amperes)

Figure 2.16 shows the line diagram of the RCPT set up.

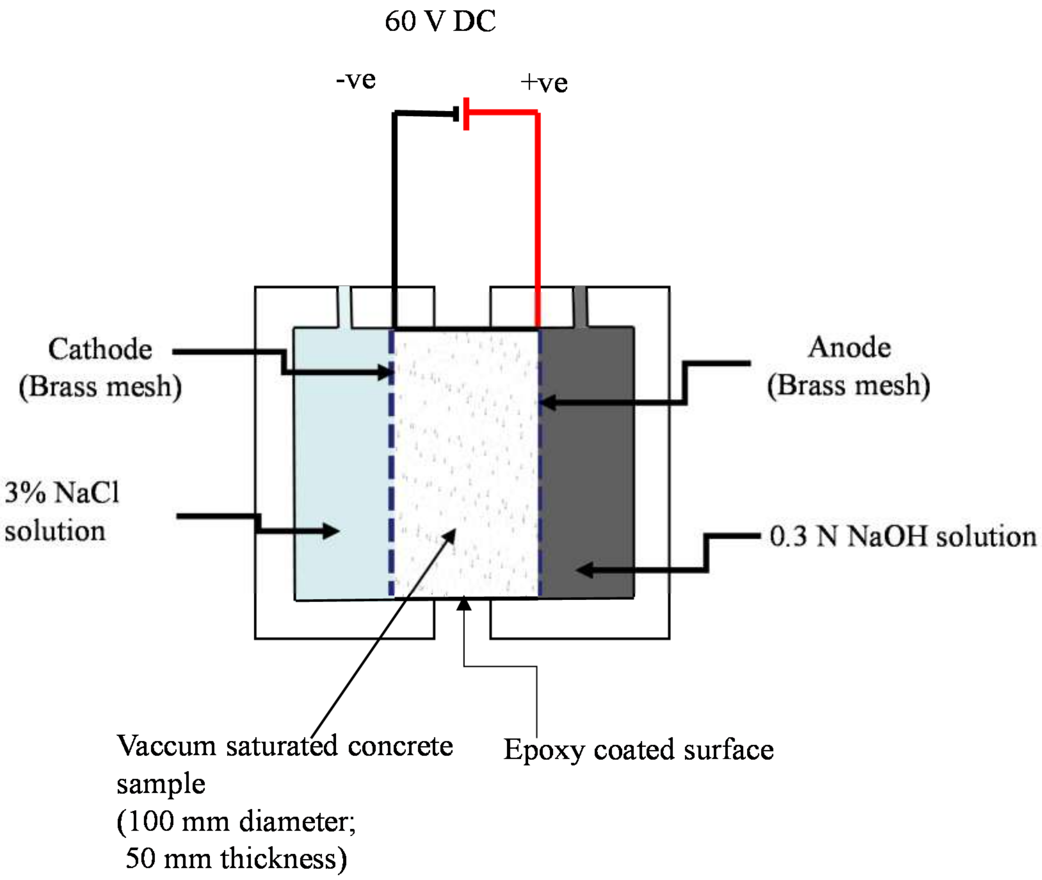

Figure 2.16 Line diagram of RCPT set up

Andrade (1993) had made a critical review of RCPT and identified the different mechanisms occurring in concrete during the test and came up with their scientific explanation. She had proposed the Nernst-Planck equation to calculate the diffusion coefficient from RCPT. The unidirectional flux of a particular ion (J_j) is explained to be a function of diffusion, migration and convection. The equation of the total flux is given in Equation 2.34.

Table 2.6 indicates the classification of chloride ion penetrability in concrete based on the charge passed as given in ASTM C1202 (2010).

Table 2.6 Chloride ion penetrability based on charge passed (ASTM C1202, 2010)

Charge passed (Coulombs)	Chloride ion penetrability
>4000	High
2000 - 4000	Moderate
1000 - 2000	Low
100 - 1000	Very Low
<100	Negligible

The merits and demerits/criticisms of RCPT are discussed below (Saraswathy and Song, 2006, Chindaprasit et al., 2007, Cheng et al., 2005, Aldea et al., 2000, Stanish et al., 1997, Andrade, 1993, Ali Akbar Ramezanianpour et al., 2011).

Merits

- Widely used test method because of its simplicity
- Gives qualitative classification of concrete

Demerits/Criticisms

- The test measures ionic movement and not permeability (as name indicates).
- Many transport mechanisms act together in this test.
- The current passed is related to all ions in the pore solution and not just chloride ion.
- The measurements are made before steady state migration is achieved.
- The high voltage applied leads to an increase in temperature, especially for low quality concretes and the rise in temperature can further accelerate ionic movement.
- The results are influenced by the conductivity of concrete. The pore solution characteristics are altered when pozzolanic materials or corrosion inhibitors are incorporated, thus changing the pore solution conductivity. Thus, the test is biased to concrete containing blends such as silica fume which have very less pore solution conductivity.
- The results are influenced by the presence of rebars and other fibers in the concrete matrix.

Even though the test is subjected to widespread criticism, many researchers have been able to get correlation between RCPT and other long term test methods to assess chloride penetration (Papadakis, 2000, Lu et al., 2006).

2.4.3 Rapid migration test

The rapid migration test (RMT) was developed by Tang and Nilsson in 1992 at the Charmers Technical University, Sweden (High performance concrete structural designers' guide, 2005). Thus, this test is also known as the CTH test. This test method is standardized by NORD as NT BUILD 492, 1999 and AASHTO as AASTO TP 64:2003 (2007). The test principle is similar to RCPT, and involves the application of a 30 V potential gradient across the vacuum saturated concrete specimen, one side of which is in contact with 0.3 M NaOH solution and the other side with 10% NaCl solution. The potential is applied for longer duration (varies from 6 to 96 hours, in most cases 24 hours) compared to the RCPT. After this time period, the specimens are split and silver nitrate solution is sprayed on the split surface. Chlorides react with silver nitrate to form silver chloride which is white in colour, the extent of white precipitate indicates the depth of chloride penetration. The non-steady state diffusion coefficient is calculated by using the depth of chloride penetration using Equation 2.45.

$$D_{nssm} = \frac{RT}{zFE} . \frac{X_d - \propto \sqrt{X_d}}{t} \tag{2.45}$$

where

$$E = \frac{U-2}{L} \tag{2.46}$$

$$\propto = 2\sqrt{\frac{RT}{zFE}} . erf^{-1}\left(1 - \frac{2c_d}{c_0}\right) \tag{2.47}$$

D_{nssm}	Non-steady-state migration coefficient (m^2/s)
z	Absolute value of ion valence (for chloride, z = 1)
F	Faraday constant = 9.648×10^4 J/(V·mol)
U	Absolute value of the applied voltage (V)
R	Gas constant = 8.314 J/(K·mol)
T	Av. value of the initial and final temperatures in the anolyte solution (K)

L	Thickness of the specimen (m)
X_d	Average value of the penetration depth (m)
t	Test duration (s)
erf^{-1}	Inverse of error function
c_d	Chloride concentration at which the colour changes (≈ 0.07 N for OPC concrete)
c_0	Chloride concentration in the catholyte solution (≈ 2 N)

Figure 2.17 shows the line diagram of the RMT set up (adapted from NT BUILD 492, 1999).

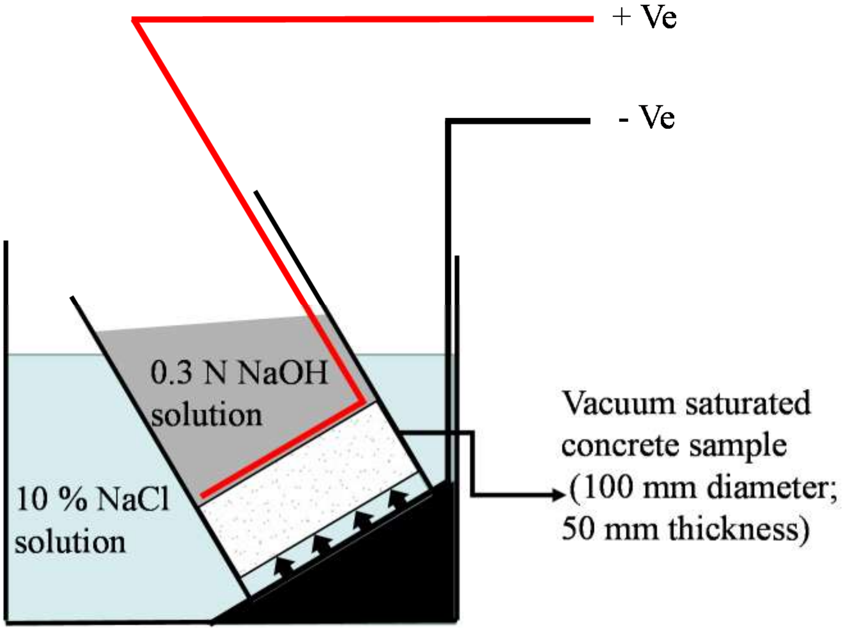

Figure 2.17 Line diagram of RMT set up (Adapted from NT BUILD 492, 1999)

The classification criteria suggested by the developers of the test (Tang and Nilsson) is given in Table 2.7, which is based on the non-steady state migration coefficient (Bjegović et al., 2015). This test method was developed to overcome the shortcomings of RCPT and it does so in some of the aspects. The heating effect is avoided due to the use of higher quantity of sodium chloride solution and due to the application of lower potential. The depth of chloride penetration is used to calculate the non-steady state migration coefficient. Hence, there is direct evidence of chloride penetration. Further, the set up enables easy removal of any escaping gases. The test is not affected by the presence of calcium nitrite corrosion inhibitor. Moreover, the correlation between RMT and long term test methods is better compared to that with RCPT (Vivas et al., 2007).

Table 2.7 Concrete quality classification based on the migration coefficient (Bjegović et al., 2015)

Non-steady state migration coefficient ($\times 10^{-12}$ m^2/s)	Concrete quality
< 2	Very good
2 – 8	Good
8 – 16	Normal
> 16	Poor

The following are the merits and demerits of this test method.

Merits

- Non-steady state migration coefficient is related only to chloride ion penetration and thus the test is more intuitive in nature.
- Reduces the problem related to heating of the specimen
- The test shows lesser variation compared to RCPT.

Demerits

- Presence of conductive materials affects the test results.
- Many transport mechanisms act together.
- Large quantity of NaCl solution is required.
- It is a time consuming test. Takes up to 96 hours to complete the test for some concretes, normally 24 hours.
- Destructive in nature
- Cannot be applied on site

2.4.4 Chloride conductivity test

This test method was proposed by Streicher and Alexander of the University of Cape Town in South Africa in 1995 (Streicher and Alexander, 1995). This test is developed based on the electrochemical theory and is very rapid as it involves only single current measurement. Chloride conductivity test is standardised in the Durability Index Testing Procedure Manual, South Africa (2009) and is a widely used test method in that country.

The test consists of a two cell conduction rig in which the concrete core specimens are exposed on either side to 5 M NaCl solution. The concrete specimens are vacuum saturated in 5 M NaCl solution prior to the test. A potential difference (between 0 and 20 V) is applied to the anode (made of carbon (preferably) or stainless steel) and cathode (made of stainless steel) in such a way that the potential across the specimen is 10 V. The current is measured at this stage and is used to calculate the chloride conductivity as given in Equation 2.48.

$$\sigma = \frac{id}{VA} \tag{2.48}$$

where

σ	Chloride conductivity of the specimen (mS/cm)
i	Electric current (mA)
V	Voltage difference (V)
d	Average thickness of specimen (cm)
A	Cross sectional area of the specimen (cm^2)

Figure 2.18 shows the line diagram of chloride conductivity test set up.

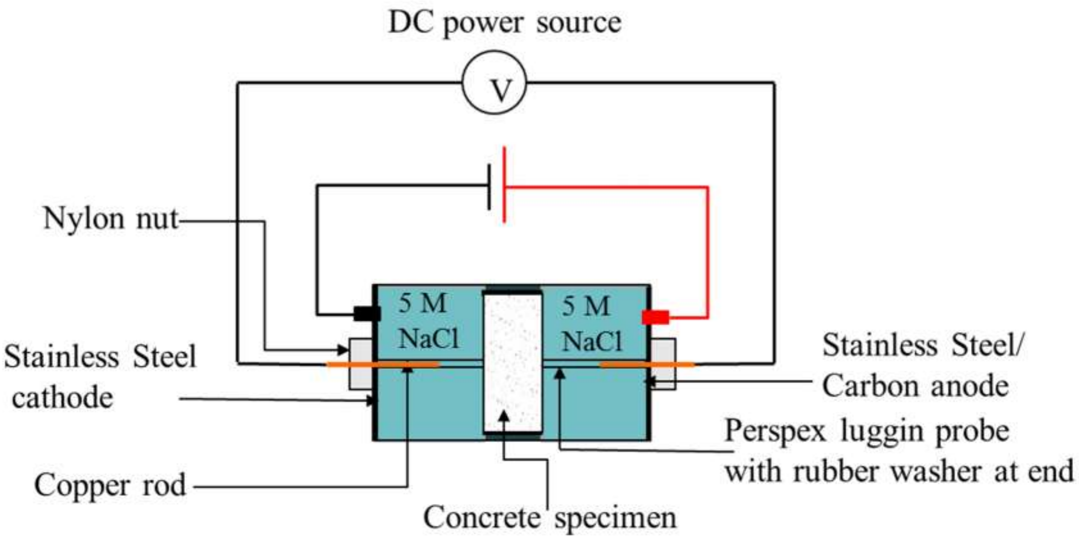

Figure 2.18 Line diagram of Chloride conductivity test set up

The classification criteria developed by Alexander et al., (1999) with respect to chloride conductivity is provided in Table 2.8.

Table 2.8 Concrete quality classification based on chloride conductivity (Alexander et al., 1999)

Chloride conductivity (mS/cm)	Concrete quality
< 0.75	Very good
0.75 – 1.50	Good
1.50 – 2.50	Poor
> 2.50	Very poor

The following are the merits and demerits of chloride conductivity test results.

Merits

- Simple and quick test
- Accelerates the steady state conditions by sample conditioning (oven drying and vacuum saturation with 5 M NaCl solution)
- Nullifies the effect of other ions in the pore solution and guarantee uniform conductivity of the pore solution

Demerits

- Destructive in nature
- Cannot be applied on site
- Pre conditioning may create micro cracks in the specimen
- May not be suitable for high performance concrete due to excessive micro-structural damage or inadequate saturation with the concentrated salt solution.

Mackechnie and Alexander (2002) had developed a chloride prediction model using chloride conductivity measurements. Fick's second law of diffusion is modified as given in Equation 2.49 to allow for diffusion coefficients with time and is used for the prediction.

$$D_c = D_i \, t^{-m} \tag{2.49}$$

where

D_i	Diffusion coefficient at one second
m	Empirical material coefficient relating to the reduction in diffusion coefficient D_c with time t

The solution to the Fick's second law of diffusion is modified and is given in Equation 2.50.

$$C_x = C_s \, (1 - \mathrm{erf}\left(\frac{x}{2\sqrt{D_i t^{(1-m)}}}\right) \tag{2.50}$$

Where

C_x	Concentration at depth x and time t
C_s	Surface concentration, assumed to be constant

Chloride conductivity test results can be used to predict long term diffusion coefficients for marine concrete. A nomogram has been developed from synthesis of marine exposure tests and case studies of the marine structures, which is presented in Figure 2.19. The nomogram shows the relationship between 28 day chloride conductivity measurements and 50 year diffusion coefficients for different concretes containing different SCMs. The modified chloride conductivity value presented in the nomogram allows for long term effects such as chloride binding and continued cementing reactions (Mackechnie, 2001).

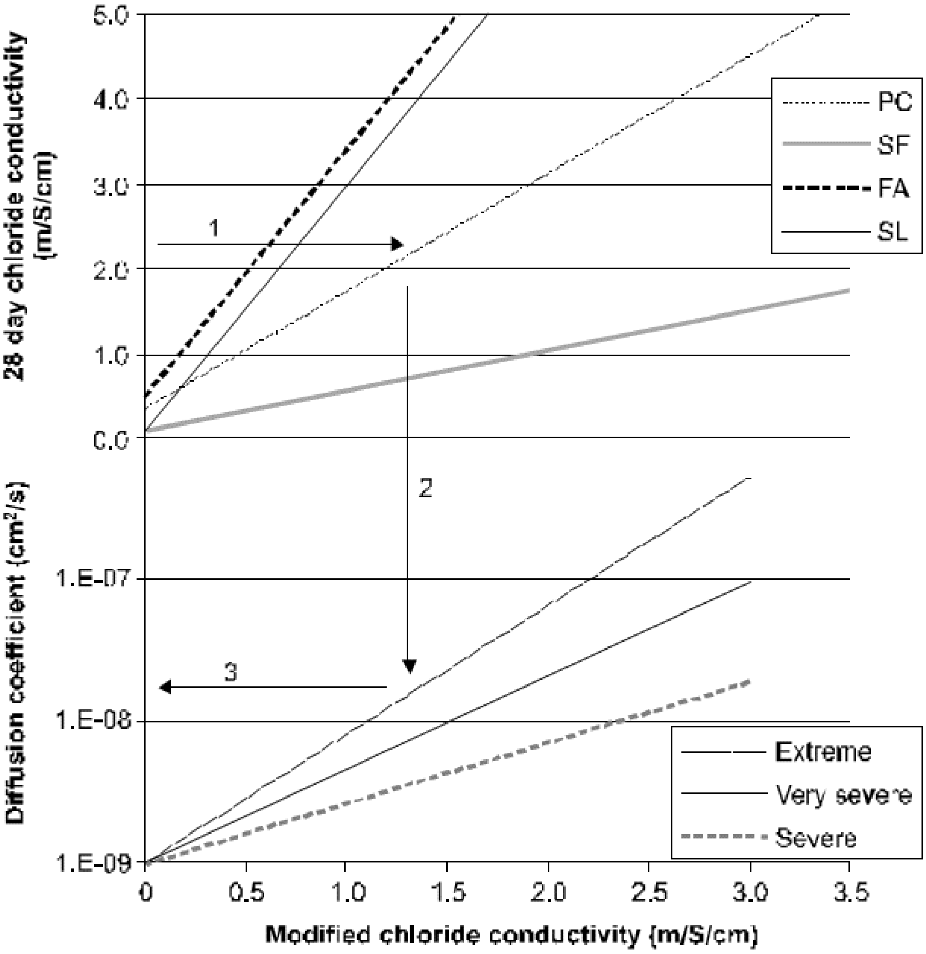

Figure 2.19 Predicting 50 year diffusion coefficients for marine concrete from 28 day chloride conductivity test results (Mackechnie, 2001)

2.4.5 Oxygen permeability index test

The oxygen permeability index (OPI) test is developed in South Africa. This test is also standardized in durability index testing procedure manual of South Africa (2009) along with chloride conductivity and water sorptivity test and is widely used in that country (Alexander, 2014). The test method involves measuring the pressure decay of oxygen passed through a concrete disk placed in a falling head permeameter. Figure 2.20 shows the line diagram of the OPI test set up.

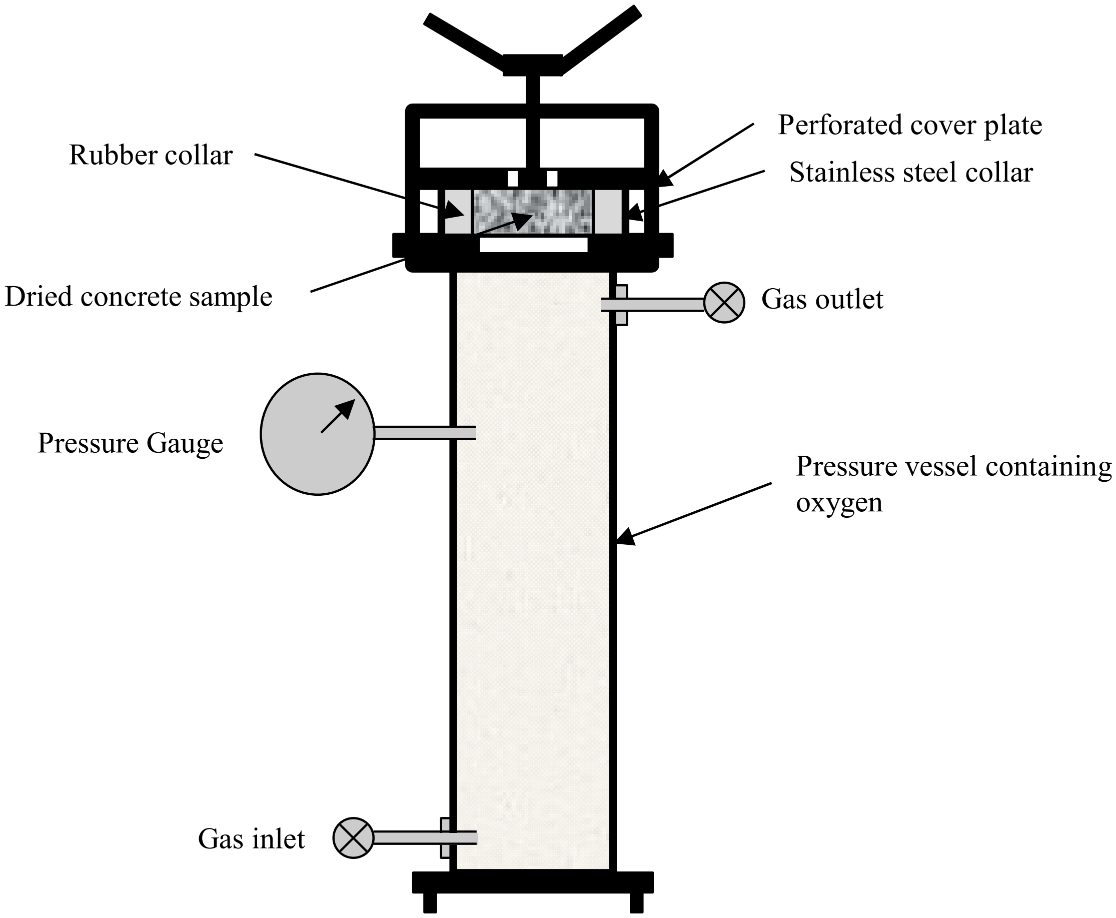

Figure 2.20 Line diagram of OPI test set up (Adapted from Durability Index Testing Procedure Manual of South Africa, 2009)

The concrete discs which are of 68 ± 2 mm diameter and 30 ± 2 mm thickness, are prepared from cores taken either from concrete structures or from 150 mm size cubes. The discs are coated with epoxy on the curved surface and are dried in an oven at 50°C for 7 days. The test specimens are cooled to room temperature for two hours prior to the testing. A pressure gradient is applied across the test specimen that is placed in the permeability cell shown in Figure 2.20. The decay in pressure is monitored over time. Using the pressure readings and the time, the coefficient of permeability is calculated based on d’Arcy’s law. The oxygen permeability index, defined as the negative log of the coefficient of permeability is calculated which is used to classify concrete qualitatively. The d'Arcy's coefficient of permeability is calculated as shown in Equation 2.51.

$$k = \frac{\omega\, V\, g\, dz}{RA\theta} \tag{2.51}$$

where

k	Coefficient of permeability of test specimen (m/s)
ω	Molecular mass of oxygen = 32 g/mol
V	Volume of oxygen under pressure in permeameter (m^3)
g	Acceleration due to gravity = 9.81 m/s^2
R	Universal gas constant = 8.313 J/K mol
d	Average specimen thickness (m) to the nearest 0.02 mm
A	Cross sectional area of the specimen (m^2)
θ	Absolute temperature (K)
z	Slope of the line determined in the regression analysis

In order to calculate the slope z, the best fit line need to be determined using linear regression of $\ln\left({}^{P_0}/_{P_t}\right)$ against t, forcing the regression line through the (0,0) point in which P_0 is the initial pressure at the start of the test (i.e., at time t_0) to the nearest 0.5 kPa; P_t is the subsequent readings in pressure to the nearest 0.5 kPa at times t, measured from t_0; and t is the time in seconds, recorded to the nearest minute. For the validity of the test, coefficient of correlation should be greater than 0.99.

The oxygen permeability index (OPI) is the negative log of the average of the coefficients of permeability of four specimens. Thus, for four specimens which are having the coefficients of permeability as k_1, k_2, k_3 and k_4 , the OPI is

$$OPI = -\log_{10}[\tfrac{1}{4}(k_1 + k_2 + k_3 + k_4)] \tag{2.52}$$

The classification criteria developed by Alexander et al. (1999) for concrete quality based on the Oxygen Permeability Index is as given in Table 2.9.

Table 2.9 Concrete quality classification based on Oxygen Permeability Index (Alexander et al., 1999)

Oxygen permeability index (OPI)	Concrete quality
> 10	Very good
9.5 - 10	Good
9.0 – 9.5	Poor
< 9	Very poor

Permeability is a measure of the capacity of concrete to transfer fluids by permeation where the driving force is the pressure difference. The permeability of concrete is dependent on different factors such as the microstructure of concrete, the moisture condition of the specimen, the features of the permeating agent etc. (Beushausen, 2008). Gas permeability measurements are important in the case of concrete durability as they are directly related to carbonation as well as propagation of corrosion. According to RILEM TC 189 report, OPI test can be used to detect differences in w/b, binder type, and curing condition of different concretes. Further, the results from OPI test are well correlated with other existing test methods such as the Cembureau method and the Torrent air permeability test (RILEM TC 189 NEC, 2007). The correlation between carbonation depth and OPI is presented in Figure 2.21(Mackechine and Alexander, 2002)

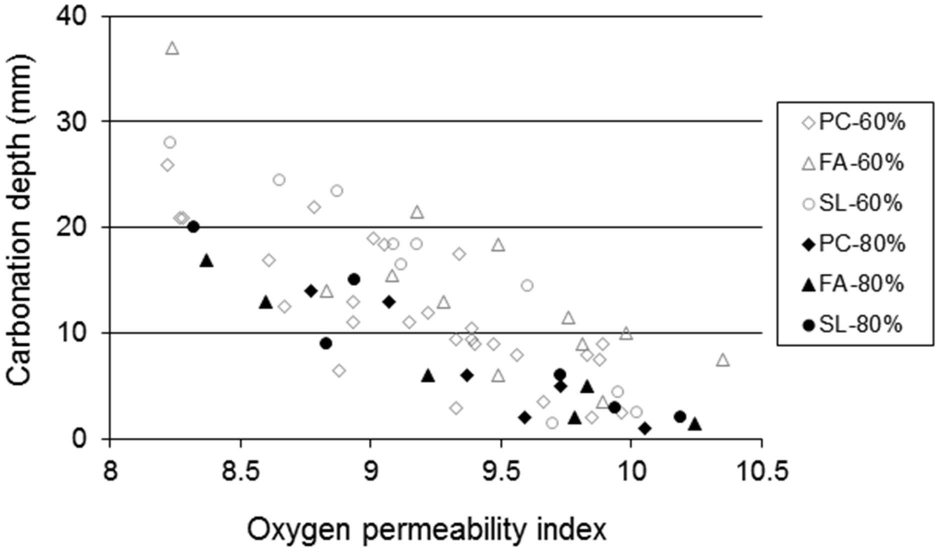

Figure 2.21 Correlation between carbonation depth and OPI test
(Mackechine and Alexander, 2002)

Salvoldi (2010) had developed a mathematical model for concrete carbonation based on the oxygen permeability coefficient that can be obtained from OPI test. The model is given in Equation 2.53.

$$X = \sqrt{\frac{2\, D_{dry}\, c\, \beta}{a}} \times \sqrt{t_e} \tag{2.53}$$

where

X	Depth of carbonation (mm)
D_{dry}	Effective diffusion coefficient (m^2/s)
c	Ambient carbon dioxide concentration (mol/m^3)
β	Relative humidity factor
a	Amount of carbonatable material in the concrete matrix (mol/m^3)
t_e	Effective time of carbonation over the service life of the concrete (years)

The effective diffusion coefficient D_{dry} can be calculated using Equation 2.54.

$$D_{dry} = \left(1.4 \times \left(\frac{k}{10^{-11}}\right)^{2.2}\right) \times 10^{-11} \tag{2.54}$$

where

D_{dry} Effective dry diffusion coefficient

k Oxygen Permeability coefficient

The following are the merits and demerits of OPI test.

Merits

- Good correlation with accelerated carbonation test
- The pore structure will not get modified during test as oxygen will not react with concrete
- Assesses the overall micro and macrostructure of the outer surface of cast concrete, thus useful to assess the state of compaction, presence of bleed voids and channels, and the degree of interconnectedness of the pore structure

Demerits

- Sensitive to macro- voids and cracks
- Sensitive to the specimen preparation
- Very difficult to conduct the tests for concrete having dense micro structure such as high performance concrete

2.4.6 Torrent air permeability test

The Torrent air permeability test was developed by Torrent in 1992 as a method to measure the coefficient of permeability to air of the concrete cover on site (Torrent, 1992). This was later standardized by the Swiss standards as SIA 262/1 E: 2003 on concrete construction. This method is non-destructive in nature and is suitable for on-site measurement of the concrete cover air permeability. The Torrent permeameter consists of a double chamber cell and a pressure regulator. The double chamber cell ensures unidirectional air flow into the inner chamber. In this method, a vacuum is created on the surface of the concrete. Once the vacuum pump is disconnected, a controlled unidirectional air flow from the pores of the concrete to the inner chamber occurs due to the design of the apparatus. The rate at which the pressure returns to the atmospheric value in the test chamber is monitored and thus the air permeability of the concrete (kT) is calculated. The conditioning requirement include temperature of element above 5 - 10°C; electrical resistivity > 10 - 20 kΩ.cm or moisture content < 5.5%, measured by an impedance based instrument. Figure 2.22 shows the line diagram of the Torrent air permeability test set up.

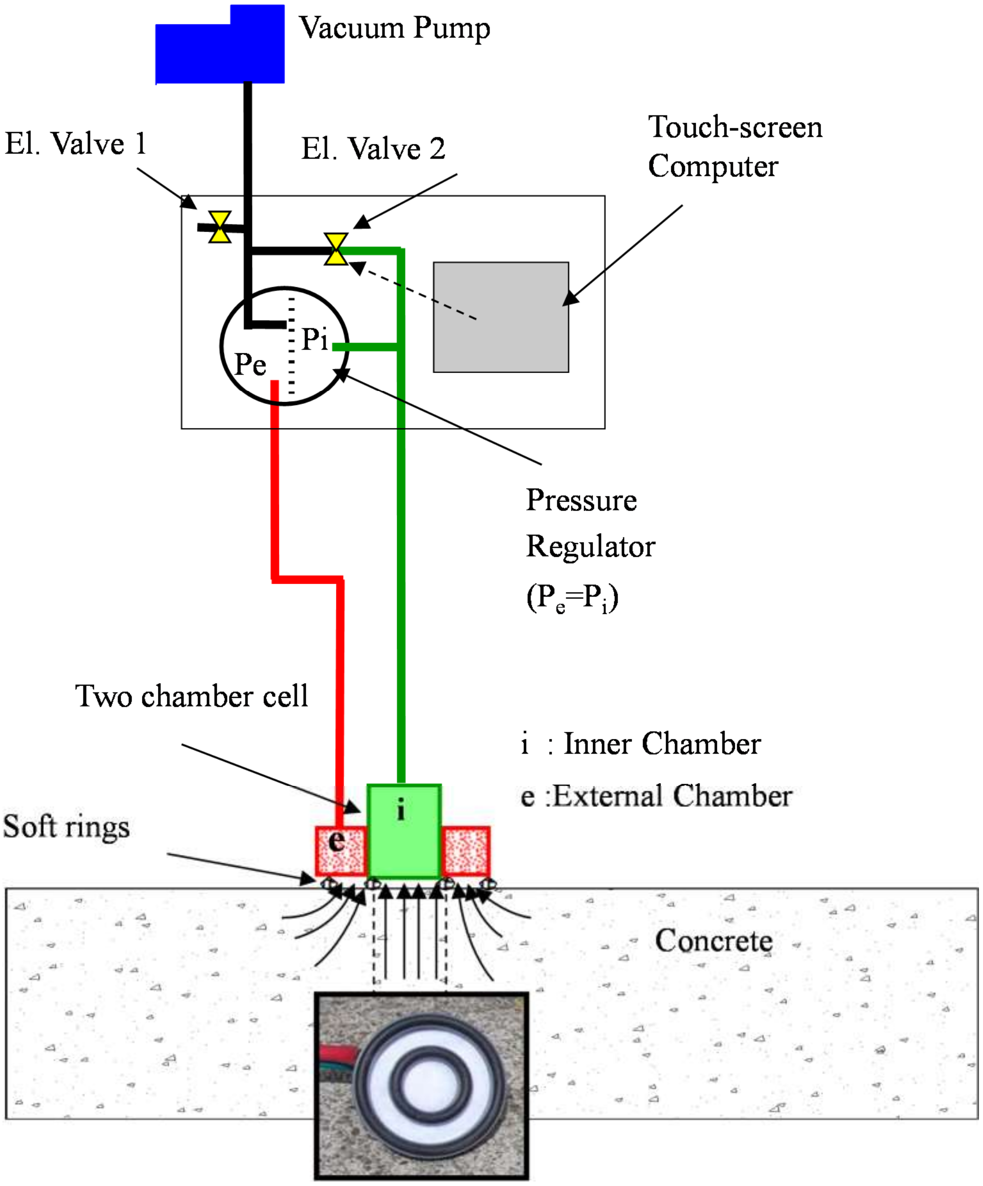

Figure 2.22 Line diagram of Torrent air permeability test set up (Permea-TORR User Manual, 2010)

The formula used to calculate the coefficient of air permeability which is based on Hagen-Poiseuille equation for compressible fluids, is given in Equation 2.55.

$$kT = \left[\frac{V_c}{A}\right]^2 \frac{\mu}{2\varepsilon P_a} \left[\frac{\ln \frac{P_a + \Delta P}{P_a - \Delta P}}{\sqrt{t_f} - \sqrt{t_0}}\right]^2 \tag{2.55}$$

where

kT	Coefficient of air permeability – Torrent method (m^2)
V_c	Volume of inner cell system (m^3)
A	Cross sectional area of inner cell (m^2)
μ	Viscosity of air = 2.0×10^{-5} N.s/m^2
ε	Estimated porosity of the covercrete = 0.15
P_a	Atmospheric pressure (N/m^2)
ΔP	Pressure rise in the inner cell at time t_f (N/m^2)
t_f	Time at the end of the test (s)
t_0	Time at the beginning of the test = 60 s

The merits and demerits of this method are discussed below.

Merits

- Simple and quick test
- Non-destructive in nature
- Both lab and site applications possible

Demerits

- Sensitive to the moisture condition of the specimen
- Test is much sensitive to the surface condition of the specimen

Table 2.10 shows the concrete quality classification based on Torrent air permeability coefficient.

Table 2.10 Concrete quality classification based on Torrent air permeability coefficient (Torrent and Frenzer, 1995)

Torrent air permeability kT ($\times 10^{-16}$ m$^{2)}$	Concrete Quality
< 0.01	Very good
0.01 - 0.1	Good
0.1 - 1.0	Normal
1.0 - 10	Poor
> 10	Very poor

Romer (2005) had done a study on the effect of moisture and concrete composition on the Torrent air permeability measurements and concluded that the results are affected by the age of the concrete and the moisture condition of the test surface. Due to the effect of high relative humidity, the apparent gas permeability got reduced. Further, application of low vacuum led to evaporation of water and thus an increase in the gas volume. This leads to overestimation of the intrinsic permeability.

Imamoto and Tanaka (2012) did a correlation study on the on-site air permeability of concrete with carbonation progress of the existing RC structures in Japan. They concluded that the carbonation velocity based on square root of time relationship increases with increase in air permeability coefficient of concrete. Figure 2.23 depicts the relation between kT and carbonation velocity for all the buildings and specimens (HK – Multi-family dwellings, TH – Lab of Tohoku University, NMWA – National museum of western art, AC – Concrete specimen, CH – Multi-family dwellings, FC – High strength concrete column) considered in their study. The overall correlation obtained was poor as evident from Figure 2.23, even though the authors have reported good correlation in the case of individual buildings.

Ebensperger and Torrent (2010) had reported that there exists strong correlation between kT and oxygen permeability (determined using the procedure recommended by the RILEM PCD – 116), capillary suction coefficient at 24 hour (determined as per SIA 262/1A), chloride migration (determined as per ASTM C1202), water penetration under pressure (determined as per EN12390-8 or DIN 1048) and age required to reach 30 mm carbonation.

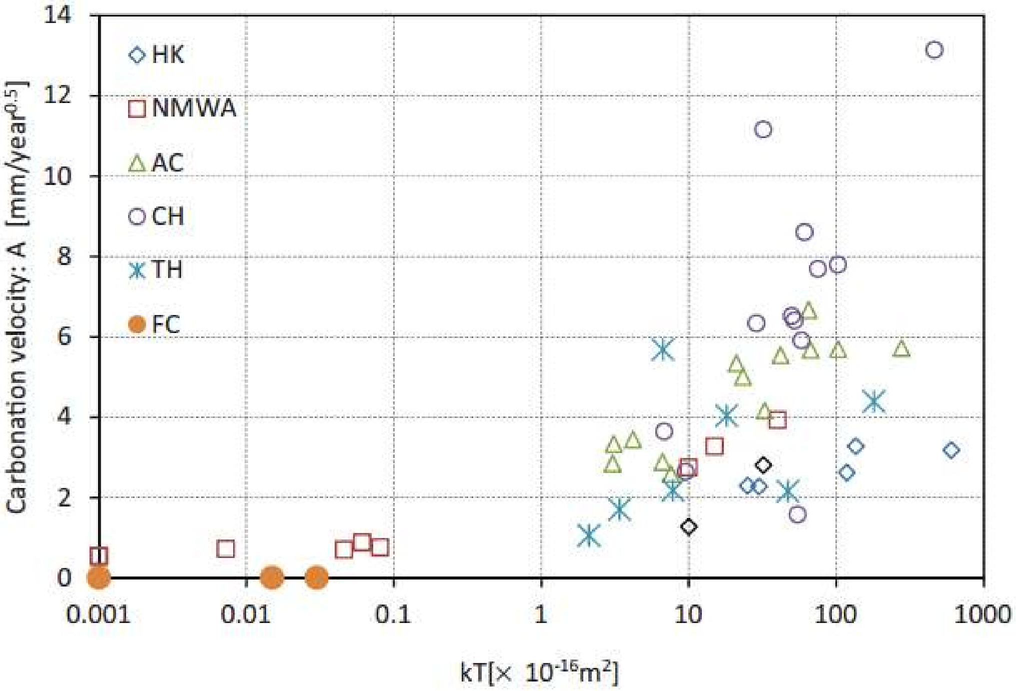

Figure 2.23 Relation between kT and carbonation velocity
(Imamoto and Tanaka, 2012)

2.4.7 Accelerated carbonation test

In the accelerated carbonation test, the concrete samples are subjected to a CO_2 concentration which is much higher than that in the atmosphere in a chamber where the temperature and relative humidity are kept optimum for the carbonation reaction to happen for a specified number of days. After exposure, the carbonation depth is measured by spraying phenolphthalein indicator on a freshly cut face of the sample. A solution of 1% phenolphthalein in 70% ethyl alcohol is suitable for determining the depth of carbonation. Phenolphthalein turns non-carbonated concrete pink, and remains colourless in carbonated concrete (RILEM TC 56 – MHM, 1988). Phenolphthalein indicator test is the simple and quick test to find the depth of carbonation. However, for research purposes, other micro-analytical techniques such as thermo gravimetric analysis (TGA), nuclear magnetic resonance (NMR), X-ray diffraction (XRD) etc. can be used to study carbonation (Castellote et al., 2009).

Curtil et al. (1993) have also described the application of polarizing microscope for the investigation of carbonation of concrete.

The measurement of carbonation depth at different points of time makes it possible to calculate the carbonation rate or carbonation velocity by applying the square root of time relationship. The square root of time law is as shown in Equation 2.56.

$$x = k.\sqrt{t} \tag{2.56}$$

where

x	Depth of carbon dioxide penetration (mm)
k	Carbonation rate (mm/√year)
t	Time (year)

Many studies have been conducted on the comparison between natural and accelerated carbonation tests. To cite an example, Sanjuán et al. (2003) had done a comparative study between natural and accelerated (5% and 100% CO_2) conditions in one set of concretes. They concluded that the accelerated testing changes the ranking of the concrete with different binders (i.e., supplementary cementitious materials) and thus, comparisons need to be made only among the concretes with same type of binders. They further recommend that the carbonation velocity, which is derived from the square root law is a useful parameter to compare the concretes in any testing condition.

Castellotte et al. (2009) had done a study on the chemical changes and phase analysis of OPC pastes exposed to accelerated carbonation at different concentrations of CO_2. They studied three concentration levels of CO_2 – 3%, 10% and 100% and concluded that up to 3% of CO_2 concentration, the microstructure developed is similar to that under natural carbonation. At higher concentration levels, the microstructure changes, mainly because of the modifications in the CSH gel.

The merits and demerits of the accelerated carbonation test are discussed below.

Merits

- Mechanism is gaseous diffusion, which is similar to the natural phenomenon

Demerits

- Microstructural alterations at high CO_2 concentrations, especially in the case of SCM mixes
- Comparatively longer duration test

2.4.8 Water sorptivity test

The foundation stone for the sorptivity test was laid by Christopher Hall in his series of papers on sorptivity named water movements in porous building materials – I to V. (Hall, 1997, Gummerson et al., 1981, Hall, 1981, Hall et al., 1982). The sorptivity test is standardized in ASTM C1585 – 13 (2013) as a standard test method for the measurement of rate of absorption of water by hydraulic cement concretes. This test is also standardized by the durability index testing procedure manual of South Africa (2009). The sorptivity test measures the rate of movement of a water front through the concrete under capillary absorption or sorption. Sorption increases with square root of elapsed time. The fundamental equation of sorptivity has already been discussed in Section 2.3.3.

In the sorptivity test, dried concrete specimens having uniform cross section are allowed to absorb water uni-directionally. In order to ensure uni-directional water absorption, the side surfaces of the specimen are coated with epoxy. The specimens are kept on knife edge supports in such a way that the water level is around 2 mm above the base of the specimen. The mass of the specimen is measured at fixed intervals.

There are some differences in the procedure and calculations in the ASTM method and the South African method, which are discussed below. The method described in ASTM C1585 is as follows. The specimens are concrete discs of 100 ± 6 mm diameter and thickness 50 ± 3 mm. The specimens are vacuum saturated and the weight measurements are taken. Then, the specimens are kept in an environmental chamber at a temperature of 50 ± 2°C and RH of 80 ± 3% for three days, followed by storage in a container at 23 ± 2°C for at least 15 days. After this period, the specimens are placed on the sorptivity test tray. The test is done using tap water. The weight measurements are taken at the following time intervals within the tolerance limits as given in brackets

– 60 s (2 s), 5 min (10 s), 10 min (2 min), 20 min (2 min), 30 min (2 min), 60 min (2 min), every hour up to 6 hour (5 min), once a day up to 3 days (2 hours), days 4 to 7, three measurements 24 hour apart (2 hours) and days 7 to 9, one measurement (2 hours). While taking the weight measurement, the timing device is stopped if the contact time is less than 10 minutes.

The absorption is defined as

$$I = \frac{m_t}{ad} \tag{2.57}$$

where

I	Absorption (mm)
m_t	Change in specimen mass at time t (g)
a	Exposed area of the specimen (mm^2)
d	Density of the water (g/mm^3)

The initial rate of absorption (mm/√s) is defined as the slope of the line that is the best fit for absorption *I* plotted against square root of time. To obtain this, a linear regression analysis of the points from 1 minute to 6 hours is performed. The secondary rate of water absorption is defined as the slope of the line that is the best fit for *I* plotted against the square root of time using all the points from one day to seven days. In both cases, if the correlation coefficient is less than 0.98, the values cannot be determined.

The method described in durability index testing procedure manual of South Africa is as follows. The specimens are concrete discs of 70 ± 2 mm diameter and thickness 30 ± 2 mm. The specimens need to be dried in an oven at 50 ± 2°C for 7 days ± 4 hr. After sealing the curved surface, the specimens are cooled in a desiccator to 23 ± 2°C for not less than 2 hours and not more than 4 hours. Following this, the specimens are placed in the sorptivity test tray. The test is done with saturated $Ca(OH)_2$ solution. The weight measurements are taken at 3, 5, 7, 9, 12, 16, 20 and 25 minutes. The stop watch is not stopped during the weighing process. Within one day, the specimens are vacuum saturated to find the absorption capacity. A graph between the mass gain and the square root of time is plotted and the slope F of the best fit line is obtained, without including the zero time reading. The water sorptivity of the specimen is calculated using Equation 2.58 as given below.

$$S = \frac{Fd}{M_{sv} - M_{s0}} \tag{2.58}$$

where

S	Water sorptivity of the specimen (mm/ √hr)
F	Slope of the best fit line (g/ √hr)
d	Average specimen thickness (mm)
M_{sv}	Vacuum saturated mass of specimen (g)
M_{s0}	Mass of the specimen at the initial time t_0 (g)

Sorptivity index is defined as the average of the water sorptivity of at least three valid individual test values. According to Alexander et al. (2008), the water sorptivity values range between 5 mm/√hr (usually for well cured grade 30 – 50 concretes) and 15 to 20 mm/√hr (for poorly cured grade 20 concretes).

The line diagram of the sorptivity test is shown in Figure 2.24.

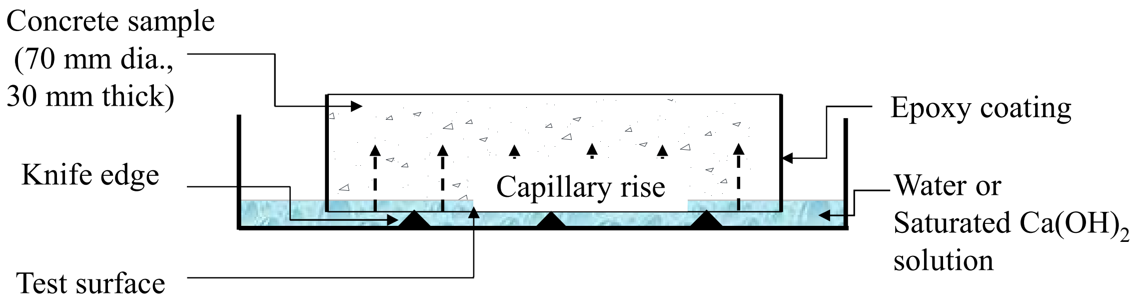

Figure 2.24 Line diagram of sorptivity test set up

Merits

- Simulates natural phenomena

- Can be performed on drilled cores
- Sensitive to the micro-structural properties of the near-surface zone of concrete

Demerits

- Sensitive to macro-voids and cracks
- Destructive

The concrete quality classification criteria developed by Alexander et al., (1999) is presented in Table 2.11.

Table 2.11 Concrete quality classification based on water sorptivity index (Alexander et al.,1999)

Sorptivity (mm/√hr)	Concrete quality
< 6	Very good
6 - 10	Good
10 - 15	Poor
> 15	Very poor

According to Alexander et al. (2008), sorptivity measurements are important in assessing the near surface quality of concrete. Although sorptivity cannot be directly related to a particular deterioration mechanism, it can be considered as a site control factor. The sorptivity values depend mainly on construction factors such as curing and are least dependent on material composition. Thus, sorptivity acts as a factor that points toward a check on the construction quality.

Hall and Kam-Ming Tse (1986) had mentioned that sorptivity is an accurate quantity which can be measured very rapidly. Leaner mixes showed higher sorptivity values. Rabehi et al. (2013) did a study on the porosity of cover zone concrete by capillary absorption test and concluded that open porosity increases with increase in w/c.

du Preez and Alexander (2004) did a study to validate the durability index tests in different site situations. They studied three blended binders and five site curing methodologies. The water sorptivity results obtained from the core samples are presented in Figure 2.25. The results indicate that there exist considerable differences between the sorptivity values of wet-cured and site-cured samples. The difference was more evident at 28 days. At 120 days, there difference in the results was little. Wet curing is proved to be the most efficient curing methodology. The improved sorptivity values at 120 days compared to those at 28 days prove the beneficial effects of continued curing.

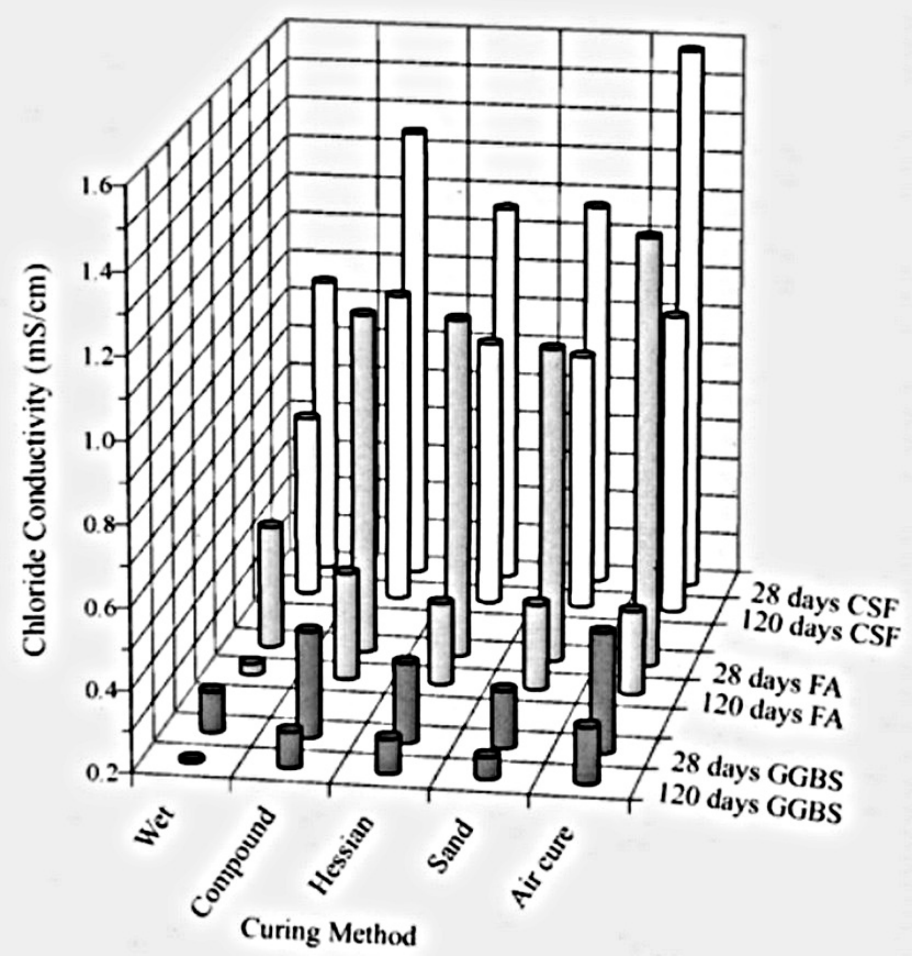

Figure 2.25 Mean water sorptivity results for slabs at 28 and 120 days (du Preez and Alexander, 2004)

2.4.9 Water permeability test

Water permeability tests measure the permeability of concrete against water ingress. This test is standardized by the German Standard DIN 1048 in which the depth of water penetration is considered as the durability parameter. Moreover, this test is being specified in most of the metro rail projects in India (Dhanya and Santhanam, 2013).

According to DIN 1048 Part 5, the concrete specimen is exposed to a constant water pressure of 0.5 N/mm^2 for a period of three days. The pressure is applied perpendicular to the mould filling direction, either from above or below the specimen. The test is done when the age of concrete is between 28 and 35 days. After three days, the pressure is released, the specimen is split into two halves and the maximum depth of water penetration is measured. If the water penetrates through the entire depth of the specimen, the test may be terminated and the specimen is rejected as the test had failed. The typical results reported by the Concrete Society, 1998 (as cited by Basheer, 2001) are as given in Table 2.12.

Table 2.12 Typical depth of water penetration results for different concretes (Concrete Society, 1998)

Concrete type	Depth of water penetration (mm)
Dense concrete with slag and superplasticizer	5
Concrete to be used in aggressive environment	< 30
Concrete to be used in water retaining structures	< 50

Figure 2.26 shows the line diagram of the water permeability test set up based on DIN 1048 Part 5.

Merits

- Depth of water penetration is measured

Demerits

- Destructive
- Air compressor is needed to keep the pressure constant

Hedegarrd and Hansen (1992) did a study on the water permeability of two series of concretes with two types of OPC and one type of fly ash by using the DIN 1048 method. They concluded that the addition of fly ash was not contributing to the improvement of water tightness of concrete as 1 kg of cement needs to be replaced by 3 kg of fly ash in order to get the same water tightness irrespective of the type of cement and curing time.

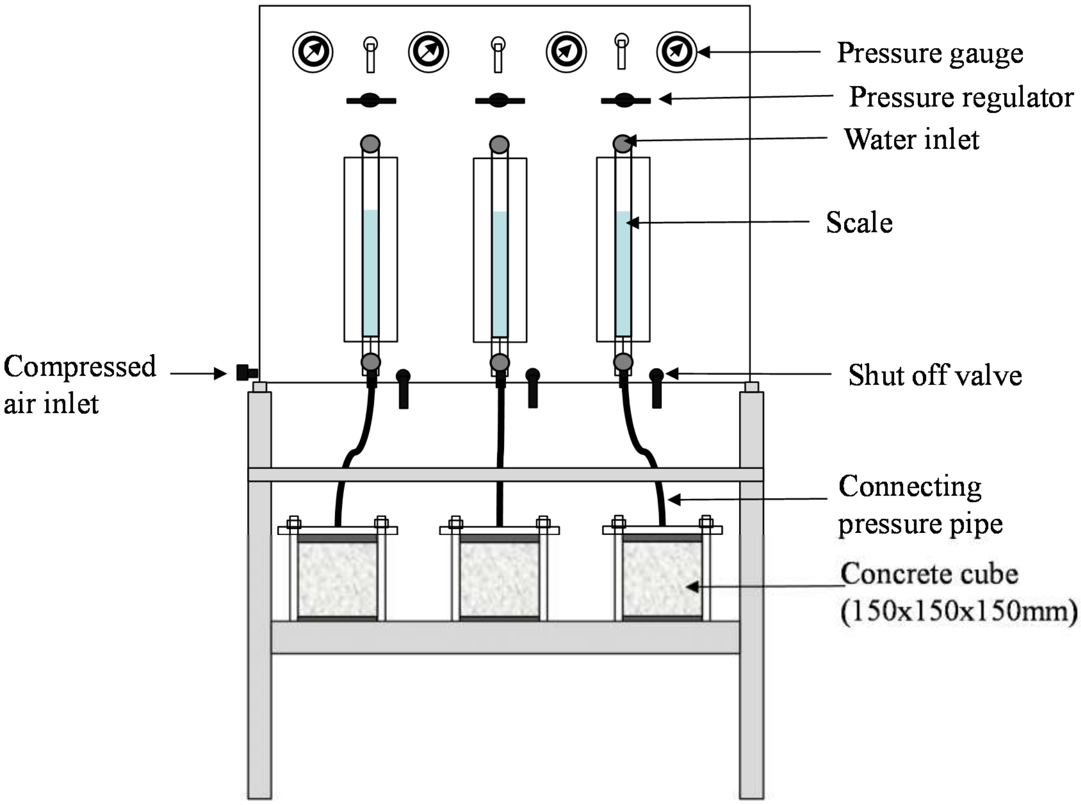

Figure 2.26 Line diagram of water permeability test set up

2.4.10 Interim summary

Section 2.4 dealt with the review of the durability test methods which have been selected to use in this work. The details of the test methods such as the theoretical back ground, line diagram, classification criteria and the merits and demerits of each test methods have discussed in detail.

2.5 SUPPLEMENTARY CEMENTITIOUS MATERIALS IN CONCRETE

There are mainly three factors deciding the durability of a concrete structure in a particular environment. These are the aggressiveness of the environment, the materials used for construction and the construction practices. Regarding the materials used for construction, it is the binder type that mainly affects the durability characteristics much more than the other materials.

According to CSA A 3001, 2003, a supplementary cementitious material (SCM) or mineral admixture may be defined as a material that, when used in conjunction with Portland cement, contributes to the properties of the hardened concrete through hydraulic or pozzolanic activity or both (Thomas, 2013). Examples of SCMs that are used to make concrete are fly ash, ground granulated blast furnace slag or slag, silica fume, volcanic ashes, calcined clay, diatomaceous earth etc.

Hydraulic activity can be explained as the property of the material by which it can react with water directly to form hydration products that have cementitious properties. Even though such materials do not need the presence of Portland cement for hardening and strength gain, these reactions get accelerated in the presence of cement. Ground granulated blast furnace slag falls in this category.

A pozzolan is defined as a siliceous or siliceous and aluminous material that in itself possess little or no cementitious value, but that will in finely divided form and in the presence of moisture, chemically react with calcium hydroxide (a hydration product of Portland cement) at ordinary temperatures to form compounds having cementitious properties (Thomas, 2013). Low calcium fly ash, silica fume, calcined clay, volcanic ash etc. belong to this group.

Some materials possess both hydraulic as well as pozzolanic activity. High calcium fly ash is an example of the same. Generally, the hydraulicity of an SCM increases with calcium content.

Figure 2.27 shows the ternary diagram depicting the chemical composition of some of the commonly used SCMs such as silica fume, Class C fly ash, Class F fly ash, slag, metakaolin along with Portland cement.

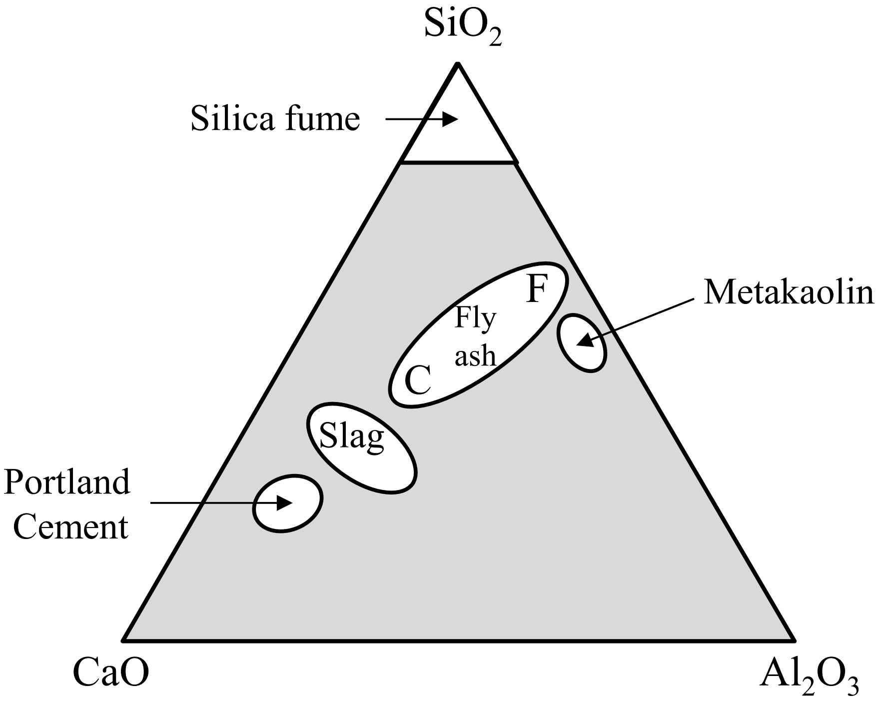

Figure 2.27 Chemical composition of some commonly used SCMs

The hydration reactions of alite (C_3S) and belite (C_2S) in the cement produce calcium silicate hydrate (CSH) and calcium hydroxide (CH). The hydration reactions are as follows (Thomas, 2013).

$$2C_3S + 11H \rightarrow C_3S_2H_8 + 3CH \tag{2.59}$$

$$2C_2S + 9H \rightarrow C_3S_2H_8 + CH \tag{2.60}$$

The actual calcium to silicon atomic ratio (C/S ratio) varies from 1.5 to 2 or more. In addition to CSH and CH, hydration of C_3A and C_4AF yield alumino ferrite phases such as AF_m and AF_t.

The pozzolanic reaction can be represented as follows.

$$xCH + yS + zH \rightarrow C_xS_yH_z \tag{2.61}$$

The C/S i.e., x/y in Equation 2.61, of the CSH formed out of the pozzolanic reaction is lower than the same for the CSH formed out of the hydration reaction. The alumina phases present in the pozzolan and cement react with CH to form many phases, the major ones being stratlingite (C_2ASH_8), hydrogarnet (C_3AH_6), calcium aluminate hydrate (C_4AH_{13}), ettringite ($C_3A.3C\bar{S}.H_{32}$), calcium monosulphoaluminate ($C_3A.C\bar{S}.H_{12}$), and calcium carboaluminate ($C_3A.C\bar{C}.H_{12}$).

In addition to pozzolanic effect, the SCMs also have filler effect. While fillers do not react by themselves, they provide additional nucleation sites on their surface for the hydrates from the cement and promote the hydration of cement by increasing the effective water to cement ratio (Deschner et al., 2012). Further, the particle packing improves when different-sized materials are used.

2.5.1 Influence of SCMs on hydrated cement phases

Supplementary cementitious materials mainly influence three different phases of the hydrated cement paste - the solid phase, the pore structure and the pore solution composition (Andrade et al., 2013, Lothenbach et al., 2011).

2.5.1.1 Solid phase

The changes in solid phase in systems containing SCMs happen primarily due to the pozzolanic and hydration reaction of the SCMs. The factors affecting these reactions are nature and content of the reactive phases in the pozzolan, content of amorphous silica, CH/Pozzolan of the mix and duration of curing (Andrade and Bujak, 2013, Thomas, 2013).

Further, SCMs influence the hydration rate of Portland cement. Most of the SCMs do not change the length of the dormant period. However, they accelerate the early age hydration of C_3S. These changes are due to the increase in the water to C_3S ratio and due to the presence of additional nucleation sites owing to the presence of pozzolans which act as fillers (Gutteridge and Dalziel, 1990). Additionally, there is an improvement in the particle packing due to the spread in particle size distribution. In fly ash, this effect is more due to the spherical particle shape (Deschner et al., 2012).

Figure 2.28 and Figure 2.29 shows the content of bound water and portlandite, determined by TGA and normalised to the OPC content in four different samples. The samples of interest in this context are OPC (Plain OPC), OPC-F1 (OPC + 50% fly ash 1) and OPC-F2 (OPC + 50% fly ash 2). The bound water content in OPC–F1 and OPC-F2 was higher after 7 days. The portlandite contents in both OPC-F1 and OPC-F2 are maximum at seven days and after that they start to decrease for mixes with fly ash. This is due to the pozzolanic reaction which leads to the consumption of portlandite (Deschner et al., 2012). The conclusions from the study by Marsh and Day (1988) also indicate that the CH content decreases as the replacement with fly ash increases with respect to OPC.

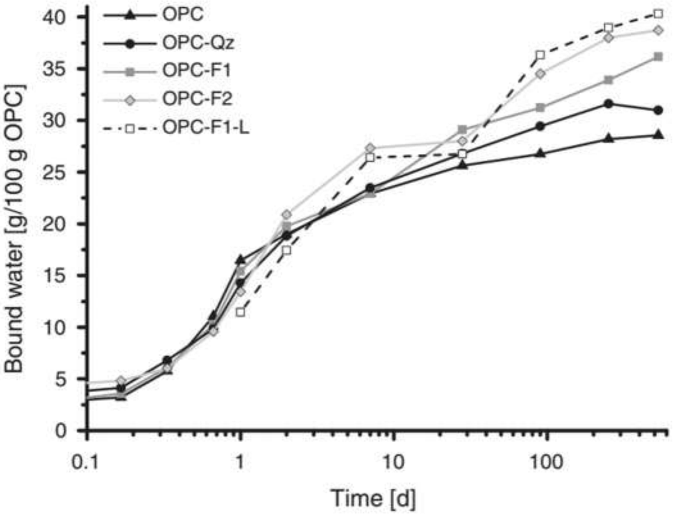

Figure 2.28 Bound water content in different binders normalized to OPC content as determined by TGA (Deschner et al., 2012)

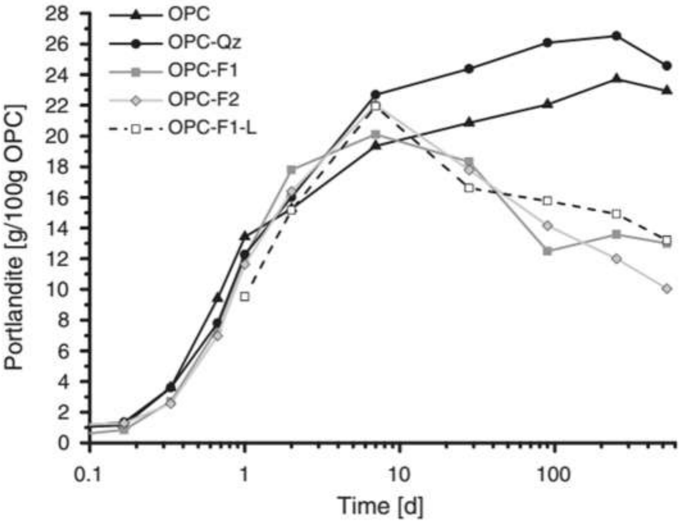

Figure 2.29 Portlandite content in different binders normalized to OPC content as determined by TGA (Deschner et al., 2012)

Figure 2.30 shows the X-ray diffractograms of the samples from the same study (as in the previous case the focus of discussion is on OPC, OPC-F1 and OPC – F2) from 2 days to 90 days. Ettringite, monosulphate (C_4AsH_{12}) and AF_m phases (solid solution of hemicarbonate and highly OH^- substituted monosulphate) are identified as the main crystalline phases formed.

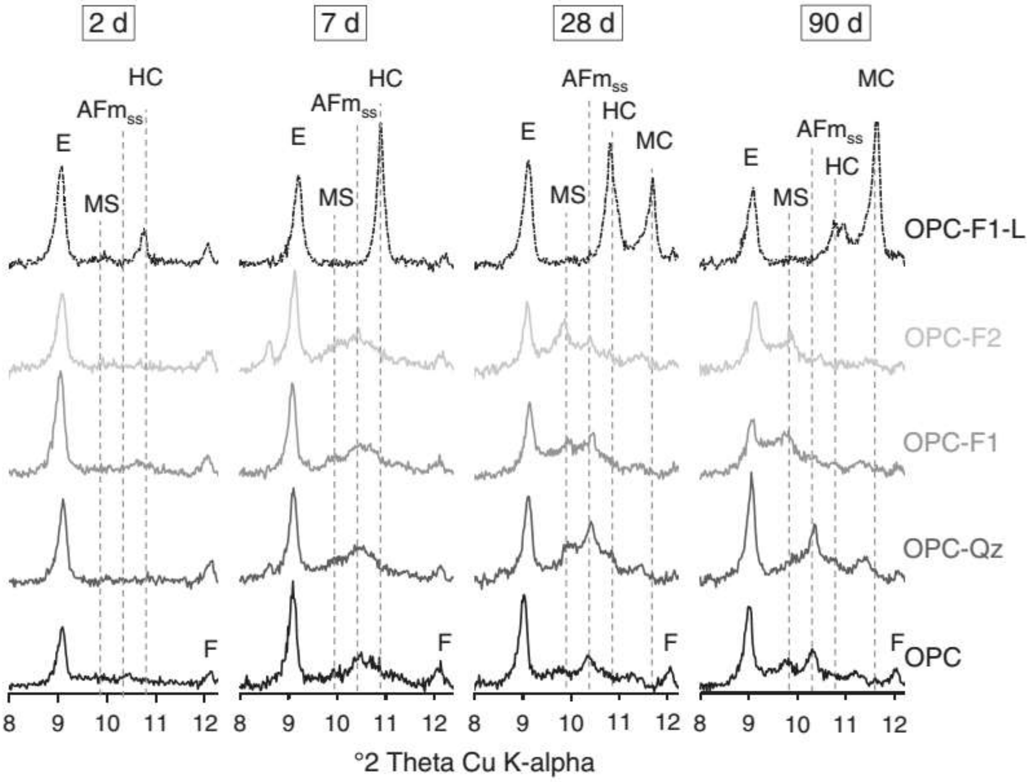

Figure 2.30 X – ray diffractograms of the hydration products of different binders (Deschner et al., 2012)

As mentioned earlier in this section, the C/S of the CSH formed out of the pozzolanic reaction is lower than the same for the CSH formed out of the hydration reaction. Further, the solid phase is a combination of different phases. For example, in the case of SCMs which contain alumina, the CSH contain substantial amount of aluminates (Lothenbach et al. 2011). Deschner et al. (2012) found through the SEM-EDS analysis that the Ca/Si and Al/Si of OPC were 1.8 ± 0.2 and 0.07 ± 0.02 whereas in the case of mixes having 50% fly ash replacement, these ratios were 1.3 ± 0.2 and 0.17 ± 0.03 respectively. The decrease in Ca/Si in fly ash mixes is due to the presence of additional

Si which got released from fly ash. This can lead to longer length of silicate chain. This step leads to the increased uptake of Al, which bridges the silicate tetrahedron.

2.5.1.2 Pore structure

The rate of hydration of the paste containing pozzolans is slower than for cement initially leading to higher porosity. However, due to the pozzolanic reaction, at later ages, the pore structure gets refined. This is primarily due to the reduction in the volume and size of the capillary pores, and less connected and more tortuous pore system. This characteristic delays the penetration of aggressive agents into the concrete system and thus gives more durability to concrete. Further, the presence of SCMs lead to densification of the interfacial transition zone (ITZ) by improving the particle packing and conversion of CH present at the ITZ to CSH (Thomas, 2013).

MIP and SEM studies on mixes with 50% and 60% slag replacements were carried out by Bouikni et al. (2009). The results indicated that slag mixes possessed more refined pore structure and denser micro-structure than plain OPC mixes. Moreover, the refined pore structure of SCM mixes help in reducing permeability and ion diffusivity (Thomas et al., 2012).

2.5.1.3 Pore solution chemistry

In general, SCMs reduce the alkalinity of the pore solution. This is because the products resulting from the pozzolanic reaction have increased alkali binding capacity. According to Thomas (2011), alkalinity depends on the composition (amount of reactive silica, calcium and alkali), amount and surface area of SCM used and the maturity of the paste. Portlandite is the alkaline reservoir of the cement paste and provides buffering capacity against lowering the pH which is the initiator of corrosion. The consumption of portlandite due to pozzolanic reaction is detrimental in case of corrosion, whereas it is favourable in the case of external acid attack and alkali aggregate reaction (Andrade, 2013). The development of elemental composition in the pore solution of OPC and OPC-fly ash blend systems are presented in Figure 2.31 and Figure 2.32 respectively.

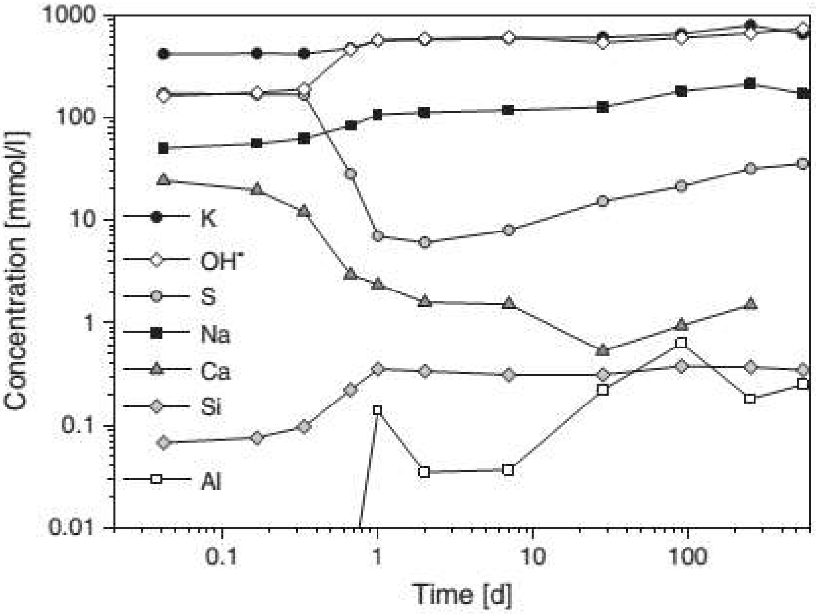

Figure 2.31 Development of elemental concentration in the pore solution of OPC (Deschner et al., 2012)

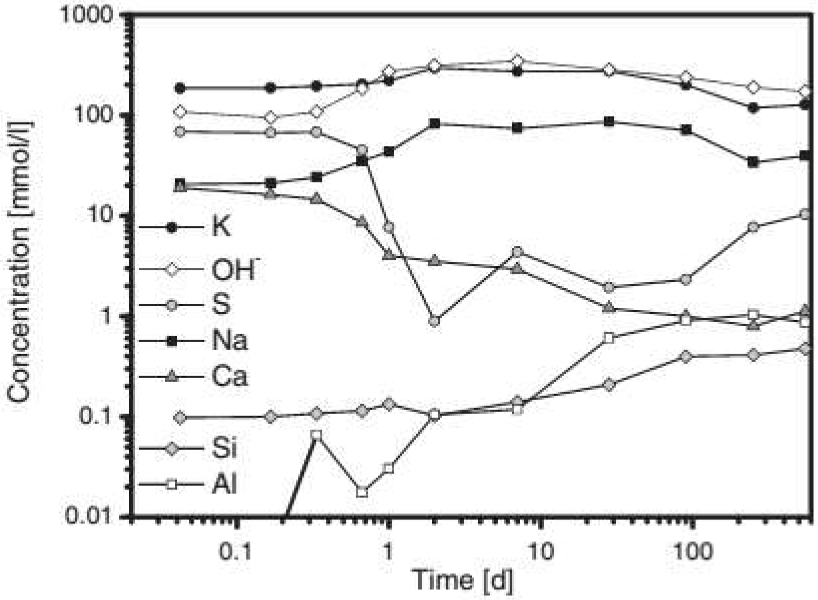

Figure 2.32 Development of elemental concentration in the pore solution of OPC - fly ash blend (Deschner et al., 2012)

From Figure 2.31 and Figure 2.32, it can be seen that there is a decrease in the Ca ion concentration in the pore solution of the fly ash mix, due to pozzolanic reaction. Further, there is a decrease in the alkali and OH^- ion concentration due to the binding of alkalis in the CSH, which is more in the fly ash mix due to the presence of additional CSH (Deschner et al., 2012).

2.5.2 Influence of SCMs on fresh and hardened properties of concrete

Table 2.13 indicates the effect of SCMs on the fresh and hardened properties of concrete (Thomas, 2013). The table mainly concentrate on two types of SCMs, slag and fly ash as these are the materials of interest in this thesis work.

Table 2.13 Effect of SCMs on the fresh and hardened properties of concrete (Thomas, 2013)

Properties	**Effect of SCM**
Fresh properties	
Workability, Consistency, Water demand	Fly ash with high fineness and low carbon content improve workability , lower water demand *Possible reasons:* Ball bearing effect, Increased paste volume, Adsorption-dispersion, Increased particle packing effect
	Slag reduces water demand and workability compared to OPC, the effect is below fly ash *Possible reasons:* Irregular particle shape, Reduced adsorption-dispersion effect
Cohesiveness	Improve cohesiveness and reduce segregation, increase pumpability
Bleeding	Finer material decrease bleeding whereas coarser material increase bleeding
Air entrainment	Low Ca fly ash concrete require more air entraining admixture due to the presence of unburnt carbon
	High Ca fly ash and slag require comparatively less increase in dosage compared to OPC
Setting time	Higher dosages of fly ash and slag increase initial and final setting time
Mechanical Properties	
Compressive strength	Fly ash and slag can reduce the early age strength whereas the later age strength gets improved.
Modulus of Elasticity	Fly ash and slag when used in moderate to high levels reduce modulus of elasticity at early ages and increase at later ages

2.5.3 Influence of SCMs on the durability properties of concrete

In general, SCMs improve the durability properties of concrete (Swamy, 2008, Gonen and Yazicioglu, 2007). Reasons for the same are attributed to the refined pore structure due to prolonged hydration and pozzolanic reaction, reduction in the alkali content, better resistance to temperature rise etc. (Swamy, 2003). In this section, the effect of SCMs on the durability properties other than chloride ingress and carbonation are discussed.

Thomas (2013) has reported that in the absence of de-icing salts, properly proportioned concretes having SCMs are expected to be durable when exposed to freeze and thaw cycles in a saturated condition. However, the performance of the same is not clear in the presence of de-icing salts. For resisting the alkali silica reaction, SCMs are found to be very effective as they reduce the alkali concentration in the pore solution. Ternary blends of silica fume and either slag or fly ash are found to be very promising in this aspect. In the case of sulphate resistance, the effectiveness of a particular SCM depends on many factors such as its composition, the level of C_3A in the cement used, the replacement level etc. Silica fume is found to be highly resistant to sulphate attack whereas high calcium fly ash is reported to be the least. Bijen (1996) has reported that slag is a good option to resist sulphate attack from soils. Concretes with fly ash or slag are more resistant to weak acid attack. Gopalan (1996) had done a study of the sorptivity of concrete with and without fly ash and found that the sorptivity of fly ash concrete is lower than that of cement concrete when the curing was proper. Gonen and Yazicioglu (2007) in their study concluded that ternary blends of silica fume and fly ash improved the strength and durability characteristics of concrete such as carbonation, capillary absorption, wetting–drying etc. When fly ash alone was used the capillary absorption got increased.

2.5.4 Influence of SCMs on chloride induced corrosion

On the whole, SCMs are beneficial against chloride induced corrosion (Shi et al. 2012, Andrade and Bujak, 2013, Thomas et al. 2012, Papadakis, 2000). Both field and lab studies by Thomas and Bamforth (1999) established that fly ash and slag are very effective in improving the long term behaviour of concrete. Figure 2.33 shows a typical field data on the chloride profile obtained from a sea wall. It can be seen that there exist considerable differences between the concrete with plain OPC and those having a replacement with fly ash.

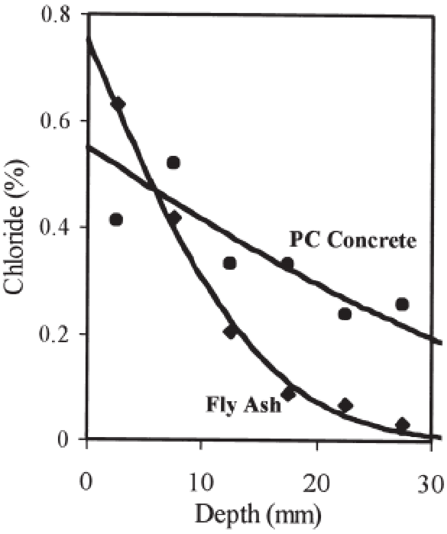

Figure 2.33 Chloride profile from a sea wall (Thomas and Bamforth, 1999)

The study by Papadakis et al. (2000), concluded that when SCMs are incorporated in concrete as a substitution either to cement or to aggregate, the total chloride content in all depths got reduced except a thin layer near the external surface. Alonso and Andrade (2013) studied the influence of fly ash in the corrosion process and concluded that both initiation time and propagation rate were reduced due to fly ash addition. Further, concretes with fly ash yielded lower diffusion coefficient and pit depths.

The primary reasons for the enhancement in performance of SCM concretes are (1) improvement of pore structure (pore volume, pore size, pore tortuosity), (2) improvement of pore solution chemistry, (3) increase in chloride binding, and (4) raising of critical chloride content (Shi et al., 2012, Andrade and Bujak, 2013, Thomas et al. 2012, Angust, 2009).

Out of the four reasons mentioned above, the effect of pore structure and pore solution chemistry has already been discussed in sections 2.5.1.2 and 2.5.1.3. The composition of the pore solution and thus its conductivity is a deciding factor when the chloride penetrability is measured by migration tests (Marriaga, 2009). The last two are specific to chloride attack in concrete and are discussed in detail in the following sections.

2.5.4.1 Chloride binding

As per ASTM C1556 (2003), chloride binding is the chemical process by which chloride ion is removed from solution and incorporated into cementitious binder hydration products. In general, chloride can be present mainly in three forms in concrete - as free chlorides in the pore solution, in physically bound form (on the surface of the hydrated products), and in chemically bound form (i.e., reacted with the hydrated products) (Yuan et al., 2009, Angst, 2009 and Andrade and Bujak, 2013). The free chlorides available in the pore solution are detrimental as they are responsible for rebar corrosion (Alonso and Andrade, 2013). Free chlorides are determined by water soluble method as per ASTM C1218 (1999) whereas the total chloride content is by acid-soluble method as per ASTM C1152 (2013) (Cheewaket, 2010).

Chloride binding leads to a reduction in the amount of free chloride availability in the pore solution. This can reduce the chance of corrosion as the free chloride availability in the vicinity of the rebar is reduced. Moreover, this can retard the penetration of chlorides into concrete as the diffusion flux gets altered. Further, due to the deposition of the reaction products, the pore structure gets modified, which also can retard the chloride ion transport (Yuan et al., 2009). In chemical binding, chlorides react with aluminate phases in cement, primarily with C_3A and form Friedel's salt ($3CaO.Al_2O_3.CaCl_2.10H_2O$). Other products formed are Kuzel's salt ($3CaO.Al_2O_3.\frac{1}{2}CaCl_2.\frac{1}{2}CaSO_4.10H_2O$), and oxy-chlorides (having a general formula $xCa(OH)_2.yCaCl_2.zH_2O$, with x:y:z varying from 1:1:1 to 3:1:12). Not only C_3A, but C_4AF also leads to the formation of the ferrite analogue to Friedel's salt ($C_3F.CaCl_2.10H_2O$) (Suryavanshi et al., 1996). Friedel's salt can be converted to Kuzel salt in situations where the paste is exposed to high chloride concentrations initially followed by exposure to chloride-free solution (Thomas et al., 2012). The morphology of Friedel's salt is hexagonal having a size between 2 and 3 µm, and the maximum intensity peak in XRD is at a d – spacing of 8.0 Å. The secondary mode image depicting the morphology of Friedel's salt is presented in Figure 2.34 in which the Friedel's salt is marked as '1'. Further, Friedel's salts yield an endothermic peak at around 360 °C in DTA (Luo et al., 2003).

Figure 2.34 Morphology of Friedel's salt (Luo et al., 2003)

A typical DTA thermograph of Friedel’s salt along with that of $Ca(OH)_2$ is presented in Figure 2.35.

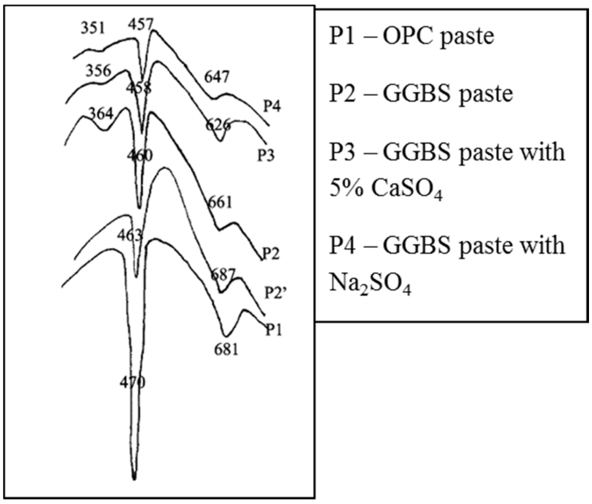

Figure 2.35 DTA thermograph of Friedel's salt and $Ca(OH)_2$ (Luo et al., 2003)

The appearance of Friedel’s salt in a SEM-BSE image is shown in Figure 2.36. The relative heights of the chloride, aluminum, and calcium peaks in its EDS spectrum confirms the presence of phase-pure Friedel's salt (Brown and Badger, 2000).

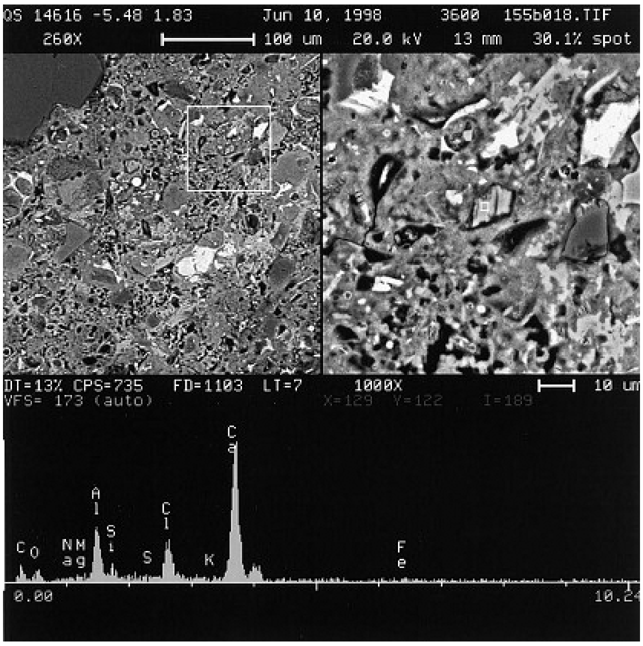

Figure 2.36 SEM BSE image with EDS of Friedel’s salt (Brown and Badger, 2000)

In a review on chloride binding of cement based materials, Yuan et al. (2009) identified the factors affecting chloride binding. These factors were reported as chloride concentration, cement composition, hydroxyl concentration, cation of chloride salt, temperature, supplementary cementitious materials, carbonation, sulphate ions, and presence of electrical field.

According to Tang and Nilsson (1993), the chloride binding capacity of concrete depends mainly on the CSH. As concretes with SCMs have more CSH gel, they have more surface area which can enhance physical absorption of Cl^- ions. Further, high alumina content in slag and fly ash lead to higher binding capacity of concretes (Dhir et al., 1996, 1997, Thomas et al., 2012). Thus, the chance of Friedel’s salt formation is more in the presence of SCMs. Chemical binding is decided mainly by the contents of C_3A and C_4AF whereas the contents of C_3S and C_2S decide physical binding (Yuan et al. 2009). According to Beaudoin et al. (1990), the binding of chloride in CSH is dependent on the C/S ratio. Lower the C/S, lesser will be the binding. Moreover, the pH of the pore solution can influence the Cl^-/OH^- and thus the binding ability of concrete (Alonso et al., 2002).

The relationships between free and bound chloride ions over a range of chloride concentrations at a given temperature are known as chloride binding isotherms. Mainly there are four kinds of binding isotherms. They are linear, Langmuir, Freundlich and BET binding isotherms. Figure 2.37 shows the relationship between the bound chloride (C_b) and free chloride (C_f) for OPC paste with w/c of 0.50. As evident from the figure, the best fit is by the Freundlich isotherm (Thomas et al., 2012). Yuan et al. (2009) also described that Freundlich isotherm is the most appropriate one to depict the relationship between bound and free chlorides. According to Thomas et al. (2012), a good knowledge about the chloride binding isotherms is needed for better prediction of service life.

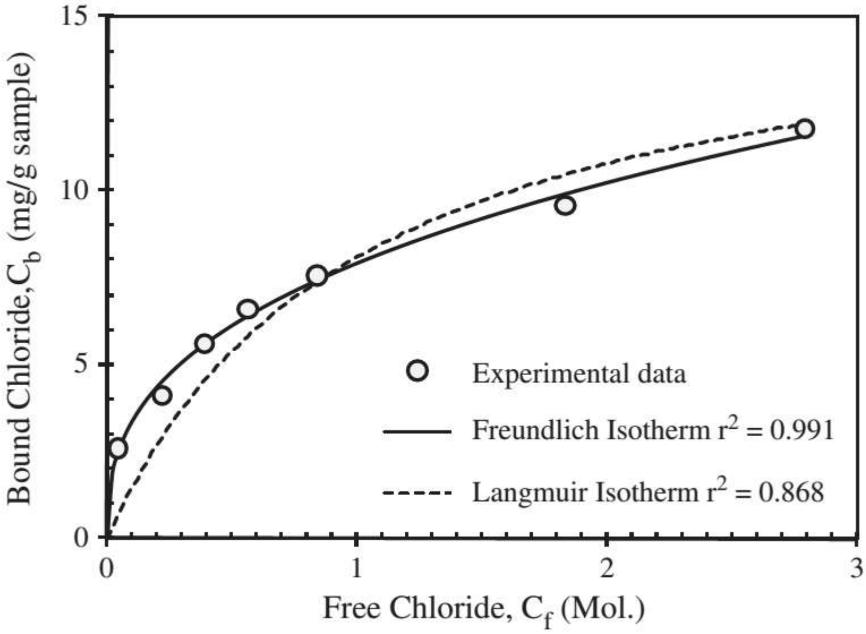

Figure 2.37 Relationship between the bound chloride (C_b) and free chloride (C_f) for OPC paste with w/c 0.50 (Thomas et al., 2012)

The X-ray diffraction patterns for paste samples made with different binders with a w/b of 0.5, immersed in 3M NaCl solution are shown in Figure 2.38. As evident, all the binders showed the presence of Friedel's salt (Thomas et al., 2012). Furthermore, Thomas et al. (2012) observed that when the free chloride content of the pore solution decreased due to leaching or some other phenomenon, a small portion of the bound chloride was released.

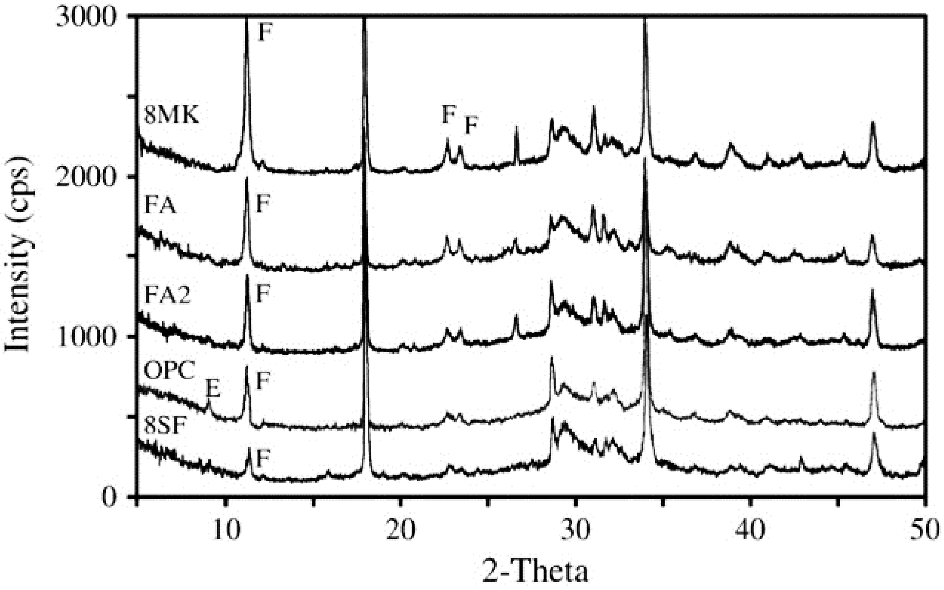

Figure 2.38 X-Ray diffraction pattern of pastes with different binders immersed in 3M NaCl solution (Thomas et al., 2012)

Fraj et al. (2012) studied the binding capacity of OPC and slag concretes and found that slag mixes bind more chlorides, which is evident from Figure 2.39. The reasons suggested by the authors include the high alumina content in slag and dilution effect of sulphate ions. Further, the porosity of the concrete reduces and improves the mechanical and transfer properties of concrete. Fineness of slag also determines to a great extent the chloride resistance of concrete.

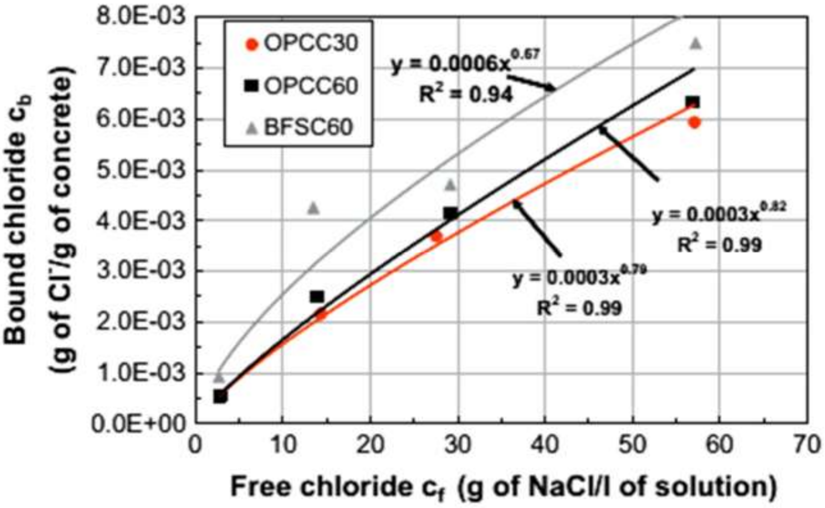

Figure 2.39 Chloride binding isotherms of OPC and slag concretes (Fraj et al., 2012)

2.5.4.2 Critical chloride content

Critical chloride content or chloride threshold value can be defined as the chloride content required for depassivation of steel (Angst, 2009). There exists a difference in opinion on the effect of SCMs on critical chloride content (Angust, 2009, Andrade and Bujak, 2013). For example, Thomas (1996) and Oh et al. (2003) found that the chloride threshold was lower with addition of fly ash whereas Schiessel and Breit (2005) got the reverse result. The investigation by Alonso et al. (2002) could not make out any difference in critical chloride content due to the presence of fly ash. According to Alonso et al. (2002), the type of binder can influence the chloride threshold value owing to the change in C_3A content and pH of the pore solution, as these two are the major factors influencing the chemical binding. Andrade and Bujak (2013) concluded that the chloride threshold level depends on the electrical potential of the reinforcement which is strongly dependent on the moisture level and temperature.

2.5.5 Influence of SCMs on carbonation induced corrosion

In general, there exists a difference in opinion among the researchers on the effect of SCMs on carbonation. Most of the literature indicate that SCM mixes are subjected to higher carbonation than OPC mixes. Osborne (1999) concluded that mixes with 70 and 80% slag were carbonated more than OPC mixes whereas the carbonation resistance of 50% slag mixes was similar to OPC mixes. Bouikni et al. (2009) studied the carbonation behaviour of concretes with 50% and 65% slag replacement and found that the CO_2 penetration was higher for 65% replacement mixes.

Thomas (2000) observed that the carbonation of concretes having fly ash up to 30% was marginally higher than OPC, whereas the difference was much higher when the replacement level was 50%. He had suggested that increasing the strength grade for fly ash mixes or extending the moist curing duration can compensate this difference. According to Sulapha et al. (2003), the higher the replacement with mineral admixtures having lower fineness, the greater is the carbonation front. When mineral admixtures with higher fineness are used, the carbonation rate reduce. They concluded that this is because when the fineness increases, the effect of pore refinement is more prominent than the reduction of $Ca(OH)_2$. Further, increase in curing duration and compressive strength lead to better carbonation resistance of mixes with and without mineral admixtures. Papadakis (2000) reported that carbonation depth decreases as aggregates are replaced by SCMs whereas carbonation depth increases when cement is replaced by SCMs. Atis (2003) found that the carbonation of 70% fly ash concrete was higher than that of 50% fly ash concrete. The carbonation of 50% fly ash concrete was reported to be lesser than the control OPC mix. However, 50% fly ash mixes had a w/b of 0.33 whereas the control concrete had a w/b of 0.55. This might be the reason for the improved performance of fly ash mixes.

Thomas (2013) has reported that concretes with and without fly ash having the same 28 day strengths performed similarly. Further, the increase in CO_2 concentration used in studies accelerates the rate of carbonation, which may overestimate the extent to which SCMs increase the rate of carbonation. Sanjuan et al. (2002) did a comparison between natural and accelerated carbonation and concluded that there is considerable difference between changes happening in concrete in both these conditions, especially when SCMs are present. Malhotra et al. (2000) tested the depth of carbonation of high performance concrete incorporating various SCMs subjected to outdoor exposure for ten years. They have reported that the depths of carbonation in all the concretes were of negligible magnitude.

Mc Polin et al. (2007) did a study on the carbonation behaviour of concrete containing different SCMs through an assessment of the pH profiles and got the relative performance of different binders against carbonation as OPC > micro silica > metakaolin > slag > fly ash. They also suggested that gas permeability test alone should not be used to find carbonation resistance of concretes as it does not take into account the diffusion of CO_2 and / or dissolved CO_2 in the pore solution. However, Mackechnie and Alexander (2002) and Andrade et al. (2000), found that there exists good correlation between gas permeability tests (OPI test and Torrent air permeability test) with accelerated and natural carbonation tests respectively. They suggested gas permeability tests as a good indicator of carbonation and service life models are also developed based on these parameters (Salvoldi, 2010).

To summarize, most of the available studies agree that the carbonation is higher in mixes having SCMs. At lower replacement levels, the difference is not much whereas as the replacement level increases the difference is much higher. The following passage explores the reasons suggested by various researchers for this behaviour.

According to Schubert (1987), the actions of SCMs in concrete are of two kinds. First, carbonation reaction leads to the consumption of $Ca(OH)_2$ which can reduce the pH of concrete, leading to increased rate of carbonation. Second, due to pozzolanic and / or hydraulic reaction, new CSH is formed which reduces capillary porosity and decreases carbonation (Torgal, 2012). Sulapha et al. (2003) also had drawn a similar conclusion from their study. Andrade and Bujak (2013) concluded that the initial reaction between CO_2 and $Ca(OH)_2$ lowers the pH of the pore solution. In order to maintain pH, portlandite dissolves first until it is fully consumed. The decalcification of CSH and other Ca bearing phases happens next. The chemical reactions lead to a drop in pH at the steel/ concrete interface, resulting in the dissociation of passive layer and initiation of corrosion. According to Jia et al. (2012), when SCMs are present, a reduction in $Ca(OH)_2$ level happens due to pozzolanic reaction, which accelerates CSH carbonation. As the addition level of SCMs increases, more CSH with low Ca/Si is formed, which accelerates the carbonation reaction as explained by Castellotte et al. (2009). Further, there is an effect of micro-cracking caused due to the deposition of $CaCO_3$ in the pore system. This was reported by Bertos (2004) also, who suggested that the micro-cracking might be due to volume expansion or due to thermal stresses developed during the carbonation reaction. Lo and Lee (2002) put forward another argument on the increased carbonation with increased SCM dosage. According to them, as the SCM replacement level increases, there is an increase in the w/c, which can increase the capillary porosity, which in turn increases the carbonation rate. However, this would imply a lack of any contribution from the SCMs.

There were many studies done comparing the natural and accelerated carbonation tests. (Sanjuan et al., 2002, 2003, Castellote et al., 2009). Sanjuan et al. (2003) found that accelerated carbonation tests change the ranking of carbonation resistance of concretes, especially for those having different SCMs. Further, there are changes in the microstructure due to high concentration of CO_2, which can be even higher when SCMs are present. Castellote et al. (2009) did a study on the chemical changes and phase analysis of OPC cement paste due to accelerated carbonation and concluded that up to 3 % of CO_2, there is not much change in the microstructure. The results of NMR spectroscopy and XRD are as shown in Figure 2.40 and Figure 2.41 respectively.

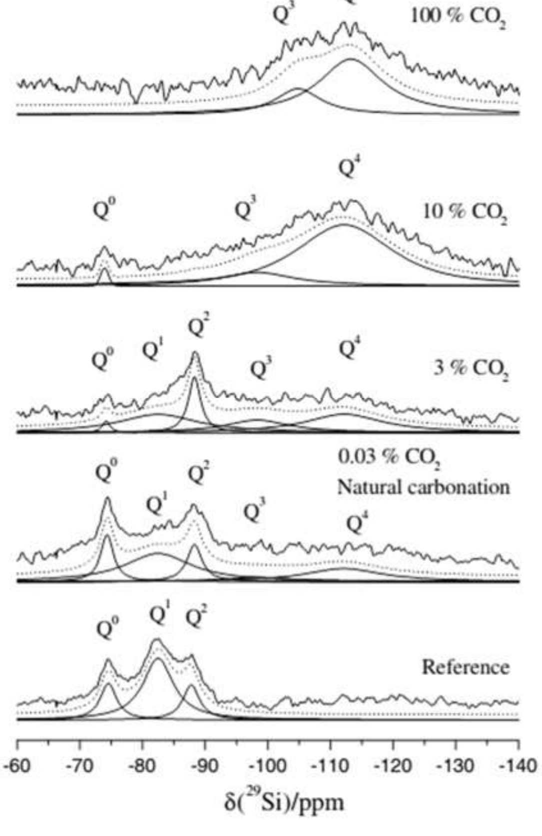

Figure 2.40 ^{29}Si M.A.S - N.M.R spectra for OPC paste samples subjected to different percentage of CO_2 concentration (Castellote et al., 2009)

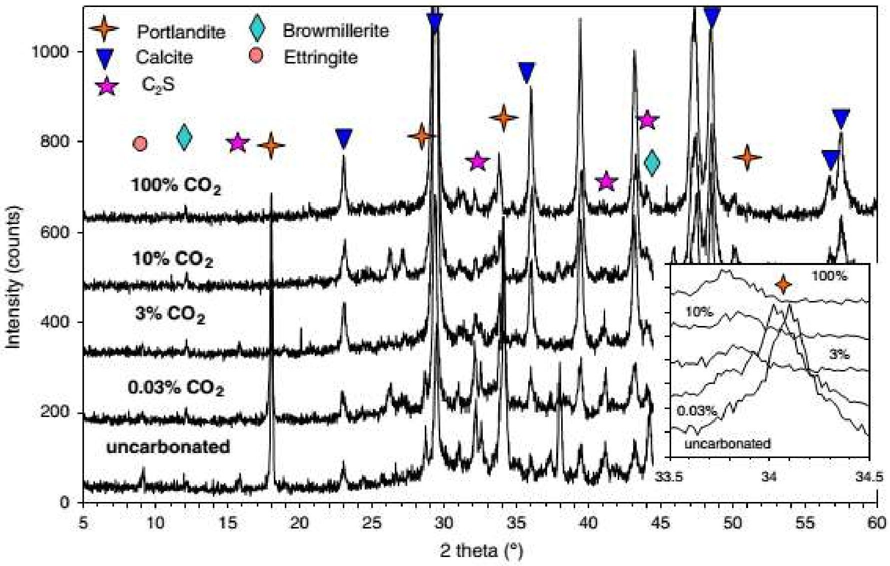

Figure 2.41 X-ray diffraction patterns for OPC paste samples subjected to different percentage of CO_2 concentration (Castellote et al., 2009)

The NMR results indicate that the intensity of the CSH gel spectrum decreases as the CO_2 concentration increases. At 100% CO_2, complete decomposition of CSH occurs. XRD results indicate the presence of portlandite in un-carbonated and 0.03% CO_2 concentration exposed samples. This observation was confirmed from TGA results. Further, the calcite peak intensity was found to increase as the CO_2 concentration increased. Ettringite was absent in 10% and 100% CO_2 concentration exposure.

Even though the effect of SCMs is reported to be detrimental in the case of carbonation, it is important to see its effect on corrosion, both in the initiation and in propagation phases. Even though the time of initiation is reduced, there can be an increase in the propagation phase. This is because, due to carbonation, the microstructure gets modified owing to the deposition of $CaCO_3$ in the pores, leading to reduced pore diameter, and pore volume, and increased pore tortuosity. These changes can lead to increased resistivity of concrete, which is a major factor determining the propagation of corrosion. However, the study by Alonso and Andrade (2013) concluded that the corrosion initiation period was reduced whereas the propagation period was accelerated depending on the fly ash content.

2.6 SERVICE LIFE PREDICTION OF REINFORCED CONCRETE STRUCTURES

Another key aspect in the concept of durability design is the prediction of service life of the structures. Most of the service life prediction models predict service life based on some physical laws like Fick's law of diffusion or are based on a single material parameter. Table 2.14 and Table 2.15 give the details of some of the commonly used prediction models to assess the service life both in terms of carbonation induced and chloride induced corrosion respectively.

Table 2.14 Models on carbonation induced corrosion

Models		Details
Basic theoretical model		• Fick's second law of diffusion • Varying the initial and boundary conditions, several solutions can be obtained
Square root of time		• Most commonly used prediction model
CO_2 diffusion coefficient	Tuutti's model (Tuutti, 1982)	• Based on mobile boundaries diffusion • Assumes that beyond carbonation front, the CO_2 concentration is zero and above that it is 100% • Reacted zone is well defined by a sharp front
	Bakker's model (Sanjuan et al., 2002)	• Combines both drying and carbonation processes, assumes that carbonation progresses only if the concrete is dry.
	Papadakis'model (Papadakis, 1991a)	• Model based on the physiochemical processes of the carbonation phenomenon • Complex model
	Castellote's UR model (Castellote and Andrade, 2008)	• Based on the principles of "Unreacted- core" systems • The controlling step in carbonation is the CO_2 diffusion through the carbonated part of the sample
	DuraCrete model (DuraCrete final Technical report, 2000)	• Probabilistic approach of service life design • Based on the principle of the Load and Resistance Factor Design (LRFD • Incorporates design equations, characteristic values of load and resistance variables and partial factors for the load and resistance variables
Air or oxygen permeability coefficient	Parrot's model (Parrot, 1994)	• Models based on air permeability coefficient • Based on the measurements from oxygen permeability test and adjusting them to the humidity content in the concrete for each environment
	Salvoldi's model (Salvoldi, 2010)	• Based on Oxygen Permeability coefficient obtained from OPI test results • Effective diffusion coefficient is calculated from the OPI value

Table 2.15 Models on chloride induced corrosion

Model	Remarks
Basic theoretical model	• Fick's second law of diffusion
Life 365 (2012)	• Widely used model • Empirical approach • Can be either deterministic or probabilistic • Based on Fick's second law of diffusion and apparent diffusion coefficient
DuraCrete (DuraCrete final Technical report, 2000)	• Empirical model • Probabilistic performance based durability design of concrete structures • Based on the non-steady state migration coefficient obtained from Rapid migration test
Clinconc (Tang, 2008)	• Considers binding effect of chlorides • Most advanced model • Based on finite difference approach
Chlodif (Oslakovic et al., 2010)	• Empirical model • Meant for the design of structures for which the data on initial chloride concentration and diffusion coefficient not available

As discussed in section 2.4, service life prediction models are also available using other durability parameters such as resistivity, chloride conductivity etc. (Andrade, 2013, Alexander, 2002).

There are many other approaches for service life prediction rather than relying on a single parameter. To cite an example, Basheer et al. (1996) explained a holistic approach of modelling of deterioration of concrete structures. There are three types of models in this approach viz., transport model, corrosion model, and structural model. The emphasis is on permeation characteristics and fracture strength of concrete. Another viewpoint of the same concept is presented by Baroghel-Bouny et al. (2009). They presented a multi-level modelling concept, to assess the durability of reinforced concrete structures, with respect to chloride induced corrosion. Both transport and corrosion models are dealt with in four levels. Depending on the importance of the structure and the time, different levels of modelling can be chosen. Here, there is no explanation regarding the structural model. Both these approaches fall under the category of rigorous approach to service life prediction. However, Andrade (2002) is of the opinion that even though rigorous models are desirable, simple tools should be available for prediction, provided their limitations are recognized. At the same time, there are many opponents to the concept of service life modelling. For example, Gulikers (2011) states that mathematical models may lead to unrealistic predictions and there should be good correlation between the parameters obtained from accelerated laboratory tests and those from real structures.

Out of the different models mentioned above, the models which will be used in the present thesis for service life prediction would be the square root of time model (for carbonation induced corrosion) and DuraCrete model (for both carbonation and chloride induced corrosion). These models are discussed in detail in the following section.

2.6.1 Square root of time model for carbonation induced corrosion

This is the simplest model available to find the depth of carbonation (Galan and Andrade, 2009). This model is expressed as

$$x = k.\sqrt{t} \tag{2.62}$$

where

x	CO_2 penetration depth (mm)
k	Carbonation rate (mm/√year)
t	Time (year)

For a particular penetration depth and time, the carbonation rate can be calculated. Using the carbonation rate, carbonation depths at any time can be determined.

Steiner (2014) had proposed that the right hand side of the Equation 2.62 need to be modified by multiplying with a factor W which takes in to account the variation in meso-climatic conditions for the specific concrete member during the design service life. Thus, Equation 2.62 takes the form

$$x = W.k.\sqrt{t} \tag{2.63}$$

For the service life estimation of the new structures, W and k need to be derived from the published data on existing structures constructed with similar materials, execution and exposure conditions. In the case of the assessment of the remaining service life of the existing structures, W and k need to be obtained from the measurement on the structure.

2.6.2 DuraCrete model for carbonation induced corrosion

This is a probabilistic approach of service life design which was developed by the European project titled Probabilistic Performance Based Durability Design of Concrete Structures or DuraCrete (DuraCrete final Technical report, 2000). The durability design method is based on the principle of the Load and Resistance Factor Design (LRFD). This method consists of different aspects such as design equations, characteristic values of load and resistance variables and partial factors for the load and resistance variables. The partial factors are incorporated in order to ensure an acceptable level of reliability with respect to the limit states considered. The acceptance criteria are given in terms of reliability index.

In the case of carbonation induced corrosion, the corrosion is assumed to be initiated when the carbonation front reaches the reinforcement. The carbonation resistance is obtained from accelerated carbonation test, which is the compliance test. The design equation, (g) stating that corrosion is initiated when the carbonation front reaches the reinforcement is given by:

$$g = x^d - x_c^d(t) = x^d - \sqrt{\frac{2.c_{s,ca}^d.t}{R_{ca}^d}} \tag{2.64}$$

Where

x^d Design value of the cover thickness

x_c^d Design value of the penetration depth of the carbonation

$c_{s,ca}^d$ Design value of the surface concentration

t	Time
R_{ca}^{d}	Design value of the carbonation resistance

The design value of the time dependent resistance is given by

$$R_{ca}^{d}(t) = \frac{R_{0,ca}^{c}}{k_{e,ca}^{c} \cdot k_{c,ca}^{c} \cdot \left(\frac{t_0}{t}\right)^{2n_{ca}^{c}} \cdot \gamma_{R_{ca}}} \tag{2.65}$$

Where

$R_{0,ca}^{c}(t)$	Characteristic value of the carbonation resistance determined on the basis of compliance tests (i.e., accelerated carbonation test)
$k_{c,ca}^{c}$	Characteristic value of the curing factor
$k_{e,ca}^{c}$	Characteristic value of the Environment factor
t_0	Age of the concrete when the compliance test is performed
n_{ca}^{c}	Characteristic value of the age factor
$\gamma_{R_{ca}}$	Partial factor for the resistance with respect to carbonation

The carbonation resistance (Visser, 2014) is calculated using Equation 2.66.

$$\frac{x_c}{\sqrt{t}} = \sqrt{\frac{1}{R_{carb}}}\,\sqrt{2C} \tag{2.66}$$

where

R_{carb}	Carbonation resistance (year (kg/m^3) /mm^2)
C	CO_2 concentration in the accelerated carbonation test
$\frac{x_c}{\sqrt{t}}$	Carbonation rate

The values of the factors are provided in the Duracrete report for different conditions.

2.6.3 DuraCrete model for chloride induced corrosion

The corrosion is assumed to be initiated when the chloride concentration around the reinforcement exceeds the critical chloride threshold value. The design equation stating that corrosion is initiated when the chloride concentration around the reinforcement exceeds the critical chloride concentration is given by

$$g = c_{cr}^{d} - c^{d}(x,t) = c_{cr}^{d} - c_{s,cl}^{d}\left[1 - erf\left[\frac{x^{d}}{2\sqrt{\frac{t}{R_{cl}^{d}(t)}}}\right]\right] \tag{2.67}$$

where

c_{cr}^{d}	Design value of the critical chloride concentration
$c_{s,cl}^{d}$	Design value of the chloride surface concentration
x^{d}	Design value of the cover thickness
R_{cl}^{d}	Design value of the chloride resistance
t	Time

The design value of the time dependent resistance is given by

$$R_{cl}^{d}(t) = \frac{R_{cl,0}^{c}}{k_{e,cl}^{c} \cdot k_{c,cl}^{c} \cdot \left(\frac{t_0}{t}\right)^{n_{cl}^{c}} \cdot \gamma_{R_{cl}}} \tag{2.68}$$

Where

$R_{cl}^{d}(t)$	Resistance with respect to chloride ingress determined on the basis of the compliance test (i.e., Rapid migration test)
$k_{c,cl}^{c}$	Characteristic value of curing factor
$k_{e,cl}^{c}$	Characteristic value of environment factor
t_0	Age of the concrete when the compliance test is performed

n_{cl} Characteristic value of age factor

$\gamma_{R_{cl}}$ Partial factor for the resistance with respect to chloride ingress

All the different factors mentioned above for different conditions are given in tables in the DuraCrete report. Even though the incorporation of different factors make the procedure for service life prediction easy, in many cases, lead to unrealistic estimation of the service life of the structure. For instance, Oslakovic et al. (2010) did an evaluation of service life of the concrete bridges exposed to marine environment. In the case of service life prediction (case study – KrK bridge, Adriatic coast), the Duracrete model leads to high reliability for better durability classes. The discrepancy came due to the influence of the theoretical input value of the age factor.

2.7 SUMMARY OF LITERATURE REVIEW AND NEEDS FOR RESEARCH

This chapter on literature review analysed the available literature pertaining to different aspects of the present project work. In the initial part of the chapter, general aspects of concrete durability were covered. Further, the challenges to achieve the durability in concrete construction were identified. The deterioration mechanisms mainly due to chloride and carbonation induced corrosion were reviewed, followed by the transport mechanisms leading to ingress of aggressive agents. The deterioration mechanisms and the transport mechanisms were linked by choosing two practical examples. The next section reviewed the details of the durability test methods such as their scientific background and the available literature. The influence of SCMs on different parameters of concrete and the available explanation for their behavior were also reviewed. Finally, three service life prediction models for assessing the service life of concrete structures in terms of chloride and carbonation induced corrosion were reviewed in detail.

From the literature study, the following research needs are identified:

- **Need for a database of durability parameters with commonly used supplementary cementitious materials, which can be used as a guideline for material selection**

Even though SCMs are specified in many of the construction projects in India, the specification is random and not based on any solid experimental database. A database of the durability parameters with the commonly used SCMs is required, so that the potential of the SCMs for ensuring durability can be reaffirmed and the database can act as a guideline for the material selection for a particular service environment.

- **Need for a classification system for concrete based on combining durability parameters addressing the transport mechanisms acting in a particular service environment**

Even if many studies have been done on environmental classification system and durability parameters, a clear picture regarding combination of test methods used for a particular exposure condition is lacking. A kind of classification system for concrete based on combining durability parameters addressing the transport mechanisms acting in a particular service environment is necessary.

- **Need for the quantification of durability parameters with SCMs for different service conditions using service life prediction modelling**

The durability parameters for different service conditions need to be quantified using service life prediction models. Moreover, the interrelationships between different durability parameters for various binder combinations need to be explored more scientifically.

- **Need to have a fundamental understanding on the effect of SCMs in concrete, both through microstructural and basic scientific approach**

Clear understanding of the microstructural changes due to carbonation and chloride ingress in concretes having different SCMs is needed.

CHAPTER 3

EXPERIMENTAL PROGRAMME

3.1 INTRODUCTION

This chapter describes the materials used, experimental design, and the detailed procedures of the experiments conducted in this research work. The section on materials describes the properties of the materials used for making concretes. Details regarding the concrete mixtures such as mixture proportions, mixing procedures, fresh properties and curing methodology are described in the section on concrete. The experimental design section describes the test variables. The experimental methods belong to three categories viz., compressive strength testing method, durability testing methods and micro analytical techniques. These durability tests belong to three groups - i.e., test methods used to measure chloride, gas and water penetrability.

3.2 MATERIALS USED IN THE STUDY

The binder materials used in this study include Ordinary Portland Cement (53 grade) and three Supplementary Cementitious Materials (SCMs) such as Ground Granulated Blast Furnace Slag (Slag), Class F fly ash and Class C fly ash. Two slags (Slag A and Slag B) obtained from two different sources were used in this study. Crushed granite was used as coarse aggregate whereas river sand was used as fine aggregate. A Sulphonated Naphthalene Formaldehyde (SNF) based admixture was used to obtain slump values between 80 mm and 150 mm.

3.2.1 Raw materials

3.2.1.1 Physical and chemical properties of binders

The physical properties of the binders such as specific gravity (determined as per IS 1727 – 1967 (2004) and specific surface area (determined using Blaine's apparatus as per ASTM C204, 2011) are presented in Table 3.1. The chemical composition of the binders was determined using X – ray fluorescence spectroscopy and the results are presented in Table 3.2.

Table 3.1 Specific gravity and specific surface area of binders

Binder	Specific gravity	Specific surface area (m^2/kg)
Ordinary Portland Cement	3.15	340
Slag A	2.86	360
Slag B	2.89	430
Fly ash (Class F)	2.49	330
Fly ash (Class C)	2.46	390

Table 3.2 Chemical composition of the different binders

Compound	Concentration (%)				
	OPC	Slag A	Slag B	Class F fly ash	Class C fly ash
Al_2O_3	4.73	17.38	21.06	29.95	31.46
CaO	65.11	35.61	31.46	1.28	13.76
Fe_2O_3	3.86	1.04	1.87	4.32	6.17
K_2O	0.54	0.58	0.88	1.44	0.12
MgO	1.20	8.03	8.57	0.61	2.28
Na_2O	0.5	0.36	0.36	0.16	0.59
SiO_2	19.44	33.82	32.38	59.32	39.89
SO_3				0.16	3.19

3.2.1.2 Physical and chemical properties of aggregates

The physical properties of the aggregates used are as shown in Table 3.3. Figure 3.1 shows the sieve analysis results.

Table 3.3 Physical and chemical properties of aggregates

Property	Coarse aggregate (20 mm)	Coarse aggregate (10 mm)	Fine aggregate
Bulk Density (kg/m^3)	1590	1510	1719
Specific gravity (SSD)	2.77	2.76	2.53
Water absorption (%)	0.41	0.43	0.72

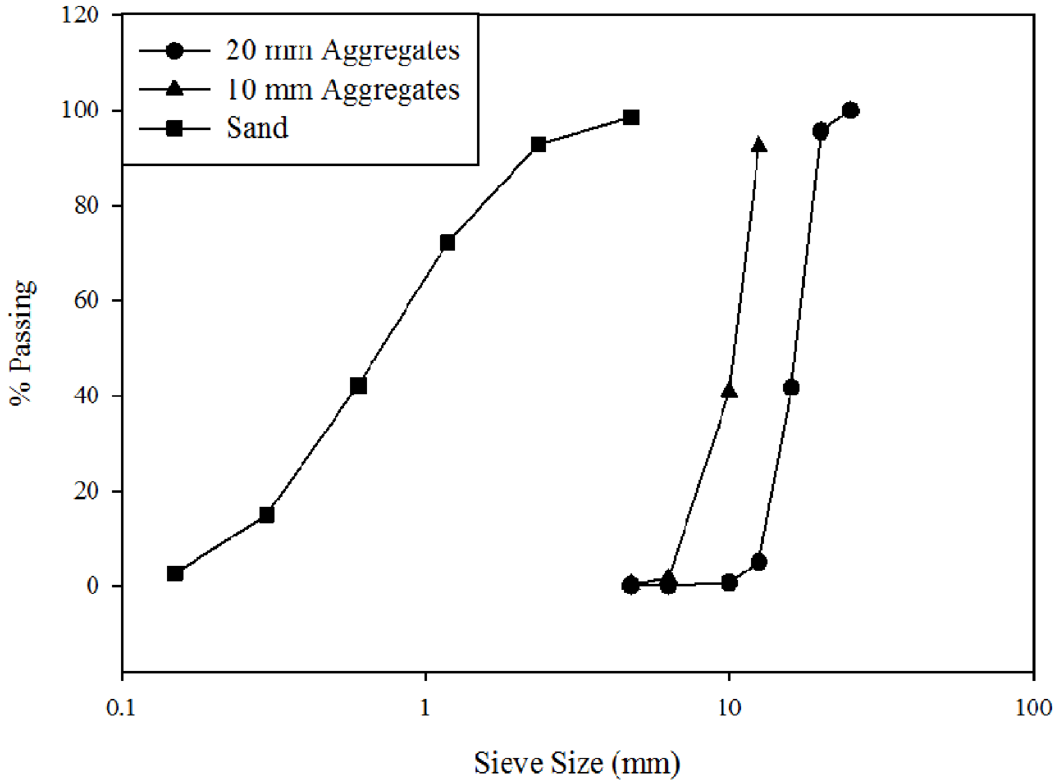

Figure 3.1 Particle size distribution of different aggregates used in the study

3.2.1.3 Properties of superplasticizer

The properties of the superplasticizer used in the study are as shown in Table 3.4.

Table 3.4 Properties of superplasticizer

Property	Results
Appearance	Dark brown colour liquid
Specific gravity	1.21
pH	6.64
% solids	40.86
% chloride	0.045

3.2.2 Concrete

For the present work, there are two categories of mixtures. Category – 1, designated as "commonly used design mixes" includes low to moderate strength grade mixes which are used commonly in construction. These are having mean strength values ranging between 20 to 60 MPa. These mixes have the following features: four total binder contents (280, 310, 340, and 380 kg/m^3), five water binder ratios (0.4, 0.5, 0.55, 0.6, and 0.65), partial replacement with four SCMs (two slags (from two different sources), Class F fly ash and Class C fly ash) and three levels of replacements (15, 30, and 50%). It is to be noted that only selected combinations were studied in this project. The second category mixes are designated as “mixes having limiting prescriptive values”. The total binder content as well as the water binder ratio of these mixes are identified both from the IS 456: 2000, the Indian Standard code of practice for plain and reinforced concrete, and from the proposal given by Saravanan and Santhanam (2012) as the recommended limiting values for different exposure conditions. In this category, only OPC is used as binder. As the name indicates, these mixtures have limiting values of total cement content and w/c specified either in the code or the proposal.

3.2.2.1 Mixture proportions

All the concretes were designed with a fine to coarse aggregate ratio of 40:60. The coarse aggregates used were combinations of 20 mm down and 10 mm down, in a proportion of 60:40. The admixture dosage was adjusted in order to obtain slump between 80 to 150 mm. Table 3.5 shows the details of the mixture proportions adopted in the study.

Table 3.5 Mixture proportion details

Sl. No.	Category	Mix ID	w/b	Binder content	SCM content	Sand (kg/m)	10 mm aggregate (kg/m)	20 mm aggregate (kg/m)	Water (kg/m)	SP (kg/m)
1	Commonly used design mixes	LFM2	0.65	280	0	760	499	749	182	0.50
2		LFM9	0.65	280	30% Slag A	760	499	749	182	0.40
3		LFM17	0.65	280	30% Slag B	760	499	749	182	0.54
4		LFM29	0.65	280	30% Class F fly ash	760	499	749	182	0.67
5		LFM4	0.55	340	0	735	483	725	187	0.00
6		LFM12	0.55	340	15% Slag A	735	483	725	187	0.24
7		LFM21	0.55	340	15% Slag B	735	483	725	187	0.98
8		LFM32	0.55	340	15% Class F fly ash	735	483	725	187	0.01
9		LFM42	0.55	340	15% Class C fly ash	735	483	725	187	0.04
10		LFM46	0.6	310	0	747	491	736	186	0.07
11		LFM10	0.6	310	15% Slag A	747	491	736	186	0.37
12		LFM19	0.6	310	15% Slag B	747	491	736	186	0.26
13		LFM30	0.6	310	15% Class F fly ash	747	491	736	186	0.13
14		LFM41	0.6	310	15% Class C fly ash	747	491	736	186	0.20
15		LFM5	0.5	310	0	759	498	748	155	2.97
16		LFM13	0.5	310	15% Slag A	759	498	748	155	3.35
17		LFM22	0.5	310	15% Slag B	759	498	748	155	3.57
19		LFM23	0.5	310	30% Slag B	759	498	748	155	3.83
18		LFM24	0.5	310	50% Slag B	759	498	748	155	4.39
21		LFM28	0.5	310	20% Slag B + 20% Class F fly ash	759	498	748	155	2.23
20		LFM33	0.5	310	15% Class F fly ash	759	498	748	155	0.37
22		LFM34	0.5	310	30% Class F fly ash	759	498	748	155	3.75
23		LFM35	0.5	310	50% Class F fly ash	759	498	748	155	2.38
24		LFM39	0.5	310	20% Slag B + 20% Class C fly ash	759	498	748	155	4.42

25		LFM40	0.5	310	20% Class F fly ash +20% Class C fly ash	759	498	748	155	3.72
26		LFM43	0.5	310	15% Class C fly ash	759	498	748	155	0.34
27		LFM44	0.5	310	30% Class C fly ash	759	498	748	155	0.50
28		ClDBS1	0.4	380	0	733	482	723	152	2.28
29		ClDBS2	0.4	380	15% Slag	733	482	723	152	2.10
30		ClDBS3	0.4	380	30% Slag	733	482	723	152	2.00
31		ClDBS4	0.4	380	50% Slag	733	482	723	152	2.28
32		ClDBS5	0.4	380	15% Class F fly ash	733	482	723	152	2.10
33		ClDBS6	0.4	380	30% Class F fly ash	733	482	723	152	1.50
34		ClDBS7	0.4	380	50% Class F fly ash	733	482	723	152	2.28
35	Limiting value mixes	MA1	0.5	300	0	764	502	753	150	2.52
36		MA2	0.55	300	0	759	498	748	165	1.58
37		MA3	0.45	320	0	759	499	748	144	3.30
38		MA4	0.45	340	0	748	492	737	153	2.45
39		MA5	0.4	340	0	755	496	744	136	5.71
40		MA6	0.4	360	0	744	489	733	144	2.16
41		MA7	0.4	400	0	723	475	712	160	2.88

3.2.2.2 Mixing procedures, fresh properties and curing methodology

The concrete is prepared in a pan mixer following the procedure below. After determining the moisture content of the aggregates using the microwave oven method (ASTM D4643, 2008), the corrections for the moisture content present in the aggregates are done. The mixing is done in a sequence, which includes buttering the mixer with cement paste, dry mixing of coarse and fine aggregates, addition of 20% of water and mixing for two minutes, giving a rest period of 4 minutes, addition of binder and mixing for one minute, mixing for two minutes with 60% water and finally two minute mixing with the remaining 20% of the water along with superplasticizer.

The fresh concrete properties of the mixes such as initial slump (as per ASTM C143, 2000), unit weight (as per ASTM C138, 2001) and air content (as per ASTM C231, 1997, by Pressure method type B) were determined and are presented in Table 3.6

The cast specimens were kept in the casting yard in a covered condition for 24 hours. After demoulding and marking, the specimens were shifted to a moist room at 27 °C and stored until the age of testing.

Table 3.6 Fresh concrete properties

Sl. No.	Mix ID	w/b	Binder content	SCM content	Ambient Temperature (°C)	Initial Slump (mm)	Unit Weight (kg/m^3)	Air Content (%)
1	LFM2	0.65	280	0	33	80	2385	2.50
2	LFM9	0.65	280	30% Slag A	33	100	2414	2.50
3	LFM17	0.65	280	30% Slag B	34	140	2442	2.20
4	LFM29	0.65	280	30% Class F fly ash	32	80	2414	2.40
5	LFM4	0.55	340	0	33	85	2428	2.40
6	LFM12	0.55	340	15% Slag A	33	80	2399	2.40
7	LFM21	0.55	340	15% Slag B	36	80	2414	2.40
8	LFM32	0.55	340	15% Class F fly ash	33	80	2399	1.80
9	LFM42	0.55	340	15% Class C fly ash	32	95	2456	0.80
10	LFM46	0.6	310	0	29	150	2456	1.00
11	LFM10	0.6	310	15% Slag A	33	95	2371	2.40
12	LFM19	0.6	310	15% Slag B	35	90	2399	2.30
13	LFM30	0.6	310	15% Class F fly ash	32	85	2456	2.10
14	LFM41	0.6	310	15% Class C fly ash	31	100	2399	0.80
15	LFM5	0.5	310	0	32	85	2428	2.50
16	LFM13	0.5	310	15% Slag A	34	125	2456	1.80
17	LFM22	0.5	310	15% Slag B	36	90	2470	2.30
18	LFM23	0.5	310	30% Slag B	33	100	2498	1.60
19	LFM24	0.5	310	50% Slag B	33	80	2484	1.80
20	LFM28	0.5	310	20% Slag B + 20% Class F fly ash	32	80	2428	1.40
21	LFM33	0.5	310	15% Class F fly ash	33	85	2428	2.00
22	LFM34	0.5	310	30% Class F fly ash	32	125	2470	1.10
23	LFM35	0.5	310	50% Class F fly ash	32	90	2385	1.50
24	LFM39	0.5	310	20% Slag B + 20% Class C fly ash	32	80	2470	1.20

Sl. No.	Mix ID	w/b	Binder content	SCM content	Ambient Temperature (°C)	Initial Slump (mm)	Unit Weight (kg/m^3)	Air Content (%)
25	LFM40	0.5	310	20% Class F fly ash +20% Class C fly ash	31	90	2442	1.40
26	LFM43	0.5	310	15% Class C fly ash	30	80	2470	0.80
27	LFM44	0.5	310	30% Class C fly ash	29	150	2498	1.20
28	ClDBS1	0.4	380	0	28	90	2428	1.20
29	ClDBS2	0.4	380	15% Slag	28	95	2428	1.00
30	ClDBS3	0.4	380	30% Slag	29	100	2442	1.50
31	ClDBS4	0.4	380	50% Slag	28	90	2428	1.00
32	ClDBS5	0.4	380	15% Class F fly ash	28	85	2385	1.80
33	ClDBS6	0.4	380	30% Class F fly ash	28	85	2498	1.50
34	ClDBS7	0.4	380	50% Class F fly ash	29	100	2470	1.80
35	MA1	0.5	300	0	32	120	2465	2.50
36	MA2	0.55	300	0	33	70	2466	1.80
37	MA3	0.45	320	0	32	75	2465	2.40
38	MA4	0.45	340	0	34	90	2465	1.60
39	MA5	0.4	340	0	33	100	2463	1.50
40	MA6	0.4	360	0	32	140	2466	1.80
41	MA7	0.4	400	0	35	140	2465	2.50

3.3 EXPERIMENTAL DESIGN

For the current research study, there are three groups of experiments. Mechanical testing forms the first group, in which the compressive strength of the concretes are determined by cube compression test. The group on durability tests is categorised into three, namely methods used to assess the penetrability of chloride, water, and gas. The chloride penetrability tests include rapid chloride permeability test (RCPT), rapid migration test (RMT) and chloride conductivity test (CCT). The Wenner 4 - probe resistivity test used to measure the surface resistivity of concrete is also included in this group. Water sorptivity test and water permeability test are the tests used to find the water penetration resistance. To study the gas penetration properties of concrete, tests such as oxygen permeability index test, Torrent air permeability test and accelerated carbonation test are carried out. The micro analytical techniques used in this study include scanning electron microscopy (SEM) with energy dispersive X-ray analysis (EDS), X-ray diffraction (XRD) and thermo gravimetric/ differential scanning caloriemetry (TG/DSC).

The details of the experimental parameters for the mechanical and durability tests are given in Table 3.7. Table 3.8 gives the details of the micro – analytical tests.

Table 3.7 Details of mechanical and durability tests

Sl. No.	**Category**	**Test**	**Standard**	**Property measured**	**Concrete Specimen details**	**No. of specimens per test**	**Age of testing (days)**	**Conditioning**	**Remarks**
Mechanical test									
1		Compressive strength	IS 516-1959	Compressive strength	Cube of size 100 mm	3	28, 90 *2,7,365	Saturated Surface Dry Samples	* for commonly used design mixes category
Durability tests									
2	Tests to measure chloride penetrability	Wenner 4-Probe resistivity		Surface resistivity	Cube of size 150 mm	1	28,90	Saturated condition	6 sides of same specimen
3		Rapid chloride permeability	ASTM C 1202	Total charge passed	Discs of 100 mm diameter and 50 mm thickness prepared from cylinder of 100 mm diameter and 200 mm height	3	28,56,90	Vacuum saturation with saturated $Ca(OH)_2$ solution	
4		Rapid migration	NT BUILD 492	Non-steady state migration coefficient	Discs of 100 mm diameter and 50 mm thickness prepared from cylinder of 100 mm diameter and 200 mm height	3	28,56,90	Vacuum saturation with saturated $Ca(OH)_2$ solution	
5		Chloride conductivity	DI Testing Manual, South Africa	Conductivity	Discs of 70 mm diameter and 30 mm thickness prepared from cube of size 150 mm	4	28,56,90	Oven drying for 7 days, followed by vacuum saturation with 5 M NaCl solution	

Sl. No.	Category	Test	Standard	Property measured	Concrete Specimen details	No. of specimens per test	Age of testing (days)	Conditioning	Remarks
6	Tests to measure gas penetrability	Oxygen permeability	DI Testing Manual, South Africa	Oxygen permeability index	Discs of 70 mm diameter and 30 mm thickness prepared from cube of size 150 mm	3	28,90	Oven drying for 7 days	
7		Torrent air permeability	SIA 262/1-E:2003	Coefficient of air Permeability	Cube of size 150 mm	1	28,90	Air drying in laboratory conditions (i.e., 65 % RH and 25 ˚C) for three weeks	4 sides of same specimen
8		Accelerated carbonation		Carbonation depth	Prismatic specimens of 100 x 100 mm cross section and 700 mm length	2	28,56,70, 112	28 days water curing followed by air curing in 65% RH and 25 ºC for 14 days	
9	Tests to measure water penetrability	Water sorptivity	SA DI Manual	Sorptivity Index	Discs of 70 mm diameter and 30 mm thickness prepared from cube of size 150 mm	4	28,90	Oven drying for 7 days. Test is followed by vacuum saturation with saturated $Ca(OH)_2$ solution	
10		Water permeability	DIN 1048 Part 5	Depth of water penetration	Cube of size 150 mm	1	28	Saturated condition	

Table 3.8 Details of micro analytical tests

Sl. No.	Technique	Purpose of study	Sample details	No. of mixes studied	Remarks
1	Scanning electron microscopy with energy dispersive X-ray analysis (SEM-EDS)	Microstructural variations due to chloride penetration	Samples from concrete penetrated by Cl, obtained from specimens immersed in 3% NaCl solution for 35 days	9	All mixes except the combination mixes
		Microstructural variations due to CO_2 penetration	Samples from concrete penetrated by CO_2 after 112 days of exposure	9	
2	X – ray diffraction spectroscopy (XRD)	Identification of crystalline compounds formed due to chloride penetration	Powder obtained from profile grinding at different depths from specimens immersed in 3% NaCl solution for 35 days	9	
		Identification of crystalline compounds formed due to carbonation reaction	Powder obtained from cement paste subjected to carbonation	9	
3	Thermo gravimetric and differential scanning calorimetry (TG/DSC)	Portlandite content, a measure of degree of pozzolanicity of concrete	Powder prepared from hardened cement paste, cured under saturated $Ca(OH)_2$ solution	13	All mixes

3.4 MECHANICAL AND DURABILITY TESTS

This section provides a detailed description of all the tests conducted in this study.

3.4.1 Compressive strength test

The compressive strength tests were done in accordance with IS 516:1959. The tests were performed on saturated surface dry cubes of size 100 mm. After measuring the dimensions, the specimens were positioned in the compression testing machine in such a way that the cast surface was perpendicular to the test surface. The load was applied at the rate of 140 kg/cm^2/minute until the failure of the specimen. Three numbers of specimens were tested at each selected age and the average value is reported as the compressive strength. For the present study, compressive strength tests were performed at 5 different ages such as 2 days, 7 days, 28 days, 90 days, and 365 days for all the concretes belonging to commonly used design mixes category. For the other concretes, both 28 days and 90 days strengths were tested.

3.4.2 Wenner 4 – probe surface resistivity test

For the present study, the surface resistivity test was conducted using Wenner 4 - Probe resistivity meter. The resistivity measurements were performed on 150 mm cubes, which were in fully saturated condition in order to nullify the effect of drying.

After the required days of moist room curing, the specimens were moved to laboratory conditions, i.e. 25°C and 65% RH. The readings were taken within 5 minutes after removing from the moist room. Before each measurement, the probes were calibrated using the standard rod provided with the Wenner resistivity meter. Two separate readings were taken on every phase of the cube, in diagonally opposite directions. Thus, the surface resistivity measurement reported is the average of twelve readings. Figure 3.2 shows the photograph of the surface resistivity measurements. The resistivity measurements were taken at two ages - 28 days and 90 days.

Figure 3.2 Surface resistivity measurement using Wenner 4 - probe resistivity meter

3.4.3 Rapid chloride permeability test

The rapid chloride permeability test (RCPT) was conducted as per the procedure given in ASTM C1202 (2010). The test specimens were concrete discs of diameter 100 mm and 50 mm thickness which were obtained from cylindrical concrete specimens of diameter 100 mm and height 200 mm. The specimens were kept in the moist room for curing until the test day. The RCPT was conducted at three ages - 28 days, 56 days and 90 days.

The specimen preparation procedure (for RCPT and rapid migration test or RMT) takes two days. On the first day, the cylindrical specimen was removed from the moist room. After surface drying, the curved face was coated with epoxy to make the surface impervious. After proper curing of epoxy, normally two to three hours, the specimens were cut using a water cooled diamond saw. 25 mm slices were discarded from both top and bottom. The remaining 150 mm was cut into three specimens, each having 50 mm height. Figure 3.3 shows the schematic of the specimen preparation whereas Figure 3.4 includes the photographs of specimen preparation for RCPT and RMT.

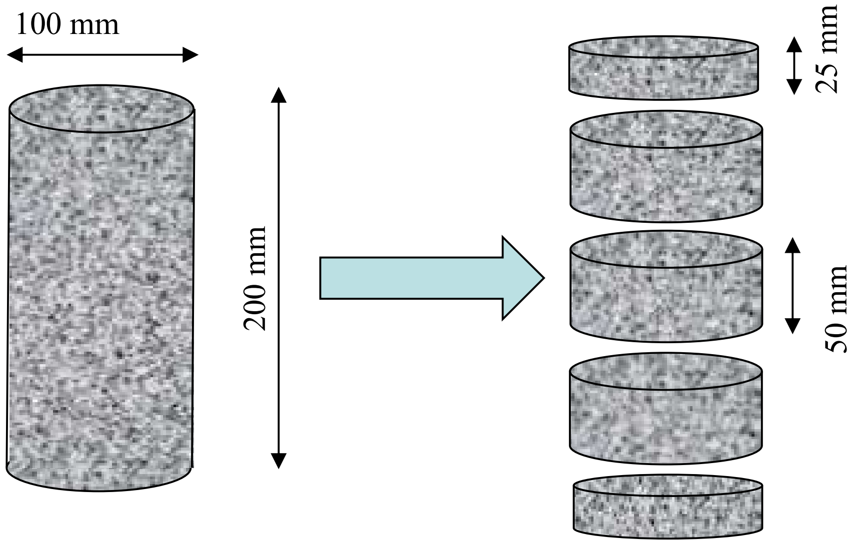

Figure 3.3 Schematic of specimen preparation for RCPT and RMT


Specimens taken out from mist room


Epoxy used for coating


Coating with epoxy


Epoxy coated specimen


Cutting of specimen

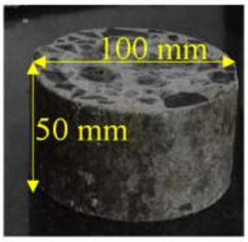

Specimen after cutting

Figure 3.4 Specimen preparation for RCPT/RMT

In the next step, the specimens were saturated by vacuum saturation method. The procedure for vacuum saturation is the same for all the tests and is described as follows. The concrete disc specimens were placed in a vacuum desiccator which was connected to a vacuum pump. The vacuum was maintained for a period of three hours so that all the pores get open. After three hours, while running the vacuum pump, the desiccator was allowed to get filled with saturated calcium hydroxide solution in such a way that all the specimens were submerged completely. The vacuum pump was kept running for another one hour. After that, the vacuum pump was stopped so that the pressure in the desiccator return to atmospheric pressure. The specimens were kept submerged in the saturated $Ca(OH)_2$ solution for another 18 hours. This step completed the vacuum saturation process and the specimens are ready to be tested in RCPT or in RMT.

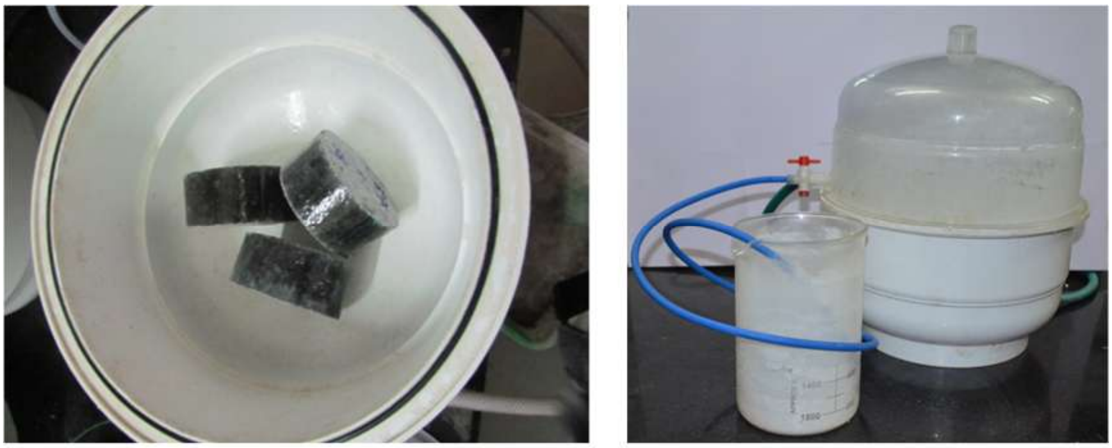

Figure 3.5 Vacuum saturation facility

After removing from the vacuum desiccator, the specimens were fixed in the acrylic cells of the RCPT set up. The cells were checked for leakage. Leakage, if found, was arrested with the help of silicon rubber sealant. The cell on one side of the specimen was filled with 3% NaCl solution, which was connected to the negative terminal of the voltage source. The other side was filled with 0.3 M NaOH solution, which was connected to the positive terminal. A voltage of 60 V was applied and the current at each half an hour was noted for a period of six hours. The test was kept running for six hours at the constant potential of 60 V. In addition to the current measurements, the temperature in the anolyte (i.e., NaOH solution) was monitored every 30 minutes. Using the current readings, the charge passed was calculated using the formula given in Equation 2.44. The average of three specimens is reported as the charge passed, which is used to qualitatively classify the concrete based on the chloride ion penetrability. Figure 3.6 shows the experimental set up of RCPT.

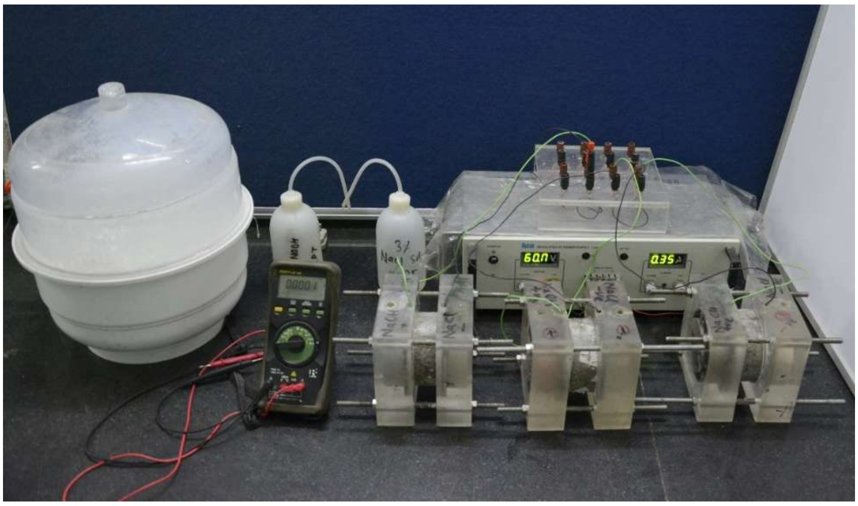

Figure 3.6 Experimental set up of rapid chloride permeability test

3.4.4 Rapid migration test

The principle of Rapid migration test (RMT) is similar to RCPT. The RMT is done as per the NORD standard NT BUILD 492. RMT was also done on 28, 56 and 90 days old concretes. The details of the specimen and the conditioning procedure are similar to that of RCPT. After noting down the exact thickness of each specimen, they were fixed tightly inside a PVC pipe, which acts as the anolyte chamber, with the help of a rubber washer. The dimensions of the specimens were measured at two diametrically opposite points. Leak proofing was ensured by the use of rubber washers and silicon rubber sealant. After ensuring complete leak proof, the upper part of the pipe was filled with 0.3 N NaOH solution. All the three cells were put inside a plastic container filled with 10% NaCl solution which acts as the catholyte. Nichrome mesh was used for the electrodes. The angle of tilt mentioned in the set up for the anode chambers was ensured by a plastic base plate. The electrode immersed in the NaCl solution was connected to the negative terminal whereas the anode was connected to the positive terminal of the voltage source. A voltage of 30 V was applied initially and the current was noted. Based on the initial current reading, the applied voltage was adjusted as per Table 3.9 and was kept constant for the specified duration.

Figure 3.7 shows the experimental set-up of rapid migration test.

Table 3.9 Test voltage and duration for concrete specimen with normal binder content (NT BUILD 492)

Initial current (with 30 V) (mA)	Applied voltage U (after adjustment) (V)	Possible new initial current (mA)	Test duration t (hour)
$I_0 < 5$	60	$I_0 < 10$	96
$5 \leq I_0 < 10$	60	$10 \leq I_0 < 20$	48
$10 \leq I_0 < 15$	60	$20 \leq I_0 < 30$	24
$15 \leq I_0 < 20$	50	$25 \leq I_0 < 35$	24
$20 \leq I_0 < 30$	40	$25 \leq I_0 < 40$	24
$30 \leq I_0 < 40$	35	$35 \leq I_0 < 50$	24
$40 \leq I_0 < 60$	30	$40 \leq I_0 < 60$	24
$60 \leq I_0 < 90$	25	$50 \leq I_0 < 75$	24
$90 \leq I_0 < 120$	20	$60 \leq I_0 < 80$	24
$120 \leq I_0 < 180$	15	$60 \leq I_0 < 90$	24
$180 \leq I_0 < 360$	10	$60 \leq I_0 < 120$	24
$I_0 \geq 360$	10	$I_0 \geq 120$	6

Specimen fixed in the anolyte chamber

Filling 0.3 M NaOH in the anolyte chamber

RMT set up

Figure 3.7 Experimental set up of rapid migration test

After the specified duration, the specimens were taken out and split into two halves. On to the freshly split surface, 0.1 M silver nitrate solution is sprayed. Silver nitrate reacts with chlorides to form silver chloride which is white in colour. The white colour is an indication of the depth to which chloride have penetrated during the experiment. The penetration depths were measured at 10 mm intervals, and are averaged to get the depth of chloride ion penetration, which is used in the formula given in Equation 2.47 to calculate the non-steady state migration coefficient. Using the criteria given in Table 2.7, the concretes are classified qualitatively. The depth of chloride penetration measurement is shown in Figure 3.8.

Figure 3.8 Depth of chloride penetration measurement

3.4.5 **Chloride conductivity test**

The chloride conductivity test (CCT) was done according to the durability index testing procedure manual of South Africa (2009). The test was conducted at three ages - 28, 56 and 90 days. For all the tests described in the South African durability index testing procedure manual, the specimens are concrete discs of diameter 70 ± 2 mm and thickness 30 ± 2 mm. These specimens were obtained by coring from 150 mm size cubes. After the required days of curing, the cubes were removed from the moist room. A 70 mm diameter cylindrical sample was cored from the cube using a water cooled diamond-tipped core cutting machine. Coring was done in the direction perpendicular to the cast direction. After drying, the curved surfaces of the cored samples were coated with epoxy. Four specimens of 30 mm thickness were obtained from each core specimen. Figure 3.9 shows the schematic of specimen preparation for South African durability index tests whereas Figure 3.10 shows the photographs of the same.

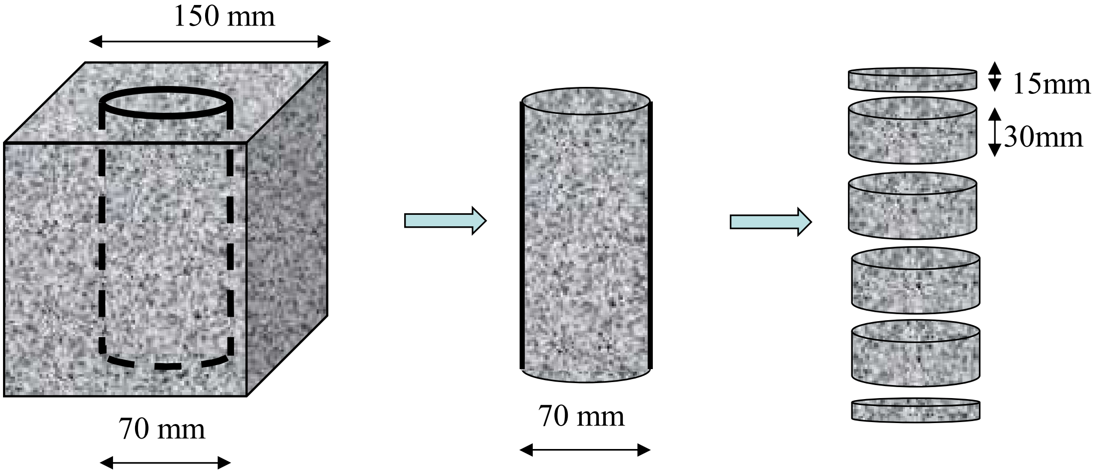

Figure 3.9 Specimen preparation for South African durability index tests

Coring Procedure **Cutting procedure**

Specimens of diameter 70 mm and thickness 30 mm

Figure 3.10 Core cutting, saw cutting, and epoxy coated (on surface) specimens for South African durability index tests

After cutting, the specimens were placed in a hot air oven maintained at 50 °C for seven days. After removing from the oven, the specimens were allowed to cool for two hours inside a desiccator. The dimensions were measured accurately from four diametrically opposite points and the average value was recorded. The weight of the specimens were also recorded. After this stage, the specimens were subjected to conditioning procedures with respect to the test conducted. The specimens for chloride conductivity test were vacuum saturated using 5 M NaCl solution following the standard procedure described in Section 3.4.3. After removing from the vacuum desiccator, the saturated weights of the specimens were measured.

Subsequently, each specimen was placed inside the rubber collar and then fitted to the chloride conductivity cells. The luggin probes were adjusted to touch the specimen. Both anodic and cathodic chambers as well as the luggin capillaries were filled with 5 M NaCl solution. The cell was connected to a power source and the voltage set to 10 V. With the help of a multimeter, the voltage developed across the specimen was measured. The voltage input was adjusted so that the voltage developed across the specimen became 10 V. At this stage, the current reading was recorded. Using the above measurements, the chloride conductivity of each of the test specimen was calculated using the formula given in Equation 2.48. Chloride conductivity index is calculated as the average of the chloride conductivity of at least three valid individual test determinations. Moreover, the porosity was calculated using the Equation 3.1.

$$n = \frac{M_s - M_D}{At\rho_s} \tag{3.1}$$

where

M_s	Vacuum saturated mass of the specimen (g)
M_D	Mass of the dry specimen (g)
A	Cross-sectional area of the specimen (mm^2)
t	Average specimen thickness
ρ_s	Density of salt solution = 1.19×10^{-3} g/mm^3

Figure 3.11 shows the experimental set up of chloride conductivity test.

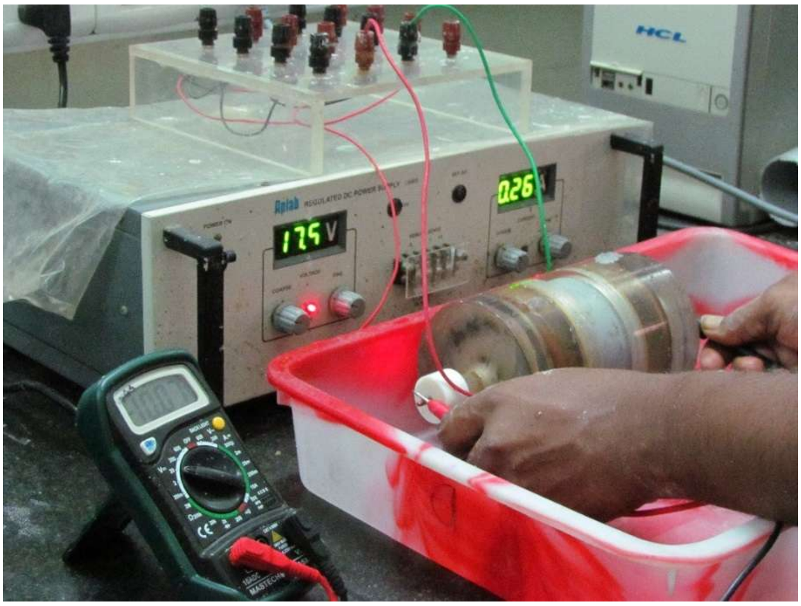

Figure 3.11 Experimental set up of chloride conductivity test

3.4.6 Oxygen permeability index test

In this test method, the pressure decay of oxygen passed through the concrete specimen placed in a falling head permeameter is measured. The coefficient of permeability to oxygen flow is determined using d'Arcy's law. This is done by finding the slope of the line obtained when the natural log of the ratio of initial pressure to the pressure at any time is plotted against time. The oxygen permeability index (OPI) which is the negative log of the coefficient of permeability, is used to classify concrete durability.

The specimens for the OPI tests were similar to those used for the chloride conductivity test. After cutting, the specimens were placed in an oven maintained at 50°C for seven days. After taking out from the oven, the specimens were placed inside the laboratory, maintained at a temperature of 25°C and RH < 60%, and allowed to cool for a period of two hours. The thickness and diameter of each specimen were measured with the help of a digital Vernier calliper. For each specimen, four measurements were taken at equally spaced points along the perimeter. The average value of the four measurements was recorded as average thickness and diameter of the specimen.

The specimens were placed inside the compressible rubber collar and then inserted into the stainless steel rigid sleeve such that the external face rested against the lip of the collar. The entire assembly was placed on top of the oxygen permeability cell to cover the opening. The O-ring present in the permeability cell ensured perfect fit. The apparatus was tightened properly. The inlet and outlet valves of the permeability cells were opened and oxygen was allowed to flow through the permeameter for about five seconds in order to purge other gases present in the cell. After this stage, the outlet valve was closed and when the pressure was just above 100 kPa the inlet valve was closed. The pressure was checked and if necessary, the inlet and outlet valves were adjusted so that the initial pressure reading was 100 ± 5 kPa. The pressure readings were noted and monitored. If the pressure dropped at a rate greater than 5 kPa per minute, leakage was suspected and the set up was rechecked. If there was no leakage, the readings were noted at fixed intervals or at every 30 minutes or 15 minutes. The test was terminated after 6 hours or when the pressure had dropped to 50 kPa, whichever happened first. Using the pressure and time readings, the OPI was calculated using Equations 2.51 and 2.52. Figure 3.12 shows the photograph of the OPI test set up.

Drying of specimens in oven set at 50°C

Specimens with compressible rubber collar and stainless steel rigid sleeve

Oxygen Permeability Index test set up

Figure 3.12 Oxygen permeability index test set up

3.4.7 Torrent air permeability test

The air permeability of the concrete was determined using Torrent air permeability apparatus which is based on the Swiss standard SIA 262/1 - E. The specimens used for this test were 150 mm size cubes. All the four surfaces perpendicular to the cast surface were tested and the average value was reported as the coefficient of air permeability (kT). A time interval of 30 minutes was given between two measurements. This test was conducted at 28 and 90 days.

In order to study the effect of specimen conditioning, three kinds of drying procedures were adopted on one set of samples. These are: (1) drying in 50°C oven for seven days, (2) drying in 105°C oven for one day and (3) drying in standard laboratory conditions (at 25°C and 65% RH) for three weeks. For the other sample set, only the first conditioning methodology was followed. After removing from the oven, the specimens were allowed to cool to the laboratory conditions for a minimum of two hours.

After connecting a vacuum pump to the Permea – Torr^{TM} instrument, the machine was calibrated following the procedure mentioned in the user manual with the help of the impervious disc provided with the instrument. Before doing the test, the test surfaces were cleaned thoroughly using a plastic/nylon brush and soft cotton cloth. Once the machine is started, the vacuum pump starts automatically. After ten seconds, the vacuum cell was placed on top of the test surface. As a result, vacuum was created inside the two chambers of the cell. When the pressure in the inner chamber dropped to the pre-defined level, the electro valve 2 (in Figure 2.22) automatically closes and the inner chamber gets isolated from the pump. The air from inside the pores of the surface layer enter this chamber causing the pressure to increase. The external chamber, connected to the vacuum pump, through a pressure regulator maintains the pressure in both chambers as uniform. Data collection was started at time $t = 60$ seconds when the pressure in the inner chamber was recorded as P_0. The difference between the pressures in the inner chamber at time t ($Pi(t)$) and initial pressure (P_0) was calculated by the instrument as ΔP and recorded at each 15 second interval. The measurements were periodically taken until the following three conditions are satisfied:

a) $\Delta P_{ieff}(t) = \Delta P(t) - \Delta P_{cal}(t) \geq 20$ mbar

b) $t = 720$ s (12 min)

c) The penetration of the test L has reached or exceeded a user-defined value L_{max},

in which $\Delta P_{cal}(t)$ is the pressure increase recorded in the Calibration phase; $\Delta P(t)$ is the measured difference in pressure; $\Delta P_{ieff}(t)$ is the effective pressure increase in the inner chamber.

Using these time and pressure difference measurements, by applying the formula presented in Equation 2.55, the coefficient of air permeability kT is calculated in m^2 and is displayed by the machine. After completing the experiments, the data are downloaded from the instrument. kT value is used to classify the concrete qualitatively as per Table 2.10. Figure 3.13 shows the experimental set up of the Torrent air permeability test.

Figure 3.13 Torrent air permeability test

3.4.8 Accelerated carbonation test

The specimens for the accelerated carbonation test were prisms of size 100 mm × 100 mm × 500 mm. These specimens were cured in the moist room for a period of 28 days. Subsequently, they were air cooled in laboratory conditions for 14 days at 25°C and 65% RH. On the 42nd day, the specimens were transferred to the accelerated carbonation chamber, which was set at the conditions of 1% CO_2 concentration, 25°C and 65% RH. Before inserting into the carbonation chamber, the cross sectional surfaces were coated with an anti-carbonation coating. This step ensured the penetration of carbon dioxide through the side surfaces. The testing was done at four ages - 70, 98, 112 and 198 days from the day of casting, such that the days of exposure in the carbonation chamber were 28, 56, 70 and 112 days. On the specified dates, the specimens were taken out and cut at a distance of 10 cm from one end using a custom made concrete cutter. On the freshly cut surface, 1% phenolphthalein indicator was sprayed. As mentioned in Section 2.4.7, the non-carbonated concrete appeared pink whereas the carbonated concrete was colourless. After 5 minutes, carbonation depths were measured at each 10 mm interval and were averaged to get the depth of carbonation. Two specimens were tested in this way and the average value is reported as the depth of carbonation at that age. After splitting, the remaining portion of the specimen was placed back into the carbonation chamber after applying anti-carbonation coating on the freshly cut surface. The carbonation depth measurements obtained for the four time periods were used to calculate the rate of carbonation and carbonation resistance. Figure 3.14 shows the schematic of carbonation depth measurements whereas Figure 3.15 indicates the photographs of the accelerated carbonation test.

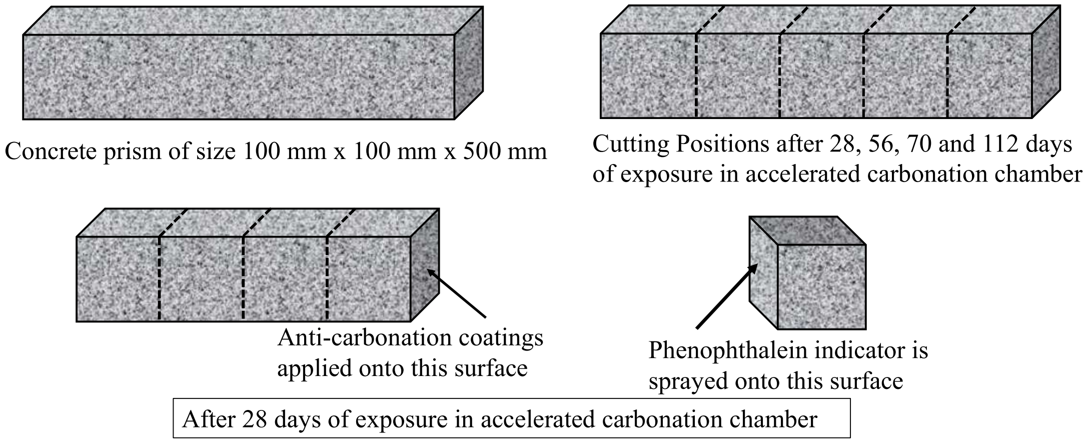

Figure 3.14 Schematic of carbonation depth measurement

Accelerated carbonation chambers

Splitting of specimens

Specimens sprayed with Phenolphthalein indicator

Figure 3.15 Accelerated carbonation test showing the chambers, splitting of specimens, and depths indicated after spraying phenolphthalein

3.4.9 Water sorptivity test

Water sorptivity test was done as per the durability index testing procedure manual of South Africa. The specimen details and the preparation methods were already described in the previous sections on chloride conductivity test and oxygen permeability index test. After removing from the 50°C oven, the specimens were cooled for two hours in the laboratory conditions (temperature 25°C and RH < 60%). The thickness and the diameter of the specimens were measured and the average values (average of four readings taken at four equally spaced points along the perimeter) were recorded. Knife edges were placed in a shallow tray and saturated calcium hydroxide solution was poured into the tray. After measuring the initial dry weights, the specimens were placed on top of the knife edges such that the level of the solution was approximately 2 mm up the side of the specimen. Immediately after placing the first specimen, the stopwatch was started and kept running until the end of the sorptivity weight measurements. The weight of each specimen was measured at 3, 5, 7, 9, 12, 16, 20, and 25 minutes after initial placement. The weights were taken in such a way that the order in which the specimens were placed into the solution was strictly maintained. Each weight measurement was taken after patting the wet surface of the specimen on a wet soft cloth. During the removal of the specimen from the tray, extreme care was taken not to drip the solution onto the top surface of other specimens. After the last reading, the stopwatch was stopped. Within a day, the tested samples were placed inside the desiccator and were vacuum saturated. Subsequently, the fully saturated weights of the specimens were obtained.

The water sorptivity is calculated using Equation 2.58. The sorptivity index is calculated as the average of water sorptivity of at least three valid individual test results. Further, the porosity of each specimen can be calculated using the formula given in Equation 3.2.

$$n = \frac{M_{sv} - M_{s0}}{A d \rho_w} \times 100 \tag{3.2}$$

where

M_{sv}	Vacuum saturated mass of the specimen (g)
M_{s0}	Mass of the dry specimen at time t_0 (g)
A	Cross-sectional area of the specimen (mm^2)
d	Average specimen thickness (mm)
ρ_w	Density of water (g/mm^3)

Figure 3.16 shows the water sorptivity test set up.

Figure 3.16 Water sorptivity test set up

3.4.10 Water permeability test

The water permeability test was done according to the German standard DIN 1048 part 5. The specimens were 150 mm size cubes which were cured for 28 days. After removing the cube from the moist room, a test surface was selected perpendicular to the cast face and was roughened using a steel wire brush. The specimens were mounted on to the permeability cells and were tightened well in order to avoid water leakage. To ensure complete water proofing, a thin layer of silicon grease was applied on the outside interface between the rubber washer and the concrete cube specimen. The air compressor was kept switched on, followed by the water inlet valve. A 5 bar (0.5 N/mm^2) water pressure was applied on the top of the cube by adjusting the air pressure through a valve system. This pressure was kept constant for a period of three days. After three days, the pressure was released and the specimens were removed from the permeability cell. Immediately after removing, the specimens were split into two. Before evaporation, the depth of water penetration was marked with the help of a marker pen. The maximum and the average depth of the water penetration were recorded. Figure 3.17 shows the water permeability test set up and measurement.

In order to study the specimen conditioning effect, one set of cubes was dried in the 50°C oven for seven days. This conditioning procedure is similar to that followed for the sorptivity determination. After cooling down for two days, these specimens were mounted onto the permeability cells and tested following the procedure described above.

Water permeability test setup

Split specimen indicating the depth of water penetrated

Figure 3.17 Water permeability test – set up and measurement

3.5 MICRO – ANALYTICAL TESTS

In order to understand the behaviour of mixes with different binders, micro analytical tests such as Scanning Electron Microscopy (SEM), X – Ray Diffraction (XRD) and Thermo Gravimetric/ Differential Scanning Calorimetry (TG/DSC) were performed on mixes having a total binder content of 310 kg/m^3 and w/b 0.5. The following sections give the details of the tests along with sample details.

3.5.1 Scanning electron microscopy

Scanning electron microscopy (SEM) is a powerful tool that is used to study the morphology and distribution of different phases present in a material. SEMs use a beam of high energy electrons to examine objects on a very fine scale. The electrons undergo different types of interactions with the specimen, which leads to the production of secondary electrons (SE), backscatter electrons (BSE) and X-rays. Analysis of the BSE image produced along with the energy dispersive X-ray analysis (EDS) helps to identify different products or phases present in the microstructure of the material.

The identification of carbonated and chloride-bound products in the microstructure of concrete with different SCMs was done with the help of SEM. In order to study the microstructural changes happening due to carbonation, the samples were prepared from concrete specimens subjected to accelerated carbonation for a period of 154 days. After checking the depth of carbonation, 20 mm × 20 mm × 3 mm samples were prepared from the corner section. Figure 3.18 shows the schematic of the specimen preparation for SEM from specimens subjected to accelerated carbonation.

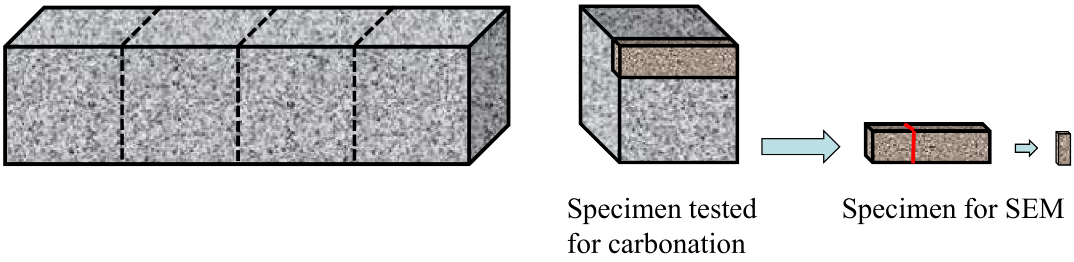

Figure 3.18 Schematic of the specimen preparation for SEM from specimens subjected to accelerated carbonation

The samples to study the micro structural alterations due to chloride ingress were obtained from specimens obtained from cylinders of diameter 100 mm and height 200 mm. After 28 days of mist room curing, the cylinder is removed from the mist room and is coated with epoxy at all surfaces. After the epoxy get cured, the concrete sample is sliced into two at the middle used a water cooled diamond saw. The two specimens thus obtained are vacuum saturated with saturated $Ca(OH)_2$ solution. After vacuum saturation, the specimens were immersed in 3% NaCl solution for 35 days. Figure 3.19 shows the schematic of specimen preparation for SEM and XRD to be immersed in chloride solution.

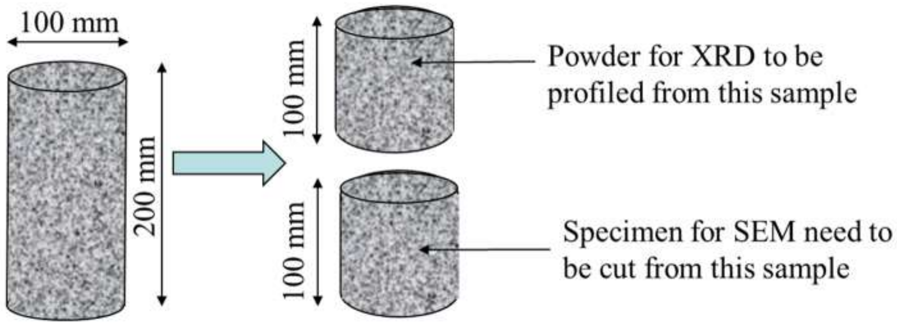

Figure 3.19 Schematic of specimen preparation for SEM and XRD to be immersed in chloride solution

After 35 days, the specimens were taken out of the chloride solution and one sample is split into two halves and the specimen for SEM is prepared as depicted in the schematic diagram presented in Figure 3.20.

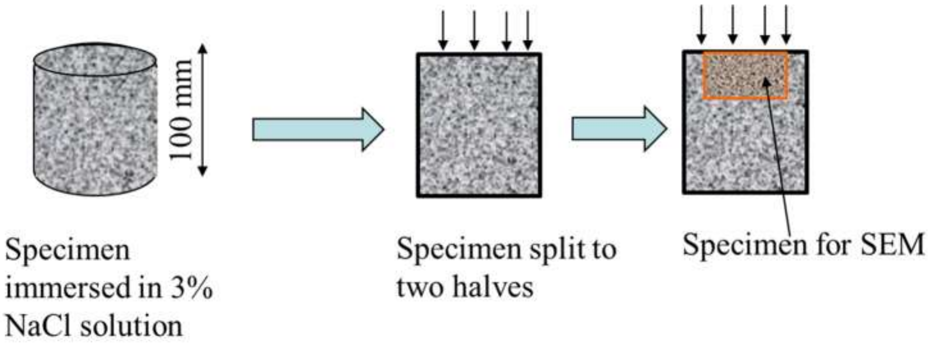

Figure 3.20 Schematic of the specimen preparation for SEM from specimens immersed in chloride solution

The samples obtained after cutting were put in acetone for 24 hours to eliminate moisture. After proper labelling, the samples were impregnated by a low modulus epoxy using a vacuum impregnating device at 0.1 bar pressure. After the epoxy got cured, the specimens were coarse polished using silicon carbide powder of # 1000 size and glycerin on a cast iron disc. Coarse polishing was done in order to remove extra epoxy from the specimen surface. After coarse polishing, the specimens were fine polished on a diamond cloth using poly crystalline diamond spray of sizes 6 µm, 3 µm and 1 µm for a period of 3 hours, 2 hours and 1.5 hours respectively. The polished specimens were coated with Au-Pd (sputter coating) to make them conductive in order to avoid charging. In addition to BSE imaging, in order to identify the composition of different products formed, the X-rays emitted from the samples were also collected by the EDX detector. Figure 3.21 shows the photographs of different stages of specimen preparation for SEM BSE imaging.

Cutting

Vacuum impregnation

Coarse polishing

Fine polishing

Prepared specimen

Sputter coating

Figure 3.21 Photographs of different stages of specimen preparation for SEM BSE imaging

Figure 3.22 shows the photograph of the Scanning Electron Microscope used in this study (Model: FEI Quanta 200, Manufacturer: FEI Company).

Figure 3.22 The Scanning Electron Microscope used in this study
(FEI Quanta 200, FEI Company)

3.5.2 X – ray diffraction

In X-ray diffraction (XRD) technique, the X-rays are scattered by atoms in a periodic lattice. The scattered monochromatic X-rays that are in-phase give constructive interference. In order to identify unknown substances, the powder diffraction pattern is recorded with the help of a diffractometer. The output of the XRD instrument is a plot between 2θ and intensity of X-ray counts, where 2θ is the total deviation between the incident beam and the diffracted beam. This output data is compared with the standard patterns for various compounds that are available in the database maintained by the International Joint Committee on Powder Diffraction Standards (JCPDS database). The comparison process can also be done with the help of a search and match software like X’Pert HighScore Plus from Pan Analytical Inc. Figure 3.23 shows the XRD instrument used in this study (Model No. D8, Manufacturer: Bruker Corporation).

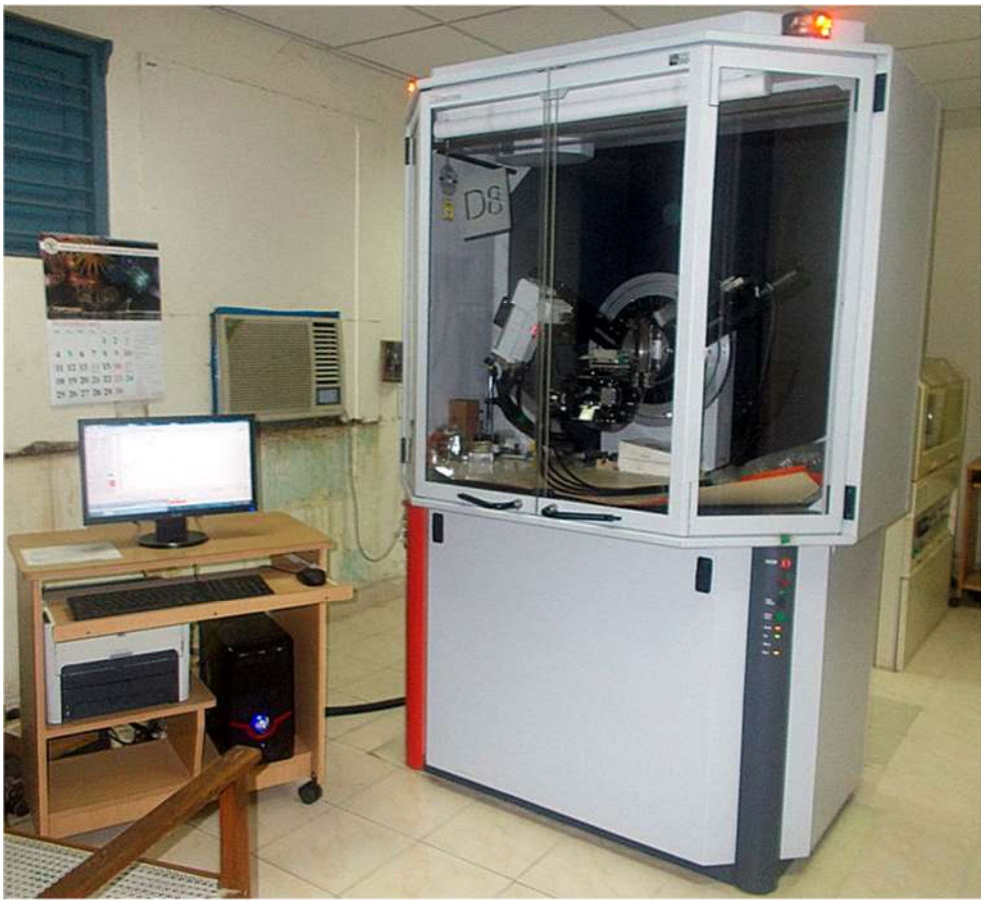

Figure 3.23 The X - Ray Diffraction instrument used in this study (D8, Bruker Corporation)

In the present project, X–ray diffraction (XRD) technique is used in two studies. In order to identify the different products formed when concrete with different binders were subjected to chloride penetration, the powder resulting from chloride profiling was subjected to XRD. The schematic of the specimen preparation has already presented in Figure 3.19. The powder samples from different layers were sieved through 75 µm sieve for the XRD. This study and the BSE imaging from SEM were used complementarily to each other.

To study the chemical and phase changes due to carbonation, powder samples which were completely carbonated were prepared from paste specimens of 9 mm diameter and 30 mm height following the procedure described below. In this case, all the paste samples had a w/b of 0.5. The specimens were cast in an acrylic mould and kept covered. On the second day, the specimens were removed from the moulds and put inside saturated lime water for curing. After 28 days of curing under saturated $Ca(OH)_2$

solution, the specimens were air dried for 14 days at 25°C and 65% RH. Then, these were introduced into the carbonation chamber maintained at 3% CO_2 concentration, 25°C and 65% RH. The weights of specimens were monitored regularly. A set of four samples were tested in each category. After reaching constant weights, complete carbonation was ensured by phenolphthalein test on the split surface of one specimen. The three other specimens were stored for a week inside acetone to remove any water and to stop hydration. Subsequently, they were dried, crushed and sieved through 75 µm sieve and were stored in polythene bags inside a desiccator until testing. These powdered samples were subjected to XRD to analyse crystalline phases that are formed due to carbonation. Figure 3.24 shows the paste specimens of 9 mm diameter and 30 mm height that were used to study the chemical and phase changes due to carbonation.

Figure 3.24 Paste specimens of 9 mm diameter and 30 mm height to study the chemical and phase changes due to carbonation

3.5.3 Thermo gravimetric analysis

The thermal analysis performed in this study was TG/DSC in which thermo gravimetric analysis (TGA) data was provided as a supplementary characterization information to differential scanning caloriemetry (DSC). DSC is a thermal analysis technique in which heat is supplied or removed to a sample that undergoes thermal transformation in order to keep it at the same temperature as the reference material. In TGA, the amount and rate of change in the mass of a sample is measured as a function of temperature or time in a controlled atmosphere. This technique can be used to study materials that show either mass loss or gain due to decomposition, oxidation/reduction or loss of volatiles such as moisture.

Two studies were performed using TGA in this project work – one to determine the portlandite content and the other to find the degree of carbonation. To find the portlandite content, paste samples were cast and were cured in saturated lime water. This test was conducted at two ages 28 days and 90 days. After the required days of curing, the samples were crushed and sieved through 75 μm sieve and analysed using TG/DSC technique. The test was conducted from 30°C to 1200°C, at a heat rate of 10 °C per minute. In order to study the degree of carbonation, the powder samples were prepared using the method described in Section 3.5.2. The thermal analysis investigation was conducted from 30°C to 1000°C, at a heat rate of 10°C per minute. Figure 3.25 shows the TG/DSC instrument used in this study (Model No. STA 409 TC, Manufacturer: Netzch Technologies).

Figure 3.25 The TG/DSC instrument used in this study
(STA 409 TC, Netzch Technologies)

3.6 SUMMARY

The details of the materials used, experimental design and the procedures of different experiments used in this study were described in this chapter. The details presented include the properties of the materials used for making concretes, concrete mixture proportions, mixing procedures, fresh properties and curing methodology, the test variables, the testing procedure adopted for mechanical, durability and micro-analytical tests.

CHAPTER 4

DATABASE OF DURABILITY PARAMETERS AND STRENGTH GRADE CLASSIFICATION

4.1 INTRODUCTION

Even though SCMs are specified in many construction projects in India, the specifications are random and are not based on any solid experimental database (Dhanya and Santhanam, 2013). A database of the durability parameters with the commonly used SCMs is required, which can act as a guideline for the material selection for a particular service environment. Further, the influence of the SCMs on the durability parameters can be reaffirmed.

In the present chapter, the concept of strength grade classification is developed based on four durability parameters, namely the surface resistivity (from Wenner 4-probe surface resistivity test), charge passed (from rapid chloride permeability test), sorptivity index (from water sorptivity test) and oxygen permeability index (from oxygen permeability index test). The first two tests are related to chloride ion penetrability. Water sorptivity test is a measure of the water penetrability whereas oxygen permeability index test measures the resistance against gas penetrability.

The test methods are selected in such a way that one commonly used test method representing the chloride ion penetrability, water penetrability and gas penetrability is addressed. Surface resistivity is selected because it is a simple test which can be done on site, and additionally there is good correlation between surface resistivity and other tests related to chloride ion penetrability such as RCPT, RMT, CCT etc. Moreover, these tests are performed for all the mixes studied in this project. Thus, while classifying the mixes in strength grade, there was possibility to get the representative mixes in almost all categories. Hence, these test methods were selected for developing the strength grade classification.

Based on the performance in these durability tests, the concretes were classified into four durability classes such as Poor, Moderate, Good and Excellent centered on the four different durability parameters under consideration. The classification criteria were adopted from the current standards or from available literature. As mentioned in Section 2.4.1, there are many classification criteria available for surface resistivity and the test is yet to get standardized. The criteria adopted here is recommended by ACI Committee report 222R (2001), which relates resistivity and corrosion rate presented in Table 2.5. The benchmarks for charge passed were developed from the ASTM standard (ASTM C 1202, 2010), in which it is related to chloride ion penetrability as already presented in Table 2.6. The category of negligible chloride ion penetrability (i.e., total charge passed less than 100 Coulombs) is eliminated here as the present criteria deals with low to medium grade concrete where this level of very low penetrability is rare. With regard to oxygen permeability index and sorptivity index, the classification criteria adopted is based on Alexander et al. (1999), who are the developers of these tests. This criteria is widely used in South Africa to classify concrete qualitatively. Table 4.1 indicates the different durability classes along with the limiting values of each parameter.

Table 4.1 Classification criteria based on durability parameters

Durability Class	Durability parameter			
	Surface Resistivity (kΩ.cm)	Charge passed (Coulombs)	Oxygen Permeability Index	Sorptivity Index (g/√hr)
Poor	<5	>4000	<9	>15
Moderate	5-10	2000-4000	9-9.5	12-15
Good	10-20	1000-2000	9.5-10	6-12
Excellent	>20	<1000	>10	<6
Basis of selection	ACI 222R, 2001	ASTM C1202, 2010 *	Alexander et al., 1999	Alexander et al., 1999

*Category <100 is eliminated as is not suitable for ordinary concrete

4.2 DATABASE OF DURABILITY PARAMETERS AND COMPRESSIVE STRENGTH

The database of the durability parameters and compressive strengths for the concretes in the current study is presented in the appendix in Tables B1 to B10.

Based on the results obtained, the concrete mixtures with different binders are ranked on a scale of 1 to 4 with 1 being the best. Table 4.2 gives the qualitative ranking based on the performance at 28 days whereas

Table 4.3 gives qualitative ranking based on the performance at 90 days.

The ranking is developed based on an absolute analysis. In this analysis, all the mixtures were given ranking based on the classification criteria adopted in this study. Based on the ranking obtained for each mixture from the classification criteria, the average ranking for mixes having different SCM dosages for a particular test is determined. In the case of ranking related to chloride ion penetrability, based on the average ranking for each tests, the average ranking for all the tests related to chloride ion penetrability are calculated and is then converted to a scale from 1 to 4. In the case of ranking for concretes with regard to water sorptivity, gas penetrability and CO_2 penetration, the ranking depends on only one test in each category such as water sorptivity test, OPI test and accelerated carbonation test. Here also, the ranking is based on the average value of the ranks obtained from the classification criteria.

Table 4.2 Qualitative ranking of concretes with different binders based on the performance at 28 days

Concrete resistance against	Binder type								
	OPC	Slag			Class F fly ash			Class C fly ash	
		15%	30%	50%	15%	30%	50%	15%	30%
Chloride ion penetration	4	3	2	1	2	2	1	4	3
Water sorptivity	3	2	2	1	3	2	2	3	2
Gas permeability	2	1	1	1	1	1	1	1	1
CO_2 penetration	1	1	2	2	3	4	4	3	4

Table 4.3 Qualitative ranking of concretes with different binders based on the performance at 90 days

Concrete resistance against	Binder type								
	OPC	Slag			Class F fly ash			Class C fly ash	
		15%	30%	50%	15%	30%	50%	15%	30%
Chloride ion penetration	3	2	2	1	2	1	1	3	2
Water sorptivity	3	2	2	1	2	2	2	2	2
Gas permeability	1	1	1	1	1	1	1	1	1

It can be seen from Table 4.2 that the best performance with regard to chloride penetration is for concretes with Class F fly ash and slag at 50% replacement level. Slag at 30% replacement level and Class F fly ash at 30 and 15% replacement levels are ranked next whereas 15% slag and 30% Class C fly ash mixes are at the next lower level. OPC mixes showed the worst performance in this category. In the case of water sorptivity, the best performance was again by concretes with 50% slag mixes. Mixes with OPC and Class C fly ash at 15% replacement were at the lowest level whereas all the other mixes fell in the second level. With respect to gas permeability, all the mixes were either in the good or very good category. Further, a similarity in trends is observed in the results from both OPI and Torrent tests. There was only a marginal decrease in the performance level of the OPC mixes, which were ranked 2. With regard to CO_2 penetrability, the best performance was by OPC and 15% slag mixes followed by 30% and 50% slag mixes. Fly ash mixes showed poor performance, with higher replacement levels getting low ranks. Both Class F and Class C fly ash mixes at 15% got a ranking of 3 whereas the other replacement levels were ranked 4.

At 90 days, most of the concretes showed a jump to the next higher durability level. All the concretes achieved the best durability class in the gas permeability tests. With regard to chloride penetration, the best performances were exhibited by 50% slag and 30% and 50% Class F fly ash mixes. OPC and Class C fly ash at 15% replacement levels showed the poorest performance at this age also; however, the durability rank got improved by one level, i.e., they were ranked 3 compared to the previous (28 days) rank of 4. Other mixes showed intermediate performance. For water sorptivity, the best performance was by slag mixes at 50% replacement level. The poorest performance was by OPC while the other mixes showed intermediate performance.

4.3 DURABILITY PARAMETERS VERSUS COMPRESSIVE STRENGTH

Conventionally, compressive strength is considered as the only crucial performance parameter for concrete, and it is assumed that if the strength is good, the durability can automatically be achieved. However, both research and practical experiences show clearly that strength and durability are not related (Mehta, 2001, Alexander et al., 2011, Basheer et al., 2005). Strength depends on the total porosity of the structure whereas durability depends on the pore connectivity.

The plots in Figure 4.1 to 4.4 explore the relationships between the durability parameters (surface resistivity, total charge passed, Oxygen Permeability Index and sorptivity index respectively) and compressive strength. The figures clearly show the extent of scatter in the data, and no semblance of a correlation can be picked out.

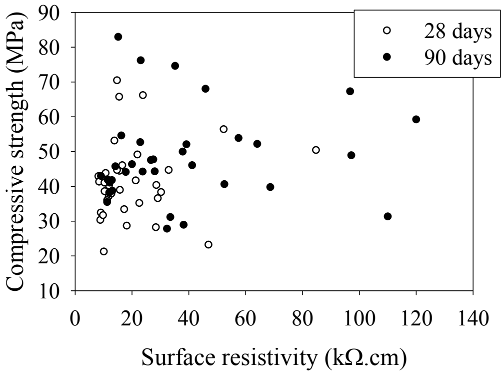

Figure 4.1 Plot showing poor correlation between compressive strength and surface resistivity

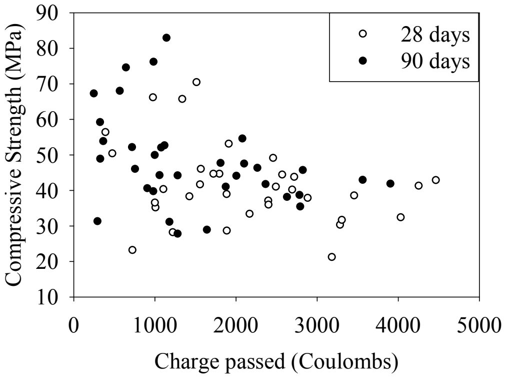

Figure 4.2 Plot showing poor correlation between compressive strength and charge passed

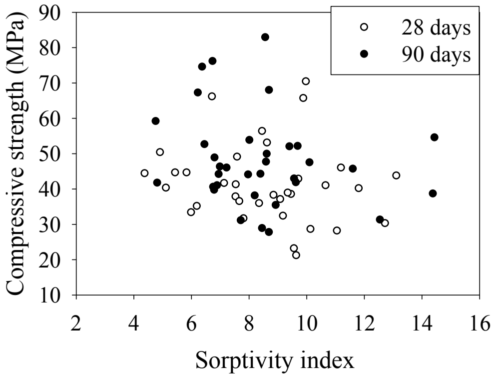

Figure 4.3 Plot showing poor correlation between compressive strength and sorptivity index

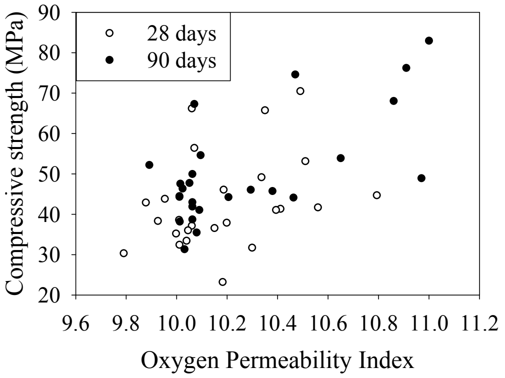

Figure 4.4 Plot showing poor correlation between compressive strength and oxygen permeability index

From the figures presented above, it is clear that for the current set of data, there is no direct correlation between compressive strength and the durability parameters. Thus, an alternative strategy is required to provide an engineering perspective to the database. This is attempted in the following section, which explores the use of a durability class within specific strength grades.

4.4 STRENGTH GRADE CONCEPT

Achievement of durability in high strength and high performance concrete is not that difficult as the microstructure in these types of concretes is well developed. Producing durable concrete at lower strength levels is still a challenge. There is a distinct need to address durability in such concretes, as they are used majority of the time for a variety of projects ranging from residential to infrastructure. The goal of achieving durability in low strength grade concretes can only be achieved by the use of SCMs. However, there is lack of clarity on how much is the extent of improvement in each of these parameters when SCMs are used. Thus, a combined study of all these parameters in the same concrete is essential.

Ramezanianpour et al. (2011) did a comparative study on the relationship between concrete resistivity, water penetration, RCPT and compressive strength. The authors were able to get good correlation between resistivity and water penetration as well as resistivity and RCPT. However, they were not able to achieve any correlation between compressive strength and surface resistivity. In another study by Burden (2006) on concrete mixtures with different w/b and fly ash replacement levels, the author drew the conclusion that fly ash had greater influence on durability parameters than on strength. The tests conducted included compressive strength, RCPT and accelerated carbonation test. The author re-emphasized that strength is not a good indicator of durability. On the contrary, in a correlation study between compressive strength and certain durability indices of plain and blended cement concretes, Al-Amoudi et al. (2009) obtained good correlation between compressive strength and certain selected durability indices corresponding to chloride permeability and coefficient of chloride diffusion irrespective of the mix design parameters. This observation differs with other available literature. The binders used in the study included Type I cement, silica fume and fly ash. Indeed, most of the literature agrees to the fact that SCMs influence the durability parameters more compared to strength. The reasons for the same are due to the filler effect as well as pozzolanic reaction, which eventually leads to more tortuous pore structure and alterations in the pore solution chemistry (Deschner et al., 2012, Andrade and Buják. 2013).

Baroghel-Bouny et al. (2006) classify the durability indicators into two, viz., universal indicators and complementary parameters. The universal indicators are basic physical and chemical properties that are directly related to transport properties as well as microstructural characteristics such as initial $Ca(OH)_2$ content, porosity, chloride diffusion coefficient, gas/liquid permeability etc. The complementary or optional parameters need to be evaluated many a times because they appear in many predictive models. Examples of such parameters include the surface chloride concentration, chloride binding capacity etc. Potential durability classes corresponding to each durability indicator such as very low, low, medium, high and very high were developed, which can be used as a tool for mixture comparison. The DIs were determined at different ages (28, 90, 120 and 180 days) on saturated concretes along with 28 day characteristic compressive strength values (Baroghel-Bouny, 2002). Even though an overall correlation between chloride diffusion coefficients and 28 day compressive strength has been reported, it is proved that mineral additives like fly ash can produce durable concrete at lower strength level, which violates the correlation. Further, using the same database, a multi-level modelling concept by combining the durability indicators and physical/chemical models was proposed, which can be applied at four levels of sophistication. However, this approach seems to be very complicated for practicing engineers. Further, combining the DIs measured at different ages (28, 90, 120 and 180 days) with 28 day compressive strength seems to be illogical. For engineering purposes, simple qualitative tables are more suitable rather than complicated models on quantification.Table 4.4 and

Table 4.5 indicate the durability parameters in the present study at 28 and 90 days respectively. Different colour codes are used to demarcate the levels of durability. The colour codes used are: red – poor; orange – moderate; yellow – good and green – excellent category. The mixes are divided into 5 strength classes or grades such as 20-30, 30-40, 40-50, 50-60, and >60. Concrete mixes having mean compressive strength between 20 to 30 MPa fall under strength grade 20 - 30. Typically this category would include mixes having characteristic compressive strength of 20 MPa, in other words M20 grade concrete. In a similar way, the entire matrix involves low to medium strength concretes that are used for general purposes, i.e., from M20 to M50.

Table 4.4 Matrix of durability parameters and compressive strength at 28 days

Strength grade	w/b	Binder content (kg/m^3)	SCM content	Compressive strength	Surface Resistivity test	RCPT	OPI test	Sorptivity test	
				f_{ck} av.,28 MPa	SR av.,28 kΩ.cm	TC av.,28 Coulombs	OPI av., 28	SI av., 28 mm/√hr	Slope av.,28 g/√hr
20-30	0.65	280	30% Class F fly ash	21.27	10.08	3180		9.63	4.77
	0.5	310	50% Class F fly ash	23.22	46.92	720	10.18	9.56	2.80
	0.65	280	30% Slag A	28.22	28.42	1220		11.05	3.54
	0.65	280	30% Slag B	28.69	18.17	1885		10.13	3.39
	0.65	280	0	29.90	8.88	3285		12.72	4.27
30-40	0.6	310	15% Class C fly ash	31.71	9.80	3305	10.30	7.81	3.11
	0.6	310	0	32.44	9.02	4030	10.01	9.18	4.14
	0.5	310	20% Class F fly ash+ 20% Class C fly ash	33.42	17.25	2170	10.48	5.99	1.71
	0.5	310	30% Class F fly ash	35.20	22.58	1010	10.01	6.18	2.15
	0.6	310	15% Slag A	36.01	11.27	2400	10.05	8.35	2.58
	0.4	380	50% Class F fly ash	36.58	29.08	1000	10.15	7.66	1.70
	0.55	340	15% Slag A	37.15	11.83	2400	10.06	9.08	3.26
	0.5	310	30% Class C fly ash	37.89	12.75	2885	10.20	7.53	3.12
	0.5	310	20% Slag B+ 20% Class F fly ash	38.34	30.25	1425	9.93	8.85	2.85
	0.6	310	15% Slag B	38.58	10.38	3460	10.01	9.45	4.04
	0.6	310	15% Class F fly ash	38.96	15.75	1885	10.08	9.34	4.15

Strength grade	w/b	Binder content (kg/m^3)	SCM content	Compressive strength	Surface Resistivity test	RCPT	OPI test	Sorptivity test	
				f_{ck} av.,28 MPa	SR av.,28 kΩ.cm	TC av.,28 Coulombs	OPI av., 28	SI av., 28 mm/√hr	Slope av.,28 g/√hr
	0.55	340	15% Class F fly ash	39.90	11.92	2690	10.16	11.80	5.29
40-50	0.5	310	20% Slag B + 20% Class C fly ash	40.01	28.58	1105	10.04	5.11	1.45
	0.5	310	15% Class C fly ash	41.06	10.31	2490	10.39	10.65	4.01
	0.55	340	15% Class C fly ash	41.33	8.45	4250	10.41	7.54	3.41
	0.4	380	30%Flyash F	41.69	21.33	1555	10.56	7.13	1.75
	0.55	340	0	42.89	8.19	4465	9.88	9.71	4.09
	0.5	310	0	43.81	10.73	2720	9.95	13.11	3.32
	0.55	340	15% Slag B	44.47	15.58	2570	10.01	4.37	1.27
	0.5	310	15% Slag A	44.69	14.75	1795	10.79	5.83	1.77
	0.5	310	30% Slag B	44.69	32.92	1720	10.66	5.43	1.18
	0.5	310	15% Class F fly ash	46.07	16.58	1570	10.19	11.19	3.58
	0.5	300	0	46.14	10.86	3295	10.13	9.21	3.62
	0.4	340	0	47.49	16.08	2225	9.98	2.93	0.87
	0.45	340	0	47.83	9.96	3130	9.76	4.65	1.42
	0.45	320	0	48.44	10.81	2735	9.93	4.30	1.25
	0.4	400	0	48.84	9.575	2135	9.87	6.64	2.3
	0.5	310	15% Slag B	49.15	21.92	2460	10.34	7.58	2.18

Strength grade	w/b	Binder content (kg/m^3)	SCM content	Compressive strength	Surface Resistivity test	RCPT	OPI test	Sorptivity test	
				f_{ck} av.,28 MPa	SR av.,28 kΩ.cm	TC av.,28 Coulombs	OPI av., 28	SI av., 28 mm/√hr	Slope av.,28 g/√hr
50-60	0.5	310	50% Slag B	50.41	84.75	475	10.73	4.91	1.29
	0.55	300	0	50.83	10.17	4200	9.80	11.02	3.78
	0.4	380	15%Flyash F	53.14	13.83	1910	10.51	8.62	1.79
	0.4	360	0	54.05	13.5	2770	9.87	5.37	1.86
	0.4	380	50% Slag	59.08	52.25	390	10.07	8.45	1.44
>60	0.4	380	15% Slag	65.74	15.50	1340	10.35	9.88	2.41
	0.4	380	30%Slag	66.2	23.83	975	10.06	6.71	1.02
	0.4	380	0	70.48	14.75	1515	10.49	9.97	2.35

Table 4.5 Matrix of durability parameters and compressive strength at 90 days

Strength grade	w/b	Binder content	SCM content	Compressive strength	Surface Resistivity test	RCPT	OPI test	Sorptivity test	
				f_{ck} av.,90 MPa	SR av.,90 kΩ.cm	TC av.,90 Coulombs	OPI, av.,90	SI av., 90 mm/√hr	Slope av.,90 g/√hr
20-30	0.65	280	30% Slag B	27.81	32.33	1280		8.69	2.41
	0.65	280	30% Slag A	28.95	38.17	1640		8.45	2.70
30-40	0.65	280	30% Class F fly ash	31.14	33.50	1180	10.01	7.71	2.90
	0.5	310	50% Class F fly ash	31.33	110.00	290	10.03	12.54	2.39
	0.65	280	0	35.46	11.27	2790	10.08	8.92	2.69
	0.6	310	15% Slag B	38.17	11.99	2630	10.01	8.20	2.75
	0.6	310	15% Class C fly ash	38.72	13.08	2780	10.06	14.38	5.67
	0.5	310	30% Class F fly ash	39.77	68.67	980	10.73	6.79	1.33
40-50	0.5	310	20% Slag B + 20% Class C fly ash	40.61	52.50	905	10.82	6.75	1.67
	0.55	340	15% Slag A	41.04	12.17	1875	10.09	6.89	1.71
	0.6	310	15% Slag A	41.78	12.92	2365		4.81	1.23
	0.6	310	0	41.89	11.45	3905	10.06	9.62	4.10
	0.55	340	0	42.98	9.08	3560	10.06	9.56	3.90
	0.5	310	15% Class C fly ash	44.12	17.83	2005	10.46	7.97	2.61
	0.5	310	30% Class C fly ash	44.22	23.75	1280	10.21	6.94	2.41
	0.6	310	15% Class F fly ash	44.30	28.00	1060	10.01	8.39	3.21
	0.55	340	15% Class C fly ash	45.74	14.17	2825	10.38	11.60	5.03
	0.5	310	20% Class F fly ash + 20% Class C fly ash	46.05	41.17	755	10.29	7.22	1.51
	0.55	340	15% Slag B	46.35	20.00	2265	10.02	6.98	1.75

Strength grade	w/b	Binder content	SCM content	Compressive strength	Surface Resistivity test	RCPT	OPI test	Sorptivity test	
				f_{ck} av.,90 MPa	SR av.,90 kΩ.cm	TC av.,90 Coulombs	OPI, av.,90	SI av., 90 mm/√hr	Slope av.,90 g/√hr
	0.5	310	15% Slag B	47.55	26.67	2100	10.01	10.10	1.95
	0.55	340	15% Class F fly ash	47.73	27.50	1810	10.05	8.59	3.12
	0.4	380	50% Class F fly ash	48.92	97.18	325	10.97	6.80	1.44
	0.5	310	15% Class F fly ash	49.96	37.83	995	10.06	8.61	1.58
50-60	0.55	300	0	50.97	12.50	4030	9.86	12.61	3.6
	0.5	310	30% Slag B	52.06	39.17	1075	10.75	9.40	1.17
	0.5	310	20% Slag B + 20% Class F fly ash	52.19	64.08	720	9.89	9.68	1.85
	0.5	310	15% Slag A	52.69	22.92	1118		6.45	1.32
	0.4	380	30% Class F fly ash	53.88	57.5	365	10.65	8.01	1.61
	0.5	310	0	54.62	16.25	2080	10.09	14.43	3.55
	0.5	300	0	56.22	12.08	2640	9.66	12.38	3.76
	0.45	320	0	57.37	12.02	1890	9.77	12.95	3.4
	0.45	340	0	57.37	13.17	2465	9.76	10.45	3.51
	0.5	310	50% Slag B	59.23	120.00	325	10.81	4.76	0.83
>60	0.4	360	0	61.38	27.92	1825	9.82	10.65	3.18
	0.4	340	0	62.19	21.75	1440	9.98	8.83	2.29
	0.4	400	0	65.72	15.83	1685	9.82	12.01	3.75
	0.4	380	50% Slag	67.3	96.74	250	10.07	6.22	0.67
	0.4	380	15% Class F fly ash	68.03	45.87	570	10.86	8.69	1.50
	0.4	380	30% Slag	74.6	35.17	645	10.47	6.37	0.79
	0.4	380	15% Slag	76.2	23.08	985	10.91	6.73	1.02
	0.4	380	0	82.95	15.16	1145	11.00	8.56	1.73

The overall trends, which have been described earlier in the section on the ranking, can be summarized as follows. Slag and Class F fly ash are the best performers for chloride penetration resistance. Improvement of durability parameters from 28 to 90 days is best for Class F fly ash. Only OPC and Class C fly ash mixes fall in the low durability category. Class C fly ash performance is similar to OPC at 28 days, but improves at 90 days. The spread in the data for SCM mixes is large compared to that of OPC mixes.

Strength grade classification is a tool for the practicing engineers to get an assessment of durability at an equivalent strength level. Different options are available for the practicing engineers to design a mix having a particular strength in terms of the type of binder, binder content, water binder ratio, the levels of replacement of SCM etc. For example, in order to design a concrete mix having a mean strength between 30 and 40 (typically M 30 grade concrete), as per the 28 day results matrix, 12 options are available (as seen in Table 4.4). If the binder chosen is OPC alone, the mix having a binder content of 310 kg/m^3 and w/b 0.60 is an option. However, the durability performance of this mix is not good. The charge passed is in the Poor category, and surface resistivity falls in the Moderate category. The sorptivity results are in the good range and OPI is in Excellent category. If in the same mix, the binder proportion is slightly altered, i.e., when 15% slag is added, then the surface resistivity and the charge passed get improved by one level, i.e. they get classified into the Good and Moderate categories respectively. The classes for sorptivity index and OPI remain at the same level. When the replacement is with 15% Class F fly ash, similar trends are obtained with an exception that the category for charge passed gets improved by two levels (new category is Good). With 30% Class F fly ash and w/b of 0.5, Surface resistivity and OPI results are classified in the Excellent category. Even though the charge passed and the sorptivity index are in the Good category, it can be seen that the results are very close to the limiting values. When the option is total binder content 380 kg/m^{3}and w/b 0.4 with 50% Class F fly ash replacement, all the durability parameters are classified in the Excellent category except the sorptivity index. However, considering the slope of the best fit line between the mass gain versus square root of time (which is 1.70), this mixture can be considered in the Excellent category. Further, it can be seen from the matrix that the mix having 20% Class C fly ash and 20% Class F fly ash, yielded a sorptivity index value of 5.99 and a slope of 1.71. Therefore, the mixture with a binder content of 380 kg/m^3 and w/b 0.4 having 50% fly ash replacement can be considered as falling into the Excellent durability category in terms of all the durability parameters considered. Another thing to be noticed is that the mixture having a binder content of 310 kg/m^3 and water binder ratio 0.5, having 50% fly ash replacement, satisfies all the requirements for Excellent durability category except sorptivity index. However, this is not a good option for the current group because the strength is 23.2 MPa, which is in the strength category 20-30.

Based on the results, the following conclusions can be drawn. Within the same strength grade, mixes with SCMs are better compared to their OPC counterparts. As the replacement level increases, the durability parameters get improved. However, this is associated with a lowering of the compressive strength in the case of Class F fly ash, especially at 28 days. As strength grade increases, the mixes attain higher durability categories. As the age of concrete increases from 28 to 90 days, in the case of strength, all mixes move up by one category. However, in the case of durability classes, OPC mixes move up by only one category or remain in the same category, whereas SCM mixes move two steps ahead as the increases from 28 to 90 days. For the present study, the age of the concrete is same as the number of days of curing.

Another important observation from the strength grade classification table is that, as water binder ratio decreases, more mixes are qualifying to higher durability classes, the trend of which is already well established.

The qualitative ranking system and the strength grade classification developed will be useful for the engineers who are practicing in the field of concrete technology for choosing the right blend of material depending on their requirement at site. The trend of the behaviour of different SCMs in durability parameters are evident from this study. Depending on the service requirement (i.e., level of durability required), the mixture proportion can be tailor made.

4.5 A PRACTICAL EXAMPLE OF STRENGTH GRADE CONCEPT

In order to show a practical example of the strength grade concept, the mixture design for three grades of concretes were considered from a live metro rail construction project in India. Three grades of concretes were considered for this analysis. These are

M 30, M 35 and M 50. M 30 grade concrete was used for the construction of parapet wall, M 35 grade for the construction of pile cap and the M 50 grade for the construction of the top segments. In all the mixture designs, only OPC of 53 grade was used as the binder. The mixture designs used in the field are: for M 30, total cement content 430 kg/m^3; w/c 0.35 and CA: FA 60:40.; for M 35, total cement content 420 kg/m^3; w/c 0.4 and CA:FA 58:42.; for M 50, total cement content 460 kg/m^3; w/c 0.31 and CA:FA 60:40.

With respect to the strength grade classification at 28 days, as presented in Table 4.4, it is clear that for all these grades, there are better economical options available by the use of SCMs. For example, for M 30 grade concrete, the mean strength requirement is 38.25 MPa. The different options which satisfy this requirement are mixes with (1) total binder content of 310 kg/m^3 having w/b 0.5 with 20% slag and Class F replacement; (2) total binder content 310 kg/m^3, w/b 0.6 with 15 % slag replacement; (3) total binder content 310 kg/m^3, w/b 0.6 with 15 % Class F fly ash replacement; and (4) total binder content 340 kg/m^3, w/b 0.55 with 15 % Class F fly ash replacement. All these mixes can result in either good or very good level of durability. Unfortunately, for this project, the durability requirements were not clearly defined, which makes it difficult to propose the mix proportions accurately.

Similarly, we can see that more economical and durable options are available for M 35 and M 50 grades also. In the case of M 50 grade concrete, the mixture having a total binder content of 380 kg/m^3 and w/b of 0.4 with 50% slag replacement is the option which satisfies this condition. Further, all the durability parameters for this particular combination are in the excellent category. This proportion should definitely be a better option than what is adopted in the site (total cement content 460 kg/m^3; w/c 0.31). The economic benefit for the first option will be much higher. Thus, we can see that there are possibilities to reduce the quantity of cement used in this construction, which can lead to more sustainability in construction, both from economic and ecological point of view. Further, the resulting enhancement of durability of the structure can also contribute to sustainability in an indirect manner.

4.6 SUMMARY

An attempt has been made in the present chapter to develop a new concept called strength grade classification. Different mixes in the same strength range are classified into different durability classes based on qualitative criteria adapted from standards and literature. The durability parameters used here to classify concrete include surface resistivity, charge passed, sorptivity index and oxygen permeability index.

The results show that the options available to make concrete at a particular strength grade can result in different levels of durability. It is clear that even with mixes having high w/b and low binder content, with the use of SCMs, high level of durability is achievable. Depending on the requirement of the service environment, the mixture can be tailor-made. The database generated in this study can act as a guideline for material selection and it demonstrates the potential of SCMs to improve durability. Further, strength grade classification supports the concept of performance specification. There need not be any limit for the mixture parameters. The concrete producer can have flexibility on type and dosage of SCMs as well as other mixture parameters. The SCM can be chosen based on availability.

CHAPTER 5

EVALUATION OF THE INFLUENCE OF DIFFERENT TEST RELATED FACTORS ON DURABILITY PARAMETERS

5.1 INTRODUCTION

In this chapter, four most commonly specified durability tests were explored for different test related factors. For these tests, additional data on the test related factors were collected along with the normally recorded parameters. Even though these additional measurements are not included in the main focus of the thesis, an understanding of the factors affecting the test results is necessary in order to specify a set of durability test methods and parameters.

5.2 RAPID CHLORIDE PERMEABILITY TEST

Rapid chloride permeability test (RCPT) is the most widely specified and most criticized durability test method (Bickley et al., 2006). The criticisms of this test have already been discussed in Chapter 2. As a result, a number of studies (Feldman et al., 1994, Julio-Betancourt and Hooton, 2004, Andrade et al., 1999) were conducted by various researchers in order to suggest modifications for this test as well as on the factors influencing this test. However, most of these studies were concentrated on mixes having OPC as the binder. The applicability of RCPT to mixes having SCMs is questioned by many researchers (Russel 2001, Pfeifer et al., 1994; Scanlon and Sherman, 1996). Hence, the attempt in the current study is to verify the modifications suggested to RCPT for mixes having SCMs. The effect of temperature rise during the experiment as well as the depth of chloride ion penetration on different mixes are evaluated. Further, the correlation between the initial current and the total charge passed is also examined.

5.2.1 Initial current versus charge passed

In order to reduce the time required to conduct the test and to eliminate the effect of other factors such as Joule effect (or heating effect) on the output of RCPT, Feldman et al. (1994) suggested the use of the initial conductivity as a quality indicator for concrete. The authors were able to get good correlation between initial current and charge passed as well as conductivity and charge passed. However, the investigations were focused only on mixtures with OPC.

The relation between initial current and charge passed for all the mixtures in the current study at three ages is presented in Figure 5.1. It can be seen that there exists strong correlation between total charge passed and initial current reading. Further, these observations agree to those of Feldman et al. (1994), which was a study on only OPC concretes. From the results of this study, it is clear that this relationship also applies to mixtures having supplementary cementitious materials. Thus, the initial current reading can be used as a good, quick indicator of concrete quality. The initial current readings are not affected by the test temperature. However, the effect of other ions in the pore solution on the charge carrying ability cannot be eliminated.

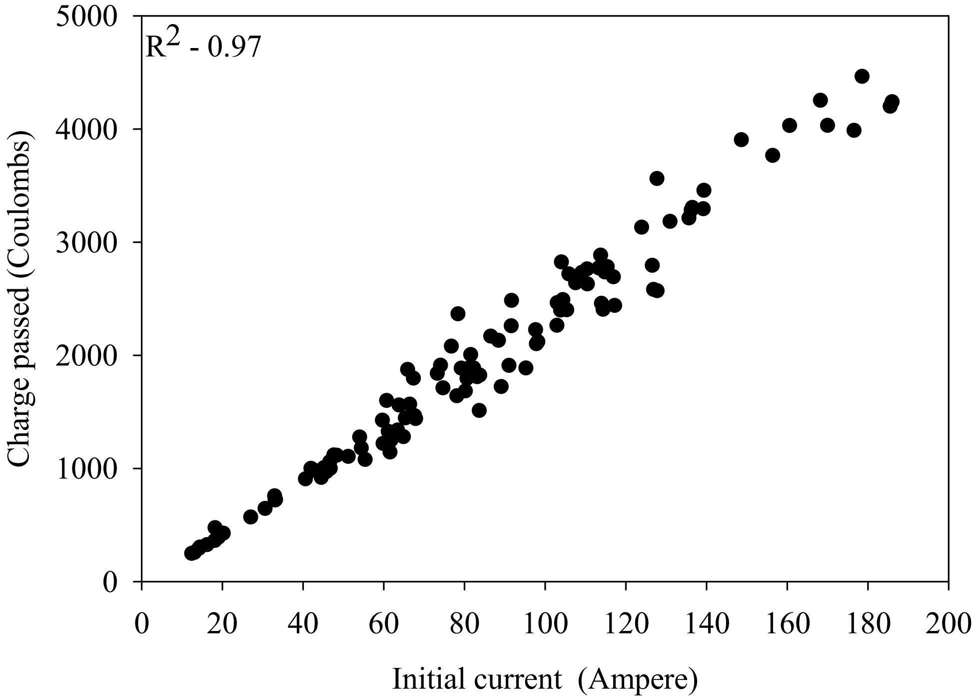

Figure 5.1 Relation between charge passed and initial current in RCPT

5.2.2 Depth of chloride penetration versus charge passed

In a parametric study on RCPT, Andrade et al. (1999) analyzed the relation between chloride penetration depth determined by colourimetric technique and the total charge passed and got a good correlation. In a similar way, the depths of chloride penetration of the samples in this study were also monitored by spraying 0.1 N $AgNO_3$ on the split surface of the specimens after conducting the test. The depth of the white AgCl precipitate formation is plotted against the charge passed in Figure 5.2. It can be seen that the correlation is satisfactory for the vast range of mixtures studied in this project.

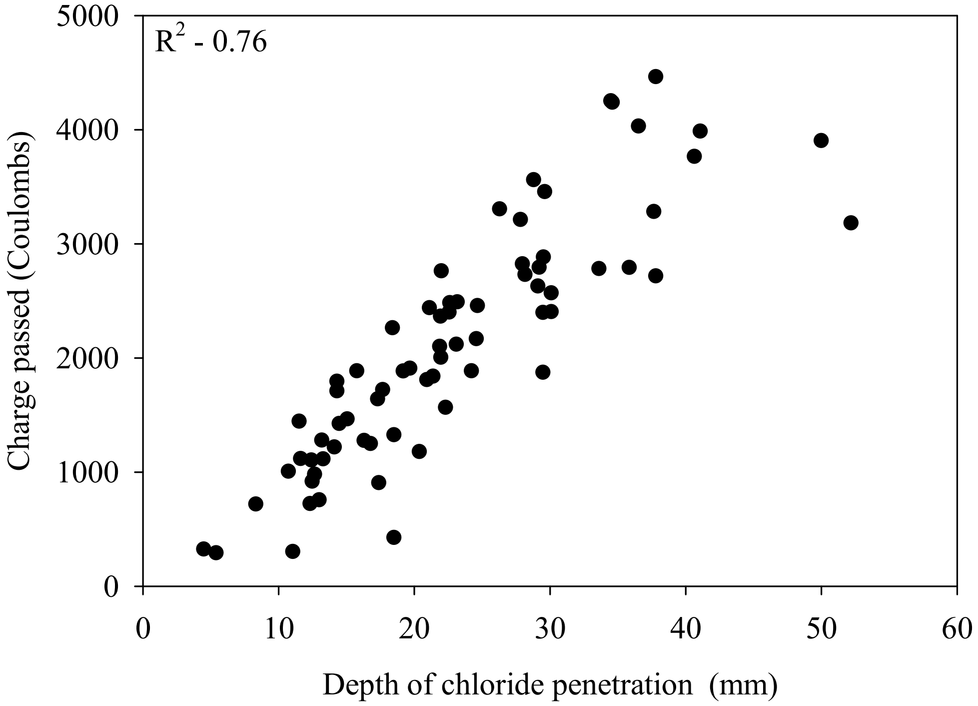

Figure 5.2 Relation between charge passed and depth of chloride penetration in RCPT

5.2.3 Maximum temperature versus charge passed

The increase in temperature during the test and its influence on the total charge passed (Joule effect) is pointed out to be one of the major drawbacks of RCPT (McGrath and Hooton, 1999). In order to study this phenomenon, the temperature of the downstream cell i.e., the cell having NaOH solution, was monitored during each half hour of the experiment and the maximum temperature reached during the experiment was recorded. This temperature is plotted against the charge passed in Figure 5.3. It can be seen that there exists a good correlation between the charge passed and the maximum temperature reached during the experiment, which indicates that there is a substantial influence of temperature on the charge passed.

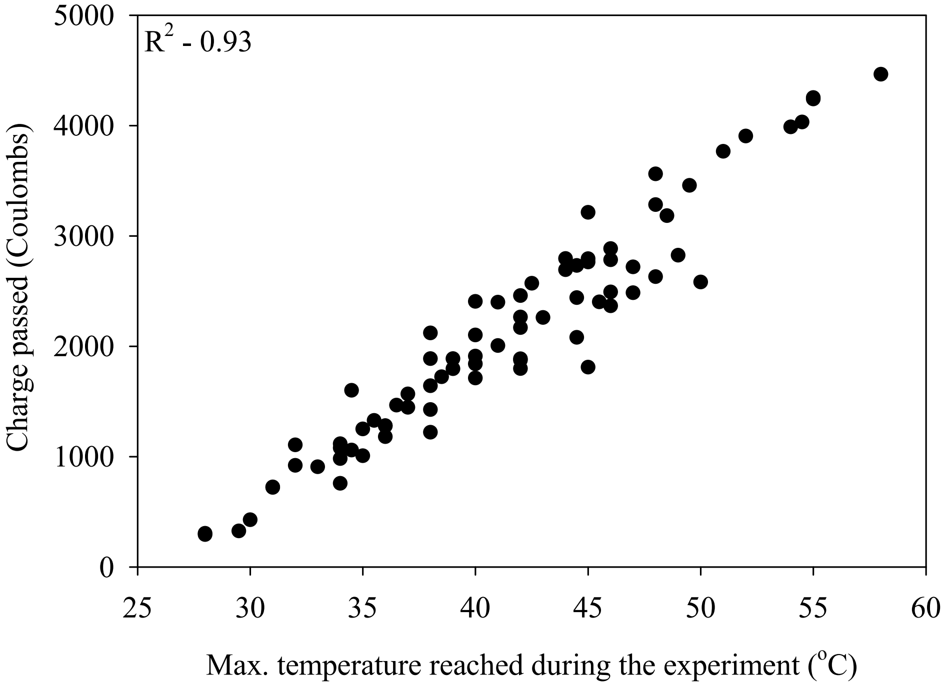

Figure 5.3 Relation between charge passed and maximum temperature in RCPT

In a similar way, Julio-Betancourt and Hooton (2004) had concluded that there was a good correlation between the total charge passed and the difference between initial and final temperatures during the test.

5.2.4 Temperature profile during the experiment

It is well discussed in the literature about the influence of temperature on the total charge passed (McGrath and Hooton, 1999, Julio-Betancourt and Hooton, 2004). However, the influence of SCMs on the temperature rise during RCPT is not studied well in the literature. In order to understand the influence of SCMs on the temperature rise, the temperature profile for different concretes is plotted in Figure 5.4 to Figure 5.7 for mixes having a total binder content of 310 kg/m^3 and w/b 0.5. Figure 5.4 shows the temperature profile of the OPC mix. The temperature profiles of mixes in which 30% of total binder are replaced with SCMs such as slag, Class F fly ash and Class C fly ash are presented in Figure 5.5 to Figure 5.7.

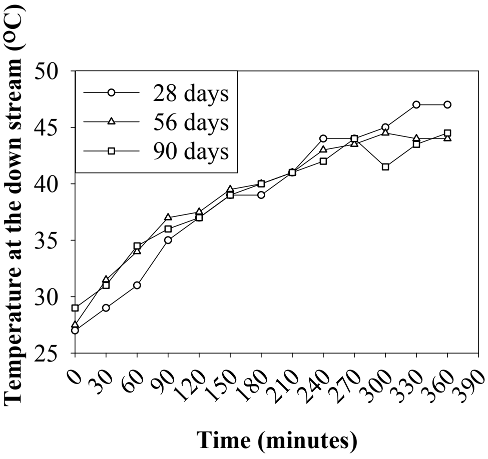

Figure 5.4 Temperature profile during RCPT for OPC mix

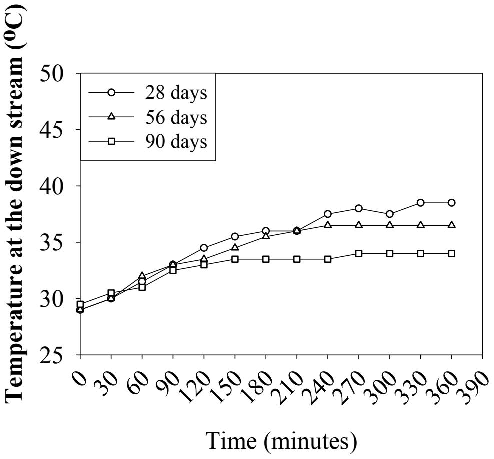

Figure 5.5 Temperature profile during RCPT for 30% slag mix

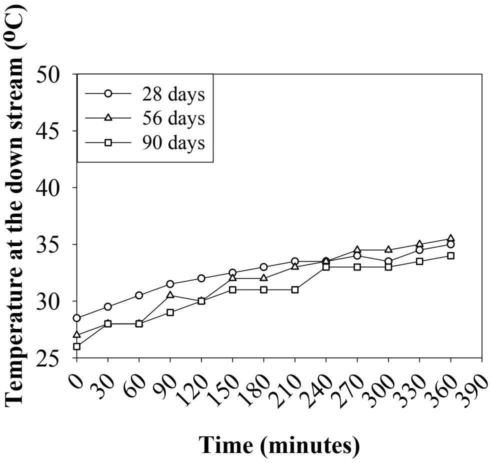

Figure 5.6 Temperature profile during RCPT for 30% Class F fly ash mix

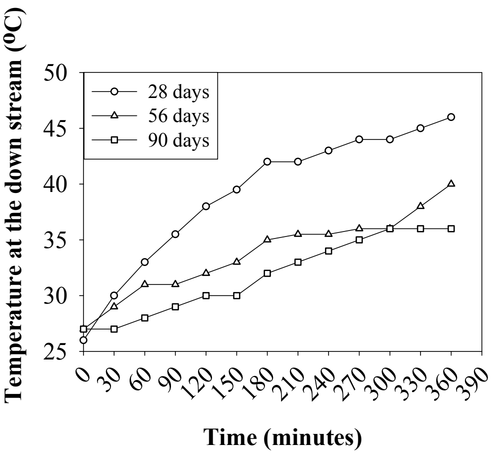

Figure 5.7 Temperature profile during RCPT for 30% Class C fly ash mix

It can be seen that the OPC mixes are showing the highest increase in temperature during RCPT. As the age of the concrete increases, the maximum temperature decreases. As OPC is replaced with SCMs, the maximum temperature reached during RCPT decreases. The lowest temperature is displayed by slag and Class F fly ash mixes at 90 days. The maximum temperature reached for Class C fly ash mixes at 28 days is almost the same as that for OPC mixes, but is substantially lower at 90 days. A similar trend is observed in other mixes (having different water binder ratio and total binder content) also. Thus, it can be concluded that the presence of SCMs reduces the temperature rise during RCPT.

5.3 WATER PERMEABILITY TEST

The water permeability test based on DIN 1048 (Part 5) is a commonly specified durability test method. According to DIN 1048, the water permeability test needs to be started when the specimens are in fully saturated condition. However, in many cases it is observed that the specimens get dry during transportation from the site to the laboratories for testing. In order to study the influence of drying on the water permeability test results, two sets of specimens were cast for mixes having a total binder content of 380 kg/m^3 and w/b 0.4. All the specimens were cured for 28 days in a moist room. The test was conducted on one set of specimens as soon as they were taken out of the moist room. The second set of specimens were dried in a ventilated hot air oven set at 50 °C for 7 days prior to testing. The drying criteria adopted here is similar to that adopted for sorptivity test based on durability index testing procedure manual of South Africa (2009).

The results of the water permeability test for the two sets of specimens subjected to different pre-conditioning are presented in Figure 5.8. The demarcation criteria shown in Figure 5.8 is the specification for good quality concrete to resist aggressive environment (< 30 mm penetration) reported by Concrete Society, 1998 (as cited by Basheer, 2001).

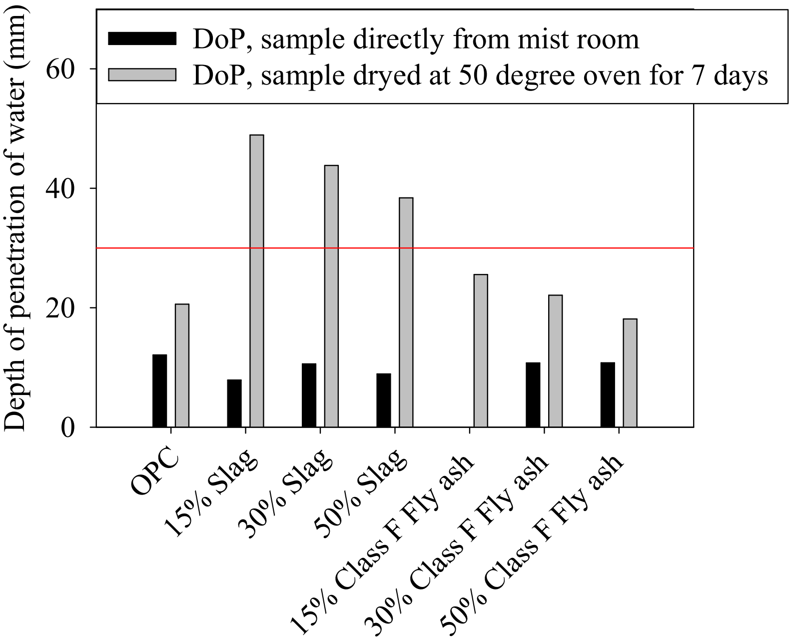

Figure 5.8 Effect of specimen drying on the water permeability test results

It can be seen that drying influences the test results considerably. The drying effect is more prominent in the case of slag mixes compared to OPC and Class F fly ash mixes.

5.4 SORPTIVITY TEST

The sorptivity index is the main result of the water sorptivity test based on the durability index testing procedure manual of South Africa. Concrete is classified qualitatively based on sorptivity (mm/√hr) under the criteria that higher the sorptivity index, poorer the concrete quality. The formula to find sorptivity is already presented in Equation 2.58. It is obtained by multiplying the slope of the best fit line of the plot of the mass gain verses square root of time, with the specimen thickness and then dividing by the water absorption. In some cases, it is observed that the sorptivity index seems to increase from 28 to 90 days. This is because as the pore structure gets more developed, the water absorption capacity reduces, yielding higher sorptivity index. The counter argument to this is that as the pore size reduces, the capillary rise is expected to increase. Thus a normalization with water absorption is necessary. Hence, an attempt is made to compare all the parameters obtained from water sorptivity test.

The water sorptivity test can yield four parameters which are useful to classify the concrete qualitatively. These are sorptivity index (mm/√hr), slope of the best fit line between the mass gain and square root of time (g/√hr), porosity (%) and water absorption (%). Figure 5.9 to Figure 5.12 show these results for the mixes having a total binder content of 380 kg/m^3 and a water binder ratio of 0.4. It can be seen that in the case of mixes with 15 and 30% Class F fly ash, the values of sorptivity index are increasing from 28 to 90 days, which is opposite to the expected behavior. However, the other results such as slope of the best fit line between mass gain and square root of time, water absorption and porosity are decreasing from 28 to 90 days. Thus, in order to get correct idea of the behavior, it is better to compare all the four parameters together.

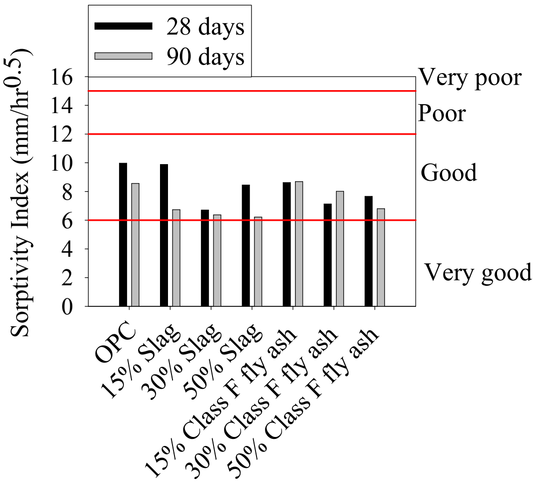

Figure 5.9 Sorptivity index

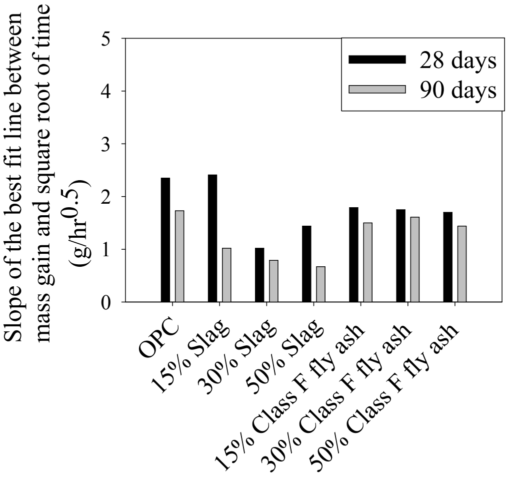

Figure 5.10 Slope of the best fit line between mass gain and square root of time

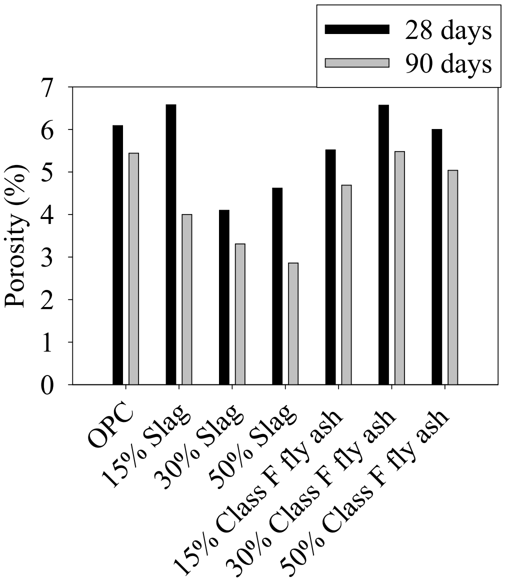

Figure 5.11 Porosity

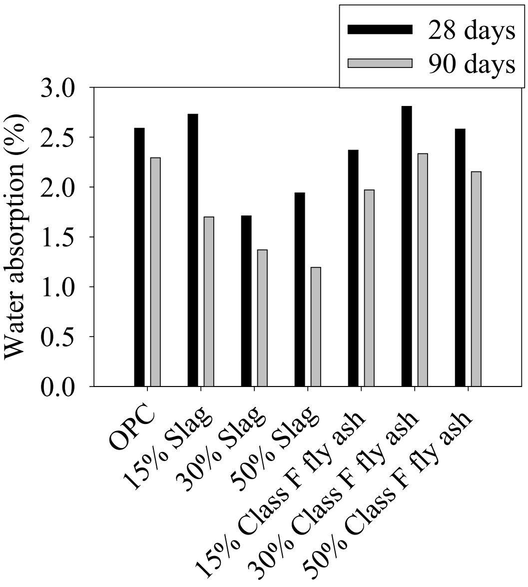

Figure 5.12 Water absorption

5.5 TORRENT AIR PERMEABILITY TEST

Torrent air permeability test is adopted both as a laboratory as well as site test. Even though there are specifications associated with this test regarding the moisture condition and resistivity levels of concrete structures on site, there is no guideline available for the conditioning of the specimens for laboratory testing. Hence, for one set of mixes (having total binder content 380 kg/m^3 and w/b 0.4), Torrent air permeability test was conducted on specimens dried in three conditions such as drying in a ventilated hot air oven at 105 °C for 1 day, drying in a ventilated hot air oven at 50°C for 7 days and drying in laboratory conditions at 25 °C and 65 % RH for three weeks. The results are presented in Figure 5.13.

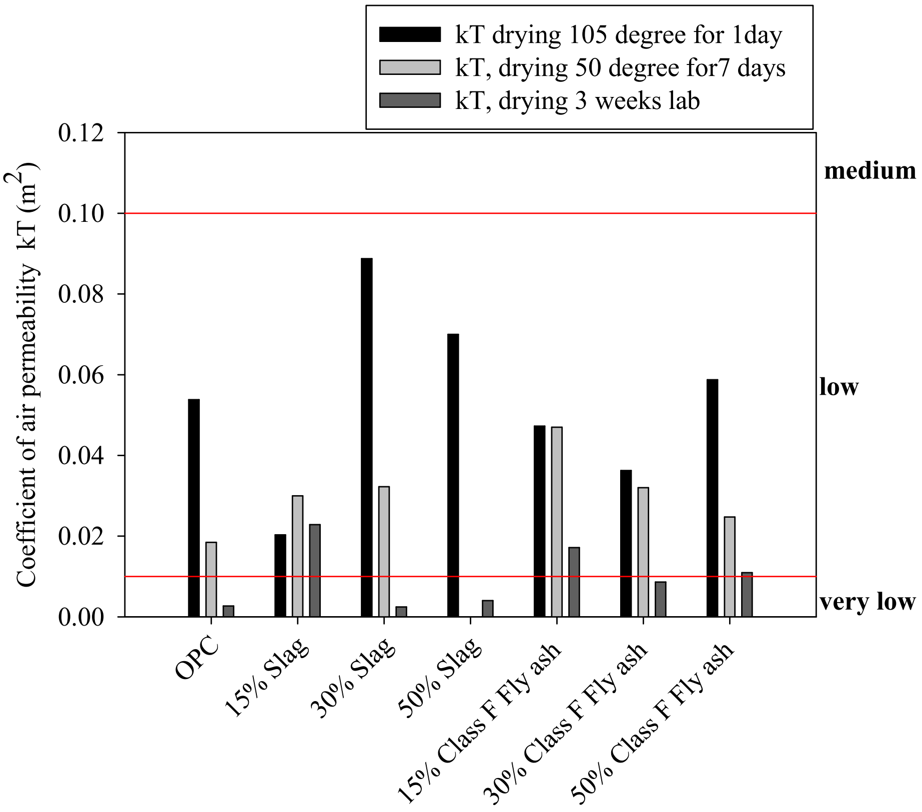

Figure 5.13 Effect of specimen drying on Torrent air permeability test results

It can be seen that drying affects the results considerably. Drying at 105°C led to very high permeability of concrete. In many cases, the equipment was not able to produce a result at all. Upon close examination of the specimens, it was found that oven drying led to hairline cracks on the specimen surface and hence yielded wrong (or no) results. The specimens used in the present study were 150 mm size cubes. Figure 5.14 shows the photograph of typical cracks found on the surface. These cracks were present in many specimens, especially on those from high water cement ratio mixes for both conditioning temperatures (i.e., 50°C and 105°C). Thus, drying in lab conditions for 3 weeks seems to be the best conditioning practice for this test. More research needs to be done correlating this result with those obtained from site to make this conclusion more authentic. Presence of cracking was found on multiple specimens. The cracking might have happened because of the specimen size of the cubes, as there was no cracking observed on concrete disc specimens prepared for DI tests. The reliability of the reading was found to improve when the drying was performed in lab conditions for three weeks.

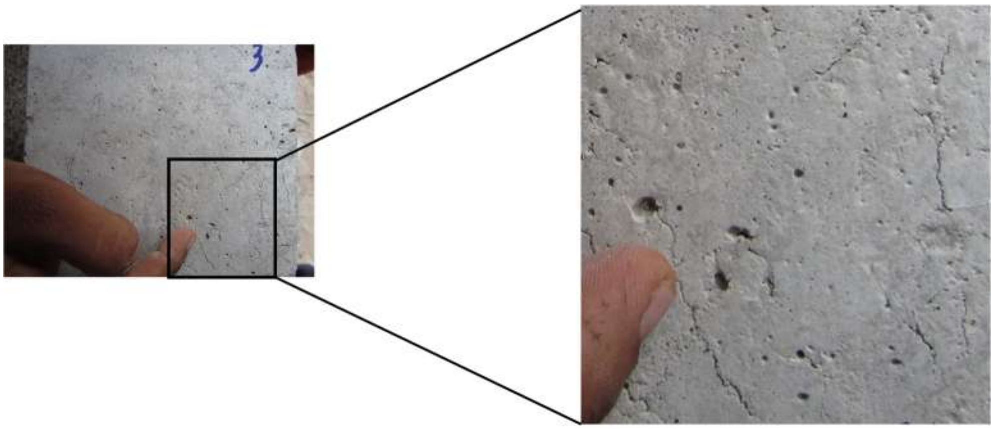

Figure 5.14 Photograph of the hairline cracks developed on the cube surface due to oven drying

5.6 SUMMARY

In this chapter, some of the most commonly used durability test methods are critically analysed to derive more useful, simple results. In the case of RCPT, very good correlation is obtained between total charge passed and other simple observations such as initial current and depth of chloride penetration. Further, substantial influence of temperature on total charge passed is established as indicated by the good correlation between total charge passed and the maximum temperature reached during the experiment. It is also found that presence of SCMs reduces the temperature rise during RCPT. Study of the influence of specimen conditioning on the results of water permeability test and Torrent air permeability test indicates that specimen conditioning methodology influences the test results considerably. Even though sorptivity index is the major parameter obtained from water sorptivity test, comparison of the other parameters obtained from the test such as slope of the best fit line between the mass gain and square root of time, porosity and water absorption can definitely yield more clarity in understanding the behaviour of a particular concrete in assessing its capillary absorption capacity. Thus, the additional measurements taken helped to understand the tests better.

CHAPTER 6

ASSESSMENT OF THE INFLUENCE OF SCMs ON THE DURABILITY PARAMETERS

In this chapter, the influence of SCMs on different durability parameters of concrete is presented. Results are presented in two sections. In the first section, the influence of SCMs on durability parameters obtained from a single category of mixtures is presented. The rest of the data and the graphs are incorporated in the Appendix D. The second section presents the results for all the concretes studied under this thesis work. These two sections give a qualitative comparison of the performance of SCMs in different durability tests. The quantification of the effect of SCMs is then done using service life prediction models. For carbonation induced corrosion, the service life prediction is done using the square root of time law and the DuraCrete model whereas for chloride induced corrosion, service life is predicted using DuraCrete model. At the end of the chapter, a comparison of all durability tests done in this project work is also presented.

6.1 INFLUENCE OF SCMs ON DURABILITY PARAMETERS RELATED TO CHLORIDE ION PENETRABILITY

The durability parameters discussed include surface resistivity (from Wenner 4 – probe resistivity test), charge passed (from rapid chloride permeability test), non-steady state migration coefficient (from rapid migration test) and chloride conductivity (from chloride conductivity test).

6.1.1 For concretes having same total binder content and water binder ratio

In this section, the influence of SCMs on durability parameters for concretes in the same category (mixes having same total binder content and water binder ratio) is discussed. Figure 6.1 to Figure 6.4 indicate the effect of replacement of OPC with SCMs on the selected durability parameters. All the mixes under consideration have a total binder content of 310 kg/m^3 and water binder ratio of 0.5. In all the plots, the limiting values suggested by the relevant standards (RILEM TC 154-EMC, 2004, ASTM C1202, 2010, Bjegović et al., 2015, Alexander et al., 1999) are also shown for comparison of the data.

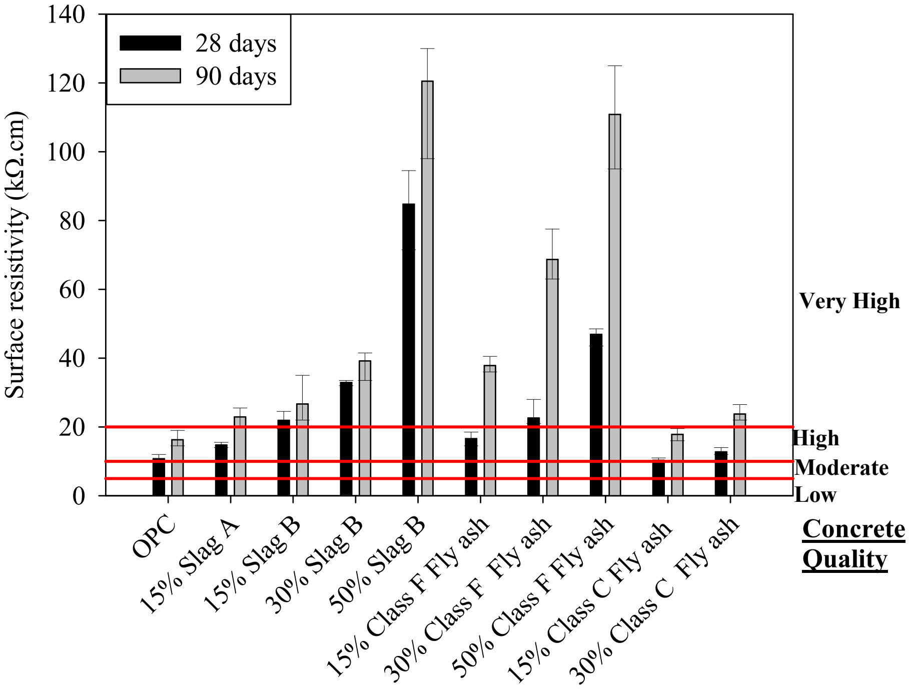

Figure 6.1 Influence of SCMs on the surface resistivity of mixes in the same category (Total binder content 310 kg/m^3 and w/b 0.5)

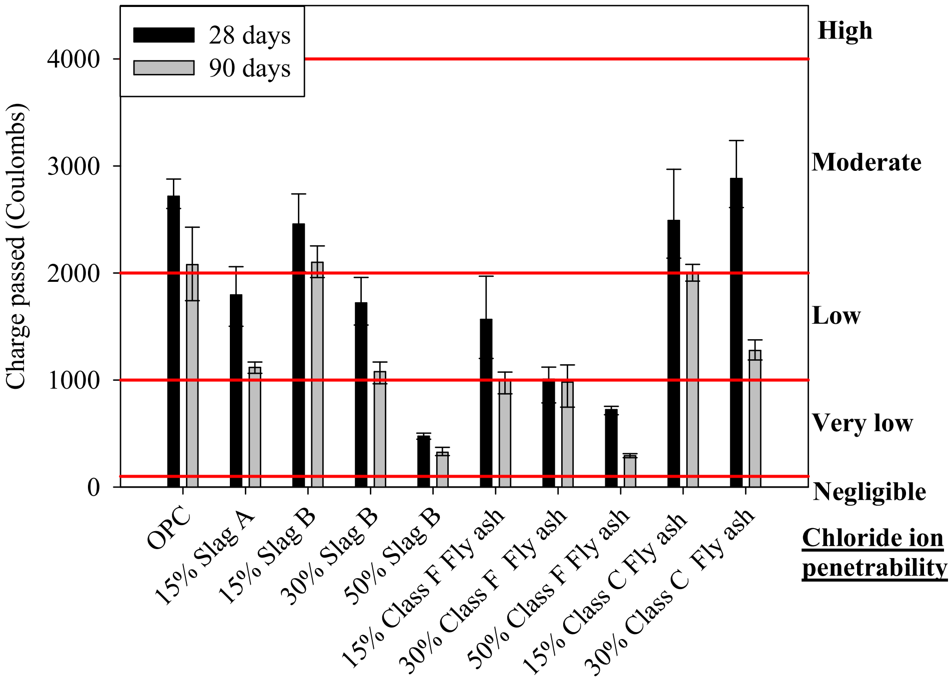

Figure 6.2 Influence of SCMs on charge passed of mixes in the same category (Total binder content 310 kg/m^3 and w/b 0.5)

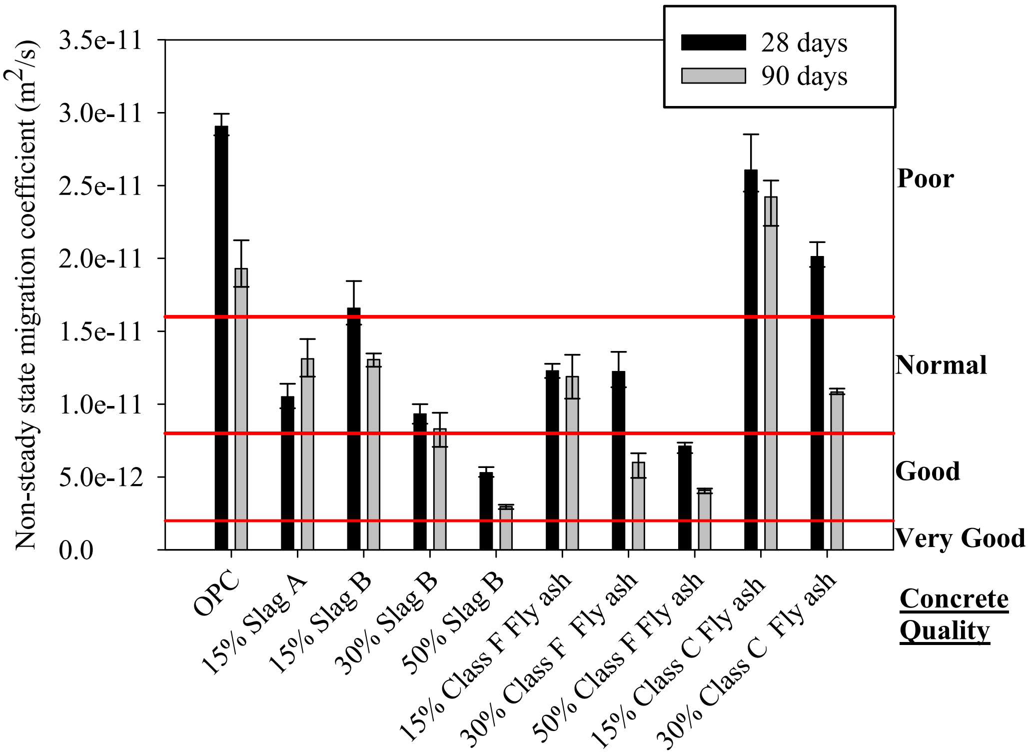

Figure 6.3 Influence of SCMs on non-steady state migration coefficient of mixes in the same category (Total binder content 310 kg/m^3 and w/b 0.5)

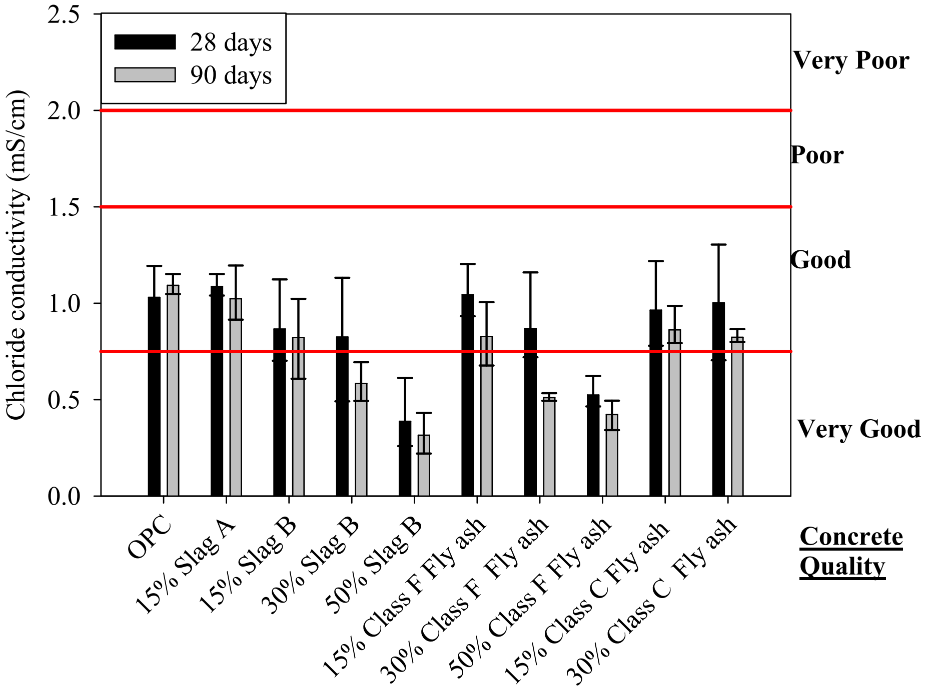

Figure 6.4 Influence of SCMs on chloride conductivity of mixes in the same category (Total binder content 310 kg/m^3 and w/b 0.5)

It can be seen from Figure 6.1that surface resistivity gets improved with replacement by SCMs and with the number of days of curing. Concretes with 50% slag replacement and 90 days of curing exhibit the best result, followed by Class F fly ash mix with 50% replacement at 90 days of curing. The greatest enhancement of surface resistivity from 28 to 90 days is exhibited by Class F fly ash, and this is significantly higher than that of slag. Even though the surface resistivity of Class C fly ash is comparable to OPC at 28 days, there is a distinct improvement at 90 days.

In a similar way, as the SCM dosage increases, the other parameters such as charge passed, non-steady state migration coefficient and chloride conductivity decrease, as evident from Figure 6.2 to Figure 6.4. Correspondingly, there is an improvement in the concrete quality. The results are quite evident in the case of parameters such as surface resistivity, charge passed and non-steady state migration coefficient. In the case of chloride conductivity, even though the trends are same, there is not much difference in the concrete quality described by this parameter. All the concretes except those having higher dosages of slag and Class F fly ash (which are in the 'Very Good' category) are qualified as having a concrete quality 'Good'.

Thus, it is obvious from the results of all the parameters relating to chloride ion penetrability that as OPC is replaced with SCMs, the concrete quality gets improved. Slag and Class F fly ash at 50% replacement at 90 days of curing are the best performers with slag occupying the first position. There is substantial improvement in the concrete quality at higher dosages (30% and above) of slag and Class F fly ash. Class F fly ash mixes displayed greatest improvement in these parameters as the curing duration increased from 28 to 90 days. In all the cases, the worst performance is exhibited by OPC mixes. The performance of Class C fly ash is similar to OPC at 28 days. However, there is considerable improvement in the performance when the curing duration increases to 90 days. This trend is clearer for mixes having a replacement level of 30% compared to that of 15%.

All the results show that there is an improvement in the concrete quality as the curing duration increases from 28 to 90 days. This points to the fact that in order to realize high levels of durability, extending curing is essential.

Similar results were reported by other researchers such as Bijen (1996), Baroghel-Bouny et al. (2011), Andrade et al. (2013), Thomas (2012) etc.

6.1.2 For all the concretes under study

In this section, an attempt has been made to look into the results in an overall manner. Figure 6.5 to Figure 6.8 show the influence of SCMs on the durability parameters related to chloride ion penetrability for all the concretes under study. Thus, these diagrams show the influence of SCMs on all the 41 concrete mixtures which belong to two categories - commonly used design mixes and mixes having limiting prescriptive values. The OPC mixtures vary in total cement content between 280 to 400 kg/m^3 and water binder ratio from 0.4 to 0.65. OPC mixtures are represented as mixtures having 0% replacement with SCMs. In the case of mixes having SCMs, there is a variation of total binder content between 280 to 380 kg/m^3 and water binder ratio between 0.4 and 0.65. SCMs are replaced at three levels - 15, 30 and 50%. The overall trend is presented for two curing durations - 28 and 90 days.

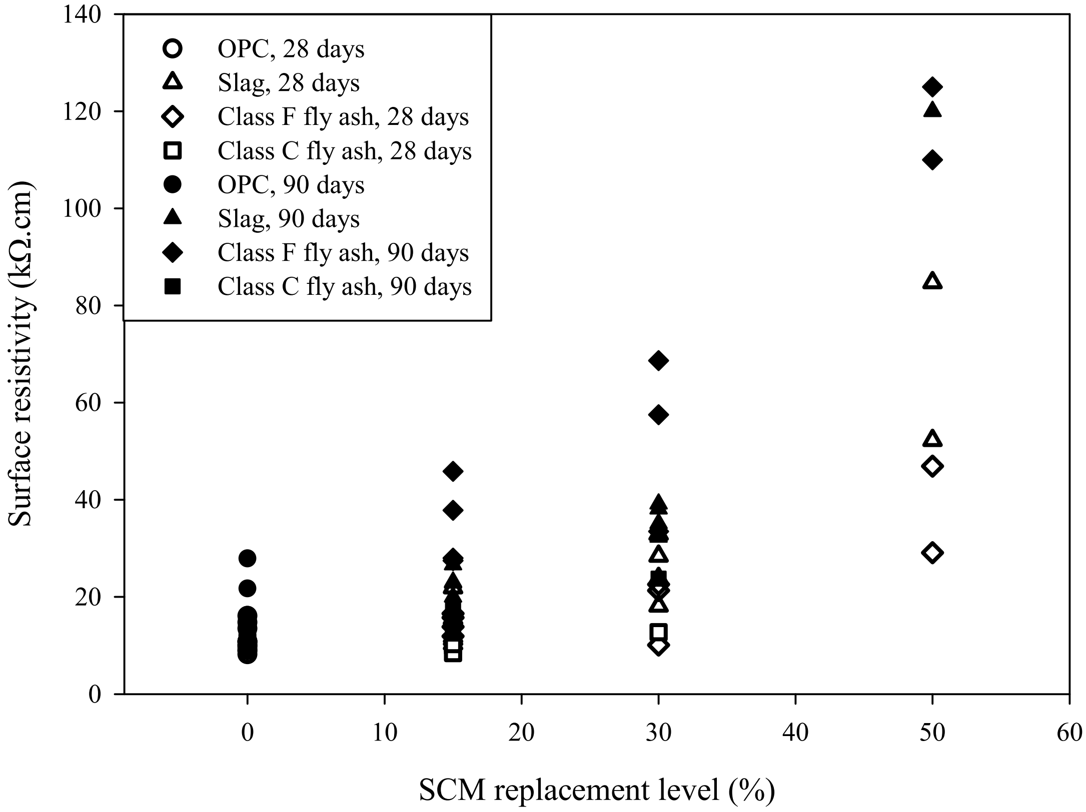

Figure 6.5 Influence of SCMs on the surface resistivity for all the concretes under study

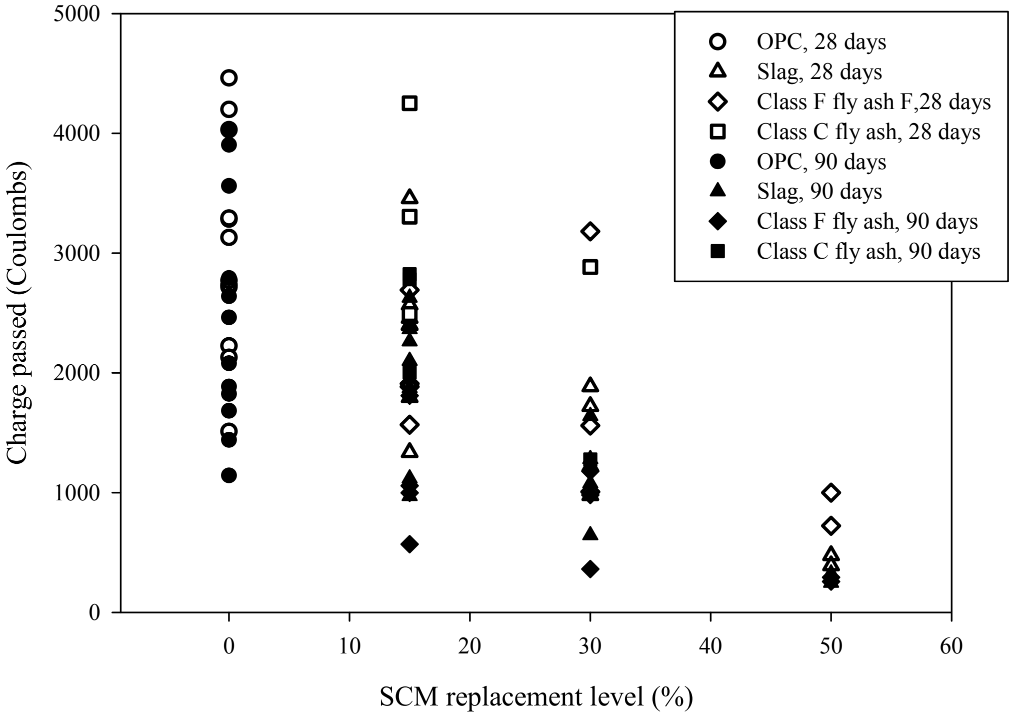

Figure 6.6 Influence of SCMs on the charge passed for all the concretes under study

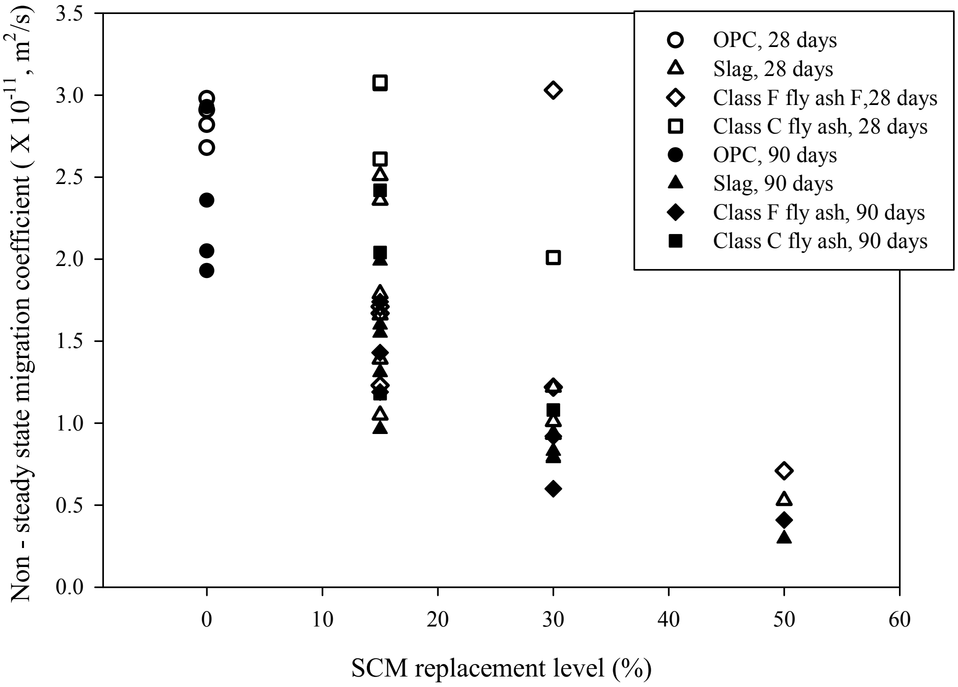

Figure 6.7 Influence of SCMs on the non-steady migration coefficient for all the concretes under study

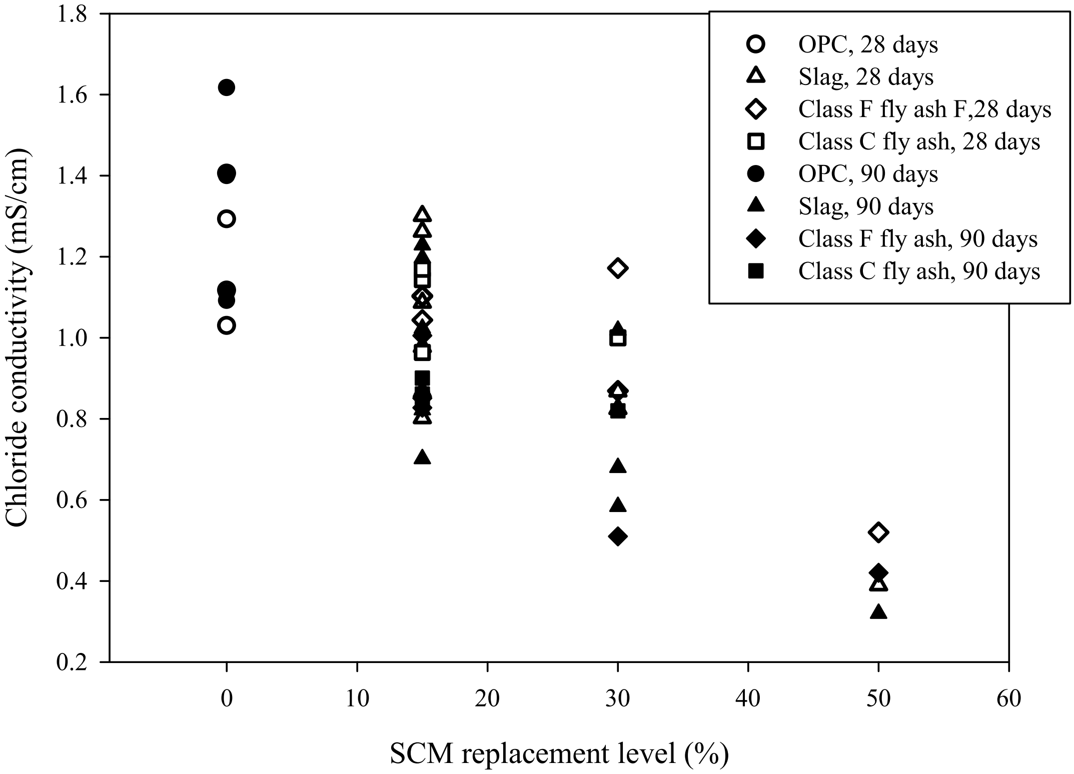

Figure 6.8 Influence of SCMs on the chloride conductivity for all the concretes under study

From the results presented in the Figure 6.5 to Figure 6.8, it is clear that SCM mixes show better resistance against chloride ion penetration (as measured by the electrical methods) than OPC mixes. As the SCM dosage increases, concrete quality increases in terms of chloride ion penetrability. These trends are obvious at 28 days itself. In all the cases, the best performance is exhibited by mixtures having 50% replacement with SCMs.

In all the diagrams presented above, the values at the lower end for the OPC mixes (which are showing better durability) are for the mixtures having high total cement content. In some cases, it can be seen that OPC mixes are attaining a durability level comparable to that of SCM mixes. For example, in Figure 6.6, for the OPC mixture at 90 days, the charge passed is close to 1000 Coulombs. At the same time, SCM mixes at 50% replacement with slag produce charge passed close to 500 Coulombs. It is worthwhile to note that the OPC mix that produced a charge passed of 1000 Coulombs had a total cement content of 400 kg/m^3 and a water binder ratio of 0.4 whereas the slag mixture that produced a charge passed less than 500 Coulombs had a total binder content of 310 kg/m^3 and water binder ratio 0.5. Thus, it can be concluded that use of SCMs can lead to economy in construction by saving the material in addition to enhancing the durability of concrete.

Further, the resistance against chloride penetration, as obvious from the overall trends of surface resistivity, total charge passed, non-steady state migration coefficient and chloride conductivity, increases from 28 to 90 days of curing. This emphasizes the fact that to realize high levels of durability, extended curing is essential. It is to be noted that the specimens tested at an age of 90 days are cured for 90 days. Hence the age of the specimen as well as the curing age matches. There is a remarkable improvement in the durability properties, especially in terms of chloride ion penetrability as the testing age increases from 28 to 90 days. That indicates the importance of extended curing. There is no testing conducted on 90 days on specimens which are cured for 28 days.

Another noticeable trend is that, in order to achieve higher levels of durability, the replacement levels need to be higher, in this case 30% and 50%. In the case of mixes having a replacement level of 15%, even though the durability parameters got improved, the enhancement is not much significant.

The reasons for increased performance of SCMs include pozzolanic reaction leading to the development of pore structure and modification in the pore solution chemistry due to the incorporation of SCMs. A detailed analysis of these factors is provided in the next chapter.

6.2 INFLUENCE OF SCMS ON DURABILITY PARAMETERS RELATED TO GAS PENETRABILITY

6.2.1 For concretes having same total binder content and water binder ratio

For the present work, two categories of tests were done to assess the gas penetrability of concrete – gas diffusion test and gas permeability tests. Accelerated carbonation test belongs to gas diffusion test whereas Oxygen permeability index test and Torrent air permeability test belong to the category of gas permeability tests. Figure 6.9 shows the influence of SCMs on depth of carbonation for concretes having total binder content 310 kg/m^3 and w/b 0.5.

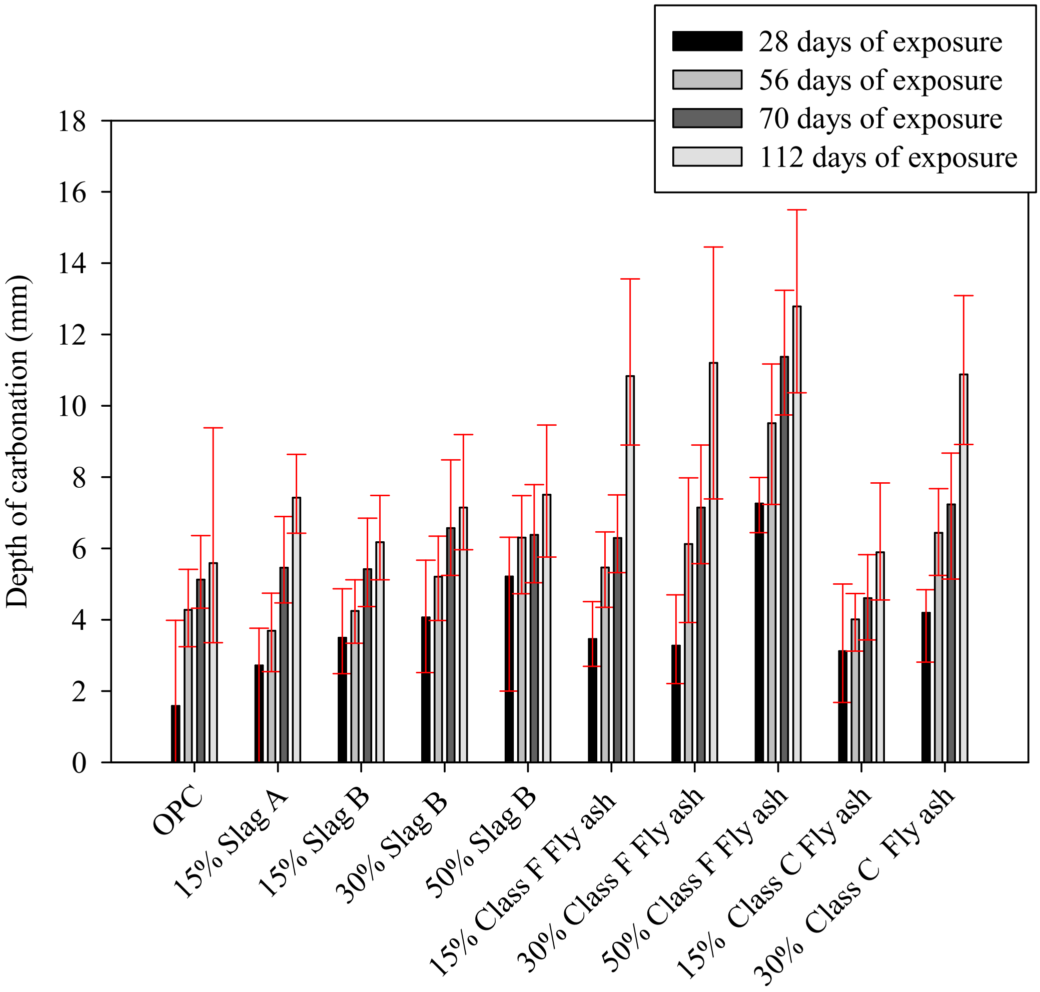

Figure 6.9 Influence of SCMs on depth of carbonation of mixes in the same category (Total binder content 310 kg/m^3 and w/b 0.5)

From Figure 6.9, it is can be seen that the depth of carbonation is more for SCM mixes compared to that of OPC mixes. Fly ash mixes show greater depth of carbonation, whereas slag mixes show relatively less depth of penetration. As the replacement level increases, the depth of carbonation increases. At lower replacement levels, the difference is not much significant even at 112 days of exposure for slag and Class C fly ash. This is more evident in Figure 6.10 which shows the spread of the data. The depth of carbonation for 15% Class F fly ash mix having a w/b of 0.5 is higher than that of 15% Class F fly ash mix having a w/b of 0.6. This might be because of an experimental error due to the poor surface condition of the specimen. Similar conclusions on the performance of fly ash mixes at lower replacement level (15%) were reported by Alonso and Andrade (2002). They have concluded that if the replacement level is low, the service life in terms of carbonation induced corrosion can be guaranteed if fly ash is employed at lower replacement level.

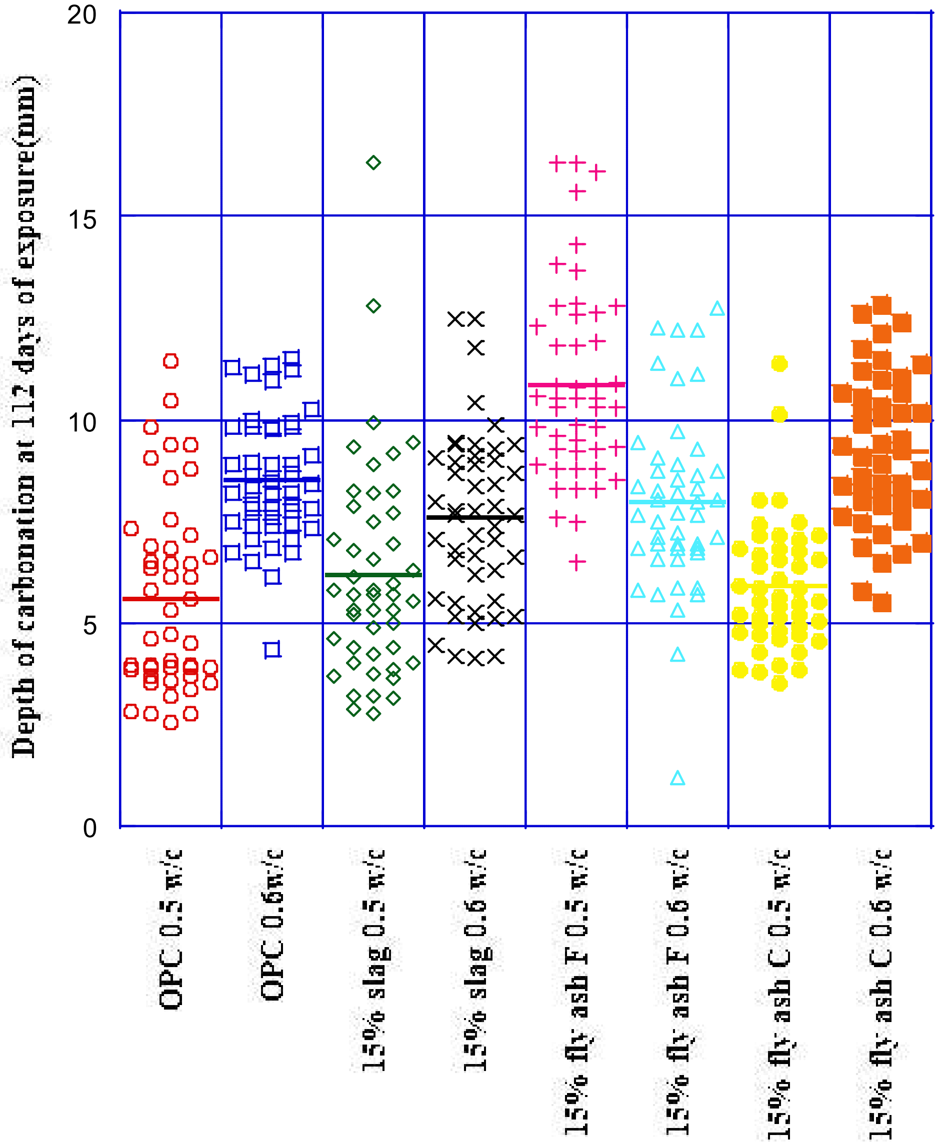

Figure 6.10 Depth of carbonation at lower replacement levels of SCMs
(Exposure period - 112 days)

Using the depth of carbonation data, the carbonation rate, which is the slope of the graph between depth of carbonation and the square root of time of exposure, is calculated. A typical graph between depth of carbonation and the square root of time of exposure is presented in Figure 6.11.

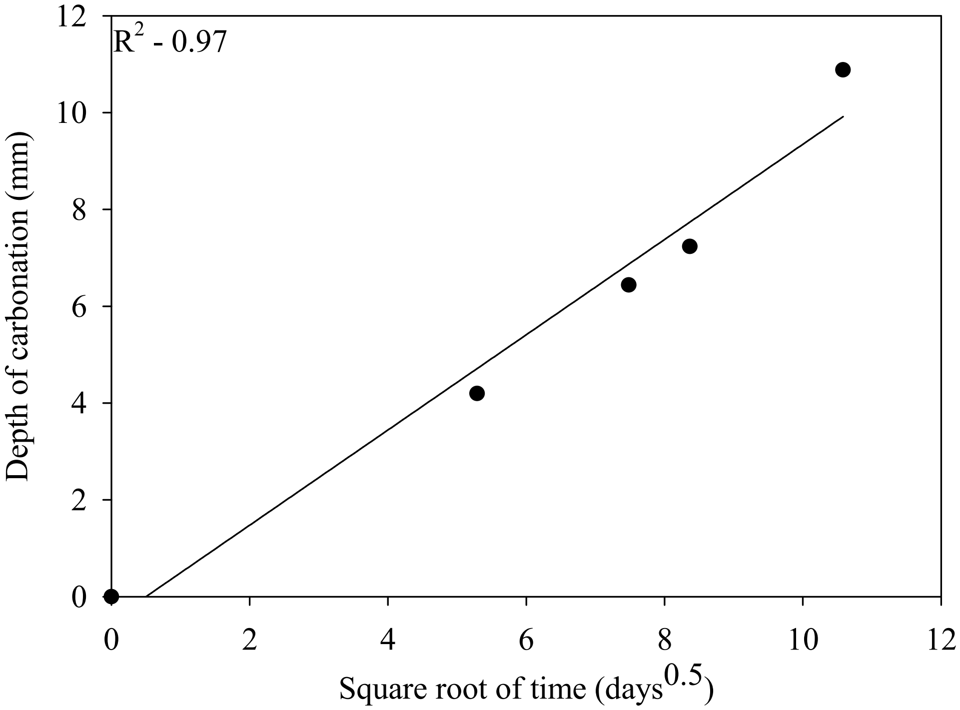

Figure 6.11 Typical plot between depth of carbonation and the square root of time of exposure (Total binder content 310 kg/m^3; w/b 0.5; 30% Class C fly ash)

The carbonation rate for various concretes with a total binder content of 310 kg/m^3 and w/b 0.5 is presented Figure 6.12. The carbonation rate is considered to be a material parameter of concrete. From Figure 6.12, it can be understood that the carbonation rate for OPC mix is lower than that of the other SCM mixes (except Class C fly ash at 15% replacement level). In all other categories, the carbonation rate of the Class C fly ash mixes at all replacement levels are lower and thus the current trend may be due to some experimental error or due to the scatter of the data. Using the carbonation rate, the carbonation resistance is calculated as per Equation 2.67 and is presented in Figure 6.13. As evident, the carbonation resistance of OPC mix (except in the case of 15% Class C fly ash mix) is more than for SCM mixes.

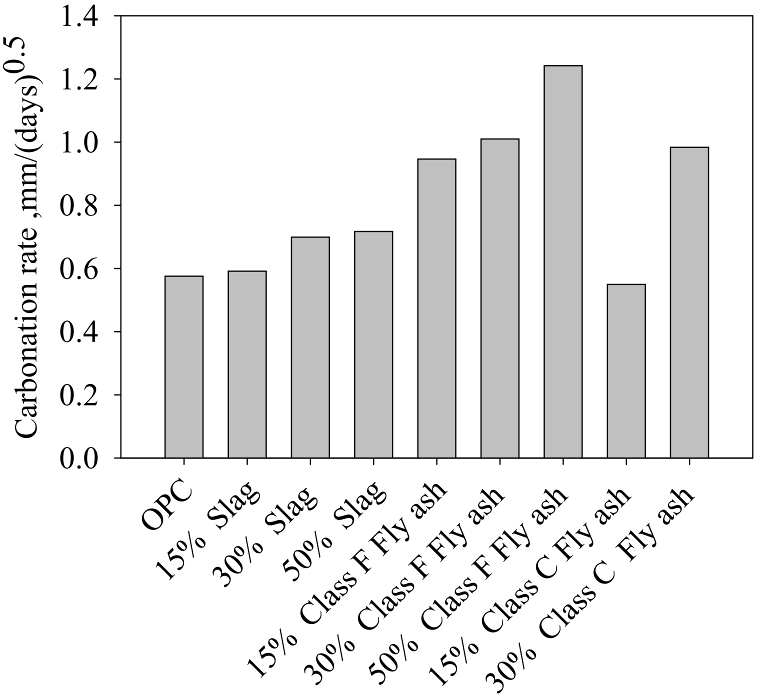

Figure 6.12 Influence of SCMs on the carbonation rate of mixes in the same category (Total binder content 310 kg/m^3 and w/b 0.5)

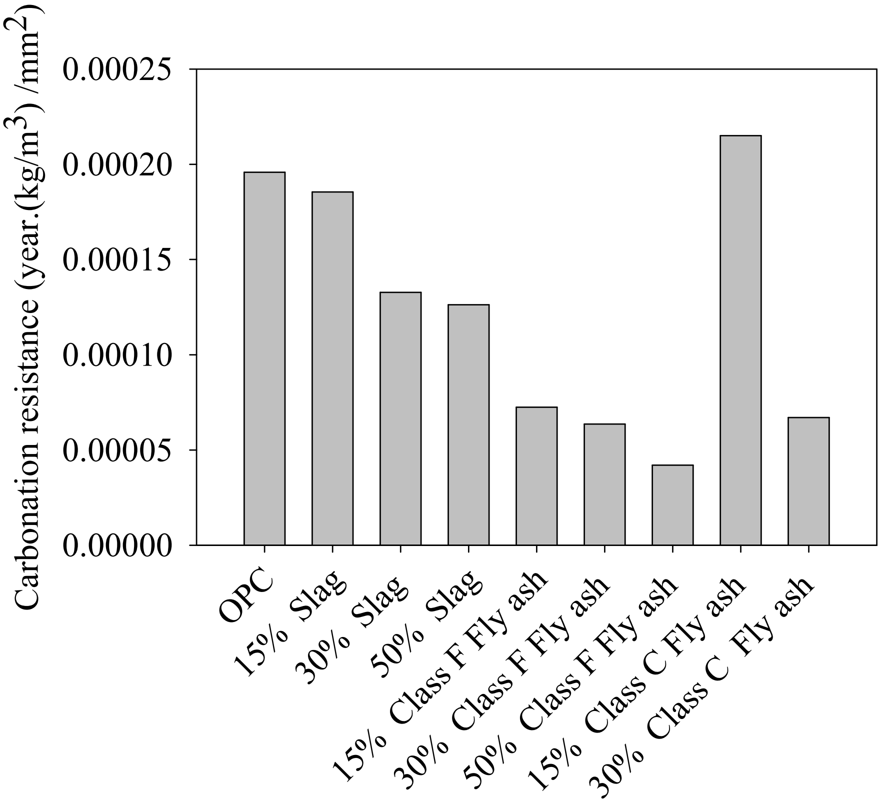

Figure 6.13 Influence of SCMs on the carbonation resistance of mixes in the same category (Total binder content 310 kg/m^3 and w/b 0.5)

It is interesting to note from Figures 6.12 and 6.13 that although there is only a marginal difference in the carbonation rates with slag and Class F fly ash at low replacement levels, the concretes differ significantly in terms of the carbonation resistance. Class F fly ash concretes are seen to have the lowest resistance, irrespective of the replacement level. Slag concretes, on the other hand, perform better than Class F fly ash concretes. The increase of replacement from 15 to 30% for Class C fly ash makes a major difference to the carbonation resistance.

The influence of SCMs on the Oxygen Permeability Index and Torrent air permeability is presented in Figure 6.14 and Figure 6.15.

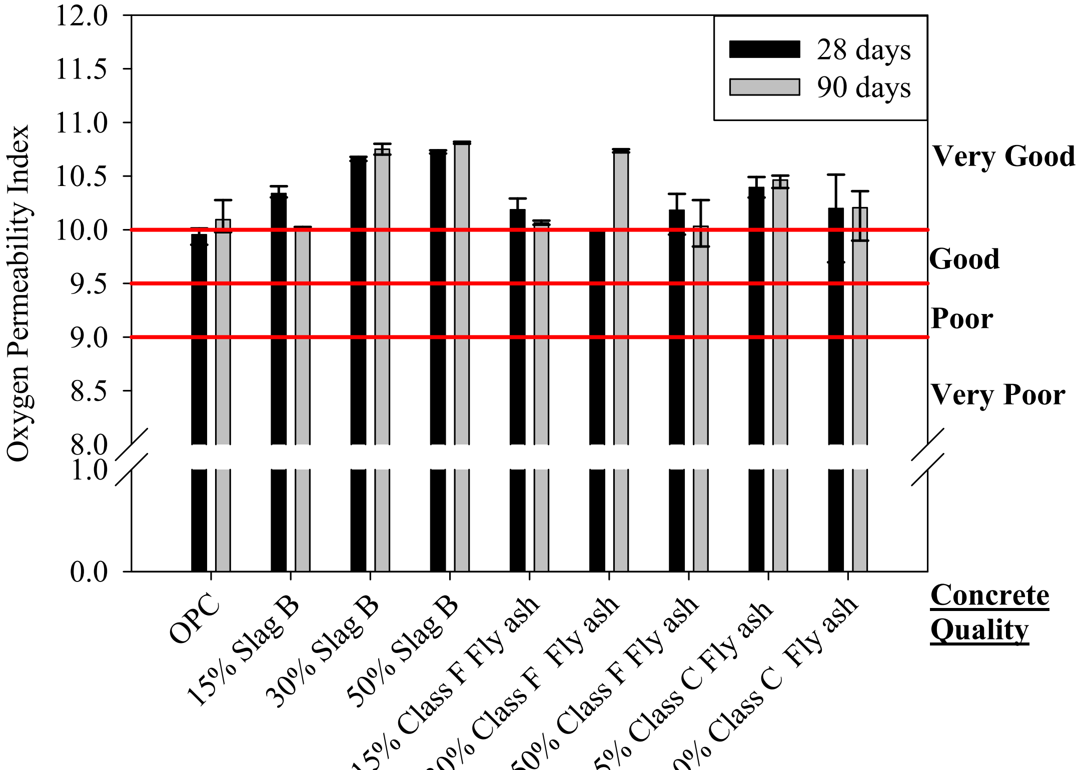

Figure 6.14 Influence of SCMs on Oxygen Permeability Index of mixes in the same category (Total binder content 310 kg/m^3 and w/b 0.5)

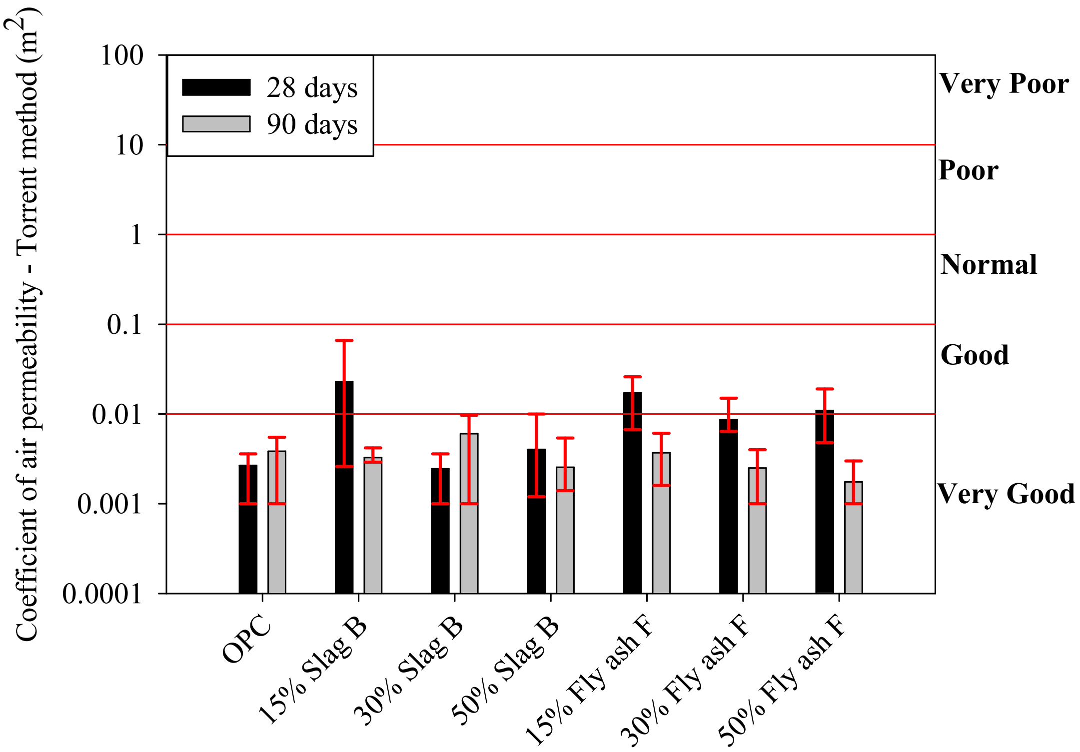

Figure 6.15 Influence of SCMs on the coefficient of air permeability of mixes in the same category (Total binder content 380 kg/m^3 and w/b 0.4)

It can be seen from Figure 6.14 and Figure 6.15, in terms of gas permeability, all the mixes fall into either very good or good category. This is similar for both the tests conducted in this testing programme. In the case of Torrent air permeability test, the results presented belong to specimens which are dried in the laboratory condition for three weeks. There was difficulty in getting consistent results in the other categories of the mixes, as in those cases, the specimens were dried in a 50°C oven for seven days. That's why the experiments to study the effect of specimen drying on the Torrent air permeability results were designed as discussed in chapter 5. From those studies, the drying in the laboratory conditions for three weeks is found to be the best conditioning methodology for Torrent air permeability test.

6.2.2 For all the concretes under study

The overall trends for the influence of SCM replacement on the carbonation rate is presented in Figure 6.16.

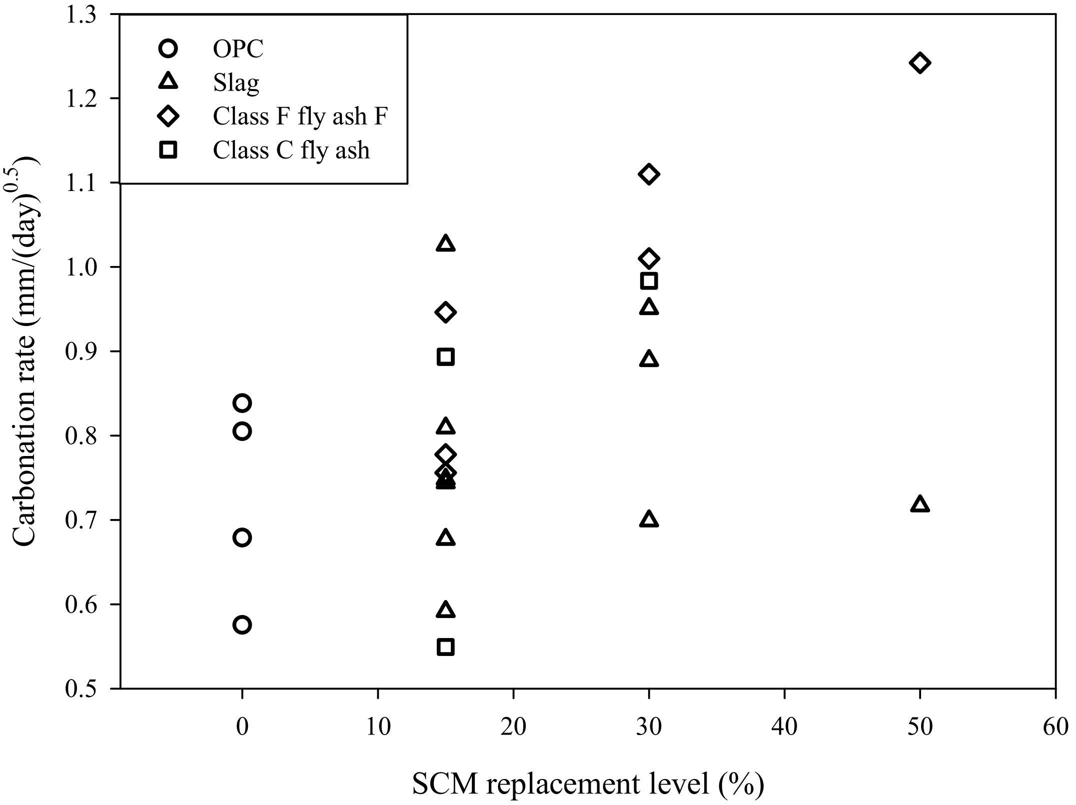

Figure 6.16 Influence of SCMs on the carbonation rate for all the concretes under study

In the case of carbonation rate, the trends are very clear from Figure 6.16. The carbonation rate is minimum for the OPC mixes. As OPC is replaced with SCMs, the carbonation rate increases. Mixtures in which 50% OPC is replaced with SCMs exhibit the highest rates of carbonation. This trend is in agreement with the findings of Andrade et al., (2013), Bijen et al. (1996), and Papadakis (2000). The reasons for the reduced performance of SCMs may be attributed to their pozzolanic reaction due to which $Ca(OH)_2$ is consumed; the depletion of $Ca\ (OH)_2$ by pozzolanic reaction implies that the first line of defense against carbonation is ineffective, and this can lead to decalcification of CSH by carbonation. Due to the carbonation of CSH, dense products are formed, which increase the porosity of the system. This can further accelerate the carbonation reaction.

The overall trend in the oxygen permeability index test is presented in Figure 6.17.

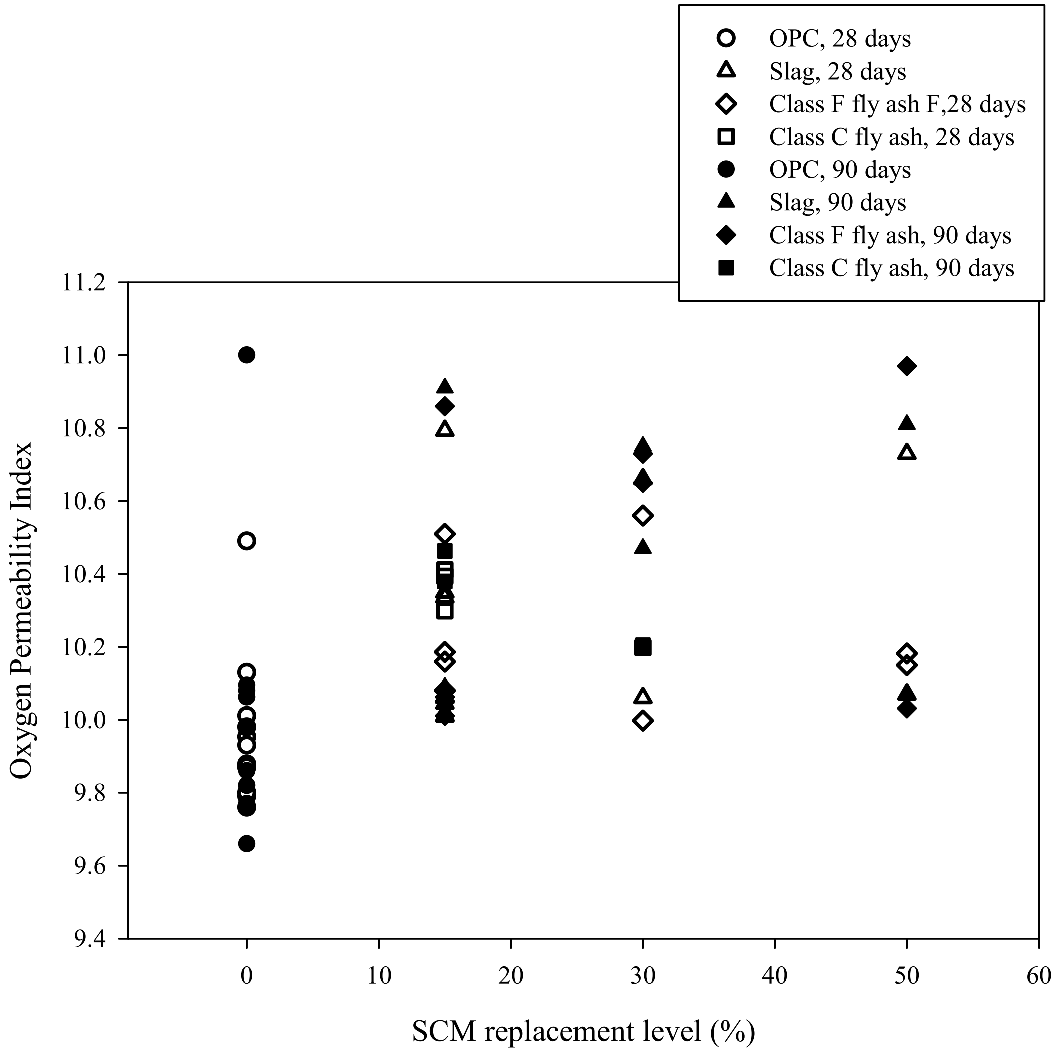

Figure 6.17 Influence of SCMs on the Oxygen Permeability Index for all the concretes under study

In the case of Oxygen Permeability Index test, it is difficult to identify a clear difference between different concretes selected for the study. All the results fall either in the good or very good category.

In the case of Torrent air permeability test results, the plot of the overall trend is not made as data with specimen conditioning in the laboratory environment for three weeks is not available for the entire set.

6.3 INFLUENCE OF SCMS ON DURABILITY PARAMETERS RELATED TO WATER PENETRABILITY

The test methods related to water penetrability carried out in this project include water sorptivity test and water permeability test. Initially, the water permeability test was conducted on specimens dried in a 50°C oven for 7 days. Later, as discussed in Chapter 5, it was found that drying affected the water penetration considerably. Thus, the results of the mixes having a total binder content of 380 kg/m^3 and water binder ratio 0.4 are only included in this section – in this case the tests were conducted as soon as the specimens were taken out of the moist room. To discuss the sorptivity results, results of the mixes having a total binder content of 310 kg/m^3 and water binder ratio 0.5 are considered.

6.3.1 For concretes having same total binder content and water binder ratio

The influence of SCMs on both sorptivity index and on the slope of best fit line between mass gain and square root of time are presented in Figure 6.18 and Figure 6.19. Owing to the difficulties in the interpretation of the sorptivity index, as discussed in Chapter 5, both these data are presented.

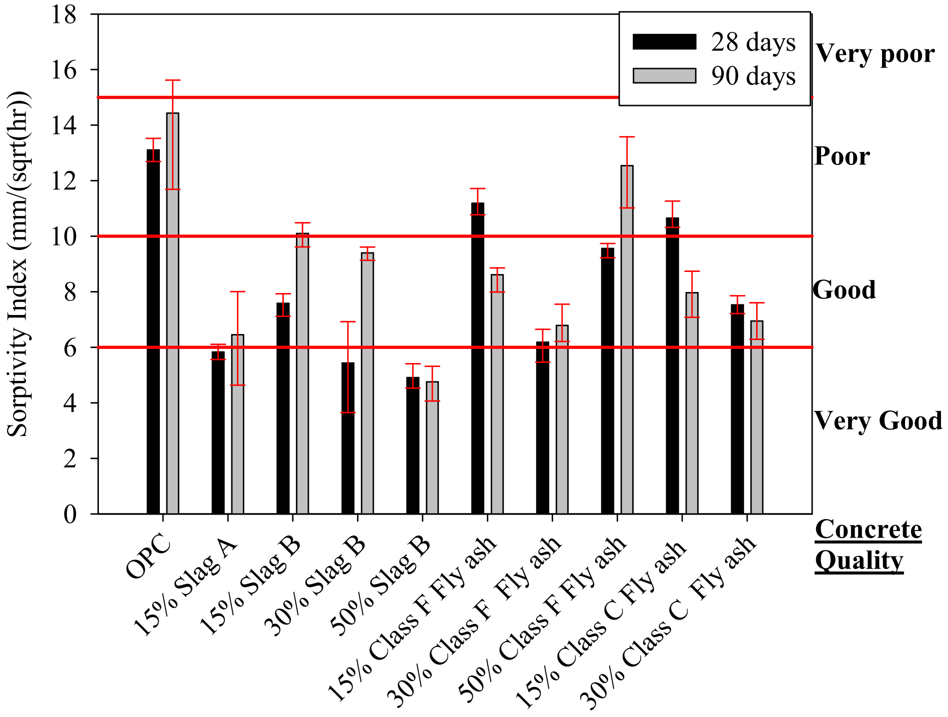

Figure 6.18 Influence of SCMs on sorptivity index of mixes in the same category (Total binder content 310 kg/m^3 and w/b 0.5)

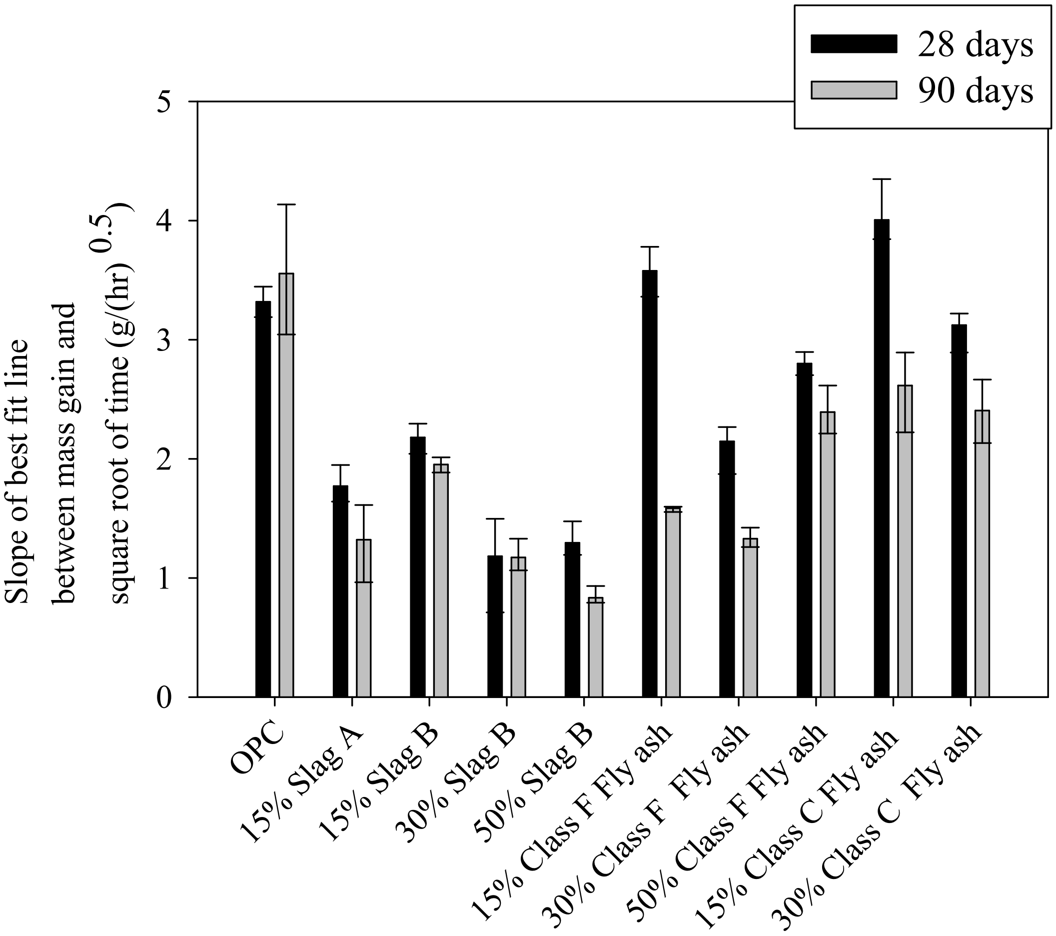

Figure 6.19 Influence of SCMs on slope of best fit line between mass gain and square root of time of mixes in the same category (Total binder content 310 kg/m^3 and w/b 0.5)

It is found from Figure 6.18 that SCM mixes perform better compared to mixes having 100% OPC as binder. Most of the mixes fall in the good category. However, there is lack of clarity in the performance when the curing duration changes from 28 to 90 days. This can be understood better by interpreting Figure 6.19. As the curing duration increases, the slope gets reduced, which indicates that the rate of capillary absorption is reduced. The performance of slag mixes is close to very good range, especially at higher dosages. Incorporation of Class F and Class C fly ash also contributes to the enhancement of durability against capillary absorption.

The results of the water permeability test results are presented in Figure 6.20. It is seen that all the mixes qualify as good quality concrete to resist aggressive environment, i.e., depth of water penetration < 30 mm. However, no significant contribution of SCMs is found.

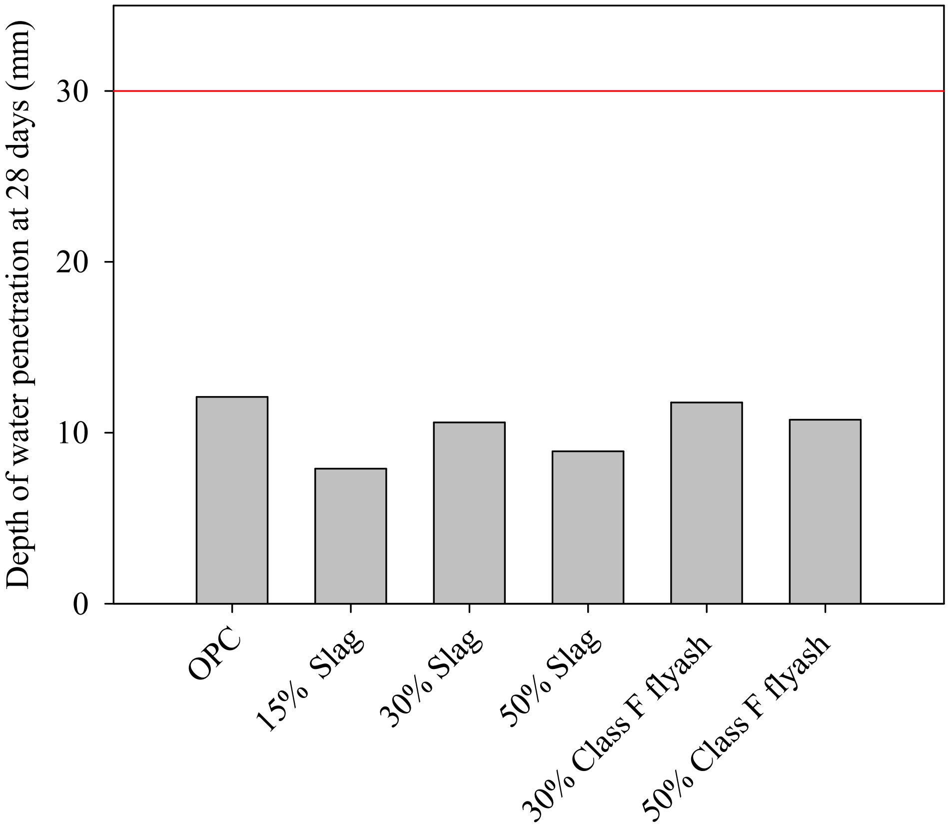

.

Figure 6.20 Influence of SCMs on the depth of water penetration of mixes in the same category (Total binder content 380 kg/m^3 and w/b 0.4)

6.3.2 For all the concretes under study

The influence of SCMs on the sorptivity index and on the slope of best fit line between mass gain and square root of time for all the concretes under study is presented in Figure 6.21 and Figure 6.22.

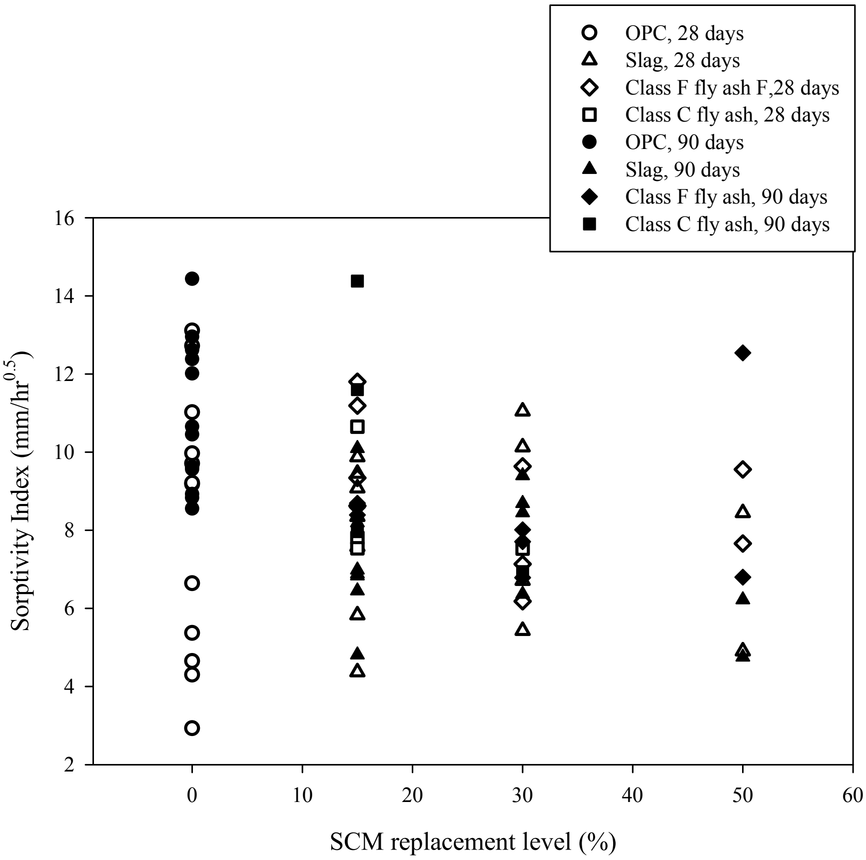

Figure 6.21 Influence of SCMs on the sorptivity index for all the concretes under study

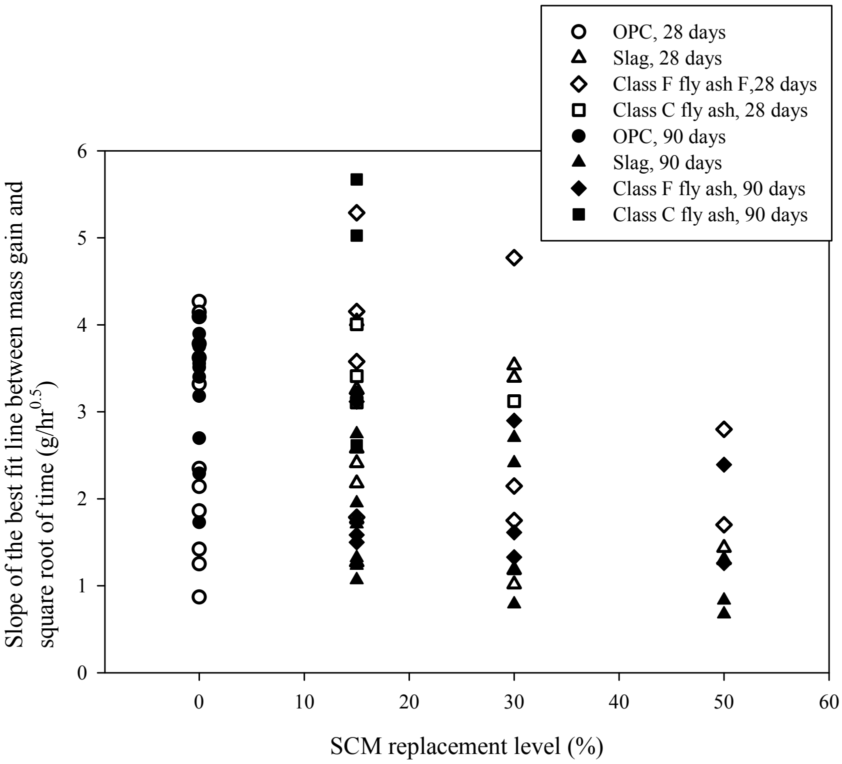

Figure 6.22 Influence of SCMs on the slope of best fit line between mass gain and square root of time for all the concretes under study

It can be seen from Figure 6.21 and Figure 6.22 that SCMs positively influence the water sorptivity test results. Mixes with SCMs perform better than OPC mixes. The improvement in the sorptivity is not significant at 28 days. However, the trends are more obvious at 90 days. This indicates the importance of extended curing. The improvement in the water sorptivity test result may be attributed to the development of pore structure caused by the pozzolanic reaction.

6.4 QUANTIFICATION OF THE INFLUENCE OF SCMS ON DURABILITY USING SERVICE LIFE PREDICTION MODELS

In this section, the effect of SCMs is quantified with the help of existing service life prediction models. For carbonation induced corrosion category, two existing service life models such as square root of time model and DuraCrete model are used to do the prediction. In the case of chloride induced corrosion, DuraCrete model is used to do the service life prediction. The prediction of service life is done for the mixes having a total binder content 310 kg/m^3 and w/b 0.5. The results are presented in terms of the service life of SCM mixes relative to OPC mix. The service life prediction helps to get the quantification of the pattern of results obtained in the previous sections of this chapter.

6.4.1 Carbonation induced corrosion

The service life of concrete structures in terms of carbonation induced corrosion is calculated based on two models, the square root of time model and the DuraCrete model. In both models, the carbonation resistance of the concrete mixtures is calculated based on the results from the accelerated carbonation test. The DuraCrete model considers, in addition to carbonation resistance, other influencing factors that affect service life such as curing factor, environment factor, age factor, partial factor for carbonation resistance etc.

6.4.1.1 Square root of time model for carbonation induced corrosion

It is well established that the depth of carbonation and the square root of time are directly proportional (Galan and Andrade, 2009). The constant of proportionality is the carbonation rate, which is considered to be a material parameter. The calculation of carbonation rate has been presented already in Equation 2.63. To bring out the difference in concentration of the CO_2 used in the accelerated test and that in the natural conditions, Visser (2014) had used the Equation 2.67. This equation is used here to predict the depth of carbonation at the end of a particular service life (in this case, 50 years) to get a comparison between different mixes. Table 6.1 gives the details of the carbonation depths predicted based on the square root of time law at 50 years. The predicted carbonation depths are presented as relative to the OPC concrete. Figure 6.23 shows a pictorial representation of the same.

Table 6.1 Carbonation depth prediction based on square root of time law

SCM replacement	Carbonation rate (mm/√days)	Carbonation resistance (year.(kg/m^3) /mm^2)	Carbonation depth relative to OPC concrete, predicted at 50 years
0	0.58	1.96E-04	1.00
15% Slag	0.59	1.85E-04	1.02
30% Slag	0.70	1.33E-04	1.21
50% Slag	0.72	1.26E-04	1.24
15% Class F fly ash	0.95	7.24E-05	1.63
30% Class F fly ash	1.01	6.36E-05	1.74
50% Class F fly ash	1.24	4.21E-05	2.14
15% Class C fly ash	0.55	2.15E-04	0.95
30% Class C fly ash	0.98	6.71E-05	1.70

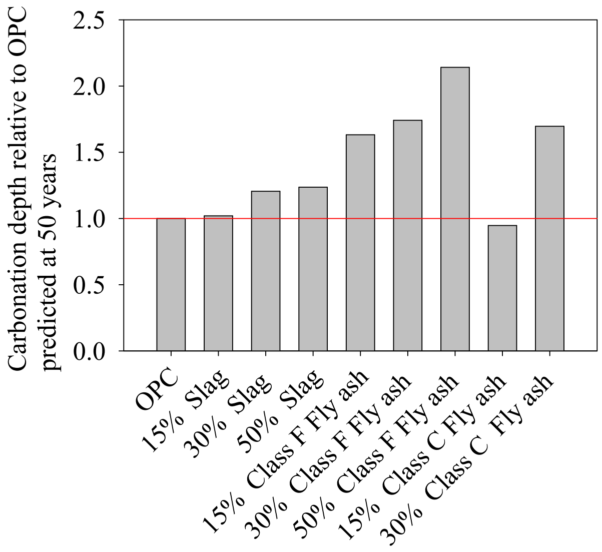

Figure 6.23 Carbonation depth relative to OPC predicted at 50 years for different concretes with binder content of 310 kg/m^3 and 0.5 w/b ratio

It can be seen from Figure 6.23 and Table 6.1 that as OPC is replaced with SCMs, the carbonation depth increases except for 15% Class C fly ash mix. The increase in carbonation depth is not significantly large in the case of Slag mixes (1.24 in the case of 50% slag mix). However, there is substantial increase in the depth of carbonation in the case of fly ash mixes. The relative carbonation depth is more than 2 (2.14) in the case of 50% Class F fly ash mix. When the carbonation front reaches the steel surface, or when the depth is equal to the concrete cover, it is considered as the end of service life. This implies that the service life of OPC mixes in a carbonation environment will be high compared to SCM mixes.

6.4.1.2 DuraCrete model

The inputs required to predict service life in terms of carbonation induced corrosion based on DuraCrete model include characteristic value of the carbonation resistance determined on the basis of compliance test (Accelerated carbonation test), characteristic value of the curing factor, characteristic value of the environment factor, age of the concrete when the compliance test is performed, characteristic value of the age factor and partial factor for the resistance with respect to carbonation.

For the present case, the following assumptions were made for service life prediction. In order to calculate the environmental factor, the laboratory condition having 65% RH is considered. However, this factor is suggested in the DuraCrete report only for OPC and slag. For fly ash concretes in this study, the factor corresponding to slag was adopted. All the concretes were cured for 28 days. The cost of mitigation is assumed to be normal and the concrete is assumed to be uncracked. Equation 2.67 is used to calculate the carbonation resistance. The service life predicted is represented in Table 6.2 and Figure 6.24 as service life relative to OPC.

Table 6.2 Service life relative to OPC in terms of carbonation induced corrosion predicted by DuraCrete model

SCM replacement	Carbonation rate (mm/√days)	Carbonation resistance (year.(kg/m^3) /mm^2)	Service life relative to OPC
0	0.58	1.96E-04	1.00
15% Slag	0.59	1.85E-04	0.95
30% Slag	0.70	1.33E-04	0.68
50% Slag	0.72	1.26E-04	0.64
15% Class F fly ash	0.95	7.24E-05	0.37
30% Class F fly ash	1.01	6.36E-05	0.32
50% Class F fly ash	1.24	4.21E-05	0.21
15% Class C fly ash	0.55	2.15E-04	1.10
30% Class C fly ash	0.98	6.71E-05	0.34

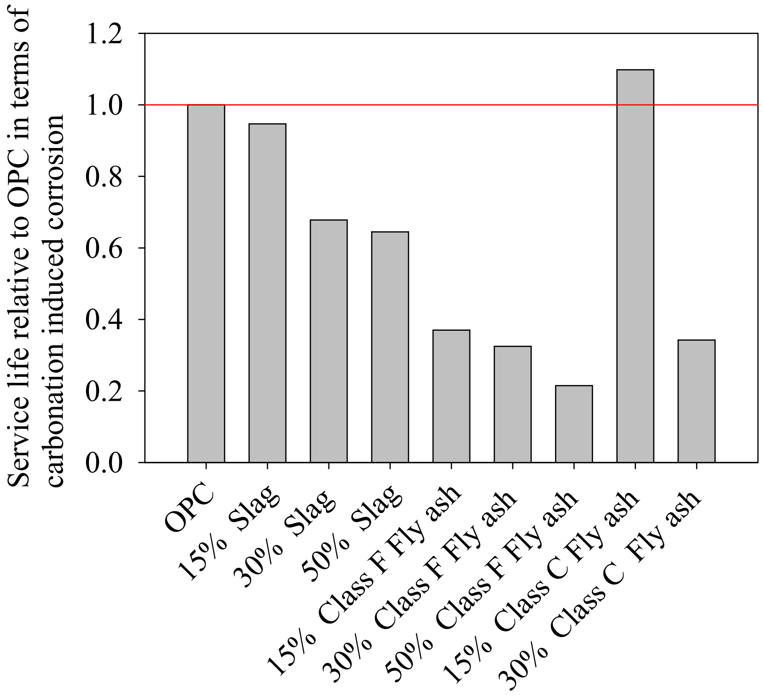

Figure 6.24 Service life relative to OPC in terms of carbonation induced corrosion predicted by DuraCrete model

From Table 6.2 and Figure 6.24, it can be inferred that the service life with respect to carbonation induced corrosion is less for SCM mixes compared to OPC mix except in the case of Class C fly ash mix at 15% replacement level. Slag at 15% replacement level does not significantly affect the service life of concrete (relative performance 0.95). However, at higher replacement levels, this effect is more significant. The relative performance of 50% slag mix is 0.68. In the case of Class F fly ash, a tremendous decrease in the performance is observed. The relative service life performances of Class F fly ash mixes at 15, 30 and 50% replacements are 0.37, 0.32 and 0.21 only. Even though, Class C fly ash at lower replacement level performed better than OPC, the relative performance of 30% Class C fly ash mix is obtained as 0.34 only. The service life prediction also underlines the conclusion made in the previous section that the performance of SCM mixes is not as good as that of pure OPC mixes.

6.4.2 Chloride induced corrosion

The service life of concrete structures in terms of chloride induced corrosion is calculated based on the DuraCrete model. In this model, the service life is calculated based on the non-steady state migration coefficient obtained by conducting the Rapid migration test.

6.4.2.1 DuraCrete model

For the present case, the service life prediction assumes the following conditions: the structure is located in a tidal zone; a cover depth of 75 mm is provided corresponding to the extreme environment in IS:456-2000; the cost of mitigation of risk relative to the cost of repair is assumed to be high. The design equation, which states that corrosion is initiated when the chloride concentration around the rebar exceeds the critical chloride threshold value is already presented in Equation 2.70. The design value of time dependent resistance is calculated based on the resistance determined on the basis of rapid migration test and modifying the same based on other factors such as curing factor, environment factor, age of concrete, age factor and partial factor for the resistance with respect to chloride ingress.

During the process of modelling, the following discrepancies were encountered. Characteristic values of critical chloride concentration data were available only for OPC concretes with w/b 0.5, 0.4 and 0.3. In the case of characteristic value of environment factor, which depends on the type of binder, the data was available only for OPC and slag. As in the previous case (carbonation), the values corresponding to slag were used for prediction for concretes with fly ash also. Using these factors, the relative service life obtained for SCM mixes with respect to OPC mix is presented in column 2 of Table 6.3; it is seen that the prediction is unrealistic in the case of fly ash mixes. Upon detailed analysis, it is concluded that the age factor provided in the DuraCrete report for fly ash is the primary reason for this discrepancy. Thus, it was decided to use the same age factor for fly ash as that of slag. The service life relative to OPC predicted using the modified age factor for fly ash is given in column 3 of Table 6.3.

Table 6.3 Service life relative to OPC in terms of chloride induced corrosion predicted by DuraCrete model

Binder type	Service life relative to OPC (predicted using the age factor given in DuraCrete model)	Service life relative to OPC (predicted using the modified age factor for fly ash)
OPC	1.00	1.00
15% Slag	0.79	0.78
30% Slag	3.35	3.33
50% Slag	13.81	13.78
15% Class F fly ash	14218.30	1.47
30%Class F fly ash	14978.46	1.50
50%Class F fly ash	34912552.27	5.83
15% Class C fly ash	0.30	0.28
30% Class C fly ash	12.16	0.44

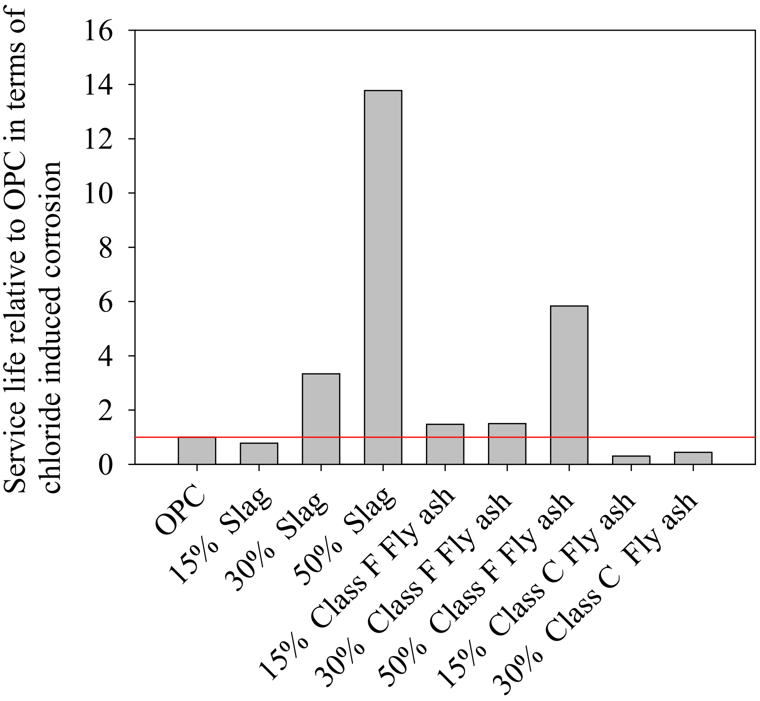

Figure 6.25 Service life relative to OPC in terms of chloride induced corrosion predicted by DuraCrete model

From Table 6.3 and Figure 6.25, it can be seen that the 50% slag mixes are capable of yielding a service life of around 14 times more than the plain OPC mix. This prediction also emphasizes that both slag and Class F fly ash mixes are better than OPC mixes in chloride penetration resistance. The reason for getting lower value of service life for Class C fly ash mixes may lie in the assumed age factor.

6.5 SUMMARY

The influence of SCMs on different durability parameters of concrete is presented in this chapter. The results are presented within one category of mixtures and across all the concretes studied under this project.

In the case of test methods where the specimens are fully saturated, the performance of SCM mixes are well ahead of OPC mixes, whereas in those tests where drying is performed, the performance of OPC and SCM mixes are close. SCM mixes show better resistance against chloride ion penetration than OPC mixes and the results are obvious at 28 days itself. This is reflected by the results of surface resistivity, RCPT, RMT and

CC tests. The reasons for this include pozzolanic reaction leading to the development of pore structure and modification in the pore solution chemistry due to the incorporation of SCMs.

Resistance against carbonation is less for SCM mixes, which agrees with the available literature. This may be attributed to consumption of $Ca(OH)_2$ in the pozzolanic reaction, which can lead to decalcification and subsequent carbonation of CSH. Due to the carbonation of CSH, dense products are formed, which increase the porosity of the system. This can accelerate further the progress of the carbonation front.

In the case of water sorptvity test, SCM mixes perform better than OPC mixes, and the trends are more obvious at 90 days. This indicates the importance of extended curing. The improvement can be attributed to the pore structure development due to pozzolanic reaction. All the water penetration depths obtained from DIN water permeability tests are below the value specified for aggressive environment. Thus, in this case, the influence of SCMs is not determine clearly.

No clear difference in durability parameters related to gas permeability test are observed in the concretes selected for the study. OPI and Torrent air permeability test results are either in the good or very good category. It is therefore difficult to identify a durability parameter to represent carbonation other than gas diffusion. This differs from the information available in the literature on this subject, in which a direct correlation between carbonation performance and the oxygen permeability index tests and Torrent air permeability tests was reported (Mackechnie and Alexander, 2002, Torrent, 2012).

The test results reconfirmed that as the water binder ratio increased, the durability parameters were adversely affected.

Table 6.4 gives a comparison of different durability tests done in this thesis work with respect to their capability to assess the influence of SCMs on the outcome of the test results.

Table 6.4 Comparison of the durability tests with respect to their capability to assess the influence of SCMs

Category	**Tests**	**Performance of SCMs in the test**	**Remarks**
Chloride penetration resistance	Wenner 4-probe resistivity	• As SCM dosage increases, surface resistivity increases • Best performance by Slag at 50% replacement • Enhancement of SR from 28 to 90 days is higher for Class F fly ash • Performance of Class C fly ash is similar to OPC	• The test is able to capture clearly the influence of SCMs and the curing duration
	Rapid chloride permeability	• As SCM dosage increases, total charge passed decreases • Best performance by Slag at 50% replacement • Enhancement of SR from 28 to 90 days is higher for Class F fly ash • Performance of Class C fly ash is similar to OPC	• The test is able to capture clearly the influence of SCMs and the curing duration • Six hour duration test; other useful parameters such as initial current, that can point towards durability, can be drawn
	Rapid migration	• As SCM dosage increases, the non – steady state migration coefficient decreases • Best performance by Slag at 50% replacement • Enhancement of SR from 28 to 90 days is higher for Class F fly ash • Performance of Class C fly ash is similar to OPC	• The test is able to capture clearly the influence of SCMs and the curing duration • Takes 24 hours generally, adaptable to service life modelling
	Chloride conductivity	• As SCM dosage increases, the chloride conductivity decreases • Best performance by Slag at 50% replacement • Enhancement of SR from 28 to 90 days is higher for Class F fly ash • Performance of Class C fly ash is similar to OPC	• The test is not able to demarcate clearly the influence of SCMs. Even though a decrease in chloride conductivity is observed, there is no substantial improvement in the category. All the mixes are falling either in the good or very good category. • Only mixes having higher dosages of SCMs are qualified to be in the very good category

Category	**Tests**	**Performance of SCMs in the test**	**Remarks**
Gas penetration resistance	Oxygen permeability	• All the results fall either in the good or very good category. • Influence of SCMs are not clear from this test based on the results obtained for the set of concretes tested in this project	• Difficult to identify a clear difference between different concretes selected for the study. • The pressure of 100kPa may not be sufficient in the case of high quality concretes
	Torrent air permeability	• All the results fall either in the good or very good category • Influence of SCMs are not clear from this test based on the results obtained for the set of concretes tested in this project	• Specimen conditioning affects the test results much • Drying in laboratory conditions at 25°C and 65% RH for 3 weeks is found to be the best conditioning methodology for laboratory specimens
	Accelerated carbonation	• Depth of carbonation is more for SCM mixes • At lower replacement level, the difference is not much significant at 112 days for slag and Class C fly ash • Fly ash mixes show greater depth of carbonation, whereas slag mixes show relatively less depth of penetration	• Represents the actual mechanism (gas diffusion) of carbonation • Even though accelerated carbonation test is linked with service life prediction models, the test takes months to complete and the products formed may be different from those formed due to natural carbonation
Water penetration resistance	Water sorptivity	• Better water sorptivity by SCM mixes • Clear trend is obtained only at 90 days testing	• To get clarity of the test results, analysis of both sorptivity index and the slope of best fit line between mass gain and square root of time together is required
	Water permeability	• DIN water permeability results below the specified value for aggressive environment	• The test needs to be done on samples at the saturated condition.

CHAPTER 7

MICRO-ANALYTICAL INVESTIGATIONS

7.1 INTRODUCTION

The micro-analytical studies were done to understand the reasons behind the effect of SCMs on different durability parameters which were discussed in Chapter 6. These studies were performed on mixes having a total binder content of 310 kg/m^3 and w/b 0.5.

A detailed review of literature on the influence of SCMs on chloride and carbonation induced corrosion and the microstructure of concrete was presented in section 2.5. The review of literature indicated that better chloride ion and water penetration resistance are exhibited by SCM mixes, due to the better microstructure development caused by the pozzolanic reaction, modification of pore solution chemistry and binding of chlorides. The carbonation resistance of SCM mixes is poor compared to OPC mixes. This is due to the reduction in calcium hydroxide (Portlandite) content because of pozzolanic reaction, decalcification of CSH and increase in the porosity of the system.

In order to establish the link between microstructure and performance, micro-analytical studies were performed in this research project. To assess the pozzolanic reaction, the portlandite contents of paste samples having different replacement levels of SCMs were determined by Thermo Gravimetric Analysis (TGA) at two ages (28 days and 90 days). The pore solution conductivities of different mixes were calculated using a software developed by the National Institute of Standards and Technology, USA, which is available at http://ciks.cbt.nist.gov/poresolncalc.html. The input parameters for this study were obtained from the chemical composition of binders analysed by X – Ray Fluorescence Spectroscopy. The microstructural features of the chloride and carbonation attacked concrete samples were studied by backscattered electron (BSE) imaging in scanning electron microscopy (SEM), carried out on epoxy impregnated polished concrete surfaces. The chloride binding was assessed by conducting X – ray diffraction (XRD) on powder obtained by profiling concrete samples which were immersed in chloride solution for 35 days. In order to study the chemical and phase changes due to carbonation, paste samples which were subjected to complete carbonation (at 3% CO_2 concentration) were analysed using XRD and TGA.

7.2 PORTLANDITE CONTENT

Portlandite content was determined by performing TGA on paste samples which were cured under saturated lime water for 28 and 90 days respectively. After curing, these samples were crushed and sieved through 75 µm sieve and tested. The temperature range chosen for the study was from 0 to 1200°C at an increment of 10°C per minute. Figure 7.1 shows the typical output of the TG/DSC experiment.

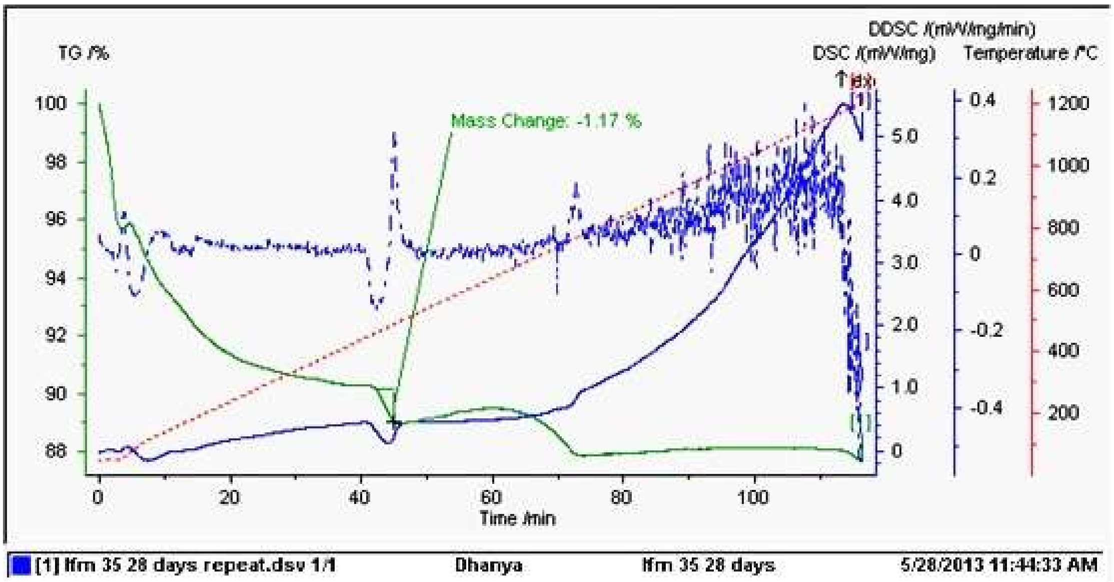

Figure 7.1 Typical output of the TG/DSC experiment

The peak between 400 and 500°C corresponds to the decomposition of $Ca(OH)_2$ or portlandite. The dehydroxylation reaction can be written as:

$$Ca(OH)_2 \rightarrow CaO + H_2O \tag{7.1}$$

Using the mass loss data, the portlandite content is calculated by Equation 7.2.

$$Portlandite\ content = Mass\ loss\ between\ 400\ to\ 500\ ℃ \times \frac{molecular\ mass\ of\ Ca(OH)_2}{molecular\ mass\ of\ H_2O} \quad (7.2)$$

The results of the Thermo Gravimetric Analysis are presented in Table 7.1.

Table 7.1 Results of the Thermo Gravimetric Analysis

Binder details	28 days		90 days	
	Mass loss (%)	Portlandite content (%)	Mass loss (%)	Portlandite content (%)
OPC	2.98	12.25	3.95	16.24
15% slag	1.8	7.40	2.1	8.63
30% slag	1.41	5.80	1.3	5.34
50% slag	0.71	2.92	0.5	2.06
15% Class F fly ash	3.16	12.99	2.27	9.33
30% Class F fly ash	1.79	7.36	1.58	6.50
50% Class F fly ash	1.17	4.81	0.44	1.81
15% Class C fly ash	2.68	11.02	3.0	12.33
30% Class C fly ash	2.05	8.43	2.0	8.22

The variation of portlandite content with the replacement level of SCMs at the two ages (28 and 90 days) is represented graphically in Figure 7.2 and Figure 7.3.

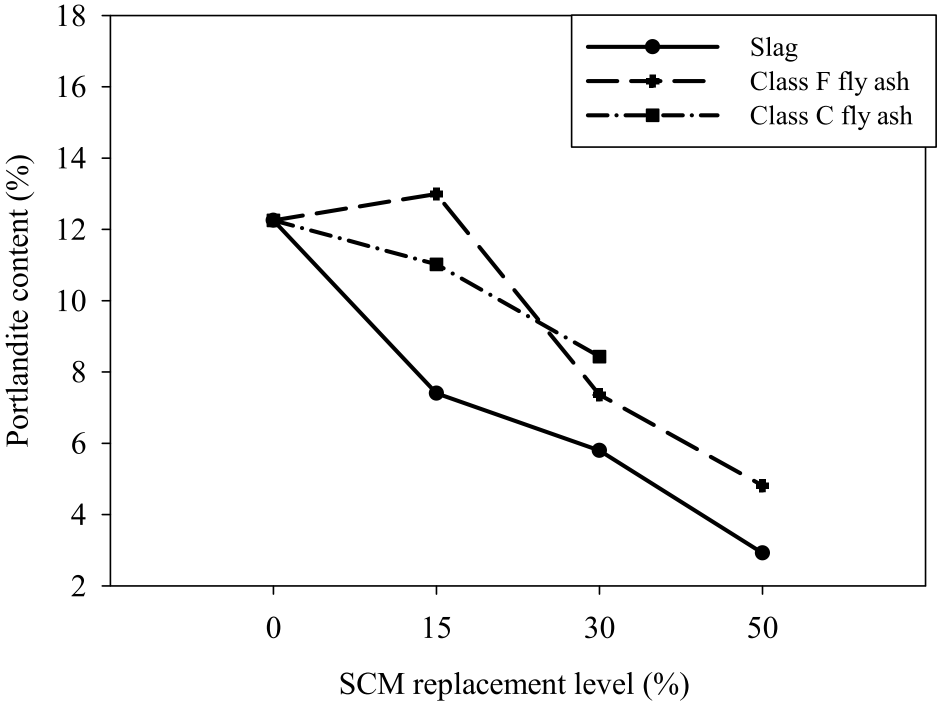

Figure 7.2 Variation of portlandite content with SCM replacement level at 28 days

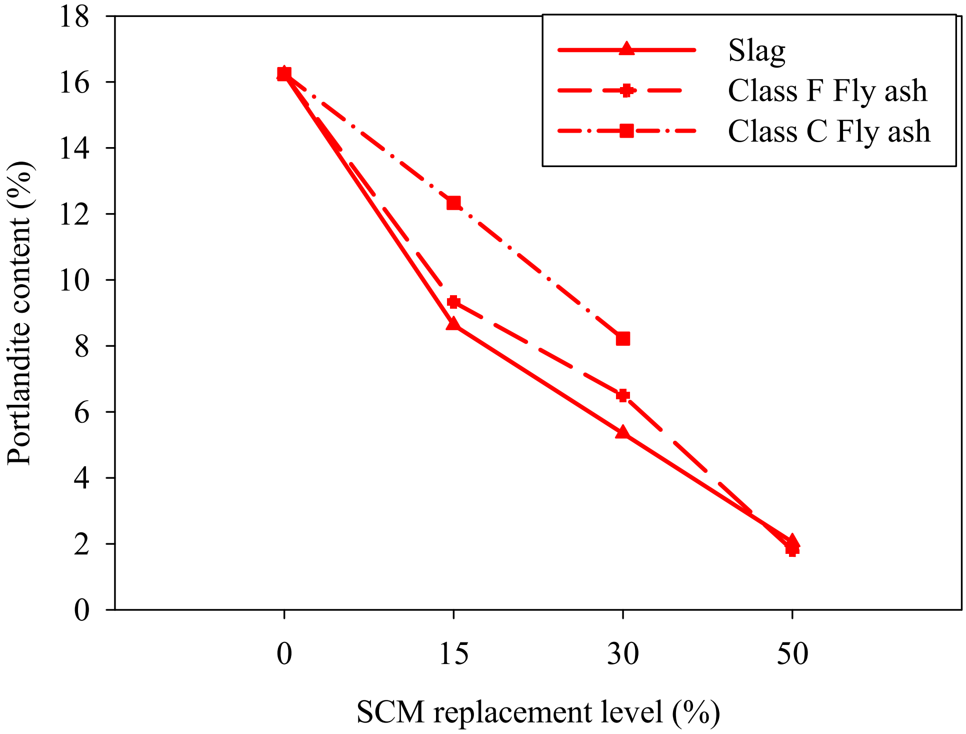

Figure 7.3 Variation of portlandite content with SCM replacement level at 90 days

In the case of OPC, the portlandite content is increasing as the curing duration increases from 28 to 90 days, indicating prolonged hydration of cement. The portlandite content is decreasing in the case of SCMs from 28 to 90 days (except 15% of slag and Class C fly ash mixes). Further, there is a decrease in portlandite content as the replacement level increases in the case of all SCMs, which is evident from Figure 7.2 and Figure 7.3. The results indicate that more pozzolanic reaction happens when the SCM dosage increases and also with increase in curing days. It is to be noted that the decrease in portlandite content is more in the case of Class F fly ash mixes as the curing duration increases from 28 to 90 days. This supports the durability test results which indicate that the enhancement of durability parameters from 28 to 90 days is more for Class F fly ash mixes. This indicates that the major mechanism is pozzolanic reaction in the case of Class F fly ash compared to cementitious reaction. The slag mixes showed lower content of portlandite even at 28 days of age. This indicates that both cementitious and pozzolanic reaction are happening in slag even at early ages. The similarity in behaviour of Class C fly ash mixes and OPC mixes in durability tests are supported by their contents of portlandite, which are close. Much variation in portlandite content can be observed compared to OPC mix, for mixes having SCMs as the curing duration increases from 28 to 90 days. This indicates that in order to explore the maximum potential of SCMs, prolonged curing is essential. This also supports the enhancement of durability parameters as observed in test results at 90 days compared to those at 28 days. The lowest content of portlandite in 50% Class F fly ash mix also supports its poor performance in the carbonation test.

7.3 PORE SOLUTION CONDUCTIVITY

The conductivity of the pore solution for different mixes was calculated using a software which was developed at the National Institute of Standards and Technology (NIST), which is an agency of the U.S. Departments of Commerce. This software is freely available on the web at http://ciks.cbt.nist.gov/poresolncalc.html. The inputs of the chemical composition for the software are obtained from the X-ray fluorescence (XRF) studies done on different binders.

Table 7.2 Pore solution conductivity values of concrete mixtures having a total binder content of 310 kg/m^3 and w/b 0.5

Binder content (kg/m^3)	Water content (kg/m^3)	Cement content (kg/m^3)	SCM content (kg/m^3)				Pore solution composition estimated (M)			Pore solution conductivity estimated (S/m)
			Slag A	Slag B	Class F fly ash	Class C fly ash	K^+	Na^+	OH^-	
310	155	310					0.2	0.42	0.62	11.92
310	155	264	46				0.17	0.36	0.53	10.34
310	155	264		46			0.17	0.36	0.53	10.34
310	155	217		93			0.14	0.29	0.43	8.69
310	155	155		155			0.1	0.21	0.31	6.41
310	155	263			47		0.27	0.37	0.64	12.44
310	155	217			93		0.34	0.33	0.66	12.95
310	155	155			155		0.43	0.27	0.7	13.64
310	155	263				47	0.18	0.42	0.59	11.5
310	155	217				93	0.15	0.42	0.57	11.09

The results show that the pore solution conductivity decreases with increase in slag replacements whereas in the case of Class F fly ash mixes, as the replacement level increases, pore solution conductivity increases. For Class C fly ash mixes, a trend similar to slag can be observed – however, the data set is smaller. The following sections explore the influence of change in pore solution conductivity on the surface resistivity of concretes having these three SCMs.

7.3.1 Effect of pore solution conductivity on surface resistivity of concrete

Figures 7.4 to 7.6 depict the variation of surface resistivity values with regard to the change in pore solution conductivity for slag, Class F fly ash and Class C fly ash respectively.

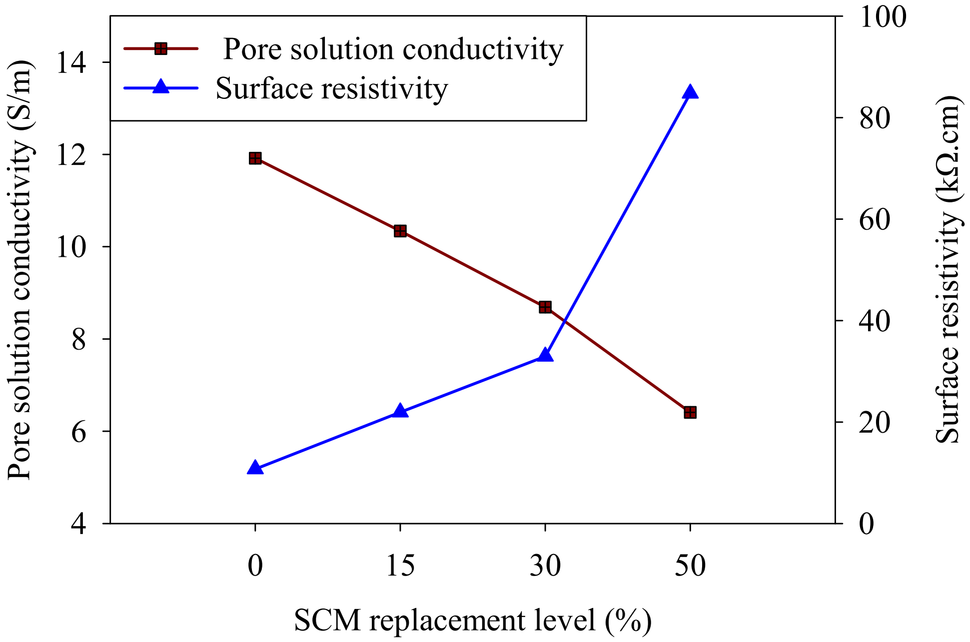

Figure 7.4 Variation of pore solution conductivity and surface resistivity of slag mixes

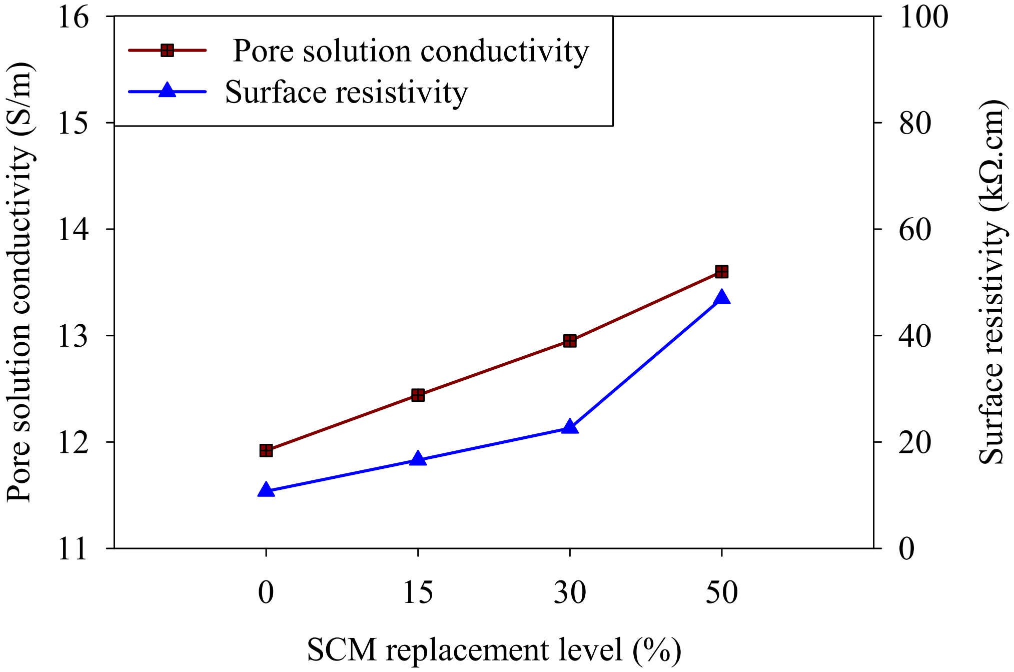

Figure 7.5 Variation of pore solution conductivity and surface resistivity of Class F fly ash mixes

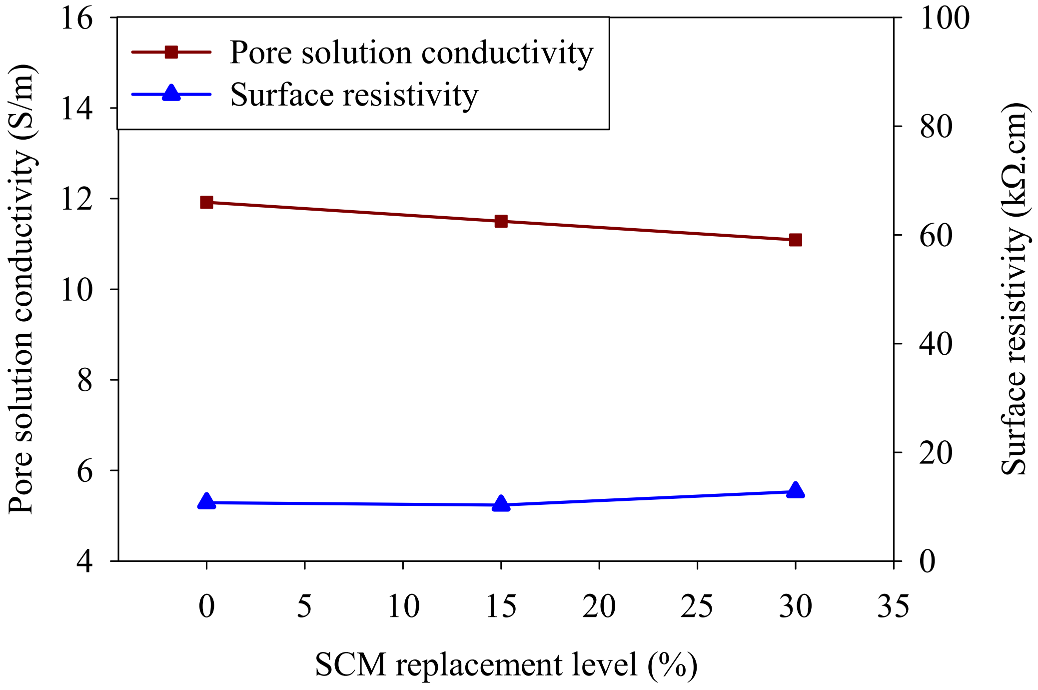

Figure 7.6 Variation of pore solution conductivity and surface resistivity of Class C fly ash mixes

Figure 7.4 shows that the pore solution conductivity decreases with increase in slag replacements and correspondingly there is an increase in the surface resistivity values. Figure 7.5 indicates that in the case of Class F fly ash mixes, as the replacement level increases, pore solution conductivity increases. Unlike the case with slag, there is an increase in surface resistivity values with increase in Class F fly ash content. For Class C fly ash mixes, the pore solution conductivity decreases with replacement level whereas the surface resistivity tend to increase, as evident from Figure 7.6. Thus, it can be concluded that surface resistivity values are not only related to pore solution conductivity, but also on the microstructure development. More experimental studies on the microstructure development using electrical impedance spectroscopy (EIS) and pore structure characterization using mercury intrusion porosimetry (MIP) are required to come up with solid conclusions in this aspect.

7.4 MICROSTRUCTURAL CHAGES IN CONCRETE DUE TO CHLORIDE INGRESS AND CARBONATION

The microstructure of different concretes subjected to chloride ion penetration and carbonation were examined by SEM in BSE mode. In order to detect the elemental composition of different phases observed in the BSE images, EDS analyses were done.

7.4.1 Evidence of binding of chlorides in concrete

Figure 7.7 presents the SEM images of concrete samples having 30 % slag as supplementary cementitious material. These samples were prepared from concretes immersed in 3% NaCl solution for 35 days after 28 days of moist curing. The highlighted portion in the Figure 7.7 is the Friedel's salt ($3CaO.Al_2O_3.CaCl_2.10H_2O$), the composition of which was identified by EDS analysis. The elemental composition of the highlighted portion is also presented.

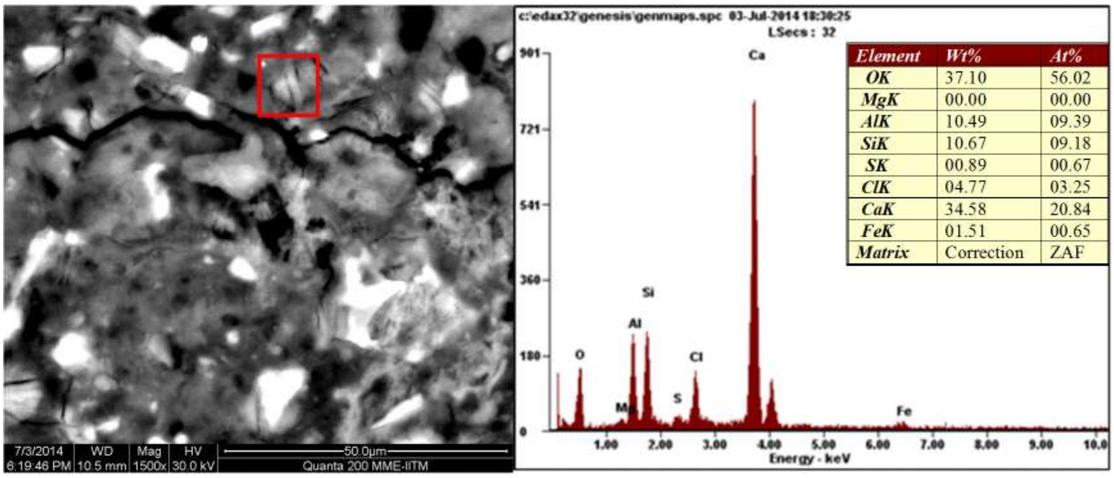

Element	*Wt%*	*At%*
OK	37.10	56.02
MgK	00.00	00.00
AlK	10.49	09.39
SiK	10.67	09.18
SK	00.89	00.67
ClK	04.77	03.25
CaK	34.58	20.84
FeK	01.51	00.65
Matrix	Correction	ZAF

Figure 7.7 SEM - BSE image of concrete having 30% slag mix subjected to chloride ion penetration

In a similar way, the evidence of chloride binding was found in the Class C fly ash mix as depicted in Figure 7.8. EDS data confirmed the presence of Friedel's salt.

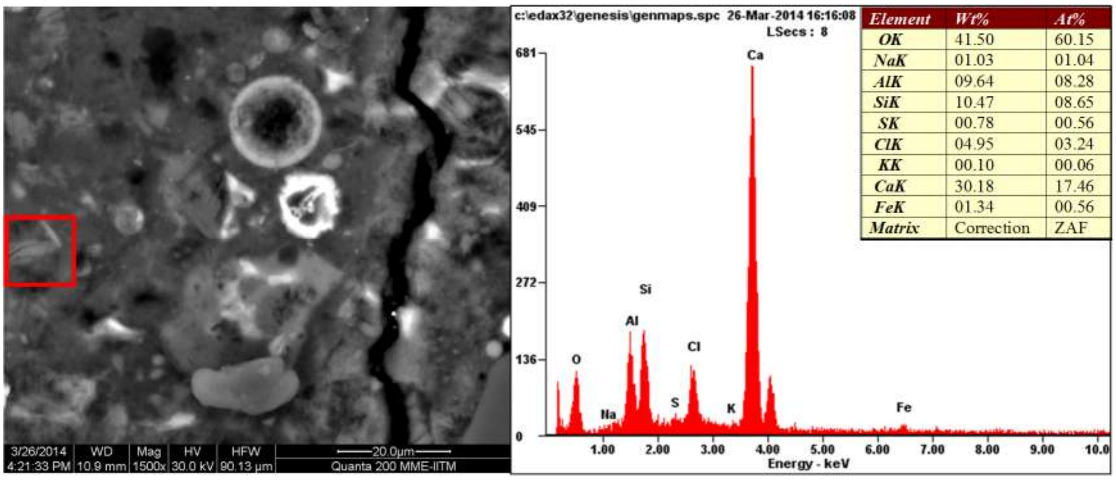

Element	*Wt%*	*At%*
OK	41.50	60.15
NaK	01.03	01.04
AlK	09.64	08.28
SiK	10.47	08.65
SK	00.78	00.56
ClK	04.95	03.24
KK	00.10	00.06
CaK	30.18	17.46
FeK	01.34	00.56
Matrix	Correction	ZAF

Figure 7.8 SEM - BSE image of concrete having 30% Class C fly ash mix subjected to chloride ion penetration

The appearance of the Friedel's salt and the EDS data (mainly the relative heights of the chlorine, aluminium and calcium peaks) were similar to those found in published literature (Brown and Badger, 2000). The BSE image from the publication by these authors is already presented as Figure 2.36 in the literature review chapter (Section 2.5.4.1).

The formation of Friedel's salt was confirmed further by the X–ray diffraction analysis which was conducted on powders obtained by profiling the samples immersed in chloride solution, as shown in Figure 7.9.

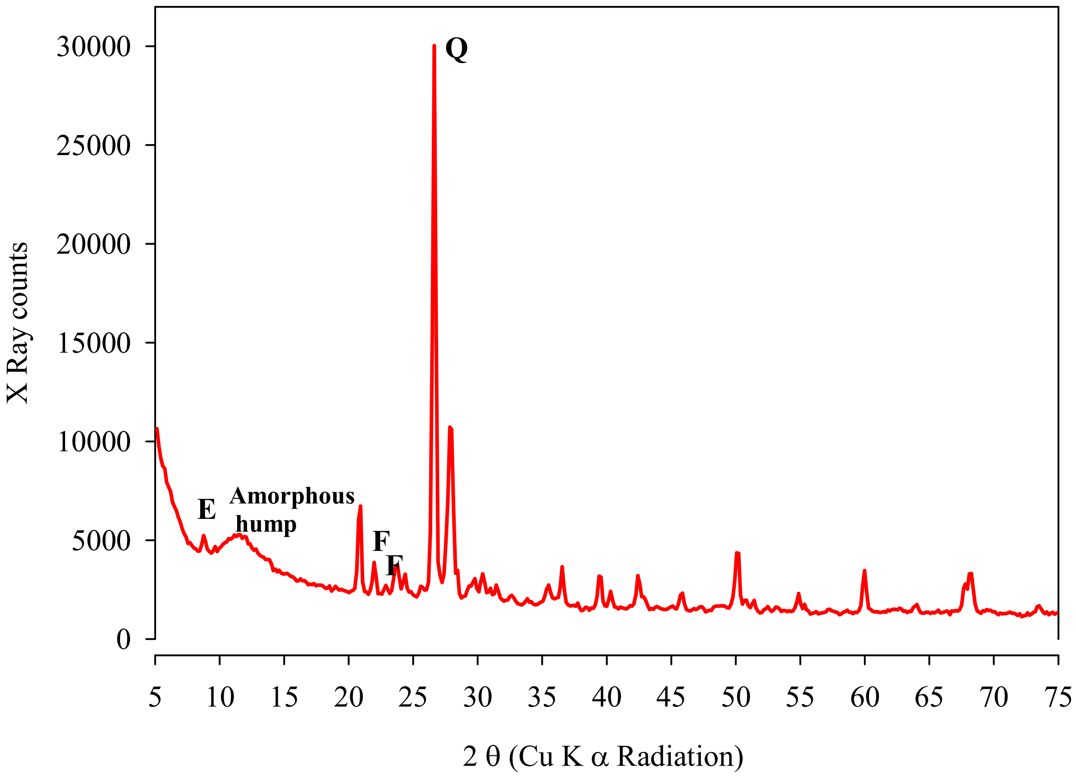

Figure 7.9 XRD pattern of concrete having 30% Class F fly ash subjected to chloride ion penetration

The analysis of XRD patterns confirmed the presence of Friedel's salt (F) in all the concretes. The peak at 11.4° of 2θ corresponding to Friedel's salt was not clearly visible in the case of SCM mixes, whereas the other peaks at 22°and 23° were clearly distinguishable. In the case of concrete having SCMs, an amorphous hump is observed between 10° and 13° of 2θ, especially in layers close to the surface. This might be due to the presence of mixture of chloride containing phases, which include Friedel's salt. Presence of ettringite (E) and quartz (Q) is also evident in the XRD pattern.

7.4.2 Modification of paste matrix due to carbonation

Many microstructural changes were observed in the paste matrix due to the carbonation reaction. These changes include formation of calcite, decalcification of CSH and an overall increase in porosity of the system. All the images presented in this section were taken in the Back Scattered Electron mode of the Scanning Electron Microscope on concrete samples which were subjected to carbonation for 112 days in the accelerated carbonation chamber at 1% CO_2 concentration.

7.4.2.1 Calcite formation

Figure 7.10 to Figure 7.13 depict the SEM – BSE images of the surface zone of the concrete with different binder combinations such as 100% OPC, 30% slag, 30% Class F fly ash and 30% Class C fly ash respectively.

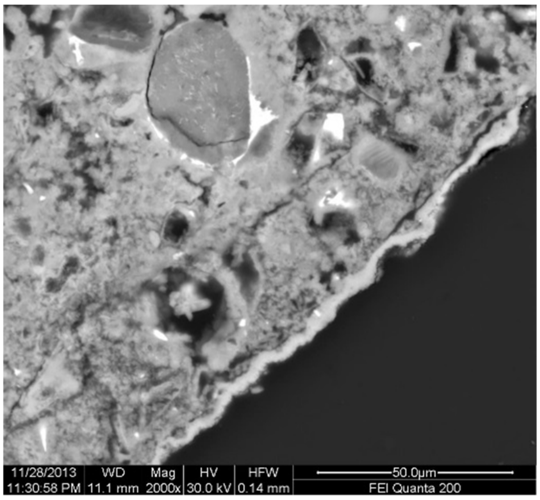

Figure 7.10 SEM - BSE image of concrete having 100% OPC subjected to carbonation

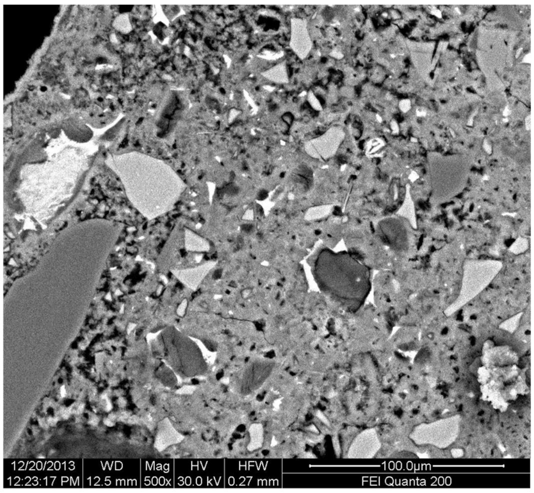

Figure 7.11 SEM - BSE image of concrete having 30% slag subjected to carbonation

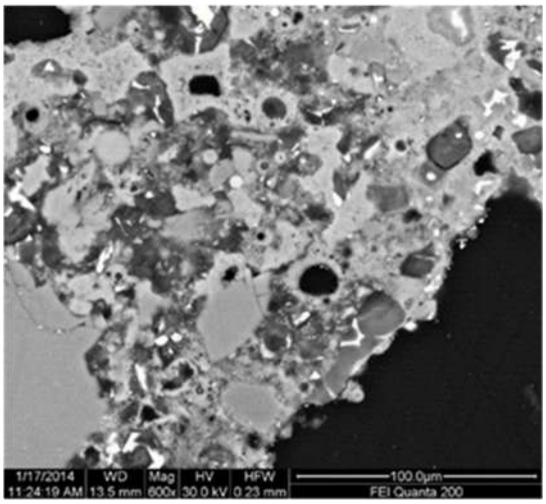

Figure 7.12 SEM - BSE image of concrete having 30% Class F fly ash subjected to carbonation

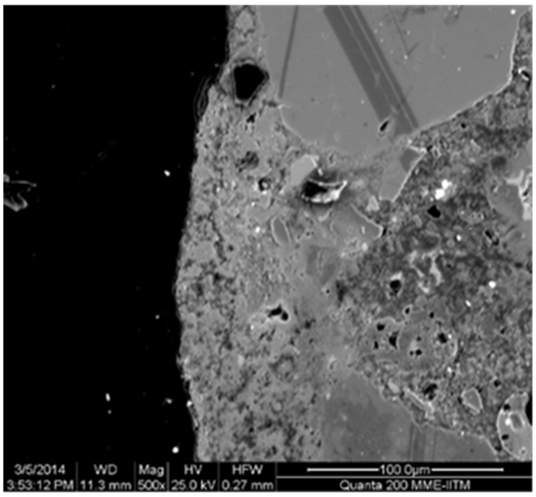

Figure 7.13 SEM - BSE image of concrete having 30% Class C fly ash subjected to carbonation

Calcite is found to be deposited especially in the surface regions in all the concretes. The presence of calcite ($CaCO_3$) is confirmed by EDS analysis. Figure 7.14 shows a typical EDS pattern which is obtained from concrete having 100% OPC.

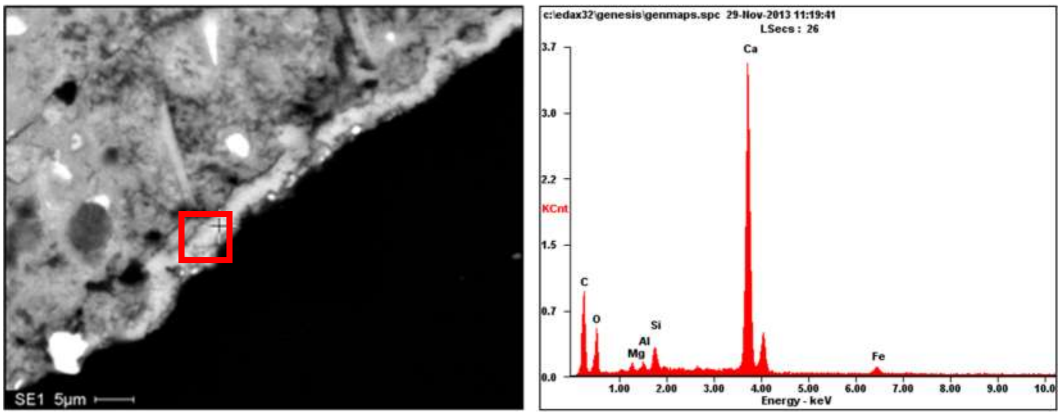

Figure 7.14 SEM - BSE image of concrete having 100% OPC subjected to carbonation

The EDS analysis confirms that the surface deposit is calcite. A large degree of calcite is formed in the surface regions, almost as a protective layer, as evident from Figure 7.14. The SEM - BSE images of the surface zone of concrete having 30% and 50% Class F fly ash subjected to carbonation are presented in Figure 7.15 and Figure 7.16 respectively.

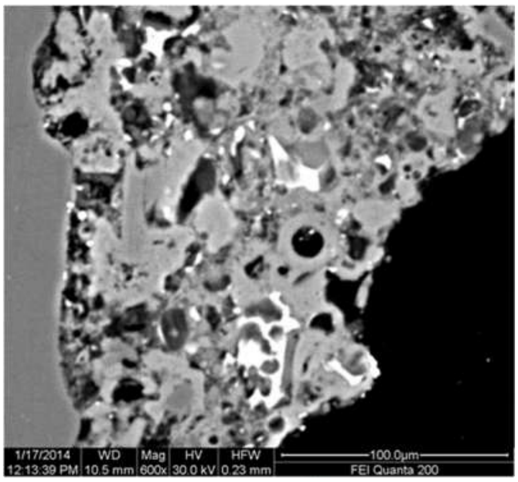

Figure 7.15 SEM - BSE image of the surface zone of concrete having 30% Class F fly ash subjected to carbonation

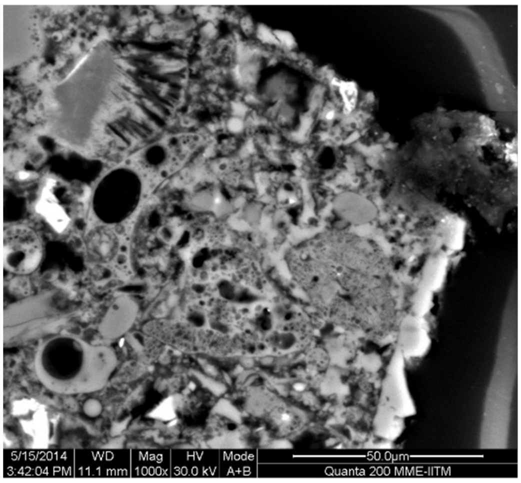

Figure 7.16 SEM - BSE image of the surface zone of concrete having 50% Class F fly ash subjected to carbonation

Figure 7.15 and Figure 7.16 indicate substantial calcite formation in the surface zones. Although the CH content was much lower compared to OPC, the evidence of major calcite deposition points to the possible carbonation of the CSH. The following section explores the EDS analysis of the CSH composition, to assess the extent of decalcification of CSH, that would have led to the formation of the calcite.

7.4.2.2 Decalcification of CSH

Figure 7.17 to Figure 7.20 present the SEM – BSE images of the concretes having different binder combinations such as 100% OPC, 30% slag, 30% Class F fly ash and 30% Class C fly ash subjected to carbonation with the EDS details.

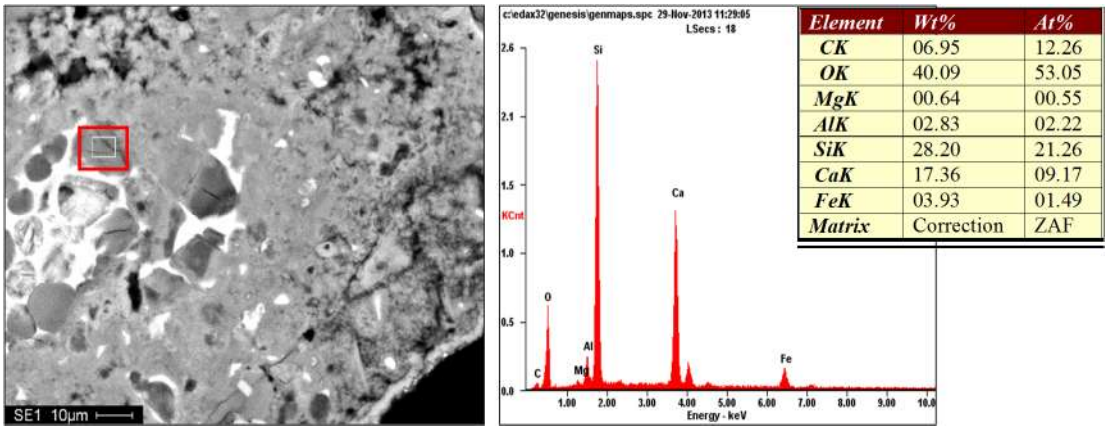

Element	*Wt%*	*At%*
CK	06.95	12.26
OK	40.09	53.05
MgK	00.64	00.55
AlK	02.83	02.22
SiK	28.20	21.26
CaK	17.36	09.17
FeK	03.93	01.49
Matrix	Correction	ZAF

Figure 7.17 SEM - BSE image of concrete having 100% OPC subjected to carbonation

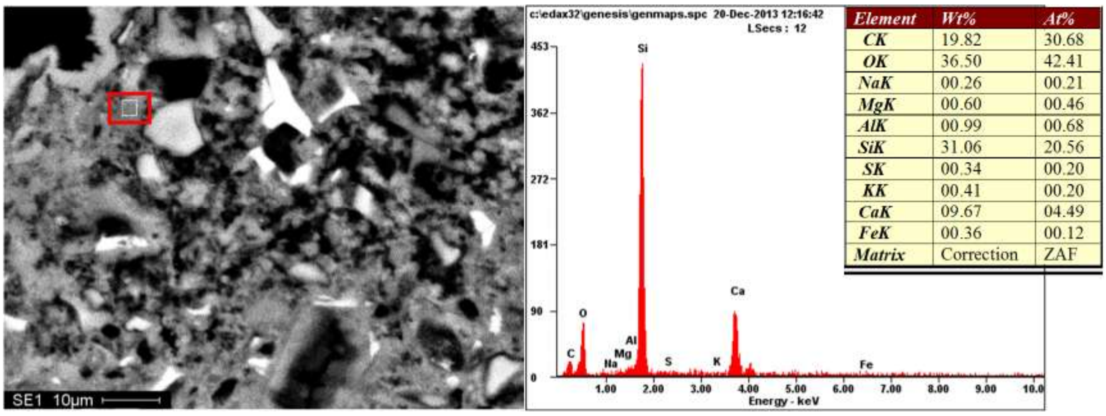

Element	*Wt%*	*At%*
CK	19.82	30.68
OK	36.50	42.41
NaK	00.26	00.21
MgK	00.60	00.46
AlK	00.99	00.68
SiK	31.06	20.56
SK	00.34	00.20
KK	00.41	00.20
CaK	09.67	04.49
FeK	00.36	00.12
Matrix	Correction	ZAF

Figure 7.18 SEM - BSE image of concrete having 30% slag subjected to carbonation

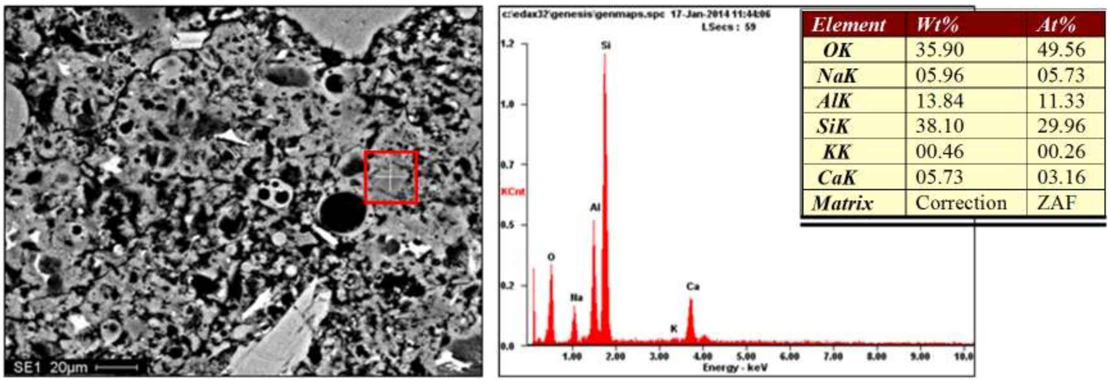

Element	Wt%	At%
OK	35.90	49.56
NaK	05.96	05.73
AlK	13.84	11.33
SiK	38.10	29.96
KK	00.46	00.26
CaK	05.73	03.16
Matrix	Correction	ZAF

Figure 7.19 SEM - BSE image of concrete having 30% Class F fly ash subjected to carbonation

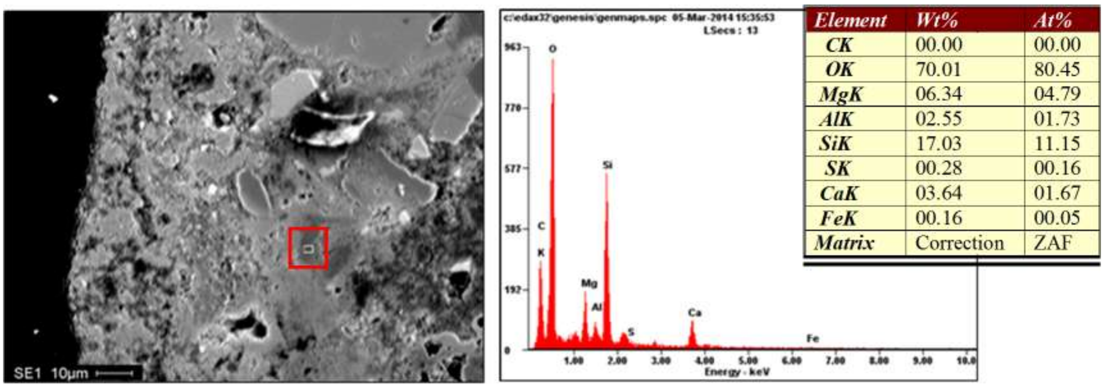

Element	Wt%	At%
CK	00.00	00.00
OK	70.01	80.45
MgK	06.34	04.79
AlK	02.55	01.73
SiK	17.03	11.15
SK	00.28	00.16
CaK	03.64	01.67
FeK	00.16	00.05
Matrix	Correction	ZAF

Figure 7.20 SEM - BSE image of concrete having 30% Class C fly ash subjected to carbonation

The EDS data confirms that decalcification happened in all the mixes as the atomic percentage of Ca is lower than that of Si. For normal concrete the Ca/Si is expected to be 1.5 to 2.0. It can be seen that the Ca/Si of the CSH in the above four figures are 0.43, 0.22, 0.11 and 0.15 respectively. This indicates that decalcification has indeed occurred. The data also indicates that the extent of decalcification is lower for the OPC mix, possibly because of greater availability of CH.

7.4.2.3 Evaluation of porosity change

Figure 7.21 to Figure 7.24 show the SEM - BSE images of concrete having different binder proportions 100% OPC, 30% slag, 30% Class F fly ash and 30% Class C fly ash respectively subjected to carbonation, at almost the same magnification level (three images at 500X and one image at 600X). Figure 7.25 and Figure 7.26 depict the SEM - BSE images of concrete having 30% and 50% Class F fly ash respectively subjected to carbonation, at a higher magnification level (1200X and 1000X respectively).

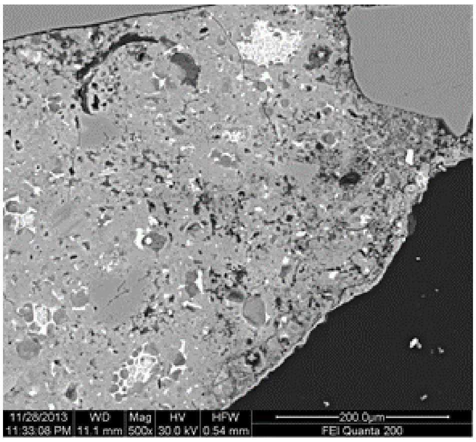

Figure 7.21 SEM - BSE image of concrete having 100% OPC subjected to carbonation (Magnification 500X)

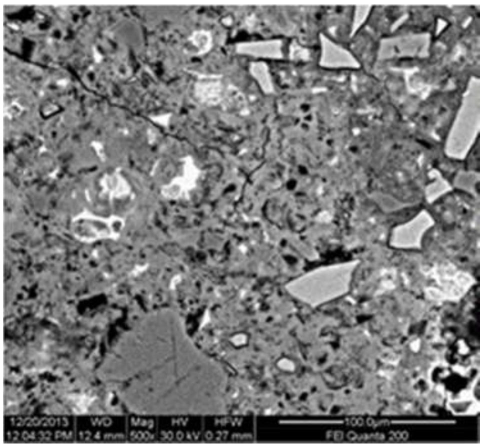

Figure 7.22 SEM - BSE image of concrete having 30% slag subjected to carbonation (Magnification 500X)

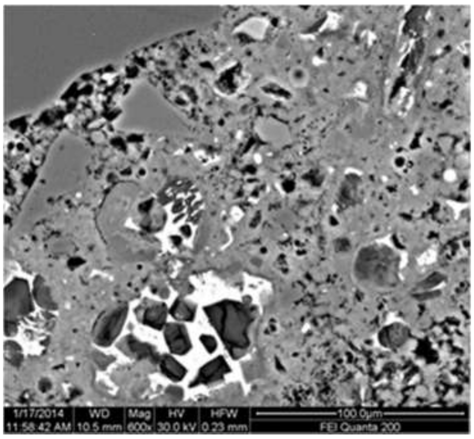

Figure 7.23 SEM - BSE image of concrete having 30% Class F fly ash subjected to carbonation (Magnification 600X)

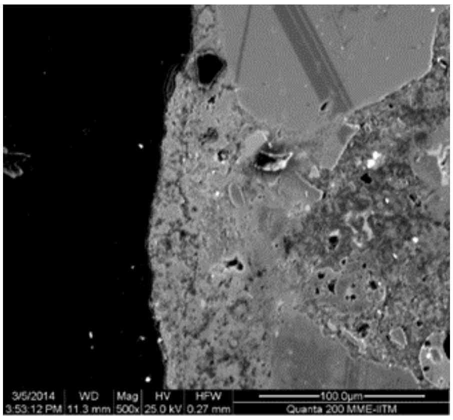

Figure 7.24 SEM - BSE image of concrete having 30% Class C fly ash subjected to carbonation (Magnification 500X)

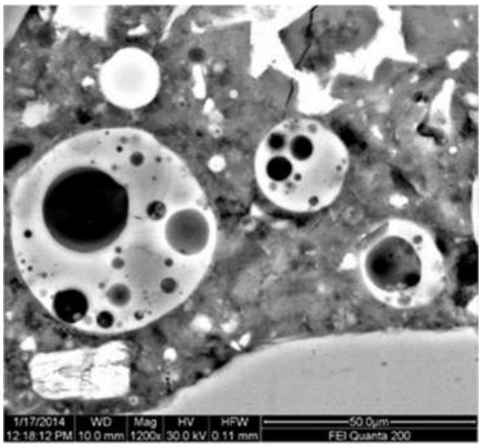

Figure 7.25 SEM - BSE image of concrete having 30% Class F fly ash subjected to carbonation (Magnification 1200X)

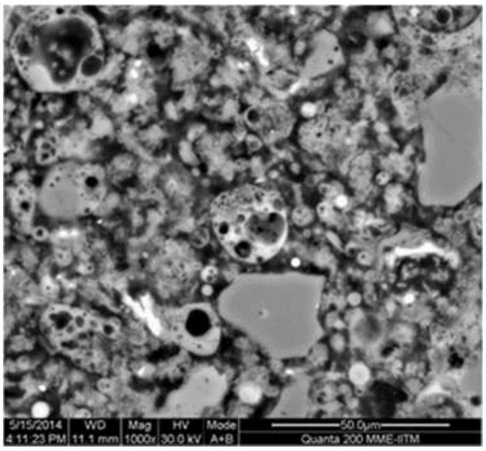

Figure 7.26 SEM - BSE image of concrete having 50% Class F fly ash subjected to carbonation (Magnification 1000X)

As evident from Figure 7.21, the overall appearance of the paste matrix indicates that the OPC concrete is having a dense appearance. With regard to Figure 7.22 and Figure 7.23, the slag and Class F fly ash mixes have greater degree of porosity compared to OPC mixes. The CSH has a much darker appearance, which might be due to the greater degree of decalcification happening in these mixes. Regarding Class C fly ash mix, some porosity is visible in the paste although not as much as in Class F fly ash.

It is clear from Figure 7.25 and Figure 7.26, in comparison with 30% Class F fly ash mix, the interior porosity of 50 % Class F fly ash mix is much higher. The paste has a leached out appearance. This indicates that, as the replacement level with Class F fly ash increases, the porosity increases due to increased decalcification and leaching of paste. The increase in porosity of the systems with supplementary materials may be due to the formation of products that occupy lesser volume than the original phases.

7.5 CHEMICAL AND PHASE CHANGES DUE TO CARBONATION

In order to study the chemical and phase changes happening due to carbonation, TGA and XRD were performed on the powder obtained by crushing the paste samples which were fully carbonated in an accelerated carbonation chamber at 1% CO_2 concentration.

7.5.1 Results of thermo gravimetric analysis

TG – DSC was conducted on paste samples up to a temperature of 1000°C. A typical output obtained from the experiment (corresponding to 30% slag as binder) is presented in Figure 7.27.

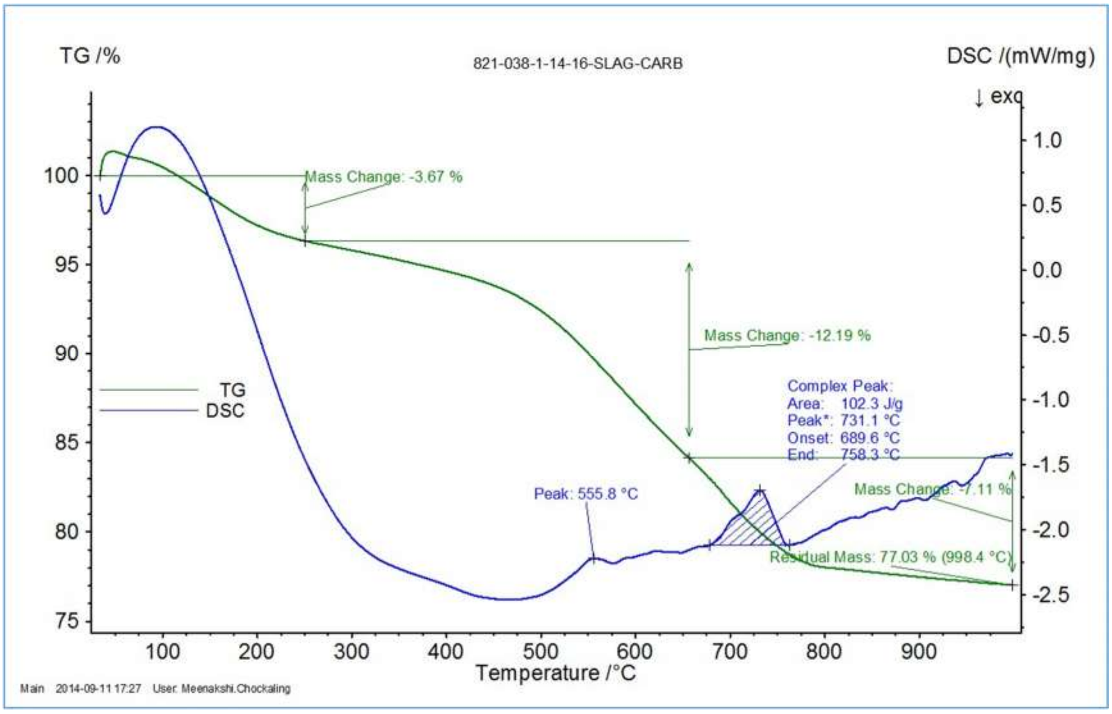

Figure 7.27 TG-DSC output of fully carbonated cement pastes having 30% slag

The decomposition of $CaCO_3$ occurs at a temperature between 700 and 800 °C. The onset temperature, peak temperature, peak mass change and end temperature of this reaction for different binders are presented in Table 7.3.

Table 7.3 Details of the decomposition reaction of $CaCO_3$ obtained from pastes having different binder combinations

Binder content	Onset temperature (°C)	Peak temperature (°C)	Peak mass change (%)	$CaCO_3$ content (%)	End temperature (°C)
OPC	738.5	784.5	9.78	22.23	812.1
30% Slag	689.6	731.1	7.11	16.15	758.3
30% Class F fly ash	719.5	750.1	7.81	17.75	785.5
30% Class C fly ash	741.6	763.0	11.00	25	780.5

From Table 7.3, it can be seen that there is much variation in the decomposition reaction details of different binders. The onset temperature changes with respect to binder type, and the type of products formed might also be different. For fly ash and slag, $CaCO_3$ may not be formed from $Ca(OH)_2$, it might be formed due to the carbonation of CSH.

7.5.2 Results of X – ray diffraction analysis

Different products formed due to carbonation of pastes having different binder combinations were analyzed using XRD on the powder obtained from fully carbonated paste samples. Figure 7.28 to Figure 7.31 indicate the XRD pattern of non – carbonated and carbonated paste samples having different binder combinations.

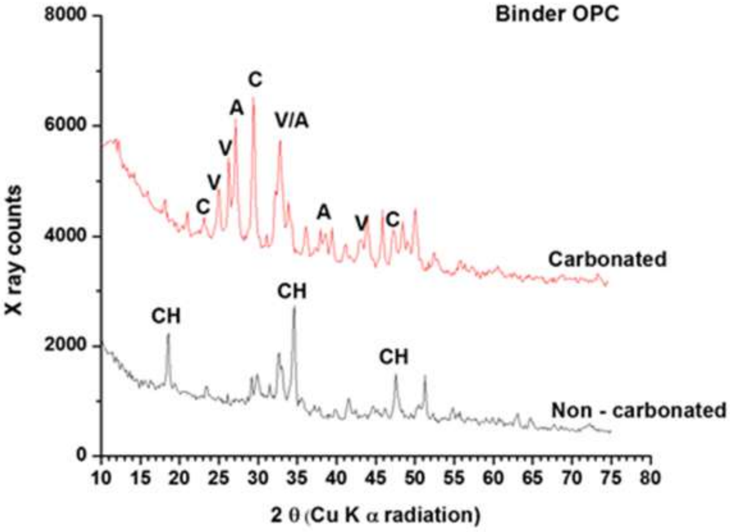

.

Figure 7.28 XRD pattern of non-carbonated and carbonated paste samples having 100% OPC

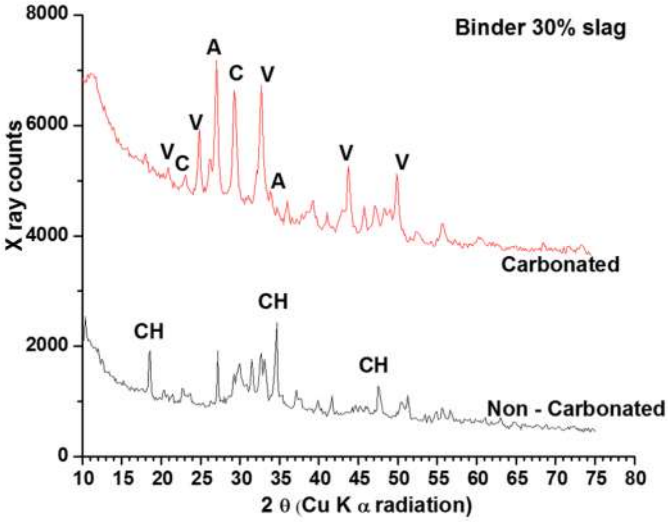

Figure 7.29 XRD pattern of non-carbonated and carbonated paste samples having 30% slag

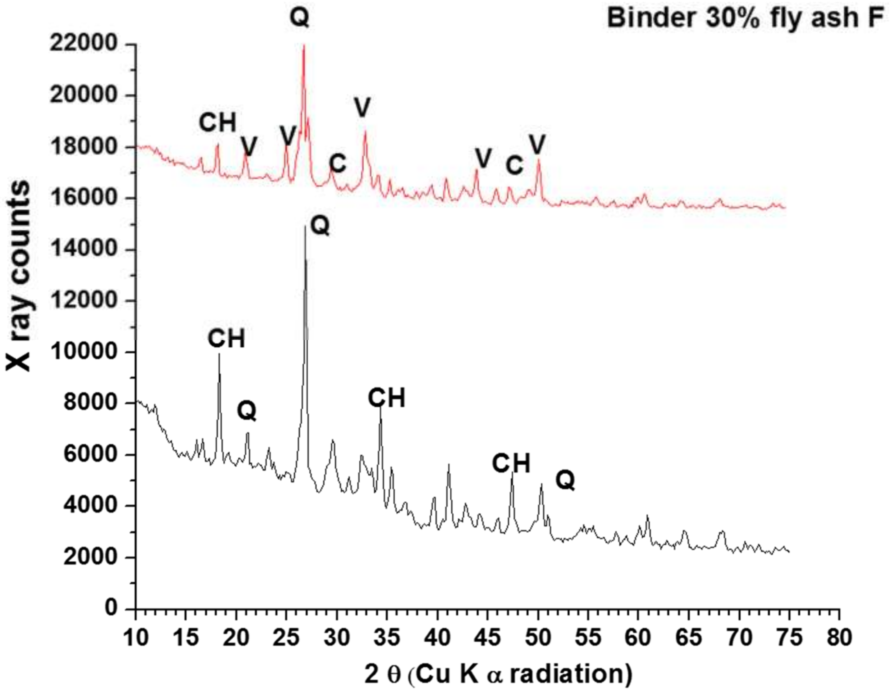

Figure 7.30 XRD pattern of non-carbonated and carbonated paste samples having 30% Class F fly ash

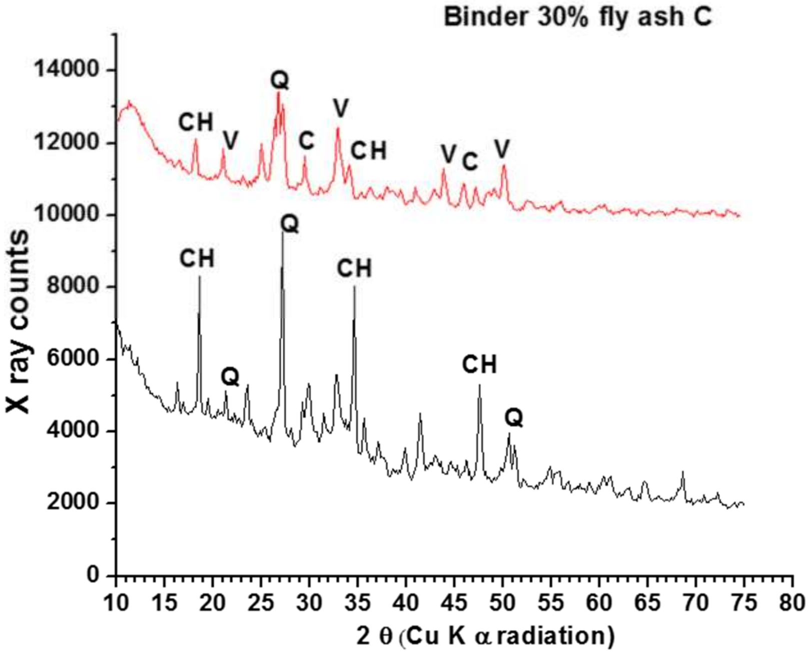

Figure 7.31 XRD pattern of non-carbonated and carbonated paste samples having 30% Class C fly ash

The XRD patterns indicate that all the polymorphs of $CaCO_3$ such as calcite (C), vaterite (V) and aragonite (A) are present as the products of carbonation in the case of paste samples subjected to 100% OPC and having 30% slag as binder. In the case of samples having 30% class F and class C fly ash, the polymorphs present are only calcite and vaterite. While calcite appears to be the dominant phase in the OPC pastes, other carbonate phases appear to dominate in the systems having supplementary materials. Further, such formation also supports the theory of carbonation of the CSH phase.

7.6 SUMMARY

The micro-analytical studies described in this chapter help to explain the influence of SCMs on different durability parameters. The results of TGA performed on paste samples show that the Portlandite content increases in the case of OPC from 28 to 90 days indicating prolonged hydration of cement. However, the Portlandite content is decreasing in the case of SCMs as the curing duration increases from 28 to 90 days and as the replacement level increases. These results indicate that more pozzolanic reaction happens when the SCM dosage increases and also with increase in curing days. The trends obtained from the results of Portlandite content are in line with those obtained from durability results. It is also observed that the surface resistivity values are not only related to pore solution conductivity, but also on the microstructure development.

Evidence of chloride binding is obtained in all the concretes with at least 30% replacement by SCMs. Presence of Friedel's salt was confirmed by SEM – BSE images supported with EDS analysis and XRD analysis. The modifications of the paste matrix due to carbonation are explained in terms of calcite formation, decalcification of CSH and change in porosity level. The supporting evidences of all these were obtained from SEM – BSE images. Results indicate that the porosity is higher for carbonated SCM mixes compared to that of OPC mixes.

The chemical and phase changes due to carbonation were studied by TGA and XRD. TGA results indicate that there is much variation in the decomposition reaction details of different binders. The onset temperature changes with respect to binder type. Because of this, the type of products formed might also be different. For fly ash and slag, $CaCO_3$ may not be formed from $Ca(OH)_2$, it might be formed due to the carbonation of CSH. From the XRD results, it is concluded that in the case of paste samples having 100% OPC and slag, all the three polymorphs of calcium carbonate such as calcite, vaterite and aragonite are formed due to carbonation reaction, and the calcite phase is dominant in the OPC system. However, in the case of paste samples made of Class F and Class C fly ash, only the presence of calcite and vaterite are confirmed by XRD analysis, with vaterite being more dominant.

CHAPTER 8

PROPOSAL FOR COMBINED QUALITATIVE CLASSIFICATION SYSTEMS

This chapter presents correlations between different durability parameters that deal with the same deterioration mechanism in concrete. The initial aim of this analysis was to check whether one durability parameter can be deduced from another parameter of a similar kind. By doing this correlation study, two concepts were evolved. Firstly, a classification system based on more than one durability parameter is developed, which can be used for the selection of materials in a more precise manner. Secondly, a combined classification system based on more than one durability parameter is evolved. This is an attempt to link the durability parameters to the transport mechanisms leading to the ingress of aggressive species into concrete in different service life environments. The service life environments selected correspond to corrosion induced by chlorides from sea water and corrosion induced by carbonation.

8.1 LITERATURE REVIEW ON CORRELATION BETWEEN DIFFERENT DURABILITY PARAMETERS OF CONCRETE

Many studies have been done in the past correlating different durability parameters with other durability parameter or with other mechanical properties such as compressive strength. Odriozola and Gutierrez (2008) had done a comparative study of different test methods to assess the durability of reinforced concrete in a marine environment. Chloride diffusion coefficient was taken as reference parameter. The correlation study compared chloride diffusion coefficient with concrete strength and other durability parameters such as porosity, water absorption, water penetration depth under pressure, capillarity, water and oxygen permeability. These tests were done on cores taken from the caissons of seven Spanish wharves, from two zones such as submerged and tidal zones. The correlation study concluded that strength is not a suitable parameter to assess concrete durability. Further, water penetration test under pressure was concluded as being the most suitable test for assessing durability of concrete in both the zones. Moreover, oxygen permeability measurements by Cembureau method was advised for checking the corrosion rate in tidal zones. An interesting observation by the authors here is that the corrosion rate is faster in submerged concretes than in tidal zone concrete. The authors support their argument by explaining that in the submerged zone, pure diffusion is the transport mechanism whereas in the tidal zone the main mechanism is capillary suction. Further, capillary suction is interrupted by wetting and drying cycles and the chloride ions diffuse outward due to external washing out of chlorides.

RILEM TC 189-NEC (2007) "Non-destructive Evaluation of the Concrete cover" had conducted a comparative study of different 'penetrability' test methods. Under this committee, the tests conducted focused on the measures to assess quality of cover zone concretes by assessing permeability to gases, permeability to water, including capillary suction and diffusion and migration of ions. The correlation between site tests and reference tests were done for this purpose. The reference tests on cored samples included O_2 permeability (RILEM TC 116-PCD), water absorption rate (RILEM TC 116-PCD), electrical resistivity (RILEM TC 154-EMC), Chloride penetration (ASTM C1202) and chloride diffusivity (NT BUILD 492). Different site tests included Autoclam air permeability test, Hong-Parrot air permeability test, Torrent air permeability test (to assess gas permeability), Autoclam sorptivity test (to assess sorption) and Wenner resistivity test (to assess electrical resistivity). These site tests yielded a correlation coefficient of 0.67, 0.92, 0.97, 0.47 and 0.83 with the corresponding reference tests addressing the same transport mechanisms.

In a review paper on the assessment of concrete durability from permeation properties, Basheer et al. (2001) presented a review of the interrelationship between permeation properties and durability of concrete. The data presented included correlation of carbonation depth of concrete with durability parameters representing gas permeability and water absorption; correlation between sorptivity index and corrosion initiation; relationship between freeze and thaw resistance and water adsorption, air permeability, water absorption etc. The work by Ramezanianpour et al. (2011) evaluated the correlation between surface resistivity (Wenner 4 probe resistivity test), water penetration (BS EN-12390-8:2000), rapid chloride penetration (ASTM C1202, 2010) and compressive strength. The authors were able to get good correlation between surface resistivity and water penetration depth. There was no correlation between surface resistivity and compressive strength. The authors suggested to use surface resistivity as a good, quick, non-destructive test to assess concrete quality.

8.2 CORRELATIONS BETWEEN DIFFERENT DURABILITY PARAMETERS IN THE CURRENT STUDY

In this section, the data from the durability tests were compared and the correlations between different durability parameters pointing towards same deterioration mechanism of concrete were evaluated. The scatter plot between surface resistivity and other durability parameters that represent chloride ion penetrability such as total charge passed, non – steady state migration coefficient and chloride conductivity respectively are presented in Figure 8.1 to Figure 8.3.

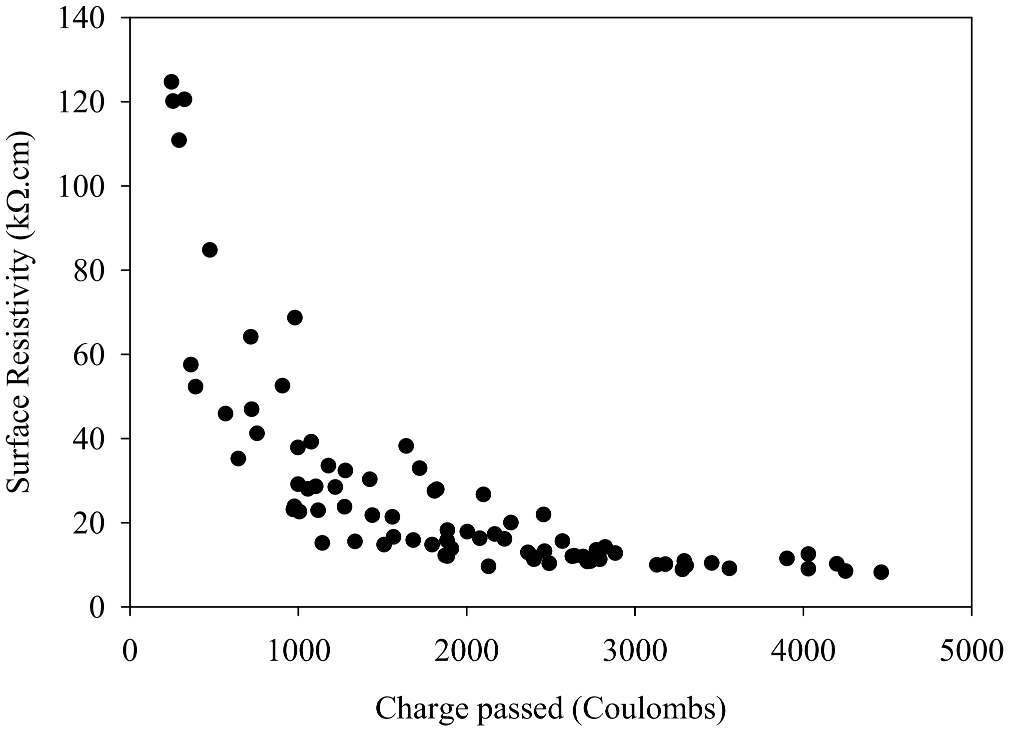

Figure 8.1 Correlation between surface resistivity and charge passed

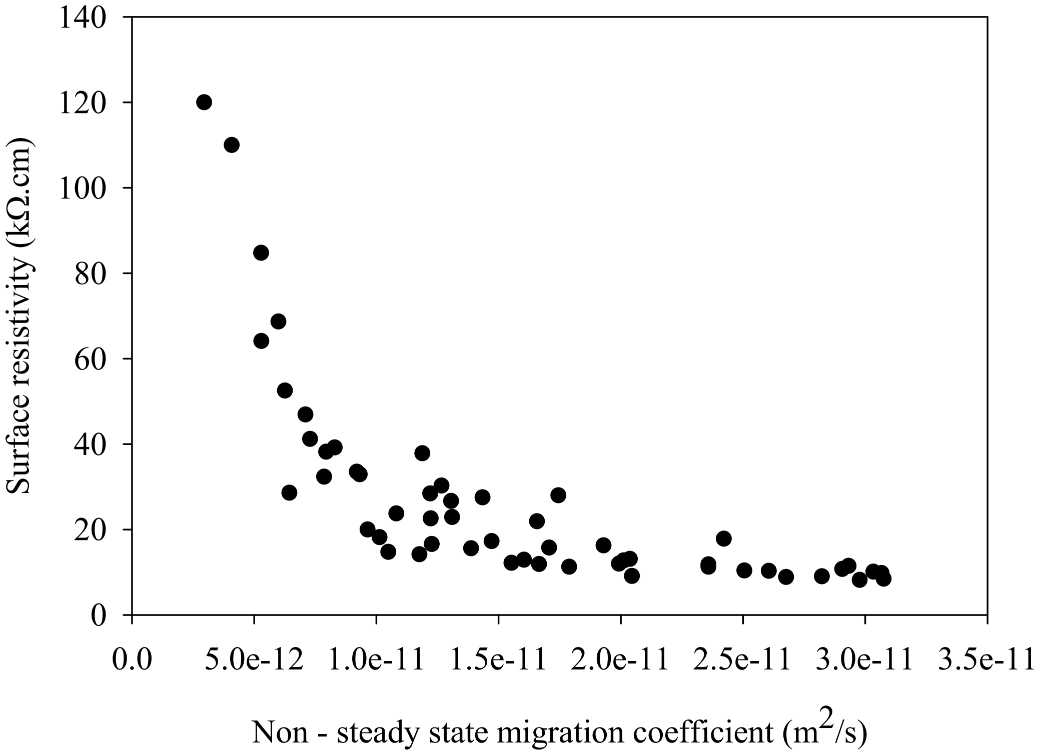

Figure 8.2 Correlation between surface resistivity and non-steady state migration coefficient

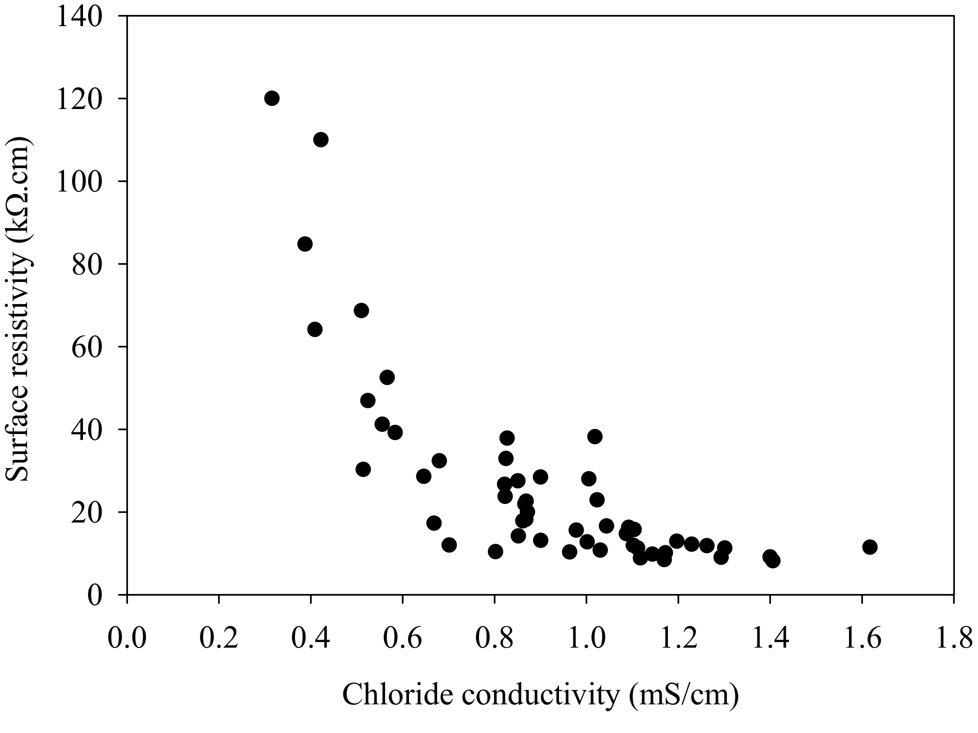

Figure 8.3 Correlation between surface resistivity and chloride conductivity

From Figure 8.1 to Figure 8.3, it can be seen that good inverse correlation (Coefficient of regression R^2 more than 0.71, 0.75 and 0.76 respectively) exists between surface resistivity and other parameters such as charge passed, non-steady state migration coefficient and chloride conductivity. These parameters are measures of the conductivity of concrete, which is the inverse of resistivity. The results indicate that either surface resistivity or any one of the above three parameters can be used when durability needs to be assessed in a chloride environment. This conclusion is in line with that made by Ramezanianpour et al. (2011), which is discussed in the previous section on the literature review on correlation studies.

The correlation between results of water permeability test and water sorptivity test is depicted in Figure 8.4. For specimens used in both water permeability test and sorptivity test, the same conditioning procedure was followed. Prior to the test, the specimens were dried at 50°C for 7 days and cooled at room temperature for 2 hours. This way, the initial absorption in both tests should be similar. The drying is not specified in the standard DIN 1048 Part 5. The drying was done in order to check whether any correlation exists between results from these two tests.

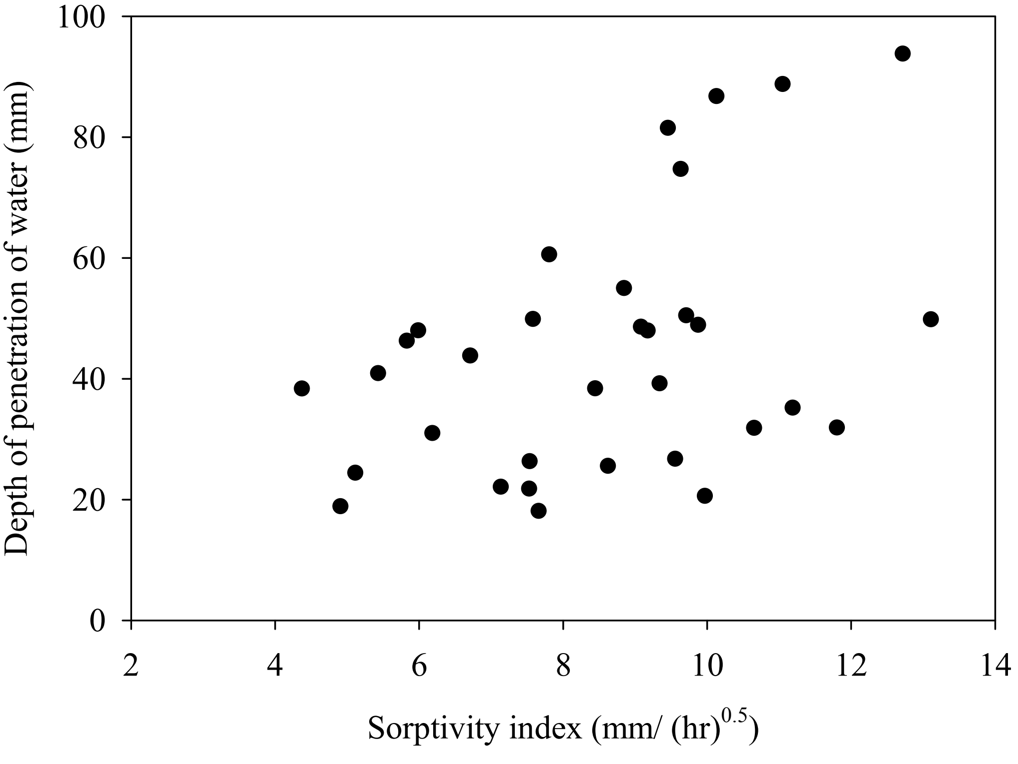

Figure 8.4 Correlation between depth of water penetration and sorptivity index

From Figure 8.4, it is understood that there is no correlation exists between the results of the water permeability test and the sorptivity test. This is because these two test methods represent two different transport mechanisms. The major mechanism is capillary suction in the case of sorptivity test whereas it is permeation in the case of water permeability test.

The scatter plot between the depth of carbonation obtained from accelerated carbonation test and the oxygen permeability index is presented in Figure 8.5. The scatter plot failed to yield any correlation. However, this result is contrary to the information available in the published literature. The correlation between carbonation depth and OPI test published by Mackechine and Alexander (2002) is already presented in Chapter 2 as Figure 2.21. On analysis of the present results, it is found that all the concretes in the present study are either in the ‘good’ or ‘very good’ category as per their classification. Because of this, the spread in the data set is not much and all the results are falling at the tail end of the graph which was presented in Figure 2.21. This might be the reason for not getting any correlation.

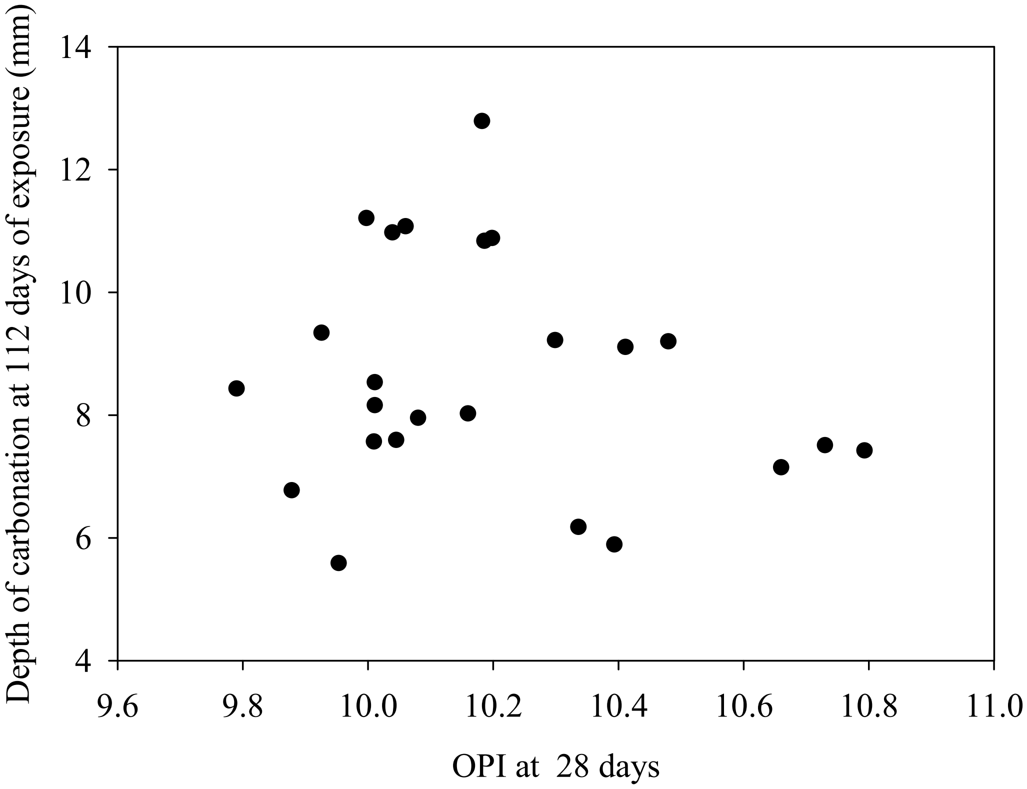

Figure 8.5 Correlation between depth of carbonation and oxygen permeability index

The correlation between depth of carbonation and Torrent air permeability was not attempted due to lack of data points belonging to same category of concretes.

8.2.1 Interchangeability of durability parameters

From Figure 8.1 to Figure 8.3, it can be concluded that results of Wenner resistivity are well correlated with results from the tests RCPT, RMT and CCT (coefficient of regression, R^2, were above 0.7). This indicates that the Wenner resistivity test can be adopted as a quick test for assessing the quality of concrete. Wenner resistivity has the advantage of being a non-destructive test, as well as one which can be carried out on concrete in the structure also, and would thus be more preferable. However, while conducting this test, care should be taken to eliminate the factors influencing the test results such as surface moisture conditions, temperature etc. as mentioned in Chapter 2.

Since the water permeability test and sorptivity test failed to yield any correlation, it is concluded that both tests would need to be performed on the same set of concretes to get a realistic estimate of the durability of concrete in terms of water penetrability. The choice of the test method depends on the type of transport mechanism leading to concrete deterioration in a particular service environment.

Even though the present data set failed to yield any correlation between OPI test and accelerated carbonation test because of the reasons mentioned in the above section, OPI can be used as a good indicative test which can be conducted at early ages such as 28 days to predict carbonation.

8.2.2 Classification systems based on more than one durability parameter

Figure 8.6 shows the effect of the replacement level of SCMs and the age of curing on the surface resistivity and total charge passed in a combined manner. The vertical lines in Figure 8.6 indicate the existing limiting values of total charge passed based on ASTM C1202 (2010) whereas the horizontal lines represent the limiting values for surface resistivity based on ACI 222R (2001). In a similar way, Figure 8.7 and Figure 8.8 represent the results of surface resistivity and non-steady state migration coefficient as well as chloride conductivity with their existing classification criteria.

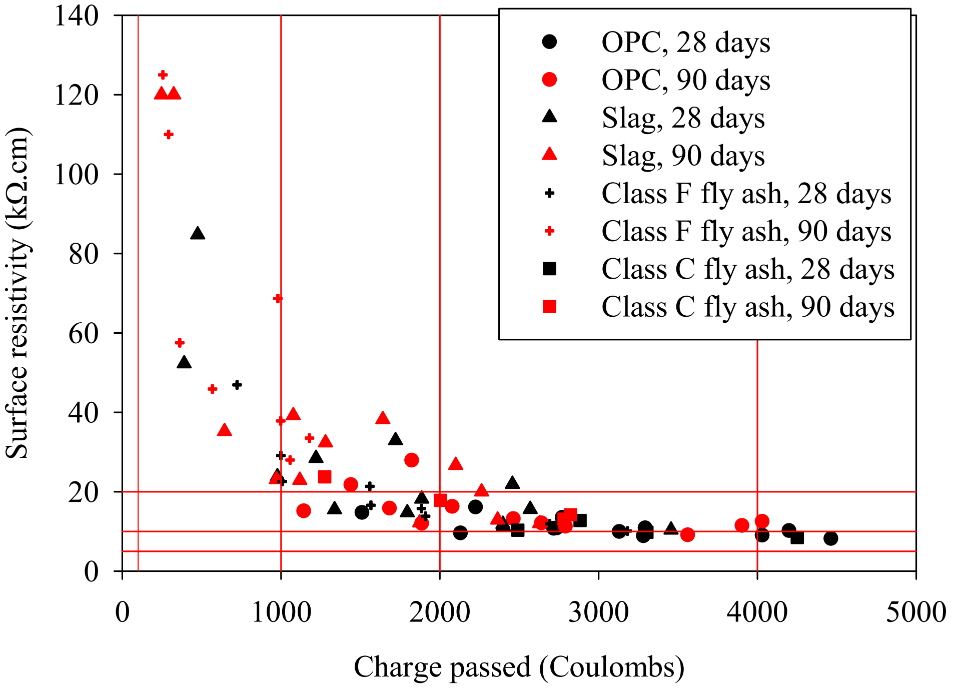

Figure 8.6 Effect of replacement level of SCMs and age of curing on surface resistivity and charge passed

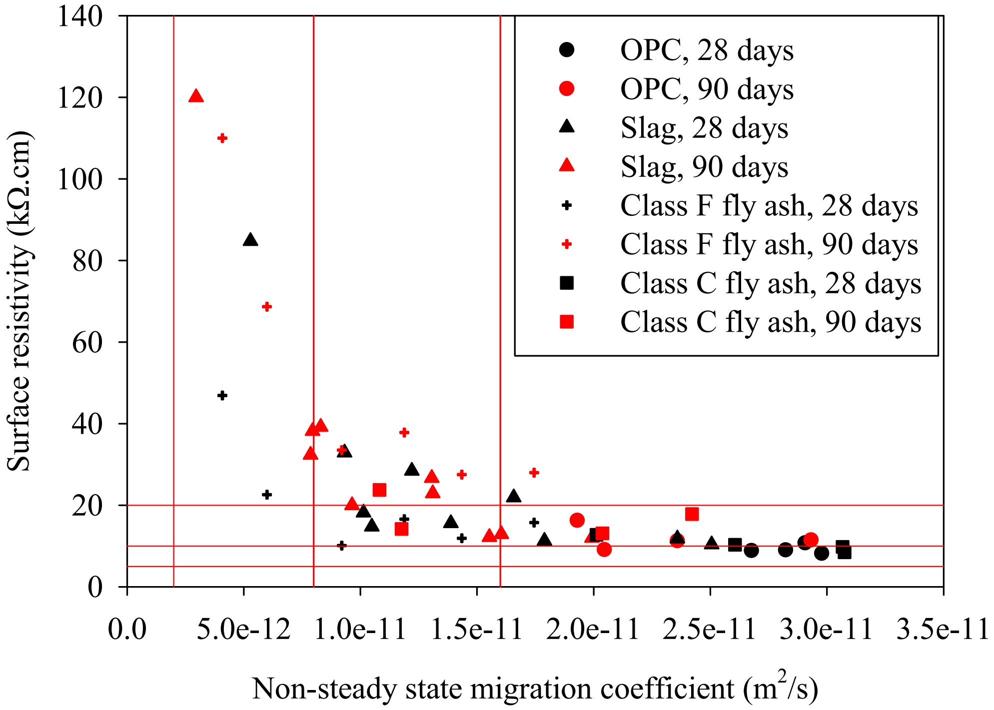

Figure 8.7 Effect of replacement level of SCMs and age of curing on surface resistivity and non – steady state migration coefficient

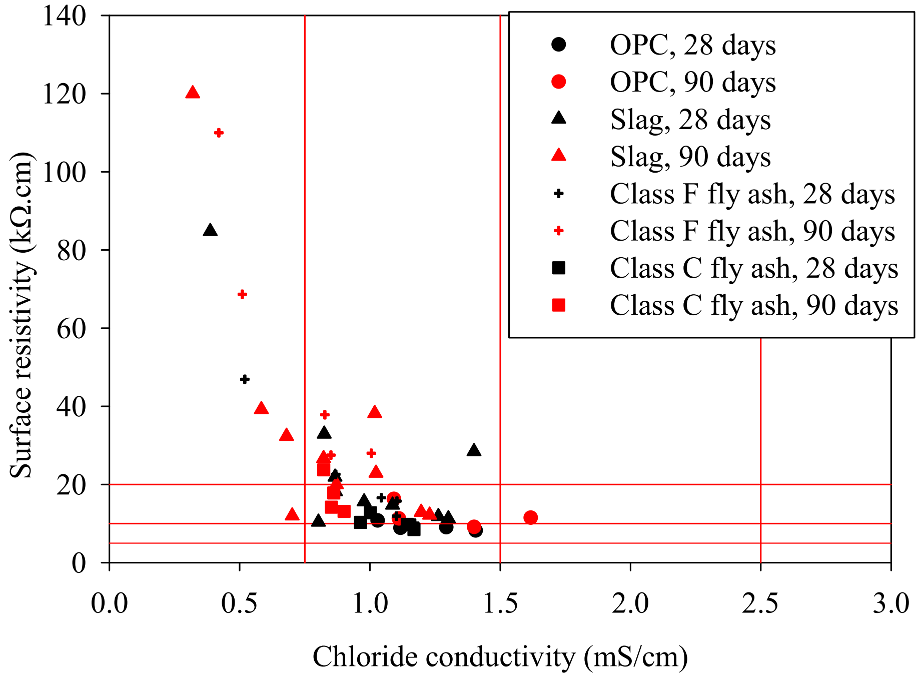

Figure 8.8 Effect of replacement level of SCMs and age of curing on surface resistivity and chloride conductivity

From Figure 8.6 to Figure 8.8, it can be seen that mixes with slag and class F fly ash occupy the top left hand region, indicating very high resistivity and very low conductivity values, which can be stated as ‘excellent’ performance. The replacement by SCM at this level is 50%. The OPC mixes and Class C fly ash mixes with 28 days of curing exhibited poor performance and occupy the bottom right hand corner. Compared to OPC mixes, all the mixes with SCMs show better performance, which is even better at 90 days. This indicates the advantages of prolonged curing when SCMs are used in concrete.

The following inferences can be made regarding the existing classification system. It is observed that none of the mixes got a surface resistivity value less than 5 kΩ.cm (very high corrosion rate according to ACI 222R, 2001). The mixes tested in this project include very lean mixes which have total binder content of as low as 280 kg/m^3 and w/b as high as 0.65. Even for these mixes, the surface resistivity values obtained were close to 8 kΩ.cm, when tested in a fully saturated condition. At an age of 28 days, this low level of resistivity (i.e., 5 kΩ. cm) is not expected to be shown by low to moderate strength concrete mixes.

The values for charge passed were not below 100 Coulombs for any mix tested. This level of durability can be achieved only by using SCMs like silica fume in high grade concrete (say, characteristic compressive strength, $f_{ck} > 60$ MPa). Thus, the classification for concrete below 100 Coulombs (negligible chloride ion penetrability as per ASTM C1202, 2010) seems to be irrelevant in the case of normal concrete. In a similar way, the non-steady state migration coefficient value of less than 2×10^{-12} m^2/s ('very good' concrete quality as per Bjegović et al., 2015) also appears to be an inappropriate limiting value in the case of normal concrete.

In the case of chloride conductivity test results, very few results went beyond 1.5 mS/cm limiting value. None of the concretes had conductivity value beyond 2.5 mS/cm. Further, too much clustering of data points is found between conductivity values 0.75 and 1.5. Most of the concretes having resistivity value between 10 and 20 kΩ.cm had a conductivity value between 1 and 1.5 mS/cm. Thus, it seems to be appropriate to introduce a new limiting value as 1 mS/cm.

Thus, a new classification criterion is proposed for concrete quality, considering chloride penetration resistance. The criterion combines both surface resistivity and one of the other durability parameters based on conduction/migration such as total charge passed, non-steady state migration coefficient or chloride conductivity. The ranges of these parameters for different categories of concrete are presented in Table 8.1.

Table 8.1Classification criteria based on more than one durability parameter

Category	Surface Resistivity (kΩ.cm)	Charge passed (Coulombs)	Non-steady state migration coefficient ($\times 10^{-12}$ m^2/s)	Chloride conductivity (mS/cm)
		AND	OR	OR
Excellent	>20	<1000	<8	<0.75
Very Good	>20	1000-2000	8-16	0.75 - 1
Good	10-20	1000 – 2000	8-16	0.75 - 1
Moderate	10-20	2000-4000	16 - 24	1 – 1.5
Poor	<10	>4000	>24	> 1.5

From Table 8.1, a concrete is classified as 'excellent' when the surface resistivity is above 20 kΩ.cm and the charge passed is less than 1000 Coulombs. Similarly, concrete mixes with surface resistivity values greater than 20 kΩ.cm and the non-steady state migration coefficient less than 8×10^{-12} m^2/s are also classified as 'excellent'. In a similar way, concrete mixes having a surface resistivity values greater than 20 kΩ.cm and chloride conductivity values less than 0.75 mS/cm are classified in the 'excellent' category. Accordingly, all the categories can be defined based on more than one parameter. This type of classification can lead to more stringency in material selection as more than one durability parameter needs to be satisfied in order to qualify for a particular service environment.

These categories and their limiting values are represented in the form of scatter plots between surface resistivity and other parameters such as charge passed, non-steady state migration coefficient and chloride conductivity in Figure 8.9, Figure 8.10 and Figure 8.11.

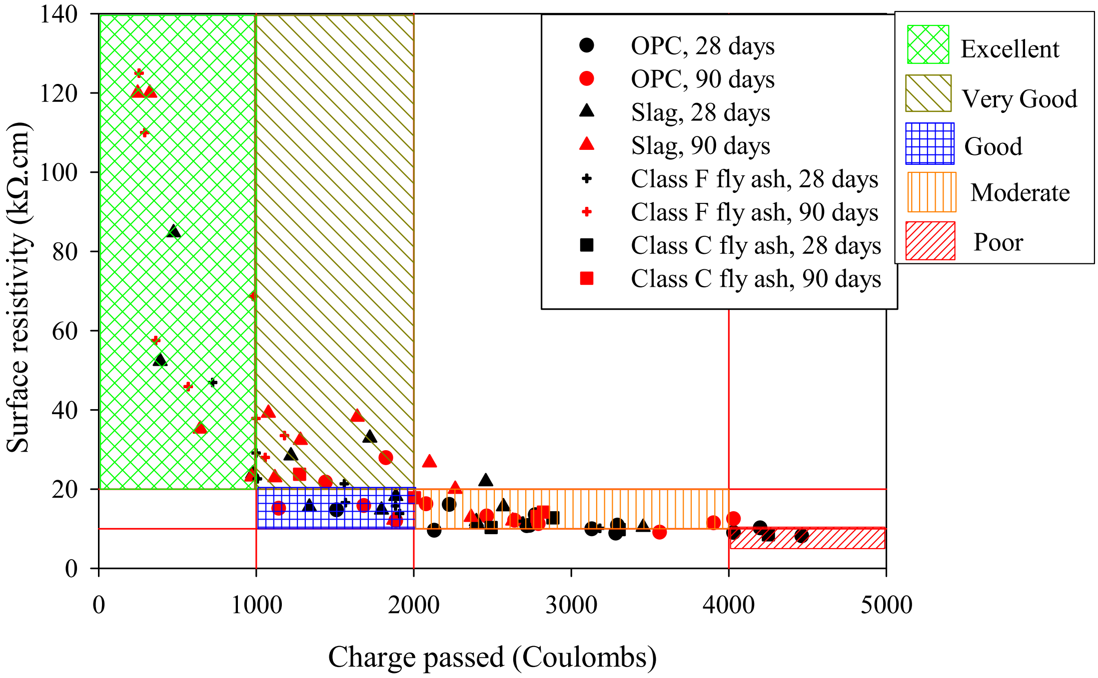

Figure 8.9 Classification criteria based on surface resistivity and charge passed

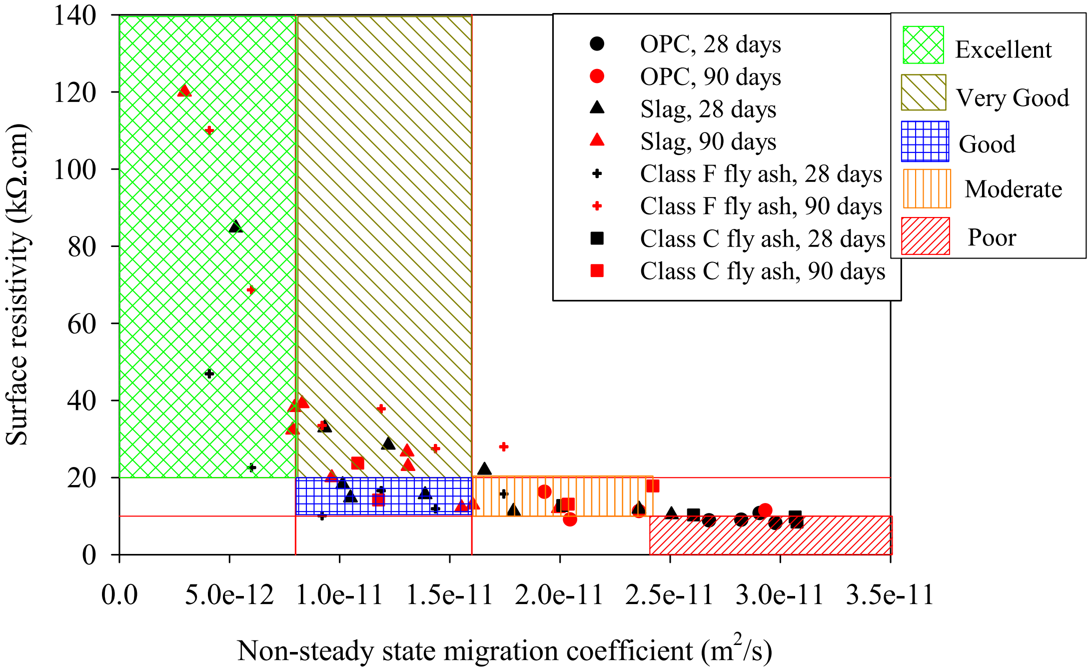

Figure 8.10 Classification criteria based on surface resistivity and non - steady state migration coefficient

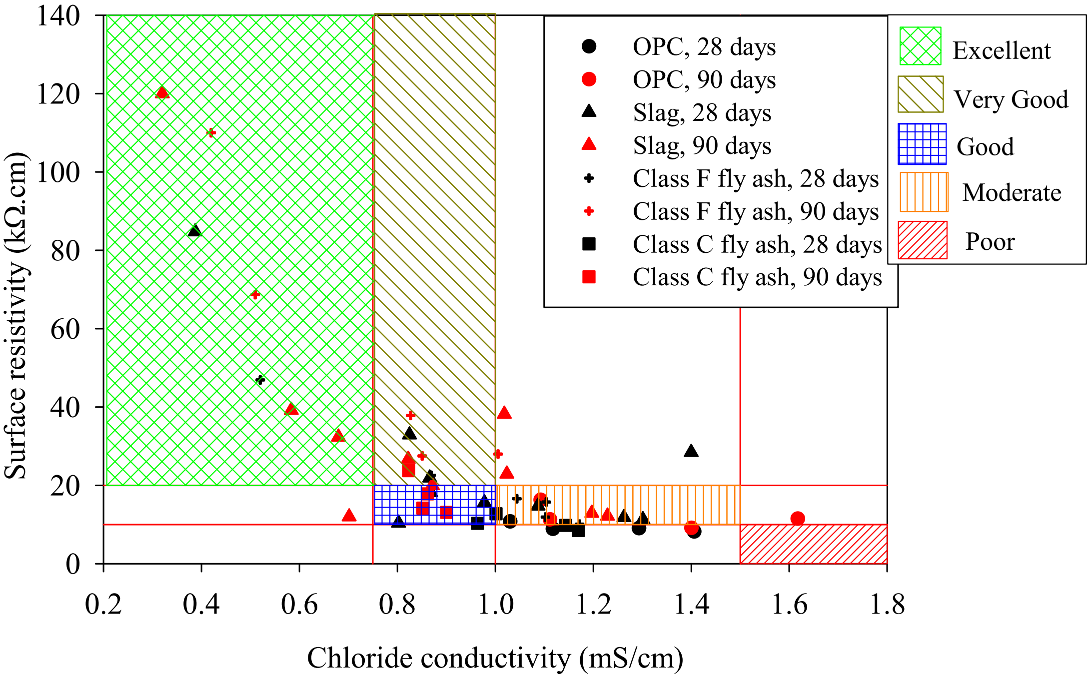

Figure 8.11 Classification criteria based on surface resistivity and chloride conductivity

8.3 COMBINED CLASSIFICATION SYSTEM FOR PARTICULAR SERVICE ENVIRONMENT

In real service environments, the aggressive species that cause deterioration enter into the concrete system because of the action of more than one transport mechanisms that act concurrently. Due to this, the durability tests specified in each environment should represent these mechanisms. Thus, it is necessary to identify the transport mechanism(s) that each durability test would address as well as the transport mechanisms acting in different service environments. The service environments considered were those prone to chloride induced corrosion and carbonation induced corrosion. For the present work, the different service conditions were identified from BS 8500 Part 1.

8.3.1 Durability test methods and transport mechanisms

As a first step towards the development of combined classification criteria, the transport mechanisms that are addressed by the durability test methods used in this thesis work were identified. Table 8.2 shows the details of the durability test methods conducted in this project work and the transport mechanism(s) that they address. A detailed review of the transport mechanisms in concrete was already presented in Chapter 2.

Table 8.2 Durability test methods and transport mechanisms

Test method	**Parameter**	**Transport mechanism(s)**
Wenner 4 - probe resistivity	Surface resistivity	Resistivity (inverse of conductivity)
Rapid chloride permeability	Charge passed	Migration/Conduction, Diffusion, Convection
Rapid migration	Non-steady state migration coefficient	Migration/Conduction, Diffusion
Chloride conductivity	Chloride conductivity	Migration/Conduction
Sorptivity	Sorptivity index	Capillary suction, Absorption, Wick action
Water permeability	Depth of water penetration	Permeation
Oxygen permeability index	Oxygen permeability index	Permeation
Torrent air permeability	Coefficient of air permeability	Permeation
Accelerated carbonation	Depth of carbonation	Diffusion

From Table 8.2, it can be seen that one transport mechanism is represented by more than one test and many transport mechanisms act together in a single test method.

8.3.2 Chloride induced corrosion

The different service conditions prone to chloride induced corrosion are (i) exposed to airborne salt but not in direct contact with sea water (ii) permanently submerged in seawater and (iii) tidal, splash, and spray zones. These categories are described in BS 8500 Part 1 as XS1, XS2 and XS3 respectively in the class 'corrosion induced by chlorides from sea water' (XS classes).

First, the transport mechanisms leading to concrete deterioration in each of the above service conditions were identified. Based on the analysis of the correlation between the test methods, specific recommendations are made regarding the combination of test methods for each service condition. The durability parameters considered to develop combined classification criteria include surface resistivity, charge passed, sorptivity and depth of water penetration. These are typical parameters indicating the transport mechanisms prevalent in these conditions. As mentioned in the previous sections, the total charge passed can be replaced with other parameters such as non-steady state migration coefficient, chloride conductivity etc. In that case, the limiting values will change.

The limiting values for the durability parameters are taken from the existing classification criteria such as ACI 222 R, 2001, RILEM TC 154-EMC, 2004 (for surface resistivity), ASTM C1202, 2010 (for charge passed), Alexander et al., 1999 (for sorptivity index), concrete society classification (for depth of water penetration). The strength criteria are chosen from BS 8500 part 1(2006) for the specified exposure condition. This proposal is presented in Table 8.3.

Strength is listed to take care of the deterioration of concrete due to the mechanical action that can happen due to splashing of waves, abrasion etc. Since the durability parameters considered in developing the combined classification criteria do not take into consideration this effect, appropriate strength levels are specified which are adopted from BS 8500 part 1 (2006) Table A4, assuming a cover depth of 50 mm.

Diffusion is the major transport mechanism primarily acting in all these conditions. That implies the fact that, one of the durability parameters specified should be related to the diffusion. As a strong correlation exists between surface resistivity and charge passed, any one of these parameters should be specified as the durability parameter governing chloride transport by diffusion in all the three cases.

In the case of concrete exposed to airborne chlorides, for surface resistivity the limit proposed is greater than 20 kΩ.cm, for which the corrosion rate category is low (ACI 222R, 2001). The total charge passed is limited to the range for which chloride ion penetrability is moderate (ASTM C1202, 2010). In this exposure condition, in addition to diffusion, sorption is another deciding mechanism, as alternate wetting and drying can happen due to rain. This may lead to physical degradation of the structure due to salt crystallization. Thus, sorptivity index and strength (in order to resist physical degradation) become the other performance criteria. The sorptivity limit recommended (i.e., 6 - 10 mm/√hr) is for "Good" concrete quality (Alexander et al., 1999). Compressive strength of 40 MPa is also recommended based on BS 8500 (2006).

Table 8.3 Combined qualitative classification criteria for service conditions subjected to chloride induced corrosion

Service condition	Description	Transport Mechanisms	Strength (MPa)	Durability Parameters			
				Surface Resistivity (kΩ.cm) OR	Charge passed (Coulombs)	Sorptivity index (mm/√hr)	Depth of water penetration (mm)
XS1	Exposed to airborne salt but not in direct contact with sea water	Diffusion, Sorption, Physical degradation	40	>20	<2000	6-10	---
XS2	Permanently submerged	Diffusion, Permeation	35	>20	<2000	---	<30
XS3	Tidal, splash and spray zones	Diffusion, Sorption, Wick action, Permeation, Physical degradation	50	>50	<1000	<6	<30

Regarding concrete fully immersed in sea, there is no effect of sorption, but on the other hand, effect of permeation will be more. Thus, impermeability will be more crucial than strength. Therefore, the charge passed is recommended to be in the 1000 - 2000 Coulomb range, which denotes low chloride ion penetrability. The depth of water penetration is limited to 30 mm, which is the limit specified by concrete society for good quality concrete to resist aggressive environment (Basheer, 2001). As before, based on BS 8500, a strength of 35 MPa is specified.

The case of concrete exposed to splash zone is the worst of all the three categories specified. All the mechanisms such as diffusion, sorption, wick action and permeation perform significant roles in the transport of aggressive species. Moreover in this zone, mechanical actions due to splashing of waves also have a major role in deterioration. Thus, both strength and impermeability are very important here. The performance criteria to be specified in this category are a combination of surface resistivity or charge passed, sorptivity index, depth of water penetration and strength. The limiting values specified are for the most impermeable concrete having a strength greater than 50 MPa.

The classification criteria recommends that the specified combination of values to be met depends on the type of environment. For example, if a mixture is to be used in XS3 condition, it should either have a surface resistivity value > 50 kΩ. cm or charge passed < 100 Coulombs, and a sorptivity value < 6 mm/√hr and a depth of water penetration < 30 mm. In addition, it should have a strength of 50MPa.

Based on the test results presented in Appendix B, the mixture proportions that are qualified to be used in the exposure conditions discussed in the above section are presented in Table 8.4. The data for depth of water penetration are unfortunately not available for all the mixtures. The mixtures are chosen based on the testing results at 28 days.

Table 8.4 Details of mixtures which are qualified to be used in different service conditions subjected to chloride induced corrosion

Service condition	Requirement	Details of the qualified mixtures (Total binder content, w/b, SCM content)
XS1	Mean strength>48.25 MPa; SR >20 or TC<2000; SI – 6-10	310, 0.5, 15% slag ; 310; 0.5, 50% slag; 380,0.4, 15% Class F fly ash; 380, 0.4, 15% slag, 380, 0.4, 30% slag, 380, 0.4, 50% slag
XS2	Mean strength 43.5 MPa; SR >20 or TC<2000; DoP <30	310,0.5, 15% slag, 310, 0.5, 30% slag, 310, 0.5, 50% slag; 310,0.5,15% Class F fly ash; 380,0.4, 15% Class F fly ash; 380, 0.4, 15% slag 380, 0.4,30% slag 380, 0.4, 50% slag; 380, 0.4, OPC*
XS3	Mean strength 58.25 MPa; SR >50 or TC<1000; SI < 6 ; DoP <30	380,0.4, 30% slag, 380, 0.4, 50% slag*
* Qualified by considering both sorptivity index and slope of the best fit line together		

From the results matrix presented in Table 8.4, it is clear that the concrete mixtures with a total binder content of 380 kg/m^3 and w/b of 0.4, having 30 and 50% slag satisfy all the criteria required for the splash zone. It is to be noted that in the case of the mixture having a total binder content of 380 kg/m^3 and w/b of 0.4 with 50% Class F fly ash, even though durability parameters are well within the range, it cannot be used in the splash zone as it fails in the strength criteria. Only one OPC mixture (with a total binder content of 380 kg/m^3 and w/b of 0.4) got qualified to be used in a chloride laden environment (XS2 category), which is the least critical one among all the three environments. The same level is achievable with a more lean mix (with a total binder content of 310 kg/m^3 and w/b of 0.5) with the use of either Class F fly ash (with a lower replacement level) or slag (with all replacement levels).

Further, this classification system reaffirms the potential of slag in the chloride laden environment. Mixtures having slag perform well in the case of durability parameters without compromising on strength. When the replacement level with Class F fly ash increases, even though the durability parameters are improved, the strength gets adversely affected. None of the Class C fly ash mixes got qualified in any of these categories. If the 90 day results are considered, more mixes are found to satisfy these criteria, which indicates the benefits of prolonged curing.

The transport mechanisms identified in this classification system are supported in BS 6349 -1 (2000) and by Odriozola et al. (2008). The details of the same were already presented in sections 2.3.8 and 8.1 respectively. Further, Basheer et al. (2001) also mentioned that durability of concrete can be evaluated by measuring the transport properties of concrete, which supports this kind of classification system.

8.3.3 Carbonation induced corrosion

As in Section 8.3.2, a combined qualitative classification criteria is developed for the exposure conditions corresponding to carbonation induced corrosion in this section. The different service conditions prone to carbonation induced corrosion are (i) dry or permanently wet (ii) wet, rarely dry and (iii) moderate humidity or cyclic wet and dry. These categories are described in BS 8500 Part 1 as XC1, XC2 as well as XC3 and XC4 respectively in the class ‘corrosion induced by carbonation’ (XC classes).

The durability parameters considered to develop combined classification criteria include carbonation rate, oxygen permeability index and sorptivity index. These are typical parameters indicating the transport mechanisms prevalent in these conditions. Carbonation rate is the exact parameter representing the CO_2 diffusion through concrete. Since the accelerated carbonation test takes months to complete, OPI test can be used as a quick test to select the mixtures. As mentioned in the Section 8.2, even though a good correlation is not obtained between OPI and carbonation rate for the results in this project, by considering the data presented in literature, this idea is put forth.

The limiting values for the OPI and SI were taken from the existing classification criteria by Alexander et al. (1999). Since there is no concrete quality classification system based on the carbonation rate, its limiting values were decided based on DuraCrete model. For a carbonation rate of 0.7 mm/√days, the service life obtained is 50 years for outdoor sheltered environment in the case of OPC mixes. The XC2 (wet, rarely dry) condition is considered to be analogous to the outdoor sheltered environment. The XC3 condition (moderate humidity or cyclic wet and dry), which is the most critical one among the all exposure categories is considered to be analogous to the lab conditions where the relative humidity and temperature are optimum for the carbonation to occur. A carbonation rate of 0.5 corresponds to a service life of 50 years in lab conditions. The strength criteria are chosen from BS 8500 part 1 for the specified exposure condition, assuming a cover of 30 mm. This proposal is presented in Table 8.5.

Table 8.5 Combined qualitative classification criteria for service conditions subjected to carbonation induced corrosion

Service condition	Description	Transport Mechanisms	Strength (MPa)	Durability Parameters		
				OPI OR	Carbonation rate (mm/√(days))	Sorptivity index (mm/√hr)
XC1	Dry or permanently wet	---	20	>9.5	---	---
XC2	Wet, rarely dry	---	25	>9.5	<0.7	---
XC3	Moderate humidity or cyclic wet and dry	Gaseous Diffusion, Sorption, Wick action, Physical degradation	30	>10	<0.5	<6

Gaseous diffusion is the major transport mechanism primarily acting in these conditions. In the case of concrete exposed to dry or permanently wet conditions (XC1), the chance of carbonation does not exist. A concrete having a minimum strength of 20 MPa will be sufficient in this case. A minimum OPI value of 9.5 is specified in order to ensure “Good” quality concrete (Alexander et al., 1999) in terms of gas penetrability.

In the case of concrete exposed to wet or rarely dry conditions (XC2), there exists a rare chance of carbonation to happen. Thus, a carbonation rate of 0.7 or OPI of 9.5 is specified. In addition, the minimum strength required in this condition is 25 MPa.

Concrete structures exposed to moderate humidity or cyclic wet and dry conditions (XC3) are those subjected to the most critical case of carbonation induced corrosion. Here, in addition to diffusion, sorption is another deciding mechanism as alternate wetting and drying can happen due to rain. This may lead to physical degradation of the structure due to leaching of the calcium hydroxide from the system. Thus, sorptivity index and strength (in order to resist physical degradation) become the other performance criteria. The sorptivity limit recommended (< 6 mm/√hr) is for "Very Good" concrete quality (Alexander et al., 1999). Compressive strength of 30 MPa is also recommended based on BS 8500, 2006. An OPI value greater than 10 or a maximum carbonation rate of 0.5 mm/√days should be achievable for the mixes to qualify to this category. Mixes having OPI greater than 10 are qualified as "Very Good" by the classification by Alexander et al. (1999) whereas a carbonation rate of 0.5 mm/√days produces 50 year service life in laboratory environments, based on DuraCrete model.

Based on the test results presented in the Appendix B, the following mixes are qualified to be used in different service conditions subjected to carbonation induced corrosion. There were difficulties in identifying mixes in terms of carbonation rate, as carbonation rate data were available only for 27 mixtures. All the mixtures except those having a total binder content of 280 kg/m^3 and w/b 0.65 qualify to be used in XC1 condition. Regarding the XC2 condition, except the mixes belonging to the 280, 0.65 category and (310, 0.6, OPC), (310, 0.6, 15 % class C fly ash) and (310, 0.5, 50% class F fly ash), all others satisfy both strength and OPI criteria. The mixes which satisfy carbonation rate criteria are (310, 0.5, OPC); (310, 0.5, 15% slag); (310, 0.5, 30% slag) and (310, 0.5, 15% class C fly ash). Mixes having a total binder content of 310 kg/m^3 and w/b of 0.5 with 15, 30 and 50% slag and the ternary blends of slag and fly ash satisfy all the criteria except that of carbonation rate. The mixes having a carbonation rate close to 0.5 are (310, 0.5, OPC) and (310, 0.5, 15% class C fly ash), having carbonation rates 0.58 and 0.55 respectively. However, in these cases, the sorptivity index value is far beyond the acceptance limit. The mixes having higher binder content and lower w/b (say, 380 kg/m^3 and 0.4 respectively) might satisfy all the requirements. Due to lack of data, a solid conclusion cannot be drawn in this regard.

8.4 SUMMARY

In this chapter, the correlations between different durability parameters that represent the same deterioration mechanism were presented. By doing the correlation study, a classification system for material selection based on more than one durability parameter is developed. Further, the transport mechanisms represented by each durability test method used in the project were recognized. The different transport mechanisms leading to concrete deterioration in different service environments subjected to chloride and carbonation induced corrosion were identified. Based on this, combined classification systems for concretes, by linking the prevalent transport mechanisms in that environment, were developed for both chloride and carbonation induced corrosion environment. Using this approach, the concrete mixtures tested in the current project work were analysed for their suitability in these service environments.

CHAPTER 9

GENERAL DISCUSSION

9.1 INTRODUCTION

This chapter discusses the practical significance of the findings from the current thesis work. The aspects discussed include the process of durability design of concrete, the formulation of a quality framework for concrete construction projects, and how the findings of the current study would help in this framework. Finally, some thoughts on the need for acceptance criteria for durability tests are also presented.

9.2 DURABILITY DESIGN OF CONCRETE

Design of concrete for durability is the need of the hour. In general, there are three different approaches to achieve durability in concrete construction. They are avoidance of deterioration approach, prescriptive approach and performance approach. Avoidance of deterioration approach implies the use of non-reactive materials such as stainless steel in construction. Prescriptive approach is followed by present codes in which limiting values on certain parameters such as water cement ratio, minimum cement content etc. are specified. If these conditions are satisfied during the mix design, that particular concrete is “deemed to satisfy” the durability requirements. In the performance approach, concrete is actually designed for durability without imposing limits either on the material characteristics or the construction methodology. However, in this kind of an approach, durability can be verified by different methodologies at different levels of sophistication. These methodologies include either the use of durability indicators or performance indicators, which are essentially concrete properties (i.e., performance test results) or the use of analytical deterioration models, which include explicit time elements. Depending on the importance of the structure and the level of sophistication, the verification methodology can be chosen. Thus, for common concrete construction, durability indicators will be a good choice for verification of concrete durability.

Out of the three different approaches, performance based approach is gathering much attention these days. A review of the literature available in this subject clearly establishes that the concept of performance based durability design approach of concrete should encompass three aspects such as aggressiveness of the environment, materials used for construction and near surface quality of concrete. Thus, the path towards durability design of concrete consists of the following steps:

- Development of environmental exposure classification system which takes into account the transport mechanisms leading to deterioration
- Identification of the durability parameter(s) relevant to a particular service environment and their limiting values for different binders
- Identification of test methods to check the as-built concrete quality and development of acceptance criteria for these parameters

Most of the present day codes (eg:- EN 206, BS 8500) have started adopting the deterioration specific environmental exposure classification system. However, in IS:456-2000, the Indian standard for plain and reinforced concrete, this modification is yet to come. The current thesis work identifies the combination of durability parameters relevant to the service environments related with chloride and carbonation induced corrosion. Further, the potential of different SCMs to achieve these parameters are also assessed in this thesis. More work is needed to identify the test methods to check the as-built concrete quality and to develop acceptance criteria. This project work had led to the development of a quality framework for concrete construction, which will be useful for the engineers working in the area of concrete technology. This framework incorporates different aspects such as strength, durability (relating it to the service condition), as-built concrete quality etc.

9.3 DEVELOPMENT OF QUALITY FRAMEWORK FOR PRACTICING ENGINEERS

Based on the present study, a quality framework is developed which will be useful for the practicing engineers. This is presented in Figure 9.1. This framework can be further modified by bringing in more explicit elements of service life and cover thickness. In this case, the limiting values of the durability parameters include the elements of service life implicitly.

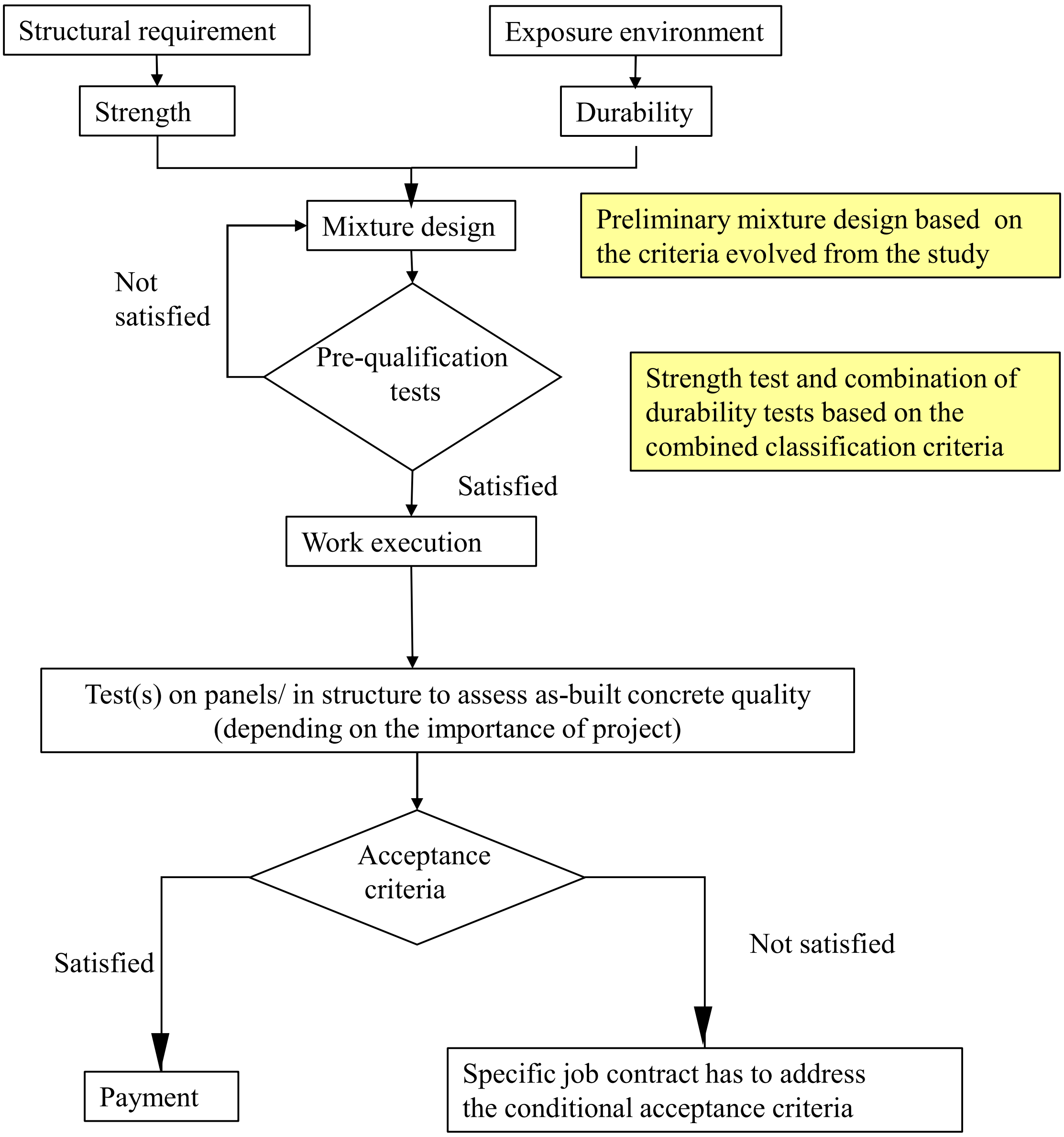

Figure 9.1 Quality framework to achieve durability in concrete construction

The concrete mix design should be based on both strength and durability. Structural requirement leads to the strength specification. However, durability requirements depend on the type of exposure condition in which the structure is going to be built. Taking into consideration both strength and durability requirements, a preliminary proportioning of the mixture can be done. Following this, the pre-qualification tests need to be done on specimens produced out of this mixture design. The pre-qualification tests should include strength test and combination of durability tests relevant to the particular service life condition. If the limiting conditions are satisfied in the prequalification tests, the work can be executed.

After the execution, the acceptance tests to check the as-built concrete quality need to be performed. These tests can be either non-destructive or invasive or a combination of both. All the non-destructive tests can be done directly on the structure. In the case of test methods which are invasive, these can be performed either on structure or on test panels, depending on the importance of the structure. The test panels having similar reinforcement detailing as that of the actual structure can be erected in the same site using the same construction methodology. Since the test panels are exposed to similar exposure conditions, and are cast and maintained in a way similar to the actual structure, the quality of concrete obtained in both structures are assumed to be the same. Once the acceptance criteria are satisfied, the payment can be given to the contractor. If the acceptance criteria is not satisfied, the steps to be followed should be clearly specified in the construction contract.

9.3.1 Contribution of the present study in the proposed quality framework

This section presents how the understanding from the present study can contribute to the proposed quality framework to achieve durability in concrete construction.

1. The preliminary proportioning of the mixture can be done based on the criteria developed in this study such as strength grade classification or based on the ranking criteria developed for concretes with different binders based on their performance in different durability tests.

2. For the pre-qualification tests, a combination of durability tests which were developed for different service life conditions for chloride and carbonation induced corrosion can be used. The mixture design can be adopted based on the limiting criteria or can also be chosen based on the developed criteria for the prequalification tests. Examples of the mixtures which will get qualify to different service conditions are discussed in Chapter 8 in the section of combined classification system.

9.3.2 Development of compliance and acceptance criteria

Through the prequalification tests, which are essentially laboratory based tests, the material potential can be assessed. However, the quality of concrete achieved on site depends much on the construction techniques such as placing, compacting, curing etc. This implies that there exists much variability between real-crete and lab-crete. Thus, it is highly necessary to develop the compliance and acceptance criteria for the tests done on site to check the concrete quality. The laboratory based prequalification tests yield results on the material potential whereas the field based tests indicate the as-built durability. Even though identification of test methods to check the as-built concrete quality and the development of compliance and acceptance criteria are out of the scope of the present thesis work, it is worthwhile to throw some light on this aspect in the background of the quality framework developed.

Alexander et al. (2008) explained the South African approach for achieving durability in concrete construction. The South African approach for achievement of quality in concrete construction deals with the use of three durability indexes - chloride conductivity, oxygen permeability index and sorptivity index. These durability indexes are "quantifiable physical or engineering parameters which characterize concrete and are sensitive to material, processing and environmental factors". Both rational and performance based durability design approaches were developed based on these indexes. Some projects have been executed in South Africa by the South Africa National Road Agency (SANRAL) incorporating the durability index tests (Nanga, 2011).

For different service environments corresponding to carbonation induced corrosion, durability requirements are specified in terms of minimum OPI value of the concrete. Similarly, for chloride induced corrosion environment, durability requirements are given in terms of chloride conductivity values. Once the concrete is delivered on site, the compliance tests are done in two stages – one to assess the material potential and the other one to check the as-built concrete quality. The tests to assess material potential are performed on samples extracted from cube specimens, which were cast from the concrete delivered on site and cured under standard conditions. These tests can be either OPI test or CC test. In order to assess the as-built concrete quality, the tests are done on cores extracted from actual structure (or from the mock-up panels). In addition to either OPI test or CC test (depending on the deterioration mechanism), sorptivity test is done compulsorily. The guidelines for testing frequency criteria are also specified clearly.

South Africans have developed both conformity criteria and acceptance criteria for the durability index results. The development of conformity criteria is grounded on the concept that these values need to be characteristic, and not average. The characteristic values can be achieved with some degree of confidence (Alexander et al., 2006). There is a reduction in average quality of the as built concrete compared to that of the material potential value because of the inconsistency in processing compared to lab specimens. Further, there exists more variability in concrete quality due to less uniformity at site. These concepts can be found in Figure 9.2 in which the conceptual relationship between material potential and as-built test distributions for chloride conductivity test is presented. In the diagram, the differences between average quality are neglected (Alexander et al., 2008). Table 9.1 presents the equations developed for finding the as-built limit, material potential limit and material target values for the SA DI tests.

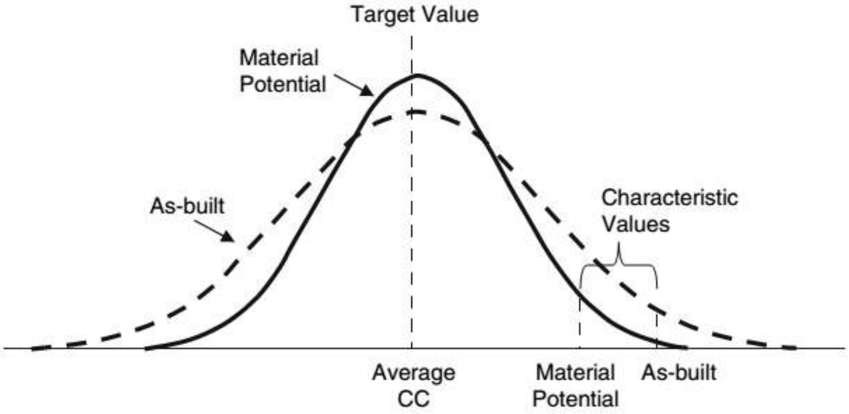

Figure 9.2 Conceptual relationships between material potential and as-built test distributions for chloride conductivity test (Alexander et al., 2008)

Table 9.1 Equations for as - built limit, material potential limit and material target value of durability indexes (Alexander et al., 2008)

	Chloride conductivity CC	OPI	Sorptivity
As- built limit (Characteristic)	$CC_{As – built}$ From service life model	$OPI_{As – built}$ From service life model	$S_{As – built}$ = 1.10 $S_{material\ potential}$
Material Potential Limit (Characteristic)	$CC_{Material\ potential}$ = 0.9 $CC_{As - built}$	$OPI_{Material\ Potential}$ = $OPI_{As\text{-}built}$ + 0.1	$S_{Material\ Potential}$ Established on site mix
Material Target Value (Average)	Lesser of: 0.9 $CC_{Material\ Potential}$ 0.82 $CC_{Material\ Potential}$ + 0.20	$OPI_{Material\ Potential}$ + 0.22	Lesser of: 0.9 $S_{Material\ Potential}$ 0.82 $S_{Material\ Potential}$ + 0.10

Further, acceptance criteria were also developed for different test results. For example, the oxygen permeability test results are considered satisfactory if both (1) the average of any three consecutive test results exceeds the characteristic value 90% of the time, and (2) no single test result is less than the characteristic value by more than 0.3. In a similar way the acceptance criteria were developed for chloride conductivity and sorptivity test results.

It is to be noted that, there is not much work has been done so far regarding the development of acceptance criteria for durability tests, except for the South African DI tests. It is high time to develop acceptance criteria for other durability parameters which are commonly used. For this purpose, large database of these parameters both from the laboratory as well as site are needed from different conditions. There is definitely a need to have collaboration of different laboratories and institutions working in this area. Further, round-robin tests on selected durability parameters can also help to assess the variability of these parameters.

9.4 SUMMARY

In this chapter, the practical significance of the present research findings is discussed. Out of the different approaches to achieve durability in concrete construction, performance based approach is gathering much attention these days. A quality framework for concrete construction is developed, which is rooted in this approach. This quality framework fits in the concept of strength grade classification and combined qualitative classification systems for different service environments subjected to both chloride and carbonation induced corrosion developed in this thesis work. Even though development of compliance and acceptance criteria for the test parameters pointing towards as-built concrete quality are out of the scope of the present work, a discussion is presented based on the existing South African model with reference to the framework.

CHAPTER 10

CONCLUSIONS

10.1 CONCLUDING REMARKS

There is an increasing concern among the engineering community regarding the durability of concrete, as numerous premature deterioration cases are getting reported from various parts of the world. Special attention needs to be given to deterioration of structures due to corrosion of reinforcement on account of its huge economic impact. In order to achieve durability in concrete construction, three major factors which control deterioration of a reinforced concrete structure are to be addressed - the aggressiveness of the environment, materials used for construction, and the near-surface quality of the concrete obtained at site.

Regarding the aggressiveness of the environment, many codes like EN 206 (2000), BS 8500 (2006) etc. have redefined the exposure classification based on the deterioration processes prevalent in different exposure conditions. Even though the Indian Standard IS 456 (2000) for plain and reinforced cement concrete defines exposure conditions in the traditional way, such as mild, moderate, severe, very severe and extreme, there have been several calls for a change to the kind of deterioration-specific classification system. Two proposals for the modification of the definition of the exposure classes along with prescriptive requirements on concrete ingredients have been published already (Kulkarni,2009, Saravanan and Santhanam, 2012).

In the current project work, the emphasis was given to the second aspect, the materials used for concrete manufacture. The effect of different Supplementary Cementitious Materials (slag, Class F and Class C fly ash) in environments subjected to chloride induced and carbonation induced corrosion were assessed through different durability tests. The durability tests included were able to assess the potential of concrete against the ingress of chloride ions, water and gas. The tests were conducted on concrete mixtures having a mean compressive strength between 20 and 60 MPa, which had different replacement levels of SCMs. Further, the influence of SCMs on the durability parameters were quantified through service life prediction models. The micro analytical studies done in this work helped to understand the behaviour of mixes with different SCMs.

The third aspect, assessment of the near-surface quality of the concrete obtained at site, is incorporated in the recommendation for quality framework for concrete construction. However, more work needs to be done in this regard.

10.2 SPECIFIC CONCLUSIONS

The specific conclusions from the present work are as arranged in specific sub-sections.

10.2.1 Creation of a database of durability parameters and compressive strength with commonly used SCMs, ranking of binders, and development of strength grade classification

A database of the durability parameters and compressive strengths for the concretes with commonly used SCMs was created, which can act as a guideline for the material selection for a particular service environment. Further, this database demonstrates the potential of SCMs to improve durability.

Ranking of different binders

- Based on the results obtained, the concrete mixtures with different binders were ranked on a scale of 1 to 4 with 1 being the best.
- The ranking can be used as a tool for material selection.

Conclusions based on 28 days results

- The best performance with regard to chloride penetration was for concretes with Class F fly ash and slag at 50% replacement level. Slag at 30% replacement level and Class F fly ash at 30 and 15 % replacement levels were ranked next whereas 15% slag and 30% Class C fly ash mixes were at the next lower level. OPC mixes showed the worst performance in this category.
- In the case of water sorptivity, the best performance was again by concretes with 50% slag. Mixes with OPC and Class C fly ash at 15% replacement were at the lowest level whereas all the other mixes fell in the second level.
- With respect to gas permeability, all the mixes were either in the good or very good category. There was only a marginal decrease in the performance level of the OPC mixes, which were ranked 2.

- With regard to CO_2 penetrability, the best performance was by OPC and 15% slag mixes followed by 30% and 50% slag mixes. Fly ash mixes showed poor performance, with higher replacement levels getting low ranks. Fly ash (both Class F and C) mixes at 15% got a ranking of 3 whereas the other replacement levels were ranked 4.

Conclusions based on 90 days results

- At 90 days, most of the concretes showed a jump to the next higher durability level.
- All the concretes achieved the best durability class in the gas permeability tests.
- With regard to chloride penetration, the best performances were exhibited by 50% slag and 30% and 50% Class F fly ash mixes. OPC and Class C fly ash at 15% replacement levels showed the poorest performance at this age also; however, the durability rank got improved by one level. Other mixes showed intermediate performance.
- For water sorptivity, the best performance was by slag mixes at 50% replacement level. The poorest performance was by OPC while the other mixes showed intermediate performance.

In practical terms, the conclusions based on 28 day results are more relevant. In order to assess the material potential in its full form, the 90 day results are presented. The specimens tested at an age of 90 days are cured for 90 days. Hence the age of the specimen as well as the curing age matches. There is a remarkable improvement in the durability properties, especially in terms of chloride ion penetrability as the testing age increases from 28 to 90 days. That indicates the importance of extended curing. There is no testing conducted on 90 days on specimens which are cured for 28 days.

Durability parameters Vs. Compressive strength

- The relationships between the durability parameters (surface resistivity, charge passed, oxygen permeability index and sorptivity index respectively) and compressive strength were explored and no semblance of a correlation could be seen.
- Hence, it is concluded from the results of this study that there is no direct correlation between compressive strength and the durability parameters.

Strength grade classification

- An attempt has been made to develop a new concept called strength grade classification. Different mixes in the same strength range are classified into different durability classes based on qualitative criteria adapted from standards and literature. The durability parameters considered to classify concrete include surface resistivity, charge passed, sorptivity index and oxygen permeability index.

- The results show that the options available to make concrete at a particular strength grade can result in different levels of durability. Even with mixes having high w/b and low binder content, with the use of SCMs, high level of durability is achievable. Depending on the requirement of the service environment, the mixture can be tailor-made.
- Strength grade classification supports the concept of performance specification. The concrete producer can have flexibility on type and dosage of SCMs as well as other mixture parameters. The SCM can be chosen based on availability.

10.2.2 Influence of SCMs on durability parameters of concrete

General Trend

- In the case of test methods where the specimens are fully saturated, the performance of SCM mixes are well ahead of OPC mixes, whereas in those tests where drying is performed, the performance of OPC and SCM mixes are close.
- Resistance against carbonation is less for SCM mixes, which agrees with the available literature
- The test results reconfirmed that as the water binder ratio increases, the durability parameters are adversely affected.

Related to chloride ion penetrability

- SCM mixes show better resistance against chloride ion penetration than OPC mixes and the results are obvious at 28 days itself. This is reflected by the results of surface resistivity test, RCPT, RMT and chloride conductivity test. The reasons for this include pozzolanic reaction leading to the development of pore structure and modification in the pore solution chemistry due to the incorporation of SCMs. In all the cases, the best performance is exhibited by mixtures having 50% replacement with SCMs.
- The resistance against chloride penetration, as obvious from the overall trends of surface resistivity, charge passed, non-steady state migration coefficient and chloride conductivity, increases from 28 to 90 days of curing. This emphasizes the fact that to realize high levels of durability, extended curing is essential.
- Slag and Class F fly ash at 50% replacement at 90 days of curing are the best performers with slag occupying the first position. There is substantial improvement in the concrete quality at higher dosages (30% and above) of slag and Class F fly ash. Class F fly ash mixes displayed greatest improvement in these parameters as the curing duration increased from 28 to 90 days. In all the cases, the worst performance is exhibited by OPC mixes. The performance of Class C fly ash is similar to OPC at 28 days. However, there is considerable improvement in the performance when the curing duration increases to 90 days.

This trend is clearer for mixes having a replacement level of 30% compared to that of 15%.

Related to gas penetrability

- Resistance against carbonation is less for SCM mixes, which agrees with the available literature. This may be attributed to consumption of $Ca(OH)_2$ in the pozzolanic reaction, which can lead to decalcification and subsequent carbonation of CSH. Due to the carbonation of CSH, dense products are formed, which increase the porosity of the system. This can accelerate further the progress of the carbonation front.
- Fly ash mixes show greater depth of carbonation, whereas slag mixes show relatively less depth of penetration. As the replacement level increases, the depth of carbonation increases. At lower replacement levels, the difference is not much significant even at 112 days of exposure for slag and Class C fly ash
- No clear difference in durability parameters related to gas permeability test are observed in the concretes selected for the study. OPI, Torrent air permeability test results are either in the good or very good category for all the concretes studied.

Related to water penetrability

- In the case of water sorptvity test, SCM mixes perform better than OPC mixes, and the trends are more obvious at 90 days. This indicates the importance of extended curing. The improvement can be attributed to the pore structure development due to pozzolanic reaction.
- No clear difference in durability parameters related to water permeability test are observed in the concretes selected for the study
- The water penetration depths (from water permeability test results based on DIN 1048) are below the specified value for aggressive environment. However, no significant contribution of SCMs is found.

Quantification of effect of SCMs

- Quantification of the effect of SCMs on carbonation was performed by two models, square root of time model and DuraCrete model and the relative performances of different mixes were calculated. The service life prediction underlines the conclusion made in the previous section that the performance of SCM mixes is not as good as that of pure OPC mixes.
- In the case of chloride induced corrosion, the service life prediction is done using DuraCrete model. Due to the unrealistic prediction obtained for fly ash mixes, the age factor is assumed to be that of slag and the relative performance is predicted. This prediction also emphasizes that both slag and Class F fly ash mixes are better than OPC mixes in chloride penetration resistance.

10.2.3 Correlation study and combined qualitative classification systems

Correlation study

- Correlations between different durability parameters pointing towards same deterioration mechanism of concrete were evaluated.
- Strong inverse correlation exists between surface resistivity and other parameters such as charge passed, non-steady state migration coefficient and chloride conductivity. These parameters are measures of the conductivity of concrete, which is the inverse of resistivity. The results indicate that either surface resistivity or any one of the above three parameters can be used when durability needs to be assessed in a chloride environment. This indicates that the Wenner resistivity test can be adopted as a quick test for assessing the quality of concrete. Wenner resistivity has the advantage of being a non-destructive test, as well as one which can be carried out on concrete in the structure also, and would thus be more preferable.
- There is no correlation between the results of water permeability test and sorptivity test. This is because these two test methods are representing two different transport mechanisms. The major mechanism is capillary suction in the case of sorptivity test whereas it is permeation in the case of water permeability test.
- Since the water permeability test and sorptivity test failed to yield any correlation, it is concluded that both tests would need to be performed on the same set of concretes to get a realistic estimate of the durability of concrete in terms of water penetrability. The choice of the test method depends on the type of transport mechanism leading to concrete deterioration in a particular service environment.
- The analysis failed to yield any correlation between the results of accelerated carbonation test and OPI test, which is contrary to the information available in the published literature. This might be due to the lack of spread in the present results. By considering this aspect, OPI can be used as a good indicative test which can be conducted at early ages such as 28 days to predict carbonation.

Classification systems based on more than one durability parameter

- A new classification criterion is proposed for concrete quality (considering chloride penetration resistance). The criterion combines both surface resistivity and one of the other durability parameters based on conduction/migration such as charge passed, non-steady state migration coefficient or chloride conductivity. The ranges of these parameters for different categories of concrete are presented. All the categories can be defined based on more than one parameter. This type of classification can lead to more stringency in material selection as more than one durability parameter needs to be satisfied in order to qualify for a particular service environment.

- For example, a concrete is classified as 'Excellent' when the Wenner resistivity is above 20 kΩ.cm and the charge passed is less than 1000 Coulombs. Similarly, concrete mixes with surface resistivity values greater than 20 kΩ.cm and the non-steady state migration coefficient less than 8×10^{-12} m^2/s is also classified as 'Excellent'. In a similar way, concrete mixes having a surface resistivity values greater than 20 kΩ.cm and chloride conductivity values less than 0.75 mS/cm are classified in the 'Excellent' category. Accordingly, all the categories can be defined based on more than one parameter.

Combined classification system for particular service environment

- The transport mechanisms represented by each durability test method used in the project were recognized.
- The different transport mechanisms leading to concrete deterioration in different service environments, indicated in BS 8500 Part 1 (2006) for chloride and carbonation induced corrosion, were identified.
- Based on this, combined classification systems for concretes, by linking the prevalent transport mechanisms in that environment, were developed for both chloride and carbonation induced corrosion environment. Using this approach, the concrete mixtures tested in the current project work were analysed for their suitability in these service environments.
- For chloride induced corrosion, the combined classification criteria is developed based on compressive strength and durability parameters such as surface resistivity, charge passed, sorptivity index and depth of water penetration, assuming a cover depth of 50 mm. In the case of carbonation induced corrosion, the parameters include compressive strength and durability parameters such as OPI, carbonation rate and sorptivity index. A cover depth of 30mm is assumed in this case.

10.2.4 Quality framework for concrete construction

- Based on the present study, a quality framework is developed which will be useful for the practicing engineers. This framework can be further modified by bringing in more explicit elements of service life and cover thickness. In this case, the limiting values of the durability parameters include the elements of service life implicitly.
- The preliminary proportioning of the mixture can be done based on the criteria developed in this study such as strength grade classification or based on the qualitative ranking criteria developed for concretes with different binders based on their performance in different durability tests.
- For the pre-qualification tests, a combination of durability tests which were developed for different service life conditions for chloride and carbonation induced corrosion can be used. The mixture design can be adopted based on the

limiting criteria, or can also be chosen based on the developed criteria for the prequalification tests

10.2.5 Micro analytical investigations

- Micro-analytical studies were performed in this research project in order to establish the link between microstructure and performance
- The results of TGA performed on paste samples show that the portlandite content increases in the case of OPC from 28 to 90 days indicating prolonged hydration of cement. However, the portlandite content is decreasing in the case of SCMs as the curing duration increases from 28 to 90 days and as the replacement level increases. These results indicate that more pozzolanic reaction happens when the SCM dosage increases and also with increase in curing days. The trends obtained from the results of portlandite content are in line with those obtained from durability results. It is also observed that the surface resistivity values are not only related to pore solution conductivity, but also on the microstructure development.
- Evidence of chloride binding is obtained in all the concretes with at least 30 % replacement by SCMs. Presence of Friedel's salt was confirmed by SEM-BSE images supported with EDS analysis and XRD analysis. The modifications of the paste matrix due to carbonation are explained in terms of calcite formation, decalcification of CSH and change in porosity level. The supporting evidences of all these were obtained from SEM – BSE images. Results indicate that the porosity is higher for carbonated SCM mixes compared to that of OPC mixes.
- The chemical and phase changes due to carbonation were studied by TGA and XRD. TGA results indicate that there is much variation in the decomposition reaction details of different binders. The onset temperature changes with respect to binder type. Because of this, the type of products formed might also be different. For fly ash and slag, $CaCO_3$ may not be formed from $Ca(OH)_2$, but rather due to the carbonation of CSH. From the XRD results, it is concluded that in the case of paste samples having 100% OPC and slag, all the three polymorphs of calcium carbonate such as calcite, vaterite and aragonite are formed due to carbonation reaction, and the calcite phase is dominant in the OPC system. However, in the case of paste samples made of Class F and Class C fly ash, only the presence of calcite and vaterite are confirmed by XRD analysis, with vaterite being more dominant.

10.2.6 Influence of test related factors on durability parameters

- Some of the most commonly used durability test methods are critically analysed to derive more useful, simple results.

Rapid Chloride Permeability Test

- There exists very good correlation between charge passed and initial current reading considering all the results. Thus, the initial current reading can be used as a good, quick indicator of concrete quality. The initial current readings are not affected by the test temperature. However, the effect of other ions in the pore solution on the charge carrying ability cannot be eliminated. The observations match with existing literature.
- Good correlation is obtained between charge passed and depth of chloride penetration obtained from RCPT for the vast range of mixtures studied in this project. This observation also agrees with literature.
- There is a substantial influence of temperature on charge passed as indicated by the good correlation between total charge passed and the maximum temperature reached during the experiment.
- In order to understand the influence of SCMs on the temperature rise, the temperature profile for different concretes is plotted and it is found that the presence of SCMs reduces the temperature rise during RCPT. OPC mixes showed the highest increase in temperature during RCPT. As the age of the concrete increases, the maximum temperature decreases. The lowest temperature is displayed by slag and Class F fly ash mixes at 90 days. The maximum temperature reached for Class C fly ash mixes at 28 days is almost the same as that for OPC mixes, but is substantially lower at 90 days.

Water permeability test

- The results of the water permeability test for the two sets of specimens subjected to different pre-conditioning (without drying and drying in ventilated hot air oven set at 50°C for 7 days) indicate that drying influences the test results considerably. The drying effect is more prominent in the case of slag mixes compared to OPC and Class F fly ash mixes.

Sorptivity test

- The water sorptivity test can yield four parameters which are useful to classify the concrete qualitatively. These are sorptivity index (mm/√hr), slope of the best fit line between the mass gain and square root of time (g/√hr), porosity (%) and water absorption (%). Comparison of all these parameters will definitely yield more clarity in understanding the behaviour of a particular concrete in assessing its capillary absorption capacity.

Torrent air permeability test

- Torrent air permeability test was conducted on specimens dried in three conditions such as drying in a ventilated hot air oven at 105°C for 1 day, drying in a ventilated hot air oven at 50°C for 7 days and drying in laboratory conditions at 25°C and 65 % RH for three weeks. It is found that drying affects the results considerably. Drying at 105°C led to very high permeability of concrete. In some cases, especially those having high w/c, drying led to hairline cracks on the concrete surface and hence yielded wrong (or no) results.

10.3 MAJOR CONTRIBUTIONS

The present thesis work resulted in the following contributions.

- Generation of a database of durability parameters for concrete having different SCMs, which can be used as a guideline in the material selection
- Recommendation for the combination of durability parameters to be used for specific exposure condition and their limiting values
- Proposal of a quality framework to incorporate durability in material selection and construction
- Understanding of the influence of microstructural alterations brought about by SCMs on the durability performance

10.4 SCOPE FOR FUTURE WORK

- In the present thesis work, only chloride and carbonation induced corrosion are dealt with. The work can be extended to study of other deterioration mechanisms. The combined classification system can be extended to other deterioration mechanisms.
- The concept of strength grade classification can be further refined by incorporating data about other types of SCMs, aggregates and more grades of concrete.
- The limiting values specified in combined classification criteria can be validated by service life modelling and by taking data from deteriorated concrete in different exposure conditions.
- More research work is needed for the development of compliance and acceptance criteria for the durability parameters.
- Influence of cover depth on the durability parameters of cover concrete achieved on site needs to be studied.
- The durability parameters need to be assessed considering the appropriate duration and type of curing used at the site, giving emphasis to the practices in different service environments.

APPENDICES

APPENDIX A

Compilation of different durability test methods

Table A1 Compilation of different durability test methods specified in different references

Table A1 Compilation of different durability test methods specified in different references

Sl. No.	Reference	Basis of classification	Test methods
1	**Lamond and Pielert, 2006**	**Gas**	Gas diffusion
			Depth of carbonation
		Water	**Water vapour diffusion**
			Standard test method for water vapour transmission of materials (ASTM E 96)
			Moisture dome test
			Absorption and rate of absorption
			Test for determining the initial surface absorption of concrete (BS1881)
			Methods for specific gravity, absorption and voids in hardened concrete (ASTM C642)
			Test method for evaluating the effectiveness of materials for curing concrete (ASTM C1151)
			Test method for measurement of rate of absorption of water by hydraulic cement concretes (ASTM C1585 / AS 1342)
			Test method for measurement of rate of absorption of water by hydraulic-cement concretes (ASTM C1558)
			Water penetration
			Water penetration test (DIN 1048)
		Ionic diffusion and chloride ingress	Bulk diffusion test (ASTM C1556/ NT BUILD 443)
			Chloride ponding test (AASHTO T259/ ASTM C1543)
			Rapid Chloride Permeability Test (AASHTO T 277/ ASTM C1202)

Table A1 Compilation of different durability test methods specified in different references

Sl. No.	Reference	Basis of classification	Test methods
			Rapid Migration Test (NT BUILD 492)
2	**Bickley et al., 2006.**	**Standard Tests for fluid penetration resistance**	Electric/Conductivity charge passed (RCPT) (ASTM C1202/AASHTO T277)
			Water permeability (Army Cops CRD 163)
			Chloride penetration / Rapid Migration (AASHTOTP 64/ NORDTEST NT 492)
			Bulk Diffusion (ASTM C1556)
			Chloride penetration profile (ASTM C1543)
			Chloride penetration (AASHTO T259)
			Surface resistivity (Wenner Resistivity)
			Rate of absorption (ASTM C1585)
			Absorption and permeable voids (ASTM C642)
		Specific Durability tests	
		Alkali aggregate reaction	Potential for expansion due to aggregate reactivity (ASTM C1260)
			Potential for expansion due to aggregate reactivity (ASTM C1293)
			Alkali reduction and silica dissolution (ASTM C289)
			Effectiveness of SCMs in reducing expansion (ASTM C441)
			Potential for expansion due to aggregate reactivity (ASTM C227)
			Mineralogy (ASTM C295)
			Effectiveness of blended cement in reducing expansion (ASTM C1157)
			Damage, gel (ASTM C856)
			Reaction product (Uranyl acetate)
			Expansion (ASTM C1567)
		Alkali Carbonate Reaction Tests	Expansion (ASTM C1105)
			Expansion (ASTM C1293, CSA A 23.214A)

Table A1 Compilation of different durability test methods specified in different references

Sl. No.	Reference	Basis of classification	Test methods
			Expansion (ASTM C586)
			Expansion (microbar test)
			Chemical composition (CSA A23.226A)
			Mineralogy (ASTM C295)
			Damage, gel (ASTM C856)
		Sulfate Resistance Tests	Potential expansion due to excess Cement sulphate Content (ASTM C1083)
			Dissolved sulphate test for detection of excess cement sulphate content (ASTM C265)
			Potential sulphate resistance as determined by expansion (ASTM C 452)
			Potential sulphate resistance as determined by expansion and mass loss (ASTM C1012)
		Freezing and Thawing Related Tests	Mass loss, dynamic modulus, length change (ASTM C 666A,B)
			Mass loss (SS 13 72 44)
			Ultra sonic pulse velocity
			Air content, spacing factor, specific surface in hardened concrete (ASTM C457)
			Air content, spacing factor, specific surface in plastic concrete (Air void analyser)
		De-Icer Scaling Related Tests	Visual (ASTM C672)
			Visual and mass loss (ASTM C672)
			Mass loss (BNQ 2621-900)
			Mass loss (Swedish SS 137244)
			Ultrasonic pulse velocity (CDF (German)
			Air content, spacing factor, specific surface (ASTM C457)
			% air, spacing factor, specific surface (Fresh air void analyser)
		Chloride content tests	Acid soluble chloride in concrete (ASTM C1152)
			Water soluble chloride in concrete(ASTM C1218)

Table A1 Compilation of different durability test methods specified in different references

Sl. No.	Reference	Basis of classification	Test methods
			Water extractable chlorides in aggregates only (ASTM C1524)
		Corrosion related tests	Voltage potential (ASTM C876)
			Time to corrosion and rate of corrosion (G 109)
			Bulk diffusion (ASTM C1556)
			Conductivity (ASTM C1202)
			Chloride penetration (ASTM C1543)
			Corrosion current and corrosion rate (Linear Polarization resistance and Galvapulse)
		Abrasion and Erosion Tests	Mass loss and depth of wear from rotating cutters (ASTM C944)
			Depth of wear by three methods: revolving disk, ball bearings, dressing wheels (ASTM C779)
			Abraded volume by sandblasting (ASTM C418)
			Abraded volume and depth of wear under water with ball bearings (ASTM C 1138)
		In-Place Testing	Rebound number (ASTM C 805)
			Penetration Resistance (ASTM C803)
			Pull out (ASTM C900)
			Break-off (ASTM C1150)
			Ultrasonic pulse velocity (ASTM C597)
			Maturity method (ASTM C1074)
			Cast-in-place cylinders (ASTM C873)
		Combined methods	Field sorptivity
			Rapid Chloride Permeability (ASTM C1202)
			Air Void Properties (ASTM C457)
3	**Bjegović et al. (2005)**	**Gas permeability**	Figg’s method
			Schönlin& Hilsdorf

Table A1 Compilation of different durability test methods specified in different references			
Sl. No.	**Reference**	**Basis of classification**	**Test methods**
			Autoclam method
			Torrent method
			Permeability exponent
			Cembureau method
			Oxygen Permeability Index Test (South Africa)
		Water permeability	Autoclam method
			Water permeability Test (GWT)
			Depth of penetration of water under pressure
		Capillary absorption	Initial surface absorption test (ISAT)
			Autoclam method
			Water absorption (RILEM CPC11.2)
			Water absorption (ASTM C1585)
			Water sorptivity test (South Africa)
		Chloride penetration	Non-steady state chloride diffusion coefficient (NORD 443)
			Non-steady state chloride migration coefficient (NORD 492)
			Electrical indication of concrete's ability to resist chloride ion penetration (ASTM C1202)
			Multiregime method (UNE 83987)
			Permit Ion Migration Test
			Chloride profiling method
		Concrete resistivity and conductivity	Direct resistivity test (UNE 83988-1)
			Concrete resistivity Wenner probe
			Chloride conductivity test (South Africa)

Table A1 Compilation of different durability test methods specified in different references

Sl. No.	Reference	Basis of classification	Test methods
4	**RILEM TC 189 , 2007**		
	Kropp and Alexander, 2007	**Diffusion**	Salt ponding test
			Bullk diffusion (NT Build 443)
		Permeation	Gas permeability
			Water permeability
			CEMBUREAU method for gas and water permeability
		Capillary suction	Sorptivity
		Migration	Rapid chloride permeability (ASTM C1202)
			Rapid migration (NT BUILD 492)
	Torrent et al., 2007	**Surface methods**	
		Single chamber method	Schonlin method
			Autoclam method
		Double chamber method	Torrent
			Zia-Guth
		Intrusive methods	Figg-Poroscope
			TUD
			Parrot
			Paulmann
			Germann Gas Test (GGT)
	Basheer et al., 2007	**Classification based on the method**	
		Surface Methods	Initial Surface Absorption Test ISAT
			Autoclam Permeability system
			Germann water test GWT

Table A1 Compilation of different durability test methods specified in different references			
Sl. No.	**Reference**	**Basis of classification**	**Test methods**
		Intrusive method	Figg-Poroscope method
			Filed permeability test FPT
		Classification based on the mechanism	
		Sorptivity methods	Initial surface absorption test ISAT
			Figg-Poroscope method
			Autoclam sorptivity test
		Permeability methods	Filed permeability test FPT
			Autoclam permeability system
			Germann water test GWT
	Andrade et al., 2007	**Electrical resistivity methods**	Four point Wenner method
			Two point method
			The disc method
		Ion migration methods	Whiting method
			Permit method
5	**Yuan and Santhanam, 2013**	**Classification based on theoretical base**	
		Fick's first law	Steady state diffusion test
		Fick's second law	Bulk diffusion test (NT Build 443)
			Bulk diffusion test (ASTM C1556)
		Nernst Plank equation	NT build 355
			Truc's method
			NT BUILD 492
			Breakthrough time method
			Multi-regime method
			Samson's method

Table A1 Compilation of different durability test methods specified in different references

Sl. No.	Reference	Basis of classification	Test methods
			Friedmann's method
		Nernst Einstein equation	Lu's method
			Andrade´s method
		Formation factor	Formation factor method
		other test methods	Rapid chloride permeability test (ASTM C1202 or AASHTO T 227)
			Conductivity test method
			90 day ponding test (AASHTO T 259)
			Water pressure method
			AC impedance method
			Integral Method
6	**ACI ITG-8R-10**	**Test methods related to resistance to fluid penetration**	Chloride ponding test (ASTM C1543 AASHTO T 259)
			Chloride bulk diffusion test (ASTM C1556)
			Water permeability (CRD 48 and 163)
			Rapid chloride permeability test (ASTM C1202 AASHTO T 277)
			Rapid migration test (AASHTO TP 64)
			Surface-resistivity test (FM 5-578 (FDOT 2004))
			Sorptivity test (ASTM C1585)
			Absorption and voids test (ASTM C642)
7	**Stanish et al., 1997**	**Long term**	Salt ponding test (AASHTO T 259)
			Bulk diffusion (NORD 443)
		Short term	Rapid chloride permeability test (AASHTO T 277)
			Electrical migration
			Rapid migration (CTH)
			Resistivity

Table A1 Compilation of different durability test methods specified in different references

Sl. No.	Reference	Basis of classification	Test methods
			Pressure Penetration
		Other test methods	Sorptivity test (Lab)
			Sorptivity test (Field)
			Propan-2-ol Counter- diffusion
			Gas Diffusion
8	**Basheer (2001)**	**Adsorption tests**	Adsorption isotherms
			BET theory
		Diffusion tests	
		Gas diffusion	Diffusion cell by Lawrence
			Diffusion cell by Richardson
		Water vapour diffusion	Water vapour transmission test (Dry cup method)
			Water vapour transpiration test
		Ionic diffusion	
		Steady state diffusion	
		Non-steady state diffusion	Immersion test
			Ponding test
		Electrical field migration	Rapid chloride permeability test
			CTH method
			Non - steady state migration test by Andrade
			Non steady state migration test by Zhang and Gjorv
			Steady state migration test
		Absorption tests	
		Water Absorption	Tests for water absorption capacity (BS1881/ ASTM C642)

Table A1 Compilation of different durability test methods specified in different references

Sl. No.	Reference	Basis of classification	Test methods
		Sorptivity	Sorptivity Test (Swiss guidelines for testing SIA 162/1, Test no. 5 water conductivity)
		Surface absorptivity test	Initial suface absorption test ISAT(BS 1881: Part 5 and part 208)
			Autoclam sorptivity test
			Standpipe absorptivity test (Chimney method, Karsten's pipe method, Australian water permeability test)
		Drill hole absorptivity tests	Figg test
			Covercrete absorption test
		Permeability tests	
		Liquid Permeability tests	
		Steady state water flow tests	API Designation RP 27; IS 2645
		Non-steady state water flow tests	Steinart Guard ring test; Autoclam Water Permeability test (In-situ tests), ISO/DIS 7032 (Lab test)
		Water penetration tests	DIN 1048; ISO/DIS 7031 Draft
		Gas permeability tests	
		Constant head gas permeability test	ASTM D4525-85
		Falling head gas permeability test	
		Drill hole suction tests	Figg Poroscope (Figg Air Permeability)
		Drill hole over pressure	Hong and Parrott
			Reinhart et al.
		Surface suction method	Hilsdorf
			SHRP method
			Torrent
		Surface over Pressure	Hansen et al.
			Lydon et al.
			Autoclam air permeability

Table A2 Details of Experimental principle/ Methodology, Parameter obtained and Duration of Gas penetrability test methods

Table A 2 Details of Experimental principle/ Methodology, Parameter obtained and Duration of Gas penetrability test methods

Sl. No.	**Test method**	**Experimental Principle / Methodology**	**Durability Parameter**	**Duration of test**
	Gas diffusion tests			
1	Diffusion cell (1) by Lawrence and (2) by Richardson	Two streams of gases having same pressure and temperature are passed through both side of the specimen. Traces of one gas (generally oxygen) are detected in the the second gas (normally an inert gas like nitrogen) by means of gas chromatograph. Gas diffusion coefficient is obtained by applying Fick's I or II law of diffusion	Gas diffusion coefficient	
2	Accelerated carbonation test	Depth of carbonation is a measure of the reaction between CO_2 and the cement paste. In accelerated carbonation test, the samples are subjected to a CO2 concentration much higher than that in the atmosphere, in a chamber in which the temperature and RH are kept optimum for the carbonation reaction to happen. The pH drop due to carbonation reaction is determined with the help of phenolphthalein indicator	Depth of carbonation	Months (depends on test variables)
3	Natural carbonation test	The specimens are subjected to carbonation in the natural environment, either as sheltered or non-sheltered. The pH drop due to carbonation reaction is determined with the help of phenolphthalein indicator	Depth of carbonation	years
	Water vapour diffusion tests			
4	Water vapour transmission tests (ASTM E 96)	The test specimen is sealed to the open mouth of a test dish having a desiccant, and the assembly placed in a controlled atmosphere. The rate of water vapour movement through the specimen into the desiccant is determined by weighing the specimen at a regular interval	Permeance	Up to 60 days
5	Water vapour transpiration test	Moisture is allowed to evaporate from a saturated specimen and the loss of weight with time is measured and reported as the water vapour transpiration	Water vapour transpiration	20-25 days

Table A 2 Details of Experimental principle/ Methodology, Parameter obtained and Duration of Gas penetrability test methods

Sl. No.	Test method	Experimental Principle / Methodology	Durability Parameter	Duration of test
	Gas permeability tests			
6	Figg's method	A negative relative pressure (55 kPa below atmospheric pressure) is created inside a small hole drilled in the concrete using a vacuum pump. The air from the concrete is allowed to enter the hole so that the pressure inside get increased. The time required for the absolute pressure to rise to 5 kPa is recorded as the air permeability index.	Air permeability index	1 minute to nearly 30 minutes
7	Schönlin& Hilsdorf	A negative pressure inside a vacuum chamber mounted on the surface of the concrete, pressure inside the chamber is allowed to increase by the air from concrete. By knowing the time required for the pressure to reach a predefined level, the air permeability index is calculated	Air permeability index	
8	Autoclam method	A metal ring is attached to the test surface and air pressure in the test surface is increased. The decay of pressure with time is noted and the slope of the graph between natural logarithm of pressure against time reported as air permeability index	Air permeability index	
9	Torrent method (SIA 262/1:2003)	A vacuum is created on the surface of the concrete and the rate at which the pressure is raising in the test chamber after the vacuum pump has been disconnected is monitored. The coefficient of air permeability is obtained by applying Hagen - Poisoullie law	Coefficient of air permeability kT	few minutes
10	Permeability exponent	Decreasing air pressure levels are applied on the specimen, which is controlled with a regulation valve between the vessel and the pressure line. After reaching steady state conditions, the air flow is maintained for the time needed to allow a drop of 50 mbar to occur in the vessel	Permeability exponent	
11	CEMBUREAU method)	Measuring the volume flow rate of the gas that passes through a specimen against which oxygen or nitrogen is pressurised		4 hours

Table A 2 Details of Experimental principle/ Methodology, Parameter obtained and Duration of Gas penetrability test methods

Sl. No.	Test method	Experimental Principle / Methodology	Durability Parameter	Duration of test
12	Oxygen Permeability Index Test	Measuring the pressure decay of oxygen passed through an oven dried concrete disc placed in a falling head permeameter d'Arcy's law is used to calculate the coefficient of permeability, negative log of the average coefficient of permeability yield Oxygen Permeability Index	Oxygen Permeability Index	6 hours
13	Zia-Guth double chamber method	The test cell comprises two concentric cylindrical chambers. Once a vacuum is established in both chambers, air is allowed to enter the outer chamber and flow into the inner chamber through the underlying concrete. The rate of increase of pressure in the inner chamber is measured and recorded	Permeability constant (m^2)	1.25 hours
14	TUD (Technical University of Delft) method	A small hole having 10mm diameter and 40 mm depth is drilled in the concrete and is sealed using a cylindrical hollow probe having an expanding rubber ring. After proper sealing, nitrogen gas at a pressure of 10 – 10.5 bar is introduced through the probe, at which time the stopcock is closed. Then the time for the pressure in the chamber to fall from 10 to 9.5 bar is recorded as the result of the test (TUD Time).	TUD time	1 minute to nearly 30 minutes
15	Hong - Parrot method	A hole of 35 mm deep and 20 mm diameter is drilled in the concrete surface and is sealed using a stainless steel plug fitted with an expanding silicone rubber sealing sleeve. The cavity is pressurised with air slightly above one atmosphere and the time taken for the relative pressure to drop from 50 to 35 kPa is measured.	Apparent permeability	Few minutes

Table A3 Details of Specimen details and conditioning, Strengths and Weakness of gas penetrability test methods

Table A 3 Details of Specimen details and conditioning, Strengths and Weakness of gas penetrability test methods				
Sl. No.	**Test method**	**Specimen details and conditioning**	**Strengths**	**Weakness**
	Gas diffusion tests			
1	Diffusion cell (1) by Lawrence and (2) by Richardson	• Concrete discs of 100 – 150 mm dia,.and 40–50 mm thickness, sealed on the curved surface. • Specimens are preconditioned to a low level of humidity (typically 40% or so) prior to the test.	• Useful for dense concretes • Used to predict carbonation rates and reinforcement corrosion rates	• Moisture content of the specimen and the relative humidity affect test results • Not adaptable to SLM • Destructive • Lab test
2	Accelerated carbonation test	• Usually Prismatic specimens • Require air curing after required days of moisture curing	• Useful for rapid evaluation of the rate of carbonation and possible corrosion risk • Adaptable to SLM	• The test only detects the pH change, which can happen due to other reasons also • Higher concentration of CO_2 may lead to microstructural alterations • Destructive • Not an acceptability test
3	Natural carbonation test	Cubes, prismatic sections, cores from site	• Gives an idea about the actual deterioration process • Can be used as acceptance test	• Long duration • Destructive
	Water vapour diffusion tests			
4	Water vapour transmission tests (ASTM E 96)	Representative sample of the material to be tested		• Test results depends on relative humidity and temperature • Very dry samples may get extensive micro-cracking

Table A 3 Details of Specimen details and conditioning, Strengths and Weakness of gas penetrability test methods				
Sl. No.	**Test method**	**Specimen details and conditioning**	**Strengths**	**Weakness**
5	Water vapour transpiration test	Representative sample of the material to be tested		• Test results depends on relative humidity and temperature • Very dry samples may get extensive microcracking • Destructive, prequalification, lab test
	Gas Permeability tests			
6	Figg's method	On actual structure	• Field test • Good correlation with carbonation • Acceptance test	• Semi-destructive
7	Schönlin& Hilsdorf	On actual structure	• Simple, lightweight instrumentation • Non-destructive • Field test • Acceptance test	• Problems in ensuring air tightness between air chamber and concrete surface
8	Auto-clam method	On actual structure	• Same equipment can be used for air and water permeability and sorptivity testing • Acceptance test • Non-destructive • Field test	•
9	Torrent method (SIA 262/1:2003)	• Can be done on actual concrete structure or on lab specimens. • The conditioning requirement include temperature of element above 5-10 °C; Electrical resistivity > 10 – 20 kΩ cm or moisture content < 5.5 wt.-%, measured by an impedance based instrument	• Double chamber ensures unidirectional flow of air • Lab and field test • Acceptance test	• Much depended on the surface condition of the specimen, even minor surface cracks affects the results

Table A 3 Details of Specimen details and conditioning, Strengths and Weakness of gas penetrability test methods

Sl. No.	Test method	Specimen details and conditioning	Strengths	Weakness
10	Permeability exponent	• For laboratory testing, specimens need to be oven dried at 105 °C • For testing site concrete, the humidity level need to be determined by drying the bore dust	• Both lab test and field test	• Destructive
11	CEMBUREAU method (RILEM TC 116 - PCD recommended)	• Concrete discs of 100 or 150 mm diameter, 50 mm height • Specimens are pre-dryed at 50°C to attain pre-set weight loss and are sealed and stored at an ambient temperature of 50°C for a minimum duration of 14 days. After attaining the temperature equilibrium, cooling is done for minimum 24 hours before testing	• Both lab test and field test	• Need to drill cores from the structures for assessing in-situ concrete quality • Semi-Destructive
12	Oxygen Permeability Index Test	• Concrete discs of 68-70 mm diameter, 30 mm height • Pre conditioning involve drying for 7 days at 50 degree oven and subsequent cooling	• Adaptable to SLM • useful to assess the state of compaction, presence of bleed voids and channels, and the degree of interconnectedness of the pore structure	• Preconditioning may lead to cracks in concrete, which can adversely affect the results
13	Zia-Guth double chmber method		• Non-destructive • Field test	
14	TUD method		• Semi-destructive • Field test	
15	Hong - Parrot method	applicable on site	• Semi-destructive • Field test	• Results depend on factors such as cracks, moisture and porosity gradients

Table A4 Details of Experimental principle/Methodology, Parameter obtained and Duration of chloride ion penetrability test methods

Table A.4 Details of Experimental principle/Methodology, Parameter obtained and Duration of chloride ion penetrability test methods				
Sl. No.	**Test method**	**Principle/Methodology**	**Parameter Obtained**	**Duration of test**
	Diffusion tests			
1	Bulk diffusion test ASTM C1556 / NT BUILD 443	Vacuum saturated concrete samples (exposed only at one surface) are immersed in 3% NaCl solution for a minimum of 35 days. Non-steady state chloride diffusion coefficient and the apparent surface chloride content are determined by curve-fitting the measured chloride profile to the Crank's error-function solution of Fick's 2nd law	Non-steady state diffusion coefficient	40-120 days after curing and conditioning
2	Salt Ponding AASHTO T 259/ ASTM C1543	3% NaCl is ponded on top of concrete slabs of 75 mm thick and 300 mm^2 surface area for 90 days. The chloride ion concentration at different layers are determined by profiling.	Non-steady state diffusion coefficient	90 days
3	Steady state diffusion test	A thin slice of the specimen is placed in a diffusion cell, one side of which is filled with a chloride solution and the other side with a solution free of chloride ions (Sink solution). Because of the concentration gradient ionic diffusion happen. The concentration of the chloride solution is maintained throughout the test. The chloride ion content in the sink solution is monitored periodically and the diffusion coefficient is calculated by using the Fick's first law of diffusion	Steady state diffusion coefficient	Months to years
4	Chloride profiling method	Samples are obtained by profiling the drilled core specimens or directly profiling at site. The concrete dust samples thus collected from different levels are tested in the laboratory for chloride content. By curve fitting using the error function solution to the Fick's second law, the surface chloride concentration as well as the apparent diffusion coefficients are calculated	Surface chloride concentration, the apparent diffusion coefficients	Days

Table A.4 Details of Experimental principle/Methodology, Parameter obtained and Duration of chloride ion penetrability test methods				
Sl. No.	**Test method**	**Principle/Methodology**	**Parameter Obtained**	**Duration of test**
	Migration tests			
5	Steady state migration test	A thin slice of the specimen is placed in a migration cell. One side of the cell is filled with a chloride solution and the other side with a solution free of chloride ions (sink solution). The ionic movement is accelerated by applying a potential difference across the specimen. The ion content in the sink solution is monitored periodically and the migration coefficient is calculated	Steady state migration coefficient	
6	Rapid Chloride Permeability Test ASTM C 1202	Vacuum saturated samples are subjected to 60V potential for 6 hours. The anolyte is 0.3 M Na OH and the catholyte is 3% NaCl solution. By noting down the current produced the charge passed is calculated, which is used to classify the concrete qualitatively.	Charge passed	6 hr
7	Rapid Migration Test NT BUILD 492	An external potential of 10 - 60 V is applied across the specimens with 10 % NaCl as catholyte and 0.3 M NaOH as anolyte for 6 to 96 hours. The specimens are split and the depth of chloride penetration is measured by spraying Silver nitrate solution	Non-steady state migration coefficient	generally 24 hr
8	Multi regime method UNE 83987	An external potential of 12V is imposed across the specimen which is exposed to 1M NaCl solution in the upstream side and to de-mineralised water in the downstream cell. Steady and non-steady state chloride diffusion coefficients are determined by monitoring the conductivity of the electrolyte in the anolyte chamber.	Steady and non-steady state chloride diffusion coefficients	few days to two weeks

Table A.4 Details of Experimental principle/Methodology, Parameter obtained and Duration of chloride ion penetrability test methods

Sl. No.	Test method	Principle/Methodology	Parameter Obtained	Duration of test
9	Permit ion migration test	The test apparatus has two concentric cylinders, the outer cell is having distilled water and the inner one is filled with 0.55 M NaCl solution. A potential difference of 60V is applied so the chloride ions can migrate from inner to the outer cell. The change in concentration of the solution in the outer cell is monitored and the migration coefficient is determined based on the rate of flow of chloride ions, the cell geometry and the test variables such as voltage applied, concentration of inner cell solution etc.	In-situ chloride migration coefficient	6 to 24 hours
10	Whiting method	Analogous to RCPT. A DC power supply is used to apply a constant voltage between the copper screen and steel reinforcing mat. A test period of 6 h at 80 V DC is used generally. A plot of current vs. time is plotted. Integration of that gives the total electric charge (in Coulombs) passing through the concrete during the test period	Total charge passed	6 hours
	Resistivity or conductivity tests			
11	Direct resistivity test UNE 83988 - 1	A voltage is applied between two electrodes having the vacuum saturated concrete sandwiched between them	Resistivity	Few seconds to minutes
12	Concrete resistivity test (Wenner 4 probe)	Wenner probe consists of a set of four points, each a constant distance apart. The current is applied between the two outer points, while the inner two points measure the potential	Resistivity	Minutes
13	Two point method	Resistance is measured by using two electrodes placed on the concrete surface or inside holes drilled to a depth of 8 mm and filled with conductive gel	Resistance	
14	Disc method	The test consists of placing one metal electrode on the concrete surface and measuring the resistance between this electrode and the reinforcement. For this purpose, a connection to the reinforcement cage and full steel continuity is to be done.	Resistivity	Few minutes

Table A.4 Details of Experimental principle/Methodology, Parameter obtained and Duration of chloride ion penetrability test methods

Sl. No.	**Test method**	**Principle/Methodology**	**Parameter Obtained**	**Duration of test**
15	Chloride conductivity test DI Testing manual, South Africa	10 V potential is applied across a concrete disc specimen which is vacuum saturated in 5M NaCl solution. The both sides are exposed on either side to a 5M NaCl solution. The chloride conductivity is determined by measuring the current flowing through the concrete specimen.	Chloride conductivity	Few minutes
	Pressure penetration techniques			
16	Pressure penetration techniques	In this method, the flow of chloride ions into concrete is accelerated by exposing one face of the concrete to a solution containing chloride that is under pressure. This will serve to drive the chlorides into the concrete under both convection and diffusion. Both the chloride profile as well as the depth of penetration is used to rate concrete quality		

Table A5 Details of Specimen details and conditioning, Strengths and Weakness of Chloride ion penetrability test methods

Table A 5 Details of Specimen details and conditioning, Strengths and Weakness of Chloride ion penetrability test methods

Sl. No.	Test method	Specimen details and conditioning	Strengths	Weakness
	Diffusion tests			
1	Bulk diffusion test ASTM C1556 / NT BUILD 443	• Minimum dimension across the finished surface of each test specimen must be at least 75 mm, but not less than three times the nominal maximum aggregate particle size. • The specimen depth must be at least 75 mm. • Vacuum saturation	• Applicable on drilled cores • Prequalification/Acceptance test • Considers chloride ion movement • unaffected by the conductors in concrete • No temperature rise • Many SLM are available based on the diffusion coefficient	• Destructive • Long term test • Need to do profiling and chloride content analysis (laborius)
2	Salt Ponding AASHTO T 259/ ASTM C 1543	• Three slabs of at least 75 mm thick and surface area of 300 mm^2 • Moist cured for 14 days and then stored in a drying room at 50 % RH for 28 days. • The sides of the slabs are sealed and only the bottom and top face are exposed.	• Unaffected by the conductors in concrete • No temperature rise	• More than one transport mechanisms act together • Over emphasises the effect of sorption and wick action • Laborious work
3	Steady state diffusion test	• Hardened cement paste disks of 3–4 mm thickness • Cement mortar disks 4 – 10 mm thickness	Prequalification laboratory test	• Destructive • long duration test • lasts for months • leaching of hydroxides and alkalies might cause error in the results •

Table A 5 Details of Specimen details and conditioning, Strengths and Weakness of Chloride ion penetrability test methods

Sl. No.	**Test method**	**Specimen details and conditioning**	**Strengths**	**Weakness**
4	Chloride profiling method	Core samples or powder samples (by profiling) from field are collected and are analysed for chloride content in the sample	Adaptable to SLM	laborious
	Migration tests			
5	Steady state migration test	Hardened cement paste disksof 3-4 mm thickness or cement mortar discs of 4-10 mm thickness	Steady state migration coefficient can be determined	• Destructive • Laboratory test • Long duration test
6	Rapid Chloride Permeability Test ASTM C 1202	• 100 mm diameter and 50 mm thick concrete discs • Vacuum saturation	• Most widely used test method • Relatively faster test • Gives qualitative classification of concrete • Prequalification test	• Many transport mechanisms are acting together • Current is related to all ions in the pore solution • Heating up of high permeable concrete • Presence of conductive materials and corrosion inhibitors affect test results • Measurements are taken before steady conditions are reacher
7	Rapid Migration Test NT BUILD 492	• 100 mm diameter and 50 mm thick concrete discs • Vacuum saturation	• Capable of addressing some of the criticisms of RCPT such as avoidance of heating, easiness for the escape of flue gases • Related to the examination of actual chloride ion movement and temperature rise • SLM are available	• Presence of conductive materials affects the test results • Many transport mechanisms acts together

Table A 5 Details of Specimen details and conditioning, Strengths and Weakness of Chloride ion penetrability test methods

Sl. No.	**Test method**	**Specimen details and conditioning**	**Strengths**	**Weakness**
8	Multi regime method UNE 83987	• Cylindrical specimens of any diameter having a thickness of 15-20 mm • Vacuum saturation with demineralised water	• Simple due to the indirect measurement of chloride concentration through a simple conductivity measurement. • The method is applicable to hardened specimens cast in the laboratory or drilled from field structures • Both steady and non-steady state migration coefficients are obtained from same test	
9	Permit ion migration test	• Field test • Chloride ions are introduced into the test surface.	• Applicabile in site	• Chloride ions are introduced into the test surface. • Slight staining because of the deposition of the ferrous by-product resulting from electro chemical reaction • Test duration is high for high performance/low permeability concretes
10	Whiting method	–98 kPa vacuum is maintained over the test area for 60 min. Limewater is introduced into the chamber and the vacuum is maintained for another 60 min. The vacuum is then broken and the limewater is heated at 60°C for approximately 18 hours. The limewater is then removed, the 3% NaCl is poured into the chamber and the test is started	• Non destructive • Field test	Introduces chloride ions into the field structure
	Resistivity or conductivity tests			
11	Direct resistivity test UNE 83988 - 1	vacuum saturation with saturated lime water		

Table A 5 Details of Specimen details and conditioning, Strengths and Weakness of Chloride ion penetrability test methods

Sl. No.	Test method	Specimen details and conditioning	Strengths	Weakness
12	Concrete resistivity test (Wenner 4 probe)	Field test For lab test, the specimens can be either cubes or cylinders	• Quick test • Resistivity is used to calculate corrosion rate in RC structures • No heating • Very low voltage is applied for a short duration	• Depends on the pore solution conductivity and moisture condition of the specimen • Inclusion of conductive materials can affect the results • Depends on specimen geometry and test temperature
13	Two point method	Two electrodes placed on the concrete surface or inside holes drilled to a depth of 8 mm	• Quick test • No heating • Applicable on site	• Inclusion of conductive materials can affect the results • Sensitive to the method of execution
14	Disc method	Field test	• Quick test • No heating • Applicable on site	• Inclusion of conductive materials can affect the results • Sensitive to the method of execution
15	Chloride conductivity test DI testing manual, South Africa	Drying in 50 degree oven for 7 days followed by vacuum saturation in 5M NaCl solution	• Simple and quick test • Nullifies the effect of other ions in the pore solution and guarantee uniform conductivity of the pore solution • Service life prediction model available	• Destructive in nature • Cannot be applied on site • Pre conditioning can lead to micro cracks in the specimen
	Pressure penetration methods			
16	Pressure penetration techniques	The concrete sample is pre-saturated with water. Permeability cell is used to conduct the test	• Depth of actual chloride penetration can be determined	• Many transport mechanisms such as diffusion, convection etc. act together

Table A6 Details of Experimental principle/Methodology, Parameter obtained and Duration of water penetrability test methods

<table>
<tr><td colspan="5">Table A6 Details of Experimental principle/Methodology, Parameter obtained and Duration of water penetrability test methods</td></tr>
<tr><th>Sl. No.</th><th>Test method</th><th>Principle/Methodology</th><th>Parameter obtained</th><th>Test duration</th></tr>
<tr><td></td><td colspan="4">Water permeability tests</td></tr>
<tr><td>1</td><td>Autoclam method</td><td>A metal ring is attached to the test surface and water pressure in the test surface is maintained at 0.5 bar. The cumulative water penetrated into concrete is plotted against the square root of time. The slope of the square root time plot between the 5th and the 15th minute is used to calculate the water permeability index.</td><td>Water permeability index ($m^3/\sqrt{min}$)</td><td>15 minutes</td></tr>
<tr><td>2</td><td>Germann Water Permeability test (GWT)</td><td>Water is filled in sealed pressure chamber which is attached to the concrete surface. The pressure is kept constant by adjusting a pin attached to the chamber. From the micro-meter reading the flux is calculated and by applying d’Arcy's law, the surface permeability is calculated</td><td>Surface permeability</td><td>Few minutes</td></tr>
<tr><td>3</td><td>Water Permeability test
DIN 1048 Part 5</td><td>The specimens are subjected to a constant water pressure of 5 kPa for three days. After that, the specimens are split into two and the maximum depth of water penetration is measured</td><td>Depth of water penetration</td><td>72 hr</td></tr>
<tr><td></td><td colspan="4">Capillary absorption tests</td></tr>
<tr><td>4</td><td>Initial surface absorption test (ISAT)</td><td>A water reservoir is filled with water and connected to the concrete through a cap with known area and the water level in the reservoir is monitored.</td><td>Initial surface absorption value ($ml/(m^2/s)$)</td><td>2 hr</td></tr>
<tr><td>5</td><td>Autoclam method</td><td>Measures the cumulative inflow of water in the first 15 minutes from a base ring of internal diameter 50 mm at an applied pressure of 0.02 bars. A plot of cumulative volume of water Vs square root of time gives a linear relationship and the slope obtained from the graph is reported as a sorptivity index.</td><td>Sorptivity index</td><td>15 minutes</td></tr>
<tr><td>6</td><td>Water sorptivity test
(South Africa)</td><td>Measures the rate of movement of a water front through the concrete under capillary suction, normalised by water absorption capacity</td><td>Sorptivity index</td><td>1 day</td></tr>
</table>

Table A6 Details of Experimental principle/Methodology, Parameter obtained and Duration of water penetrability test methods

Sl. No.	Test method	Principle/Methodology	Parameter obtained	Test duration
7	ASTM 1585 Method for measurement of rate of absorption of water by hydraulic cement concrete	This test method is used to determine the rate of absorption (sorptivity) of water by hydraulic cement concrete by measuring the increase in the mass of a specimen resulting from absorption of water as a function of time when only one surface of the specimen is exposed to water	Initial and final rate of water absorption (mm/√s)	8 days
8	Water Absorption test (RILEM CPC 11.2)	A concrete sample having a height at least twice that of the edge or diameter is placed in water with a constant level of 5mm above its bottom surface at atmospheric pressure. The specimen and the recipient are covered to prevent evaporation. The specimen is weighed at different periods of time and the absorption by capillary action is calculated.	Capillary absorption of water	72 hrs
	Absorption tests			
9	ASTM Standard test Method for Density, Absorption, and Voids in Hardened Concrete	The method consists of finding the oven dry mass, saturated mass after immersion, saturated mass after boiling and immersed apparent mass in order to find the density, absorption as well as volume of permeable pore space in concrete.	Absorption after immersion, Absorption after immersion and boiling, Bulk density, dry Bulk density after immersion Bulk density after immersion and boiling, Apparent density, Volume of permeable voids	2 days
	Field tests			
10	Field permeability test	Pressurised water is introduced into a hole made in the concrete. Pressure varies from 10 to 35 bars. After 30 minutes, the flow rate is recorded for 2 hrs by a capillary flow meter.	Apparent coefficient of permeability (cm/s)	3 hr
11	Figg poroscope method for water absorption	A hole is created in the concrete and is filled with water. After 60 seconds of water contacting the concrete, the stop-cock is closed and the rate of water suction by the concrete is monitored by the movement of the meniscus along the capillary, under a water head of 100 mm. The time taken for the concrete to absorb 0.01 ml of water is recorded and reported as the result of test.	Poroscope absorption time (s)	

Table A7 Details of Specimen details and conditioning, Strengths and Weakness of water penetrability test methods

Table A 7 Details of Specimen details and conditioning, Strengths and Weakness of water penetrability test methods				
Sl. No.	**Test method**	**Specimen details and conditioning**	**Strengths**	**Weakness**
	Water permeability tests			
1	Autoclam method	• Minimum one hour gap is required between air permeability and water permeability tests, if the same need to be done at same location. • Water permeability test and absorption test should not be done on the same location	• Quick test • Same equipment can be used for other durability indicators	• Problem for ensuring water tightness between chamber and concrete surface especially in non-horizontal surfaces • Influenced by the moisture content of the concrete
2	Germann Water Permeability test (GWT)	• Concrete cubes of size 150 mm for laboratory testing • Field concrete surface	• Quick test • Non-destructive	• If the concrete is porous, the assumption of water flow parallel to the gasket is not valid • Problems to conduct the test in non-horizontal surfaces • The test is difficult in highly impermeable concretes
3	Water Permeability test (DIN 1048 part 5)	• Concrete cubes of size 150 mm • Test should be started when the specimens are in the saturated condition so the effect of absorption can be eliminated	• Only one transport mechanism is happening	• Destructive in nature • The measurements need to be taken before the water get evaporated
	Capillary absorption tests			
4	Initial surface absorption test (ISAT)	• For lab tests, the Specimens haveto be oven dried at 105°C • For in-situ testing, drying at ambient temperature and humidity for a period of at least 48 hours is required		• Temperature can affect the results greatly • Difficulties to ensure water tightness
4	Autoclam method	Field test	Quick test	Results are highly influenced by the moisture content of the concrete surface
5	Water sorptivity test (South Africa)	Oven drying at 50 degree for 7 days	• Sensitive to the micro-structural properties of the	• Conditioning may introduce microstructural cracks in the surface

Table A 7 Details of Specimen details and conditioning, Strengths and Weakness of water penetrability test methods

Sl. No.	Test method	Specimen details and conditioning	Strengths	Weakness
		Specimens are of diameter 70 ± 2 mm and thickness 30 ± 2 mm, obtained by coring and cutting from 150 mm size cubes or from the cores taken from site	cover zone concrete and curing efficiency • Simulates natural phenomenon	• For specimens having reduced capillary porosity, the water absorption value will be low and thus the sorptivity index value may turn out to be higher, which can lead to a reversal of the trend • Destructive
6	ASTM 1585 Method for measurement of rate of absorption of water by hydraulic cement concrete	Oven drying at 50 degree for 3 days, followed by 15 days of storage in a sealable container having free air flow.		
7	Water Absorption test (RILEM CPC 11.2)	Specimens are circular discs of 150 mm diameter and 50 mm thickness not a unified specimen conditioning methodology	• Flexibility to change the suction period depending on the purpose of the test	• Absense of established values for evaluating concrete quality • Need to take cores to assess in situ concrete quality
	Absorption tests			
9	ASTM Standard test Method for Density, Absorption, and Voids in Hardened Concrete	Oven drying at 100 degree for not less than 24 hours		
	Field Tests			
10	Field permeability test	Field concrete surface	Field test	• Assumption to achieve steady state flow in 30 minutes is questionable • Not only permeation, absorption is also happening during the test • Results are much dependent on the moisture condition of the specimen
11	Figg poroscope method for water absorption	Field concrete specimen	Quick test	Semi destructive in nature

APPENDIX B

Database of durability parameters and compressive strength

Table B1 Results of Wenner 4- Probe Surface Resistivity Tests

Sl. No.	Mix ID	W/b	Binder content	SCM content	Surface Resistivity (kΩ.cm)					
					SR av, 28	Classification (RILEM TC 54 EMC) Concrete Quality	Classification (ACI 222) Corrosion Rate	SRav,90	Classification (RILEM TC 154 EMC) Concrete Quality	Classification (ACI 222) Corrosion Rate
1	LFM2	0.65	280	0	8.88	Very poor	High	11.27	Poor	Low to Moderate
2	LFM9	0.65	280	30% Slag A	28.42	Poor	Low	38.17	Poor	Low
3	LFM17	0.65	280	30% Slag B	18.17	Poor	Low to Moderate	32.33	Poor	Low
4	LFM29	0.65	280	30% Class F fly ash	10.08	Poor	Low to Moderate	33.50	Poor	Low
5	LFM4	0.55	340	0	8.19	Very poor	High	9.08	Very poor	High
6	LFM12	0.55	340	15% Slag A	11.83	Poor	Low to Moderate	12.17	Poor	Low to Moderate
	LFM21	0.55	340	15% Slag B	15.58	Poor	Low to Moderate	20.00	Poor	Low to Moderate
8	LFM32	0.55	340	15% Class F fly ash	11.92	Poor	Low to Moderate	27.50	Poor	Low
9	LFM42	0.55	340	15% Class C fly ash	8.45	Very poor	High	14.17	Poor	Low to Moderate
10	LFM46	0.6	310	0	9.02	Very poor	High	11.45	Poor	Low to Moderate
11	LFM10	0.6	310	15% Slag A	11.27	Poor	Low to Moderate	12.92	Poor	Low to Moderate
12	LFM19	0.6	310	15% Slag B	10.38	Poor	Low to Moderate	11.99	Poor	Low to Moderate
13	LFM30	0.6	310	15% Class F fly ash	15.75	Poor	Low to Moderate	28.00	Poor	Low
14	LFM41	0.6	310	15% Class C fly ash	9.80	Very poor	High	13.08	Poor	Low to Moderate
15	LFM5	0.5	310	0	10.73	Poor	Low to Moderate	16.25	Poor	Low to Moderate
16	LFM13	0.5	310	15% Slag A	14.75	Poor	Low to Moderate	22.92	Poor	Low

Sl. No.	Mix ID	W/b	Binder content	SCM content	Surface Resistivity (kΩ.cm)					
					SR av, 28	Classification (RILEM TC 54 EMC) Concrete Quality	Classifica tion (ACI 222) Corrosion Rate	SRav,90	Classification (RILEM TC 154 EMC) Concrete Quality	Classification (ACI 222) Corrosion Rate
17	LFM22	0.5	310	15% Slag B	21.92	Poor	Low	26.67	Poor	Low
19	LFM23	0.5	310	30% Slag B	32.92	Poor	Low	39.17	Poor	Low
18	LFM24	0.5	310	50% Slag B	84.75	Normal	Low	120.00	Good	Low
21	LFM28	0.5	310	20% Slag B+ 20%f Class F fly ash	30.25	Poor	Low	64.08	Normal	Low
20	LFM33	0.5	310	15% Class F fly ash	16.58	Poor	Low to Moderate	37.83	Poor	Low
22	LFM34	0.5	310	30% Class F fly ash	22.58	Poor	Low	68.67	Normal	Low
23	LFM35	0.5	310	50% Class F fly ash	46.92	Poor	Low	110.00	Good	Low
24	LFM39	0.5	310	20% Slag B + 20% Class C fly ash	28.58	Poor	Low	52.50	Normal	Low
25	LFM40	0.5	310	20% Class F fly ash + 20% Class C fly ash	17.25	Poor	Low to Moderate	41.17	Poor	Low
26	LFM43	0.5	310	15% Class C fly ash	10.31	Poor	Low to Moderate	17.83	Poor	Low to Moderate
27	LFM44	0.5	310	30% Class C fly ash	12.75	Poor	Low to Moderate	23.75	Poor	Low
28	CLDBS1	0.4	380	0	14.75	Poor	Low to Moderate	15.16	Poor	Low to Moderate
29	CLDBS2	0.4	380	15% Slag	15.50	Poor	Low to Moderate	23.08	Poor	Low
30	CLDBS3	0.4	380	30% Slag	23.83	Poor	Low	35.17	Poor	Low
31	CLDBS4	0.4	380	50% Slag	52.25	Normal	Low	96.74	Normal	Low
32	CLDBS5	0.4	380	15% Class F Fly ash	13.83	Poor	Low to Moderate	45.87	Poor	Low
33	CLDBS6	0.4	380	30% Class F Fly ash	21.33	Poor	Low	57.50	Normal	Low
34	CLDBS7	0.4	380	50% Class F Fly ash	29.08	Poor	Low	97.18	Normal	Low
35	MA1	0.5	300	0	10.86	Poor	Low to Moderate	12.08	Poor	Low to Moderate
36	MA2	0.55	300	0	10.17	Poor	Low to Moderate	12.50	Poor	Low to Moderate

Sl. No.	Mix ID	W/b	Binder content	SCM content	Surface Resistivity (kΩ.cm)					
					SR av, 28	Classification (RILEM TC 54 EMC) Concrete Quality	Classification (ACI 222) Corrosion Rate	SRav,90	Classification (RILEM TC 154 EMC) Concrete Quality	Classification (ACI 222) Corrosion Rate
37	MA3	0.45	320	0	10.81	Poor	Low to Moderate	12.02	Poor	Low to Moderate
38	MA4	0.45	340	0	9.96	Very poor	High	13.17	Poor	Low to Moderate
39	MA5	0.4	340	0	16.08	Poor	Low to Moderate	21.75	Poor	Low
40	MA6	0.4	360	0	13.50	Poor	Low to Moderate	27.92	Poor	Low
41	MA7	0.4	400	0	9.58	Very poor	High	15.83	Poor	Low to Moderate

Table B2 Results of Rapid Chloride Permeability Tests

Sl. No.	Mix ID	w/b	Binder content	SCM content	Rapid Chloride Permeability Test					
					Charge passed, av,28	CLASS,28	Charge passed, av,56	CLASS,56	Charge passed, av,90	CLASS,90
1	LFM2	0.65	280	0	3283	Moderate	3987	Moderate	2792	Moderate
2	LFM9	0.65	280	30% Slag A	1220	Low	1250	Low	1641	Low
3	LFM17	0.65	280	30% Slag B	1887	Low	1910	Low	1280	Low
4	LFM29	0.65	280	30% Class F fly ash	3182	Moderate	1887	Low	1180	Low
5	LFM4	0.55	340	0	4463	High	4239	High	3561	Moderate
6	LFM12	0.55	340	15% Slag A	2397	Moderate	2793	Moderate	1873	Low
7	LFM21	0.55	340	15% Slag B	2569	Moderate	2406	Moderate	2263	Moderate
8	LFM32	0.55	340	15% Class F fly ash	2692	Moderate	2259	Moderate	1810	Low
9	LFM42	0.55	340	15% Class C fly ash	4252	High	2763	Moderate	2824	Moderate
10	LFM46	0.6	310	0	4030	High	3765	Moderate	3904	Moderate
11	LFM10	0.6	310	15% Slag A	2401	Moderate	2484	Moderate	2365	Moderate
12	LFM19	0.6	310	15% Slag B	3457	Moderate	2581	Moderate	2629	Moderate
13	LFM30	0.6	310	15% Class F fly ash	1885	Low	1796	Low	1058	Low
14	LFM41	0.6	310	15% Class C fly ash	3305	Moderate	3212	Moderate	2782	Moderate
15	LFM5	0.5	310	0	2718	Moderate	2731	Moderate	2079	Moderate
16	LFM13	0.5	310	15% Slag A	1796	Low	1711	Low	1118	Low
17	LFM22	0.5	310	15% Slag B	2458	Moderate	2119	Moderate	2100	Moderate
19	LFM23	0.5	310	30% Slag B	1722	Low	1465	Low	1077	Low
18	LFM24	0.5	310	50% Slag B	476	Very low	304	Very low	325	Very low
21	LFM28	0.5	310	20% Slag B + 20% Class F fly ash	1425	Low	1446	Low	719	Very low
20	LFM33	0.5	310	15% Class F fly ash	1567	Low	1599	Low	999	Very low

Sl. No.	Mix ID	w/b	Binder content	SCM content	Rapid Chloride Permeability Test					
					Charge passed, av,28	**CLASS,28**	**Charge passed, av,56**	**CLASS,56**	**Charge passed, av,90**	**CLASS,90**
22	LFM34	0.5	310	30% Class F fly ash	1007	Low	1327	Low	980	Very low
23	LFM35	0.5	310	50% Class F fly ash	723	Very low	426	Very low	292	Very low
24	LFM39	0.5	310	20% Slag B + 20% Class C fly ash	1105	Low	920	Very low	906	Very low
25	LFM40	0.5	310	20% Class F fly ash+ 20% Class C fly ash	2167	Moderate	1114	Low	756	Very low
26	LFM43	0.5	310	15% Class C fly ash	2491	Moderate	2439	Moderate	2004	Moderate
27	LFM44	0.5	310	30% Class C fly ash	2884	Moderate	1839	Low	1280	Low
28	ClDBS1	0.4	380	0	1513	Low			1143	Low
29	ClDBS2	0.4	380	15% Slag	1337	Low			983	Very low
30	ClDBS3	0.4	380	30% Slag	976	Very low			643	Very low
31	ClDBS4	0.4	380	50% Slag	390	Very low			247	Very low
32	ClDBS5	0.4	380	15% Class F fly ash	1910	Low			567	Very low
33	ClDBS6	0.4	380	30% Class F fly ash	1556	Low			363	Very low
34	ClDBS7	0.4	380	50% Class F fly ash	1000	Very low			326	Very low
35	MA1	0.5	300	0	3293	Moderate			2640	Moderate
36	MA2	0.55	300	0	4200	High			4030	High
37	MA3	0.45	320	0	2737	Moderate			1887	Low
38	MA4	0.45	340	0	3130	Moderate			2463	Moderate
39	MA5	0.4	340	0	2227	Moderate			1440	Low
40	MA6	0.4	360	0	2770	Moderate			1823	Low
41	MA7	0.4	400	0	2133	Moderate			1683	Low

Table B3 Results of Rapid Migration Test Results

Sl. No.	Mix ID	w/b	Binder content	SCM content	Rapid Migration Test					
					Dnssm av,28	Classification	Dnssm av,56	Classification	Dnssm av,90	Classification
1	LFM2	0.65	280	0	2.68E-11	Poor	2.71E-11	Poor	2.36E-11	Poor
2	LFM9	0.65	280	30% Slag A	1.22E-11	Normal	1.00E-11	Normal	7.95E-12	Good
3	LFM17	0.65	280	30% Slag B	1.01E-11	Normal	1.23E-11	Normal	7.86E-12	Good
4	LFM29	0.65	280	30% Class F fly ash	3.03E-11	Poor	2.41E-11	Poor	9.20E-12	Normal
5	LFM4	0.55	340	0	2.98E-11	Poor	2.77E-11	Poor	2.05E-11	Poor
6	LFM12	0.55	340	15% Slag A	2.36E-11	Poor	2.39E-11	Poor	1.55E-11	Normal
7	LFM21	0.55	340	15% Slag B	1.39E-11	Normal	1.01E-11	Normal	9.64E-12	Normal
8	LFM32	0.55	340	15% Class F fly ash	1.67E-11	Poor			1.43E-11	Normal
9	LFM42	0.55	340	15% Class C fly ash	3.08E-11	Poor	1.57E-11	Normal	1.18E-11	Normal
10	LFM46	0.6	310	0	2.82E-11	Poor	3.05E-11	Poor	2.93E-11	Poor
11	LFM10	0.6	310	15% Slag A	1.79E-11	Poor	1.77E-11	Poor	1.60E-11	Poor
12	LFM19	0.6	310	15% Slag B	2.51E-11	Poor	1.83E-11	Poor	1.99E-11	Poor
13	LFM30	0.6	310	15% Class F fly ash	1.71E-11	Poor	1.88E-11	Poor	1.74E-11	Poor
14	LFM41	0.6	310	15% Class C fly ash	3.07E-11	Poor	2.12E-11	Poor	2.04E-11	Poor
15	LFM5	0.5	310	0	2.91E-11	Poor	2.46E-11	Poor	1.93E-11	Poor
16	LFM13	0.5	310	15% Slag A	1.05E-11	Normal	1.16E-11	Normal	1.31E-11	Normal
17	LFM22	0.5	310	15% Slag B	1.66E-11	Poor	1.35E-11	Normal	1.31E-11	Normal
19	LFM23	0.5	310	30% Slag B	9.32E-12	Normal	9.73E-12	Normal	8.30E-12	Normal
18	LFM24	0.5	310	50% Slag B	5.29E-12	Good	3.63E-12	Good	2.96E-12	Good
21	LFM28	0.5	310	20% Slag B + 20% Class F fly ash	1.27E-11	Normal	8.82E-12	Normal	5.30E-12	Good
20	LFM33	0.5	310	15% Class F fly ash	1.23E-11	Normal	1.16E-11	Normal	1.19E-11	Normal
22	LFM34	0.5	310	30% Class F fly ash	1.22E-11	Normal	6.53E-12	Good	6.00E-12	Good

Sl. No.	Mix ID	w/b	Binder content	SCM content	Rapid Migration Test					
					Dnssm av,28	**Classification**	**Dnssm av,56**	**Classification**	**Dnssm av,90**	**Classification**
23	LFM35	0.5	310	50% Class F fly ash	7.10E-12	Good	4.97E-12	Good	4.09E-12	Good
24	LFM39	0.5	310	20% Slag B + 20% Class C fly ash	6.44E-12	Good	7.10E-12	Good	6.26E-12	Good
25	LFM40	0.5	310	20% Class F fly ash+ 20% Class C fly ash	1.47E-11	Normal	9.59E-12	Normal	7.29E-12	Good
26	LFM43	0.5	310	15% Class C fly ash	2.61E-11	Poor	2.33E-11	Poor	2.42E-11	Poor
27	LFM44	0.5	310	30% Class C fly ash	2.01E-11	Poor	1.50E-11	Normal	1.08E-11	Normal

Table B4 Results of Chloride Conductivity Test Results

Sl. No.	Mix ID	w/b	Binder content	SCM content	Chloride conductivity test					
					σ av,28	Classification	σ av,56	Classification	σ av,90	Classification
1	LFM2	0.65	280	0	1.12	Good	1.65		1.11	Good
2	LFM9	0.65	280	30% Slag A	0.9	Good	1.19	Good	1.02	Good
3	LFM17	0.65	280	30% Slag B	0.87	Good	0.86	Good	0.68	Very Good
4	LFM29	0.65	280	30% Class F fly ash	1.17	Good	1.08	Good		
5	LFM4	0.55	340	0	1.41	Good	1.90	Poor	1.40	Good
6	LFM12	0.55	340	15% Slag A	1.26	Good	1.09	Good	1.23	Good
7	LFM21	0.55	340	15% Slag B	0.98	Good	0.95	Good	0.87	Good
8	LFM32	0.55	340	15% Class F fly ash	1.10	Good	1.11	Good	0.85	Good
9	LFM42	0.55	340	15% Class C fly ash	1.17	Good	1.02	Good	0.85	Good
10	LFM46	0.6	310	0	1.29	Good	1.33	Good	1.62	Poor
11	LFM10	0.6	310	15% Slag A	1.30	Good	1.30	Good	1.20	Good
12	LFM19	0.6	310	15% Slag B	0.80	Good	0.57	Very Good	0.70	Very Good
13	LFM30	0.6	310	15% Class F fly ash	1.10	Good	1.11	Good	1.01	Good
14	LFM41	0.6	310	15% Class C fly ash	1.14	Good	1.03	Good	0.90	Good
15	LFM5	0.5	310	0	1.03	Good	1.16	Good	1.09	Good
16	LFM13	0.5	310	15% Slag A	1.09	Good	1.00	Good	1.02	Good
17	LFM22	0.5	310	15% Slag B	0.87	Good	0.76	Good	0.82	Good
19	LFM23	0.5	310	30% Slag B	0.82	Good	0.78	Good	0.58	Very Good
18	LFM24	0.5	310	50% Slag B	0.39	Very Good	0.61	Very Good	0.32	Very Good
21	LFM28	0.5	310	20% Slag B + 20% Class F fly ash	0.51	Very Good	0.68	Very Good	0.41	Very Good
20	LFM33	0.5	310	15% Class F fly ash	1.04	Good	1.02	Good	0.83	Good
22	LFM34	0.5	310	30% Class F fly ash	0.87	Good			0.51	Very Good

Sl. No.	**Mix ID**	**w/b**	**Binder content**	**SCM content**	**Chloride conductivity test**					
					σ av,28	**Classification**	**σ av,56**	**Classification**	**σ av,90**	**Classification**
23	LFM35	0.5	310	50% Class F fly ash	0.52	Very Good	0.54	Very Good	0.42	Very Good
24	LFM39	0.5	310	20% Slag B + 20% Class C fly ash	0.65	Very Good			0.57	Very Good
25	LFM40	0.5	310	20% Class F fly ash +20% Class C fly ash	0.67	Very Good	0.71	Very Good	0.56	Very Good
26	LFM43	0.5	310	15% Class C fly ash	0.96	Good	0.89	Good	0.86	Good
27	LFM44	0.5	310	30% Class C fly ash	1.00	Good	0.84	Good	0.82	Good

Table B5 Results of Water Sorptivity Test Results

Sl. No.	Mix ID	w/b	Binder content	SCM content	Sorptivity test									
					Sorptivity av,28	Classification	slope av,28	Water Absorption av.,28	Porosity av.,28	Sorptivity av,90	Classification	slope av, 90	Water Absorption av.90	Porosity av.,90
1	LFM2	0.65	280	0	12.72	Poor	4.27	3.76	8.71	8.92	Good	2.69	3.34	7.89
2	LFM9	0.65	280	30% Slag A	11.05	Good	3.54	3.76	8.59	8.45	Good	2.70	3.65	8.39
3	LFM17	0.65	280	30% Slag B	10.13	Good	3.39	3.72	8.77	8.69	Good	2.41	3.05	7.20
4	LFM29	0.65	280	30% Class F fly ash	9.63	Good	4.77	5.75	13.04	7.71	Good	2.90	4.31	9.85
5	LFM4	0.55	340	0	9.71	Good	4.09	4.88	11.31	9.56	Good	3.90	4.59	10.91
6	LFM12	0.55	340	15% Slag A	9.08	Good	3.26	4.04	9.26	6.89	Good	1.71	2.68	6.71
7	LFM21	0.55	340	15% Slag B	4.37	Very Good	1.27	3.25	7.56	6.98	Good	1.75	2.81	6.53
8	LFM32	0.55	340	15% Class F fly ash	11.80	Good	5.29	5.13	11.79	8.59	Good	3.12	4.06	9.48
9	LFM42	0.55	340	15% Class C fly ash	7.54	Good	3.41	5.08	11.84	11.60	Good	5.03	4.96	11.39
10	LFM46	0.6	310	0	9.18	Good	4.14	5.25	11.89	9.62	Good	4.10	4.86	11.25
11	LFM10	0.6	310	15% Slag A	8.35	Good	2.58	3.48	7.96	4.81	Very Good	1.23	2.81	6.85
12	LFM19	0.6	310	15% Slag B	9.45	Good	4.04	4.71	11.51	8.20	Good	2.75	3.81	8.71
13	LFM30	0.6	310	15% Class F fly ash	9.34	Good	4.15	5.15	11.68	8.39	Good	3.21	4.20	9.97
14	LFM41	0.6	310	15% Class C fly ash	7.81	Good	3.11	4.44	10.45	14.38	Poor	5.67	5.03	10.51
15	LFM5	0.5	310	0	13.11	Poor	3.32	2.87	6.64	14.43	Poor	3.55	2.83	6.54
16	LFM13	0.5	310	15% Slag A	5.83	Very Good	1.77	3.39	7.95	6.45	Good	1.32	2.21	5.33
17	LFM22	0.5	310	15% Slag B	7.58	Good	2.18	3.16	7.53	10.10	Good	1.95	2.60	4.43
19	LFM23	0.5	310	30% Slag B	5.43	Very Good	1.18	2.28	5.71	9.40	Good	1.17	1.94	2.50
18	LFM24	0.5	310	50% Slag B	4.91	Very Good	1.29	2.77	7.09	4.76	Very Good	0.83	1.91	4.57
21	LFM28	0.5	310	20% Slag B + 20% Class F fly ash	8.85	Good	2.85	3.59	8.49	9.68	Good	1.85	2.08	5.00

Sl. No.	Mix ID	w/b	Binder content	SCM content	Sorptivity test									
					Sorptivity av,28	**Classification**	**slope av,28**	**Water Absorption av.,28**	**Porosity av.,28**	**Sorptivity av,90**	**Classification**	**slope av, 90**	**Water Absorption av.90**	**Porosity av.,90**
20	LFM33	0.5	310	15% Class F fly ash	11.19	Good	3.58	3.53	8.51	8.61	Good	1.58	2.46	4.22
22	LFM34	0.5	310	30% Class F fly ash	6.18	Good	2.15	3.92	9.13	6.79	Good	1.33	2.22	5.16
23	LFM35	0.5	310	50% Class F fly ash	9.56	Good	2.80	3.59	7.71	12.54	Poor	2.39	2.15	5.02
24	LFM39	0.5	310	20% Slag B + 20% Class C fly ash	5.11	Very Good	1.45	3.18	7.44	6.75	Good	1.67	2.70	6.42
25	LFM40	0.5	310	20% Class F fly ash+20% Class C fly ash	5.99	Very Good	1.71	3.17	7.52	7.22	Good	1.51	2.28	5.47
26	LFM43	0.5	310	15% Class C fly ash	10.65	Good	4.01	3.99	9.89	7.97	Good	2.61	3.66	8.59
27	LFM44	0.5	310	30% Class C fly ash	7.53	Good	3.12	4.75	11.18	6.94	Good	2.41	4.11	9.25
28	ClDBS1	0.4	380	0	9.97	Good	2.35	2.59	6.09	8.56	Good	1.73	2.29	5.44
29	ClDBS2	0.4	380	15% Slag	9.88	Good	2.41	2.73	6.58	6.83	Good	1.07	1.70	4.12
30	ClDBS3	0.4	380	30% Slag	6.71	Good	1.02	1.71	4.10	6.37	Good	0.79	1.37	3.31
31	ClDBS4	0.4	380	50% Slag	8.45	Good	1.44	1.94	4.62	6.22	Good	0.67	1.19	2.86
32	ClDBS5	0.4	380	15% Class F fly ash	8.62	Good	1.79	2.37	5.52	8.69	Good	1.50	1.97	4.69
33	ClDBS6	0.4	380	30% Class F fly ash	7.13	Good	1.75	2.81	6.57	8.01	Good	1.61	2.33	5.48
34	ClDBS7	0.4	380	50% Class F fly ash	7.66	Good	1.70	2.58	6.00	6.80	Good	1.26	2.15	5.04
35	MA1	0.5	300	0	9.21	Good	3.62	4.4	10.14	12.38	Poor	3.76	3.47	7.89
36	MA2	0.55	300	0	11.02	Good	3.78	3.72	8.79	12.61	Poor	3.6	3.52	7.32
37	MA3	0.45	320	0	4.30	Very Good	1.25	3.14	7.51	12.95	Poor	3.4	3.14	6.82
38	MA4	0.45	340	0	4.65	Very Good	1.42	3.41	7.95	10.45	Good	3.51	3.79	8.68
39	MA5	0.4	340	0	2.93	Very Good	0.87	3.31	7.72	8.83	Good	2.29	3.04	6.69
40	MA6	0.4	360	0	5.37	Very Good	1.86	3.82	8.88	10.65	Good	3.18	3.26	7.67
41	MA7	0.4	400	0	6.64	Good	2.14	3.79	8.9	12.01	Poor	3.75	3.5	8.03

Table B6 Results of Water Permeability Test Results

Sl. No.	Mix ID	w/b	Binder content	SCM content	DIN WATER PERMEABILITY TEST	
					DoP (av.), dried	DoP (av.), sample not dried
1	LFM2	0.65	280	0	93.8	21.4
2	LFM9	0.65	280	30% slag A	88.8	
3	LFM17	0.65	280	30%slagB	86.7	
4	LFM29	0.65	280	30%Class F fly ash	74.7	
5	LFM4	0.55	340	0	50.5	12.4
6	LFM12	0.55	340	15%slagA	48.6	
7	LFM21	0.55	340	15%slagB	38.4	
8	LFM32	0.55	340	15% Class F fly ash	31.9	
9	LFM42	0.55	340	15% Class C fly ash	26.3	
10	LFM46	0.6	310	0	48.0	
11	LFM10	0.6	310	15%slagA		
12	LFM19	0.6	310	15%slagB	81.5	
13	LFM30	0.6	310	15% Class F fly ash	39.2	
14	LFM41	0.6	310	15% Class C fly ash	60.6	
15	LFM5	0.5	310	0	49.8	
16	LFM13	0.5	310	15%slagA	46.3	
17	LFM22	0.5	310	15%slagB	49.9	19.3
19	LFM23	0.5	310	30% slag B	40.9	24.5
18	LFM24	0.5	310	50%slagB	18.9	
21	LFM28	0.5	310	20%slagB+20%Class F fly ash	55.0	30.9
20	LFM33	0.5	310	15% Class F fly ash	35.2	
22	LFM34	0.5	310	30%Class F fly ash	31.0	
23	LFM35	0.5	310	50%Class F fly ash	26.7	

Sl. No.	Mix ID	w/b	Binder content	SCM content	DIN WATER PERMEABILITY TEST	
					DoP (av.), dried	DoP (av.), sample not dried
24	LFM39	0.5	310	20%slagB+20%Class C fly ash	24.4	
25	LFM40	0.5	310	20%Class F fly ash+20%Class C fly ash	48.0	
26	LFM43	0.5	310	15% Class C fly ash	31.8	
27	LFM44	0.5	310	30% Class C fly ash	21.8	
28	ClDBS1	0.4	380	0	20.6	12.1
29	ClDBS2	0.4	380	15% slag	48.9	7.9
30	ClDBS3	0.4	380	30%Slag	43.8	10.6
31	ClDBS4	0.4	380	50% Slag	38.4	8.9
32	ClDBS5	0.4	380	15%Flyash F	25.5	
33	ClDBS6	0.4	380	30%Flyash F	22.1	10.8
34	ClDBS7	0.4	380	50%Flyash F	18.1	10.4

Table B7 Results of Oxygen Permeability Index Test Results

Sl. No.	Mix ID	w/b	Binder content	SCM content	OPI test					
					kav,28	OPI, 28	Classification	kav,90	OPI, 90	Classification
1	LFM2	0.65	280	0	1.64E-10	9.79	Good	8.71E-11	10.08	Very Good
2	LFM9	0.65	280	30% Slag A	3.56E-10	9.45	Poor	3.56E-10	9.52	Good
3	LFM17	0.65	280	30% Slag B						
4	LFM29	0.65	280	30% Class F fly ash						
5	LFM4	0.55	340	0	1.40E-10	9.88		9.47E-11	10.06	Very Good
6	LFM12	0.55	340	15% Slag A	9.44E-11	10.06	Very Good	8.55E-11	10.09	Very Good
7	LFM21	0.55	340	15% Slag B	9.75E-11	10.01	Very Good	9.47E-11	10.02	Very Good
8	LFM32	0.55	340	15% Class F fly ash	2.65E-10	10.16	Very Good	8.91E-11	10.05	Very Good
9	LFM42	0.55	340	15% Class C fly ash	4.05E-11	10.41	Very Good	4.17E-11	10.38	Very Good
10	LFM46	0.6	310	0	9.76E-11	10.01	Very Good	8.67E-11	10.06	Very Good
11	LFM10	0.6	310	15% Slag A	9.02E-11	10.05	Very Good	4.00E-10	9.41	Poor
12	LFM19	0.6	310	15% Slag B	9.78E-11	10.01	Very Good	9.72E-11	10.01	Very Good
13	LFM30	0.6	310	15% Class F fly ash	2.28E-10	10.08	Very Good	9.75E-11	10.01	Very Good
14	LFM41	0.6	310	15% Class C fly ash	5.03E-11	10.30	Very Good	8.67E-11	10.06	Very Good
15	LFM5	0.5	310	0	1.13E-10	9.95	Good	8.38E-11	10.09	Very Good
16	LFM13	0.5	310	15% Slag A	6.44E-11	10.79	Very Good			
17	LFM22	0.5	310	15% Slag B	4.64E-11	10.34	Very Good	9.67E-11	10.01	Very Good
19	LFM23	0.5	310	30% Slag B	4.60E-10	10.66	Very Good	3.61E-10	10.75	Very Good
18	LFM24	0.5	310	50% Slag B	3.93E-10	10.73	Very Good	2.39E-10	10.81	Very Good
21	LFM28	0.5	310	20% Slag B + 20% Class F fly ash	1.21E-10	9.93	Good	1.30E-10	9.89	Good
20	LFM33	0.5	310	15% Class F fly ash	6.86E-11	10.19	Very Good	8.67E-11	10.06	Very Good
22	LFM34	0.5	310	30% Class F fly ash	1.01E-10	10.00	Very good	3.22E-10	10.73	Very Good
23	LFM35	0.5	310	50% Class F fly ash	7.09E-11	10.18	Very Good	1.01E-10	10.03	Very Good

Sl. No.	Mix ID	w/b	Binder content	SCM content	OPI test					
					kav,28	OPI, 28	Classification	kav,90	OPI, 90	Classification
24	LFM39	0.5	310	20% Slag B + 20% Class C fly ash	1.67E-10	10.48	Very Good	2.19E-10	10.82	Very Good
25	LFM40	0.5	310	20% Class F fly ash+20% Class C fly ash	1.02E-10	10.04	Very Good	5.09E-11	10.29	Very Good
26	LFM43	0.5	310	15% Class C fly ash	4.10E-11	10.39	Very Good	3.47E-11	10.46	Very Good
27	LFM44	0.5	310	30% Class C fly ash	9.09E-11	10.20	Very Good	7.13E-11	10.21	Very Good
28	ClDBS1	0.4	380	0	3.22E-11	10.49	Very Good	9.99E-12	11.00	Very Good
29	ClDBS2	0.4	380	15% Slag	4.44E-11	10.35	Very Good	1.22E-11	10.91	Very Good
30	ClDBS3	0.4	380	30% Slag	8.64E-11	10.06	Very Good	3.39E-11	10.47	Very Good
31	ClDBS4	0.4	380	50% Slag	8.58E-11	10.07	Very Good	8.48E-11	10.07	Very Good
32	ClDBS5	0.4	380	15% Class F fly ash	3.06E-11	10.51	Very Good	1.39E-11	10.86	Very Good
33	ClDBS6	0.4	380	30% Class F fly ash	2.73E-11	10.56	Very Good	2.22E-11	10.65	Very Good
34	ClDBS7	0.4	380	50% Class F fly ash	7.09E-11	10.15	Very Good	1.06E-11	10.97	Very Good
35	MA1	0.5	300	0	7.83E-11	10.13	Very Good	2.31E-10	9.66	Good
36	MA2	0.55	300	0	1.80E-10	9.80	Good	1.48E-10	9.86	Good
37	MA3	0.45	320	0	1.66E-10	9.93	Good	1.72E-10	9.77	Good
38	MA4	0.45	340	0	1.74E-10	9.76	Good	2.10E-10	9.76	Good
39	MA5	0.4	340	0	1.06E-10	9.98	Good	1.05E-10	9.98	Good
40	MA6	0.4	360	0	1.61E-10	9.87	Good	1.53E-10	9.82	Good
41	MA7	0.4	400	0	2.11E-10	9.87	Good	1.92E-10	9.82	Good

Table B8 Results of Torrent Air Permeability Test Results

Sl. No.	Mix ID	w/b	Binder content	SCM content	Torrent test(kT x 10 $^{-16}$ m^2/s)			
					28 days	Classification	90 days	Classification
1	ClDBS1	0.4	380	0	0.003	Very low	0.004	Very low
2	ClDBS2	0.4	380	15% Slag	0.023	Low	0.003	Very low
3	ClDBS3	0.4	380	30% Slag	0.002	Very low	0.006	Very low
4	ClDBS4	0.4	380	50% Slag	0.004	Very low	0.003	Very low
5	ClDBS5	0.4	380	15% Class F fly ash	0.017	Low	0.004	Very low
6	ClDBS6	0.4	380	30% Class F fly ash	0.009	Very low	0.003	Very low
7	ClDBS7	0.4	380	50% Class F fly ash	0.010	Very low	0.002	Very low

Table B9 Results of Accelerated Carbonation Test Results

Sl. No.	Mix ID	w/b	Binder content	SCM content	Accelerated carbonation test					
					DoC,70,av	DoC, 98, av	DoC, 112, av	DoC, 154, av	Carbonation rate, mm/sqrt(days)	Rcarb - carbonation resistance (year.(kg/m^3) /mm^2)
1	LFM2	0.65	280	0	4.63	6.60	7.16	8.43	0.84	9.2E-05
2	LFM9	0.65	280	30% Slag A	6.41	8.21	8.39	8.96	0.89	8.2E-05
3	LFM17	0.65	280	30% Slag B	6.48	7.05	9.51	9.70	0.95	7.2E-05
4	LFM29	0.65	280	30% Class F fly ash	7.06	9.66	9.95	11.36	1.11	5.3E-05
5	LFM4	0.55	340	0	3.68	5.72	6.24	6.77	0.68	1.4E-04
6	LFM12	0.55	340	15% Slag A	3.93	5.62	8.52	11.07	1.03	6.2E-05
7	LFM21	0.55	340	15% Slag B	4.01	5.85	7.59	8.16	0.81	9.9E-05
8	LFM32	0.55	340	15% Class F fly ash	4.14	6.24	6.71	8.02	0.78	1.1E-04
9	LFM42	0.55	340	15% Class C fly ash	3.74	7.01	7.52	9.11	0.89	8.1E-05
10	LFM46	0.6	310	0	4.04	5.09	7.12	8.53	0.81	1.0E-04
11	LFM10	0.6	310	15% Slag A	4.37	6.21	6.68	7.59	0.74	1.2E-04
12	LFM19	0.6	310	15% Slag B	3.68	5.50	6.90	7.57	0.75	1.2E-04
13	LFM30	0.6	310	15% Class F fly ash	4.92	5.40	7.05	7.95	0.76	1.1E-04
14	LFM41	0.6	310	15% Class C fly ash	4.11	7.23	7.33	9.22	0.89	8.1E-05
15	LFM5	0.5	310	0	1.58	4.28	5.12	5.59	0.58	2.0E-04
16	LFM13	0.5	310	15% Slag A	2.72	3.69	5.46	7.42	0.68	1.4E-04
17	LFM22	0.5	310	15% Slag B	3.49	4.25	5.42	6.17	0.59	1.9E-04
19	LFM23	0.5	310	30% Slag B	4.06	5.21	6.57	7.15	0.70	1.3E-04
18	LFM24	0.5	310	50% Slag B	5.21	6.30	6.38	7.51	0.72	1.3E-04

Sl. No.	Mix ID	w/b	Binder content	SCM content	Accelerated carbonation test					
					DoC,70,av	DoC, 98, av	DoC, 112, av	DoC, 154, av	Carbonation rate, mm/sqrt(days)	Rcarb - carbonation resistance (year.(kg/m^3) /mm^2)
21	LFM28	0.5	310	20% Slag B + 20% Class F fly ash	4.01	7.38	7.54	9.34	0.90	8.0E-05
20	LFM33	0.5	310	15% Class F fly ash	3.46	5.46	6.29	10.84	0.95	7.2E-05
22	LFM34	0.5	310	30% Class F fly ash	3.28	6.12	7.14	11.21	1.01	6.4E-05
23	LFM35	0.5	310	50% Class F fly ash	7.26	9.51	11.38	12.79	1.24	4.2E-05
24	LFM39	0.5	310	20% Slag B + 20% Class C fly ash	4.07	6.95	8.01	9.20	0.91	7.8E-05
25	LFM40	0.5	310	20% Class F fly ash+20% Class C fly ash	5.93	8.48	9.59	10.97	1.05	5.9E-05
26	LFM43	0.5	310	15% Class C fly ash	3.12	4.01	4.60	5.89	0.55	2.2E-04
27	LFM44	0.5	310	30% Class C fly ash	4.20	6.44	7.23	10.88	0.98	6.7E-05

Table B10 Results of Cube Compressive Strength Test Results

Sl. No.	Mix ID	w/b	Binder content	SCM content	Compressive Strength (MPa)				
					fck2, av.	fck7, av.	fck28, av.	fck90, av.	fck365,av
1	LFM2	0.65	280	0	17.75	23.09	30.32	35.46	34.34
2	LFM9	0.65	280	30% Slag A	12.75	19.19	28.22	28.95	31.72
3	LFM17	0.65	280	30% Slag B	17.43	23.81	28.69	27.81	35.96
4	LFM29	0.65	280	30% Class F fly ash	9.99	13.87	21.27	31.14	32.00
5	LFM4	0.55	340	0	27.59	35.75	42.89	42.98	43.84
6	LFM12	0.55	340	15% Slag A	20.29	27.96	37.15	41.04	43.30
7	LFM21	0.55	340	15% Slag B	28.26	37.12	44.47	46.35	52.93
8	LFM32	0.55	340	15% Class F fly ash	18.86	31.73	40.23	47.73	49.43
9	LFM42	0.55	340	15% Class C fly ash	15.74	22.59	41.33	45.74	45.12
10	LFM46	0.6	310	0	17.29	24.10	32.44	41.89	42.68
11	LFM10	0.6	310	15% Slag A	17.08	27.94	36.01	41.78	43.90
12	LFM19	0.6	310	15% Slag B	18.16	30.58	38.58	38.17	40.32
13	LFM30	0.6	310	15% Class F fly ash	20.86	27.62	38.96	44.30	44.66
14	LFM41	0.6	310	15% Class C fly ash	15.21	22.04	31.71	38.72	41.10
15	LFM5	0.5	310	0	31.43	34.53	43.81	54.62	48.65
16	LFM13	0.5	310	15% Slag A	19.98	37.33	44.69	52.69	40.81
17	LFM22	0.5	310	15% Slag B	26.90	39.51	49.15	47.55	54.97
19	LFM23	0.5	310	30% Slag B	26.39	38.24	44.69	52.06	55.78
18	LFM24	0.5	310	50% Slag B	29.38	37.90	50.41	59.23	55.00
21	LFM28	0.5	310	20% Slag B + 20% Class F fly ash	20.63	35.0833	38.3367	52.19	53.43
20	LFM33	0.5	310	15% Class F fly ash	26.12	34.74	46.07	49.96	49.75
22	LFM34	0.5	310	30% Class F fly ash	13.37	21.40	35.20	39.77	40.85
23	LFM35	0.5	310	50% Class F fly ash	6.80	14.56	23.22	31.33	33.08

Sl. No.	Mix ID	w/b	Binder content	SCM content	Compressive Strength (MPa)				
					fck2, av.	**fck7, av.**	**fck28, av.**	**fck90, av.**	**fck365,av**
24	LFM39	0.5	310	20% Slag B + 20% Class C fly ash	21.99	29.31	40.37	40.61	45.25
25	LFM40	0.5	310	20% Class F fly ash+20% Class C fly ash	15.86	27.07	33.42	46.05	49.30
26	LFM43	0.5	310	15% Class C fly ash	25.24	26.19	41.06	44.12	45.63
27	LFM44	0.5	310	30% Class C fly ash	16.83	26.24	37.89	44.22	46.80
28	ClDBS1	0.4	380	0			70.48	82.95	
29	ClDBS2	0.4	380	15% Slag			65.74	76.20	
30	ClDBS3	0.4	380	30% Slag			66.20	74.57	
31	ClDBS4	0.4	380	50% Slag			59.08	67.36	
32	ClDBS5	0.4	380	15% Class F fly ash			53.14	68.03	
33	ClDBS6	0.4	380	30% Class F fly ash			41.69	53.88	
34	ClDBS7	0.4	380	50% Class F fly ash			36.58	48.92	
35	MA1	0.5	300	0			47.03	51.87	
36	MA2	0.55	300	0			40.51	45.66	
37	MA3	0.45	320	0			52.05	58.27	
38	MA4	0.45	340	0			49.33	52.48	
39	MA5	0.4	340	0			61.69	66.83	
40	MA6	0.4	360	0			58.59	65.98	
41	MA7	0.4	400	0			55.10	64.91	

APPENDIX C

Strength Grade Classification

Table C1 Strength grade classification of Surface resistivity

Strength class	Durability class	Surface resistivity (kΩ. cm)	Concretes at 28 days			Concretes at 90 days		
			w/b	Binder content	SCM dosage	w/b	Binder content	SCM dosage
20-30	**Poor**	**<5**						
	Moderate	**5-10**	0.65	280	0			
	Good	**10-20**	0.65	280	30% Class F fly ash			
			0.65	280	30% Slag B			
	Excellent	**>20**	0.65	280	30% Slag A	0.65	280	30% Slag B
			0.5	310	50% Class F fly ash	0.65	280	30% Slag A
30-40	**Poor**	**<5**						
	Moderate	**5-10**	0.6	310	0			
			0.6	310	15% Class C fly ash			
	Good	**10-20**	0.5	310	20% Class F fly ash+ 20% Class C fly ash	0.65	280	0
			0.6	310	15% Slag A	0.6	310	15% Slag B
			0.55	340	15% Slag A	0.6	310	15% Class C fly ash
			0.5	310	30% Class C fly ash			
			0.6	310	15% Slag B			
			0.55	340	15% Class F fly ash			
			0.6	310	15% Class F fly ash			
	Excellent	**>20**	0.5	310	30% Class F fly ash	0.65	280	30% Class F fly ash
			0.4	380	50% Class F fly ash	0.5	310	30% Class F fly ash

Strength class	Durability class	Surface resistivity (kΩ. cm)	Concretes at 28 days			Concretes at 90 days		
			w/b	Binder content	SCM dosage	w/b	Binder content	SCM dosage
			0.5	310	20% Slag B+ 20% Class C fly ash	0.5	310	50% Class F fly ash
			0.5	310	20% Slag B+ 20% Class F fly ash			
40-50	**Poor**	**<5**						
	Moderate	**5-10**	0.55	340	0	0.55	340	0
			0.55	340	15% Class C fly ash			
			0.45	340	0			
			0.4	400	0			
	Good	**10-20**	0.5	310	15% Class C fly ash	0.55	340	15% Slag A
			0.55	300	0	0.6	310	15% Slag A
			0.5	310	0	0.6	310	0
			0.55	340	15% Slag B	0.5	310	15% Class C fly ash
			0.5	310	15% Slag A	0.55	340	15% Class C fly ash
			0.5	310	15% Class F fly ash	0.55	340	15% Slag B
			0.45	320	0			
			0.5	300	0			
			0.4	340	0			
	Excellent	**>20**	0.4	380	30% Class F fly ash	0.5	310	20% Slag B + 20% Class C fly ash
			0.5	310	15% Slag B	0.5	310	30% Class C fly ash
			0.5	310	50% Slag B	0.6	310	15% Class F fly ash
			0.5	310	30% Slag B	0.5	310	20% Class F fly ash + 20% Class C fly ash
						0.5	310	15% Slag B
						0.55	340	15% Class F fly ash

Strength class	Durability class	Surface resistivity (kΩ. cm)	Concretes at 28 days			Concretes at 90 days		
			w/b	Binder content	SCM dosage	w/b	Binder content	SCM dosage
						0.4	380	50% Class F fly ash
						0.5	310	15% Class F fly ash
50-60	**Poor**	**<5**						
	Moderate	**5-10**						
	Good	**10-20**	0.4	380	15% Class F flyash	0.55	300	0
			0.4	360	0	0.5	310	0
						0.5	300	0
						0.45	320	0
						0.45	340	0
	Excellent	**>20**	0.4	380	50% Slag	0.55	300	0
						0.5	310	0
						0.5	300	0
						0.45	320	0
						0.45	340	0
>60	**Poor**	**<5**						
	Moderate	**5-10**						
	Good	**10-20**	0.4	380	0	0.4	400	0
			0.4	380	15% Slag	0.4	380	0
	Excellent	**>20**	0.4	380	30% Slag	0.4	360	0
						0.4	340	0
						0.4	380	50% Slag
						0.4	380	15% Class F fly ash
						0.4	380	30% Slag
						0.4	380	15% Slag

Table C2 Strength grade classification of Charge passed

Strength Class	Durability Class	Charge Passed, Coulombs	Concretes at 28 Days			Concretes at 90 Days		
			w/b	Binder Content	SCM Dosage	w/b	Binder Content	SCM Dosage
20-30	Poor	>4000						
	Moderate	2000-4000	0.65	280	0			
			0.65	280	30% Class F fly ash			
	Good	1000-2000	0.65	280	30% Slag B	0.65	280	30% Slag A
			0.65	280	30% Slag A	0.65	280	30% Slag B
	Excellent	<1000	0.5	310	50% Class F fly ash			
30-40	Poor	>4000	0.6	310	0			
	Moderate	2000-4000	0.6	310	15% Slag B	0.65	280	0
			0.6	310	15% Class C Fly ash	0.6	310	15% Class C Fly ash
			0.5	310	30% Class C Fly ash	0.6	310	15% Slag B
			0.55	340	15% Class F Fly ash			
			0.6	310	15% Slag A			
			0.55	340	15% Slag A			
			0.5	310	20% Class F Fly ash +20% Class C Fly ash			
	Good	1000-2000	0.6	310	15% Class F Fly Ash	0.65	280	30% Class F Fly ash
			0.5	310	20% Slag B +20% Class F Fly ash			
			0.5	310	20% Slag B +20% Class C Fly ash			
			0.5	310	30% Class F Fly ash			
	Excellent	<1000	0.4	380	50% Class F Fly ash	0.5	310	30% Class F Fly ash

Strength Class	Durability Class	Charge Passed, Coulombs	Concretes at 28 Days			Concretes at 90 Days		
			w/b	Binder Content	SCM Dosage	w/b	Binder Content	SCM Dosage
						0.5	310	20% Slag B +20% Class C Fly ash
						0.5	310	50% Class F Fly ash
40-50	**Poor**	>4000	0.55	340	0	0.55	300	0
			0.55	340	15% Class C fly ash			
			0.55	300	0			
	Moderate	2000-4000	0.5	300	0	0.6	310	0
			0.45	340	0	0.55	340	0
			0.45	320	0	0.55	340	15% Class C fly ash
			0.5	310	0	0.6	310	15% Slag A
			0.55	340	15% Slag B	0.55	340	15% Slag B
			0.5	310	15% Class C fly ash	0.5	310	15% Slag B
			0.5	310	15% Slag B	0.5	310	15% Class C fly ash
			0.4	340	0			
			0.4	400	0			
	Good	1000-2000	0.5	310	15% Slag A	0.55	340	15% Slag A
			0.5	310	30% Slag B	0.55	340	15% Class F fly ash
			0.5	310	15% Class F fly ash	0.5	310	30% Class C fly ash
			0.4	380	30% Class F fly ash	0.6	310	15% Class F fly ash
	Excellent	<1000	0.5	310	50% Slag B	0.5	310	15% Class F fly ash
						0.5	310	20% Class F fly ash +20% Class C fly ash
						0.4	380	50% Class F fly ash

Strength Class	Durability Class	Charge Passed, Coulombs	Concretes at 28 Days			Concretes at 90 Days		
			w/b	Binder Content	SCM Dosage	w/b	Binder Content	SCM Dosage
50-60	**Poor**	>4000						
	Moderate	2000-4000	0.4	360	0	0.5	300	0
						0.45	340	0
						0.5	310	0
	Good	1000-2000	0.4	380	15% Class F fly ash	0.45	320	0
						0.5	310	15%Slag A
						0.5	310	30% Slag B
	Excellent	<1000	0.4	380	50% Slag	0.5	310	20% Slag B +20%Class F fly ash
						0.4	380	30% Class F fly ash
						0.5	310	50% Slag B
>60	**Poor**	>4000						
	Moderate	2000-4000						
	Good	1000-2000	0.4	380	15% Slag	0.4	360	0
			0.4	380	0	0.4	340	0
						0.4	400	0
						0.4	380	0
	Excellent	<1000	0.4	380	30% Slag	0.4	380	15% Slag
						0.4	380	30% Slag
						0.4	380	15% Class F fly ash
						0.4	380	50% Slag

Table C3 Strength grade classification of Oxygen Permeability Index

Strength Class	Durability Class	OPI	Concretes At 28 Days			Concretes At 90days		
			w/b	Binder Content	SCM Dosage	w/b	Binder Content	SCM Dosage
20-30	Poor	<9						
	Moderate	9-9.5						
	Good	9.5-10						
	Excellent	>10	0.5	310	50% Class F fly ash			
30-40	Poor	<9						
	Moderate	9-9.5						
	Good	9.5-10	0.5	310	20% Slag B + 20% Class F fly ash	0.65	280	30% Class F fly ash
			0.5	310	30% Class F fly ash			
	Excellent	>10	0.6	310	15% Class C fly ash	0.5	310	50% Class F fly ash
			0.6	310	0	0.65	280	0
			0.5	310	20% Class F fly ash +20% Class C fly ash	0.6	310	15% Slag B
			0.6	310	15% Slag A	0.6	310	15% Class C fly ash
			0.4	380	50% Class F fly ash	0.5	310	30% Class F fly ash
			0.55	340	15% Slag A			
			0.5	310	30% Class C fly ash			
			0.6	310	15% Slag B			

Strength Class	**Durability Class**	**OPI**	**Concretes At 28 Days**			**Concretes At 90days**		
			w/b	**Binder Content**	**SCM Dosage**	**w/b**	**Binder Content**	**SCM Dosage**
			0.6	310	15% Class F fly ash			
			0.55	340	15% Class F fly ash			
			0.5	310	20% Slag B +20% Class C fly ash			
40-50	Poor	<9						
	Moderate	9-9.5						
	Good	9.5-10	0.55	340	0			
			0.5	310	0			
			0.4	340	0			
			0.45	340	0			
			0.45	320	0			
			0.4	400	0			
			0.55	300	0			
	Excellent	>10	0.5	310	15% Slag B	0.5	310	20% Slag B +20% Class C fly ash
			0.5	310	50% Slag B	0.55	340	15% Slag A
			0.5	310	15% Class C fly ash	0.6	310	0
			0.55	340	15% Class C fly ash	0.55	340	0
			0.4	380	30% Class F fly ash	0.5	310	15% Class C fly ash
			0.55	340	15% Slag B	0.5	310	30% Class C fly ash
			0.5	310	15% Slag A	0.6	310	15% Class F fly ash
			0.5	310	30% Slag B	0.55	340	15% Class C fly ash

Strength Class	Durability Class	OPI	Concretes At 28 Days			Concretes At 90days		
			w/b	Binder Content	SCM Dosage	w/b	Binder Content	SCM Dosage
			0.5	310	15% Class F fly ash	0.5	310	20% Class F fly ash +20% Class C fly ash
			0.5	300	0	0.55	340	15% Slag B
						0.5	310	15% Slag B
						0.55	340	15% Class F fly ash
						0.4	380	50% Class F fly ash
						0.5	310	15% Class F fly ash
50-60	Poor	<9						
	Moderate	9-9.5						
	Good	9.5-10	0.4	360	0	0.55	300	0
						0.5	310	20% Slag B + 20% Class F fly ash
						0.5	300	0
						0.45	320	0
						0.45	340	0
	Excellent	>10	0.4	380	15% Class F fly ash	0.5	310	50% Slag B
			0.4	380	50% Slag	0.5	310	30% Slag B
						0.4	380	30% Class F fly ash
						0.5	310	0
>60	Poor	<9						
	Moderate	9-9.5						
	Good	9.5-10				0.4	360	0
						0.4	340	0

Strength Class	Durability Class	OPI	Concretes At 28 Days			Concretes At 90days		
			w/b	Binder Content	SCM Dosage	w/b	Binder Content	SCM Dosage
						0.4	400	0
	Excellent	>10	0.4	380	15% Slag	0.4	380	50% Slag
			0.4	380	30% Slag	0.4	380	15% Class F fly ash
			0.4	380	0	0.4	380	30% Slag
						0.4	380	15% Slag
						0.4	380	0

Table C4 Strength grade classification of Sorptivity Index

Strength Class	Durability Class	SI	Concretes At 28 Days			Concretes At 90days		
			W/B	Binder Content	SCM Dosage	w/b	Binder Content	SCM Dosage
20-30	Poor	>15	0.65	280	0			
	Moderate	12-15						
	Good	6-12	0.5	310	50% Class F fly ash	0.65	280	30% Slag B
			0.65	280	30% Class F fly ash	0.65	280	30% Slag A
			0.65	280	30% Slag B			
			0.65	280	30% Slag A			
	Excellent	<6						
30-40	Poor	>15						
	Moderate	12-15				0.6	310	15% Class C fly ash
						0.5	310	50% Class F fly ash
	Good	6-12	0.55	340	15% Class F fly ash	0.65	280	0
			0.6	310	15% Slag B	0.6	310	15% Slag B
			0.6	310	15% Class F fly ash	0.65	280	30% Class F fly ash
			0.6	310	0	0.5	310	30% Class F fly ash
			0.55	340	15% Slag A			
			0.5	310	20% Slag B + 20% Class F fly ash			
			0.6	310	15% Slag A			
			0.6	310	15% Class C fly ash			
			0.4	380	50% Class F fly ash			
			0.5	310	30% Class C fly ash			
			0.5	310	30% Class F fly ash			
	Excellent	<6	0.5	310	20% Class F fly ash+20% Class C fly ash			

Strength Class	Durability Class	SI	Concretes At 28 Days			Concretes At 90days		
			W/B	Binder Content	SCM Dosage	w/b	Binder Content	SCM Dosage
			0.5	310	20% Slag B + 20% Flyash C			
40-50	Poor	>15						
	Moderate	12-15	0.5	310	0			
	Good	6-12	0.5	310	15% Class F fly ash	0.55	340	15% Class C fly ash
			0.55	300	0	0.5	310	15% Slag B
			0.5	310	15% Class C fly ash	0.6	310	0
			0.55	340	0	0.55	340	0
			0.5	300	0	0.5	310	15% Class F fly ash
			0.5	310	15% Slag B	0.55	340	15% Class F fly ash
			0.55	340	15% Class C fly ash	0.6	310	15% Class F fly ash
			0.4	380	30% Class F fly ash	0.5	310	15% Class C fly ash
			0.4	400	0	0.5	310	20% Class F fly ash + 20% Class C fly ash
						0.55	340	15% Slag B
						0.5	310	30% Class C fly ash
						0.55	340	15% Slag A
						0.4	380	50% Class F fly ash
						0.5	310	20% Slag B + 20% Class C fly ash
	Excellent	<6	0.5	310	15% Slag A	0.6	310	15% Slag A
			0.5	310	30% Slag B			
			0.5	310	50% Slag B			
			0.45	340	0			
			0.55	340	15% Slag B			

Strength Class	Durability Class	SI	Concretes At 28 Days			Concretes At 90days		
			W/B	Binder Content	SCM Dosage	w/b	Binder Content	SCM Dosage
			0.45	320	0			
			0.4	340	0			
40-50	Poor	>15						
	Moderate	12-15				0.5	310	0
						0.45	320	0
						0.55	300	0
						0.5	300	0
	Good	6-12	0.4	380	15% Class F fly ash	0.45	340	0
			0.4	380	50% Slag	0.5	310	20% Slag B + 20% Class F fly ash
						0.5	310	30% Slag B
						0.4	380	30% Class F fly ash
						0.5	310	15% Slag A
	Excellent	<6	0.4	360	0	0.5	310	50% Slag B
50-60	Poor	>15						
	Moderate	12-15				0.4	400	0
	Good	6-12	0.4	380	15% Slag	0.4	360	0
			0.4	380	0	0.4	340	0
			0.4	380	30% Slag	0.4	380	15% Class F fly ash
						0.4	380	0
						0.4	380	15% Slag
						0.4	380	30% Slag
						0.4	380	50% Slag
	Excellent	<6						

APPENDIX D

Influence of SCMs on Durability Parameters of concrete

D1 – Surface resistivity

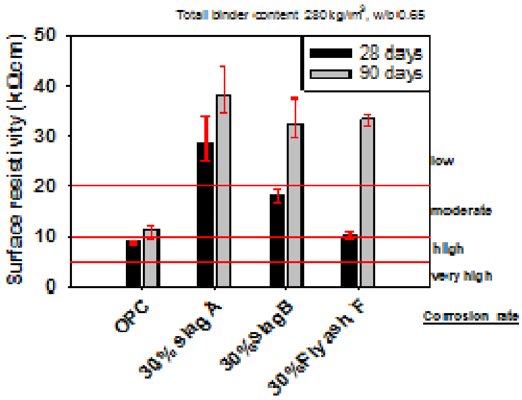

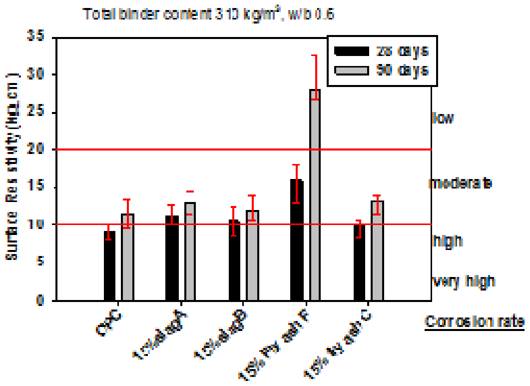

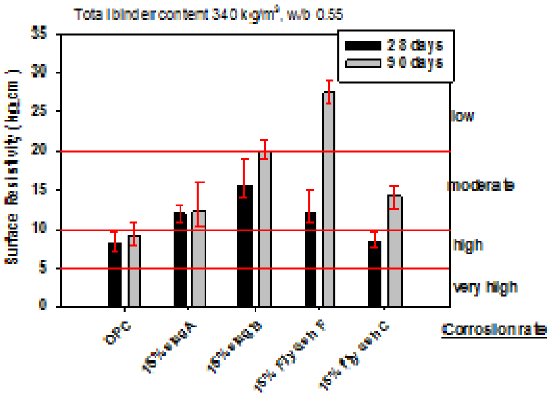

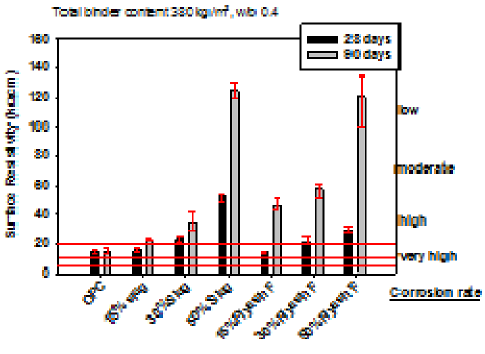

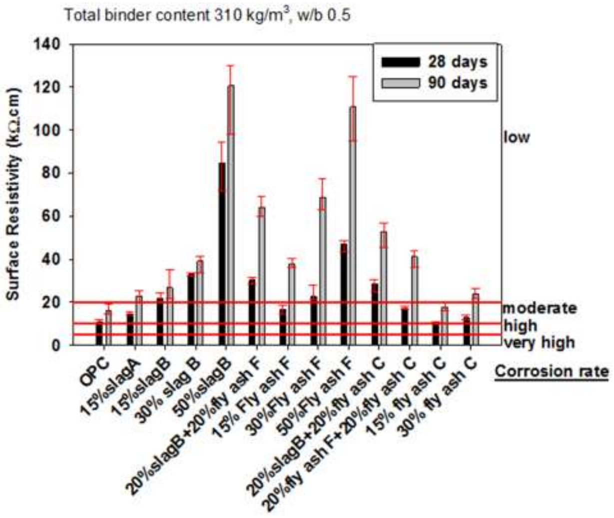

D2 – Charge passed

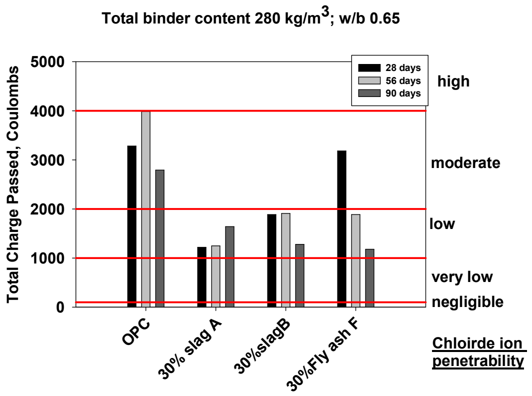

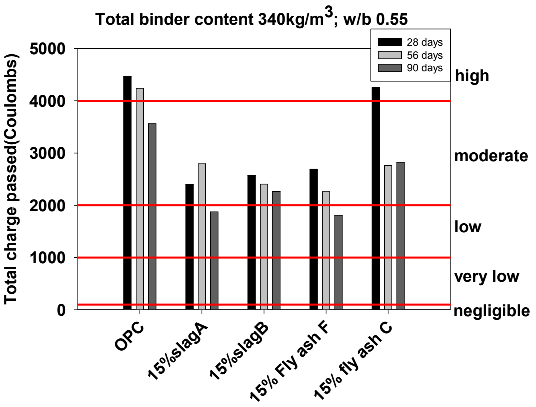

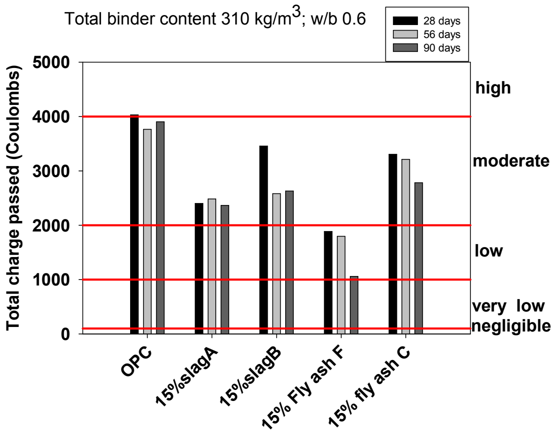

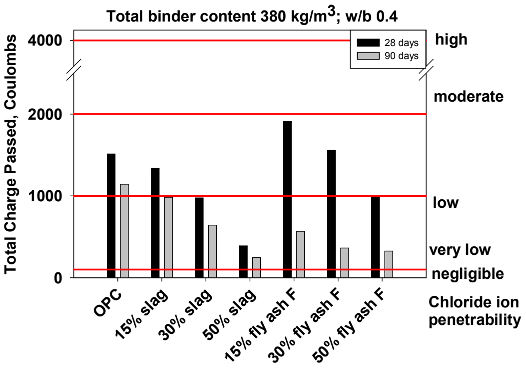

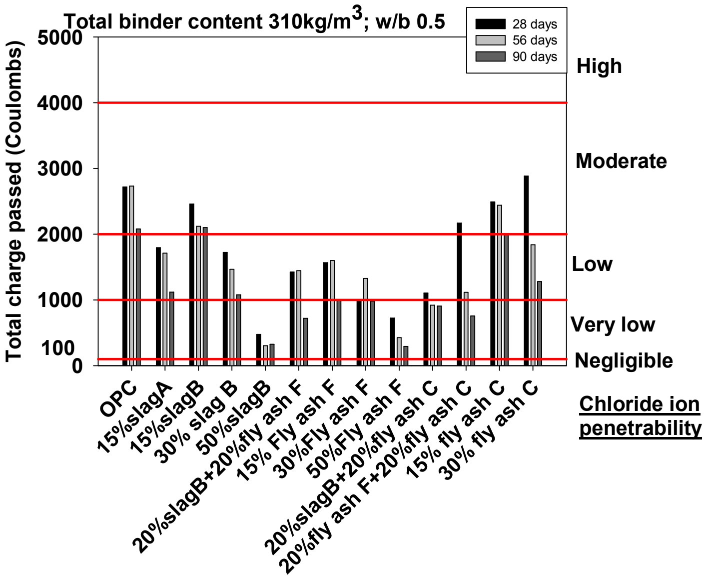

D3- Non-steady state migration coefficient

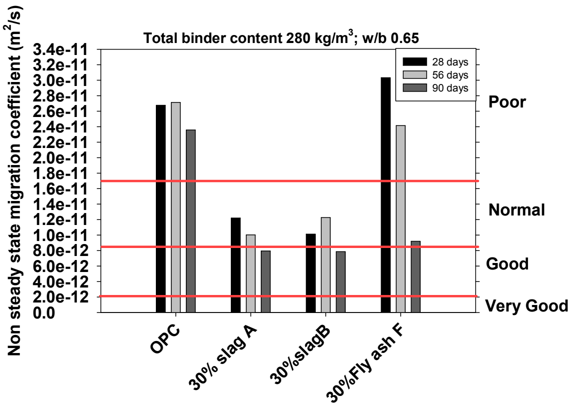

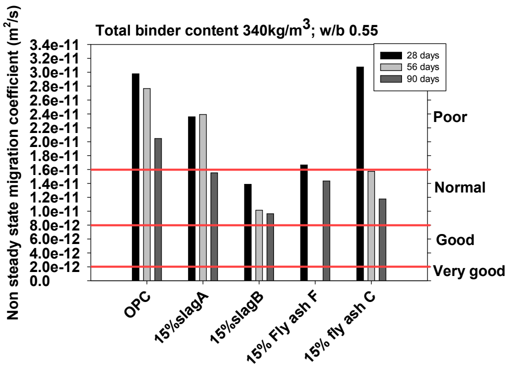

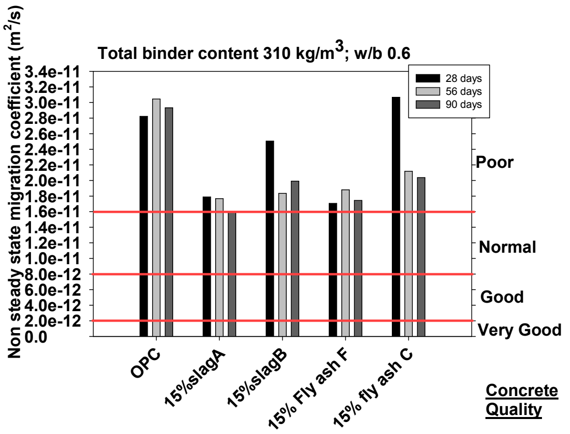

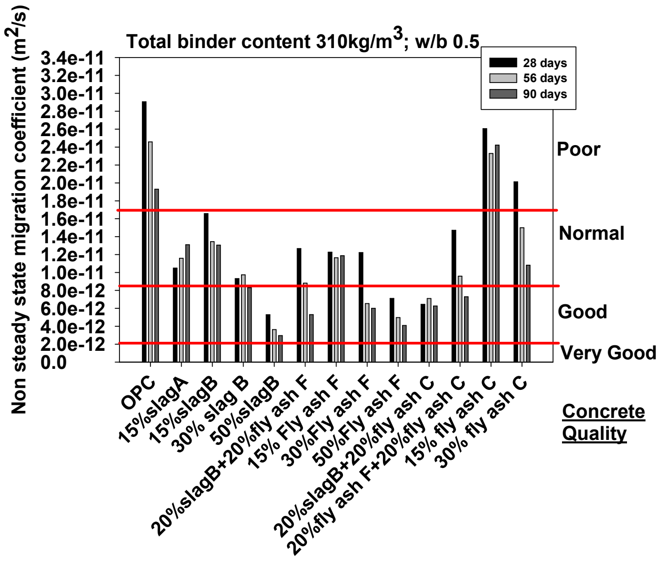

D4 – Chloride conductivity

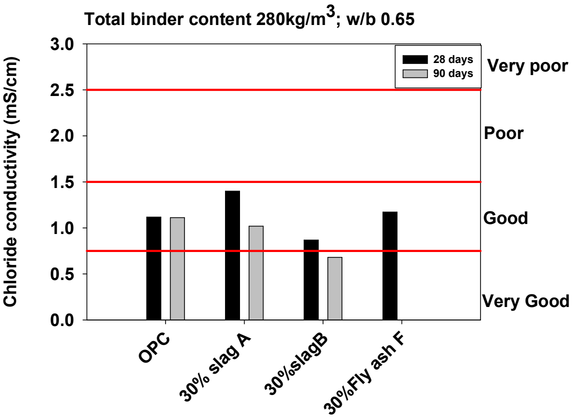

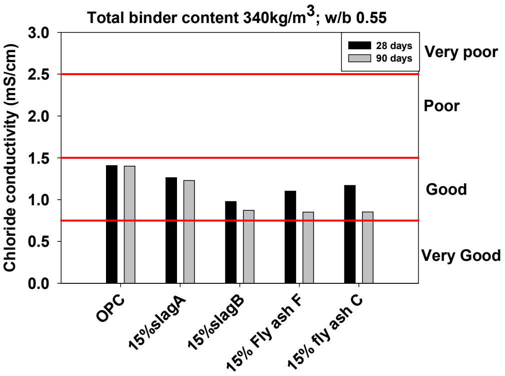

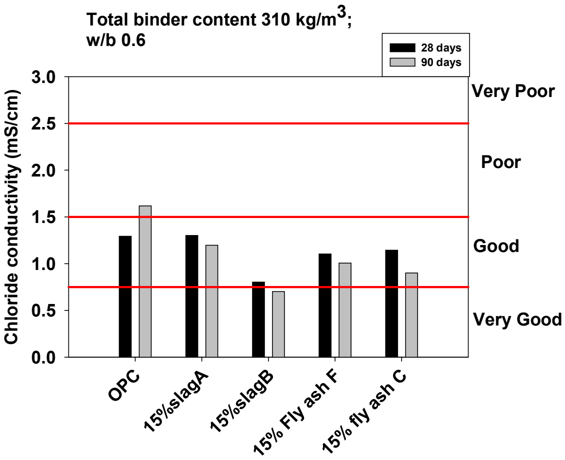

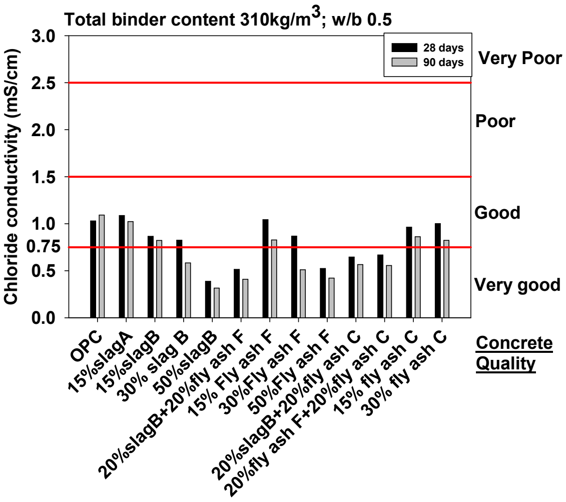

D5 – Sorptivity Index

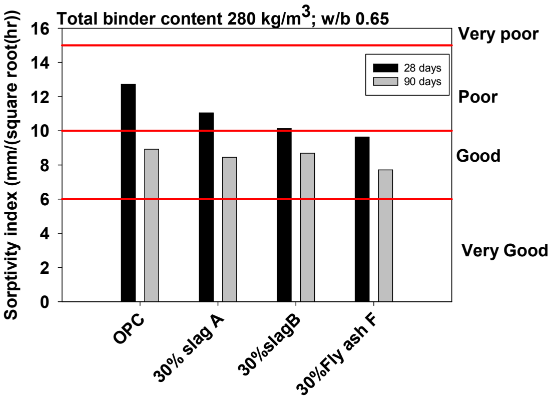

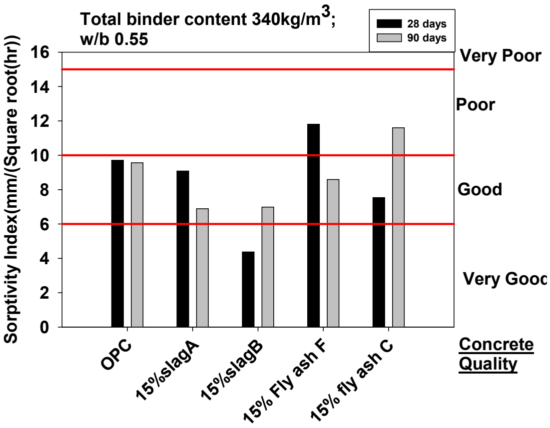

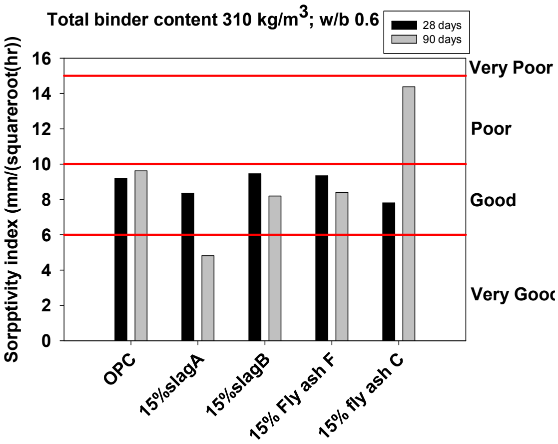

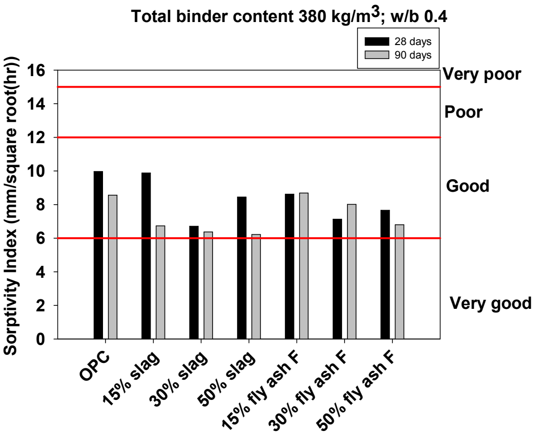

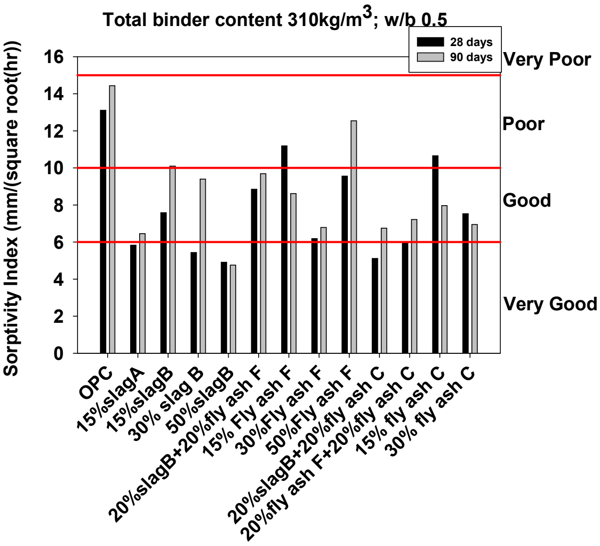

D6 – Oxygen Permeability Index

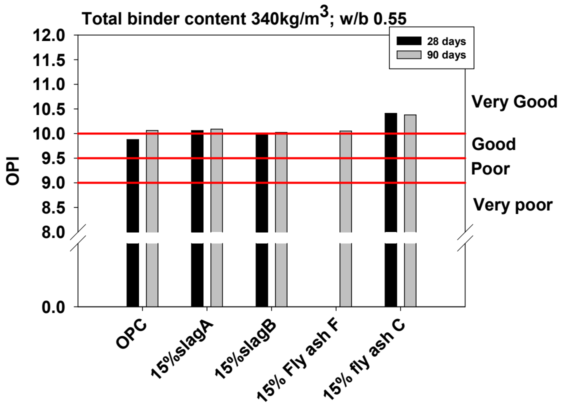

Total binder content 340kg/m^3; w/b 0.55

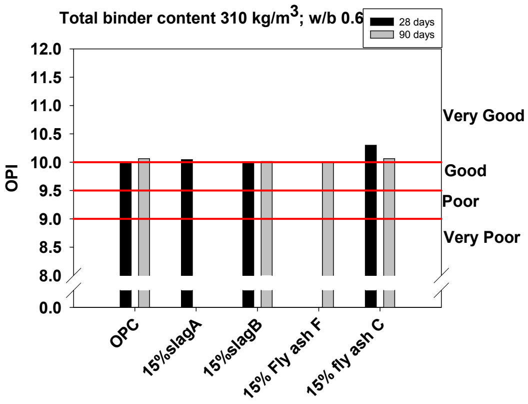

Total binder content 310 kg/m^3; w/b 0.6

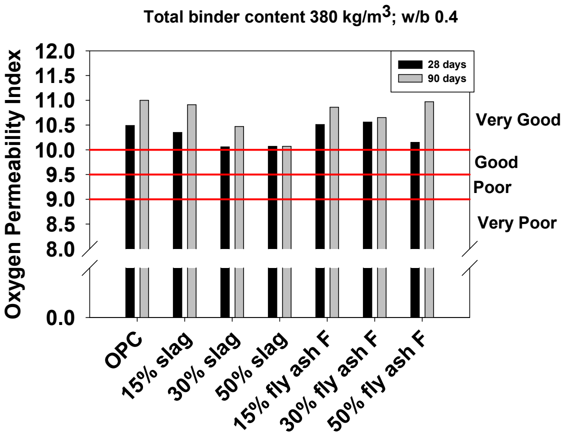

Total binder content 380 kg/m^3; w/b 0.4

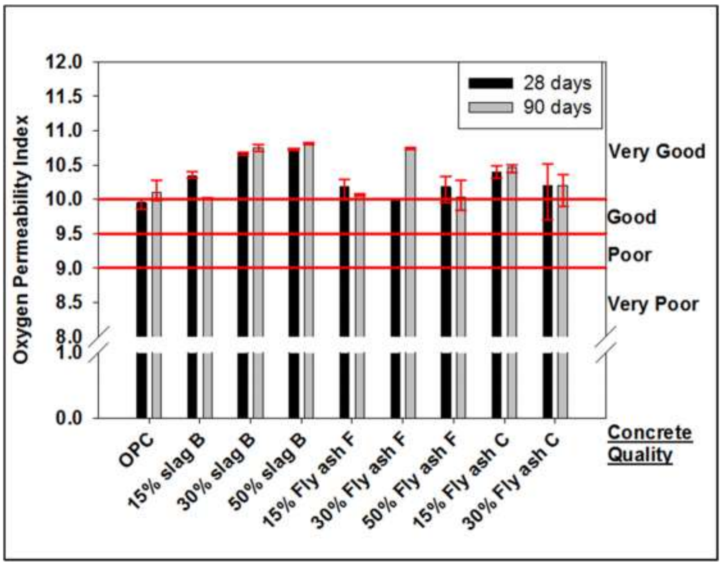

D7 – Depth of Carbonation

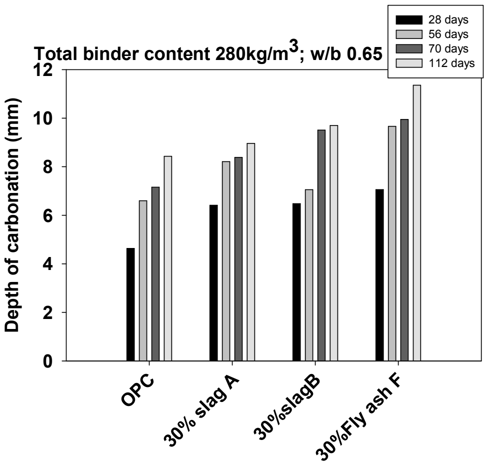

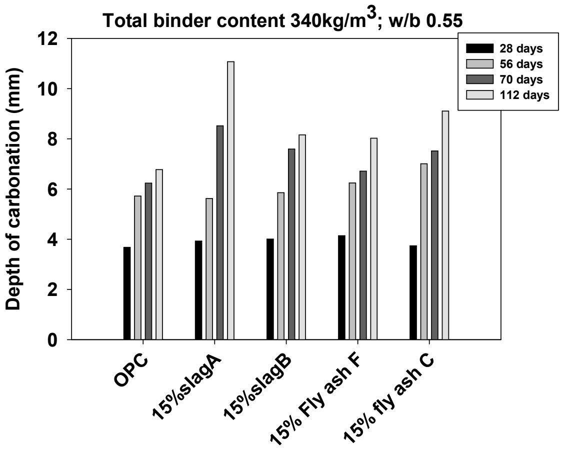

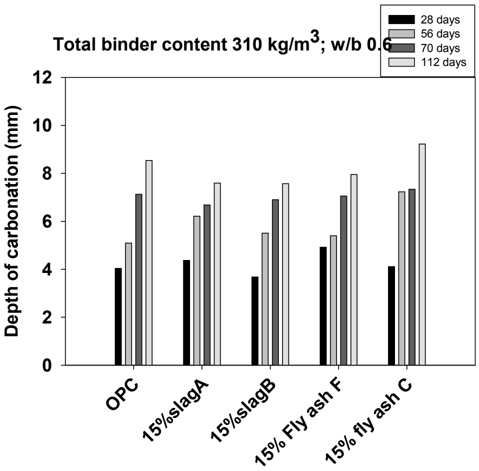

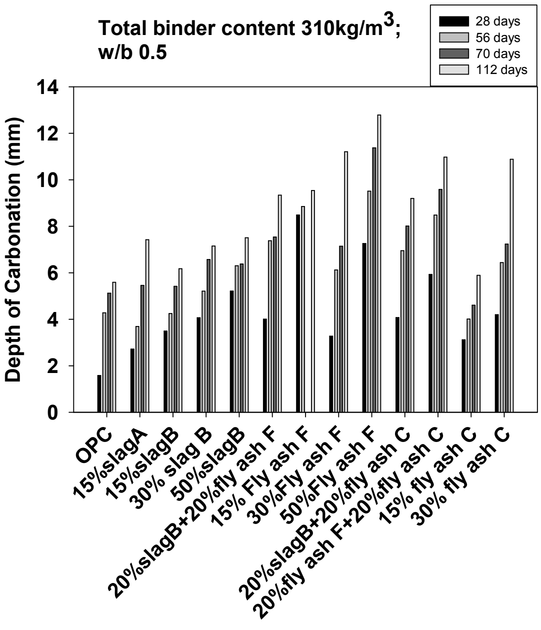

D8 – Carbonation Rate

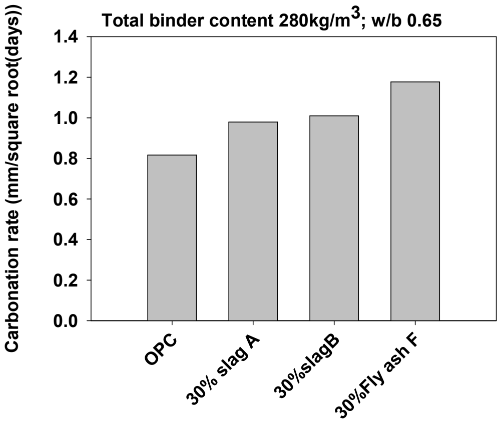

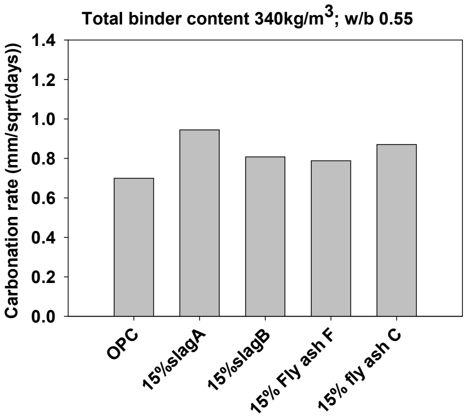

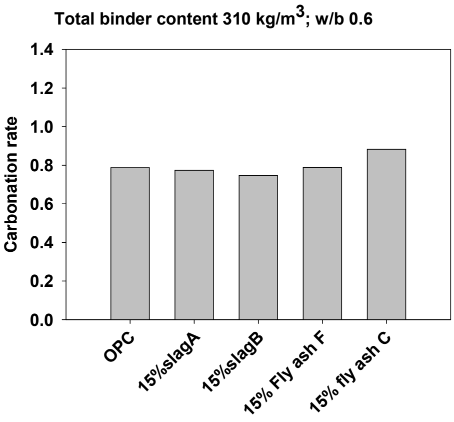

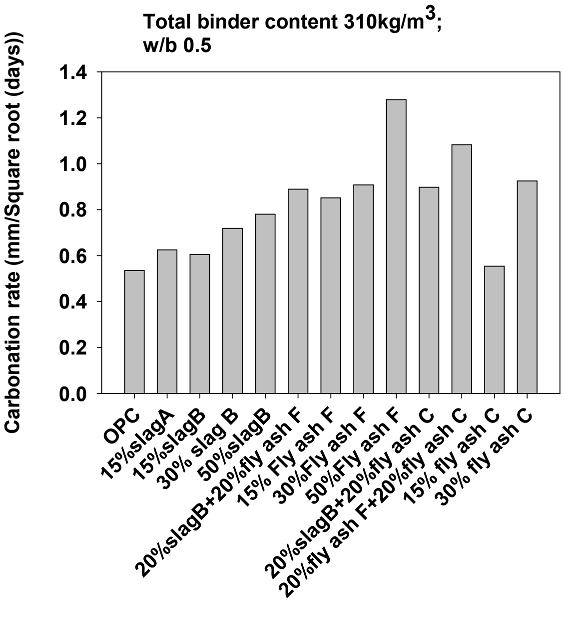

D9 - Compressive Strength

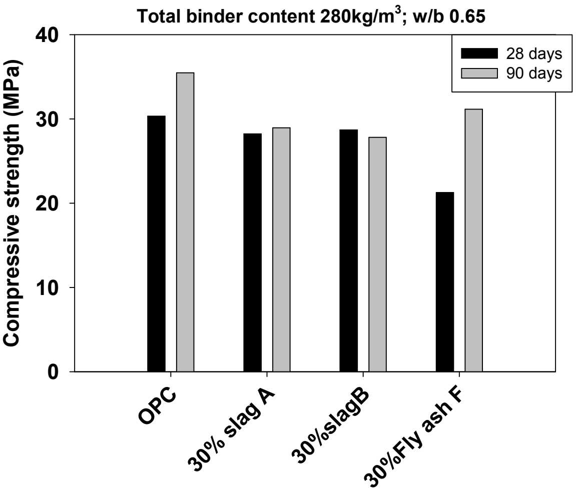
Total binder content 280kg/m^3; w/b 0.65

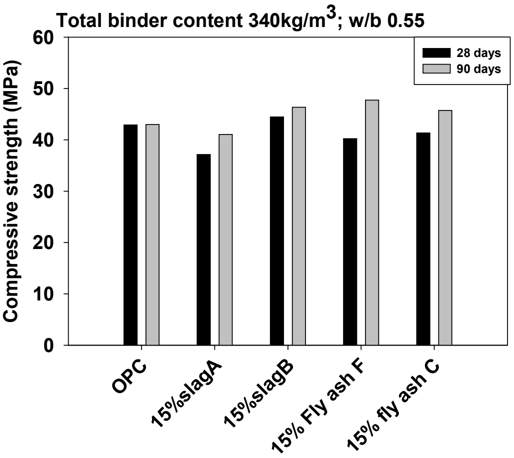
Total binder content 340kg/m^3; w/b 0.55

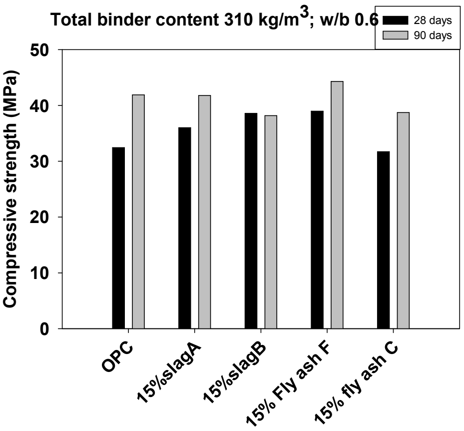
Total binder content 310 kg/m^3; w/b 0.6

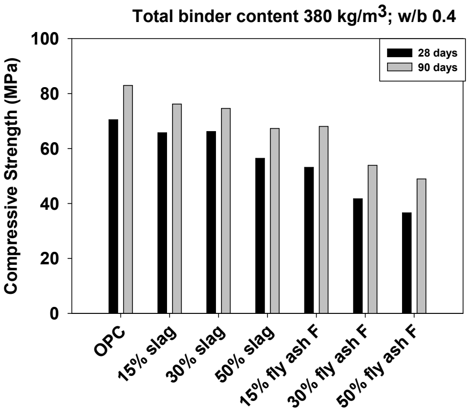
Total binder content 380 kg/m^3; w/b 0.4

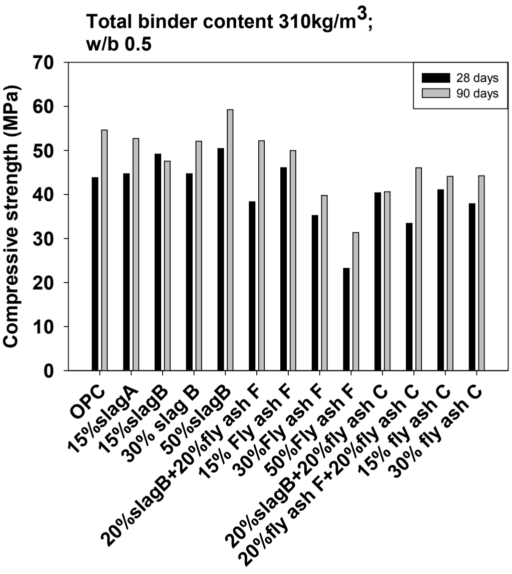
Total binder content 310kg/m^3; w/b 0.5

REFERENCES

AASHTO T 277 - 07 (2008) Rapid determination of the chloride permeability of concrete, American Association of States Highway and Transportation Officials, Washington, DC., USA.

AASHTO TP 64:2003 (2007) Standard Method of Test for Predicting Chloride Penetration of Hydraulic Cement Concrete by the Rapid Migration Procedure, American Association of States Highway and Transportation Officials, Washington, D. C., U.S.A.

Abbas, A., M. Carcasses and J.P. Olivier (1999) Gas permeability of concrete in addition to the compressive strength of concrete, *Materials and Structures*, **22**, 3-8.

Abbas, A., M. Carcasses and J.P. Olivier (2000) The importance of gas permeability in addition to the compressive strength of concrete, *Magazine of concrete research*, **52**, 1-6.

ACI 201.2R (2008) Guide to durable concrete, Reported by ACI Committee 201, American Concrete Institute, Farmington Hills, USA.

ACI 222R (2001) , Protection of metals in concrete against corrosion, Reported by ACI Committee 222, American Concrete Institute, Farmington Hills, USA.

ACI ITG-8R (2010) Report on performance-based requirements for concrete, ACI Innovation Task Group 8, American Concrete Institute, Farmington Hills, USA.

Aitcin, P. (2000) Cements of yesterday and today Concrete of tomorrow, *Cement and Concrete research*, **30**, 1349-1359.

Al-Amoudi O.S.B., W. A. Al-Kutti, A. Shamsad, and M. Maslehuddin (2009) Correlation between compressive strength and certain durability indices of plain and blended cement concretes, *Cement and Concrete Composites*, **31**, 672-676.

Aldea, C. M., F. Young, K. Wang, and S. P. Shah (2000) Effects of Curing Conditions on Properties of Concrete Using Slag Replacement, *Cement and Concrete Research*, **30**, 465-472.

Alexander, M. G. and J.R. Mackechnie (2002) A pragmatic prediction model for chloride ingress into concrete, Proceedings of *the Third International RILEM workshop on Testing and Modelling the Chloride Ingress into Concrete*, Madrid, September, 65-76.

Alexander, M. G., Y. Ballim and K. Stanish (2008) A framework for use of durability indexes in performance based design and specifications for reinforced concrete structures, *Materials and Structures*, **41**, 921-936.

Alexander, M., K. Stanish, and Y. Ballim, A two-level approach to performance-based durability specifications for corrosion prevention, pp. 281 – 291, *In*: Kovler, K. (eds.), ConcreteLife'06 - International RILEM-JCI Seminar on Concrete Durability and Service Life Planning: Curing, Crack Control, Performance in Harsh Environments, RILEM Publications, 2006

Alexander, M.G., M. Santhanam, and Y. Ballim (2011) Durability design and specification for concrete structures – the way forward, *International Journal of Advanced Engineering, Science and Applied Maths*, **2 (3)**, 95 – 105.

Alexander, M.G., Y. Ballim, and J.R. Mackechnie (1999) Guide to the use of durability indexes for achieving durability in concrete structures. Achieving durable and economic concrete construction in the South African context, Research Monograph, **2**, 5-11.

Alexander, M.G., Y. Ballim, and K. Stanish (2008) A framework for use of durability indexes in performance-based design and specifications for reinforced concrete structures, *Materials and Structures*, **41**, 921-936.

Alexander, M.G., Y. Ballim, and M. Santhanam (2005) Performance specifications for concrete using the durability index approach, *The Indian Concrete Journal*, 41-52.

Ali Akbar Ramezanianpour, A.P., M. Mahdikhani and F. Moodi (2011) Practical evaluation of relationship between concrete resistivity, water penetration, rapid chloride penetration and compressive strength, *Construction and Building Materials,* **25**, 2472-2479.

Alonso, C. and C. Andrade, Initiation and propagation of corrosion in concretes containing fly-ashes *In*: **Ferreira, R. M., J. Gulikers, and C. Andrade** (eds.) *International RILEM Workshop on Integral Service Life Modelling of Concrete Structures*, RILEM Publications SARL, 2013.

Alonso, C., M. Castellote and C. Andrade (2002) Chloride threshold dependence of pitting potential of reinforcements, *Electrochimica Acta*, **47**, 3469–3481.

Andrade C., M. Castellote, and C.L. Page (2002) Are service life models appropriate for use in design of reinforced concrete structures for exposure to chloride salts?, Proceedings of *the Third International RILEM workshop on Testing and Modelling the Chloride Ingress into Concrete*, Madrid, September, 65-76.

Andrade, C. (1993) Calculation of chloride diffusion coefficients in concrete from ionic measurements, *Cement and Concrete Research*, **23**, 724-742.

Andrade, C. and C. Alonso (1996) Corrosion rate monitoring in the laboratory and on-site, *Construction and Building Materials*, **10 (5)**, 315-328.

Andrade, C. and R. Bujak (2013) Effects of mineral additions to Portland cement on reinforcement corrosion, *Cement and Concrete Research*, **53**, 59 – 67.

Andrade, C., Alonso, C. , Gulikers, J. , Polder, R. , Cigna, R., Vennesland, O., Salta, M., Raharinaivo, A., and Elsener, B (2004) Test methods for on-site corrosion rate measurement of steel reinforcement in concrete by means of the polarization resistance method, RILEM TC 154-EMC Electrochemical techniques for measuring metallic corrosion, *Materials and Structures*, **37**, 623-643.

Andrade, C., C. Gonzalez – Gasca, and R. Torrent (2000) The suitability of 'TPT' to measure the air permeability of concrete, 5th CANMET/ACI International Conference on durability of concrete, Barcelona, June

Andrade, C., J. L. Sagrera, I. Martinez, M. Garcia and P. Zuloaga (2003) Monitoring of Concrete Permeability, Carbonation and Corrosion Rates in the Concrete of the Containers of El Cabril (Spain) Disposal, Transactions of the *17th International Conference on Structural Mechanics in Reactor Technology (SMiRT 17)*, Prague.

Andrade, C., M. Castellote, C. Alonso, and C. González (1999) Relation between colourimetric chloride penetration depth and charge passed in migration tests of the type of standard ASTM C1202-91, *Cement and Concrete Research*, **29**, 417-421.

Andrade, C., M. Prieto, P. Tanner, F. Tavares, and R. d'Andrea (2013) Testing and modelling chloride penetration into concrete,*Construction and Building Materials,* **39**, 9- 18.

Andrade, C., R. Polder and M. Basheer, Non-destructive methods to measure ion migration pp. 91 - 112 *In*: **Torrent, R., and L. F. Luco**, Non-Destructive Evaluation of the Penetrability and Thickness of the Concrete Cover - State-of-the-Art Report of RILEM Technical Committee 189-NEC, RILEM publications, 2007

Angst, U., B. Elsener, C.K. Larsen, and Ø. Vennesland (2009) Critical chloride content in reinforced concrete — A review, *Cement and Concrete Research*, **39,** 1122-1138.

Antoni, M. (2013) Investigation of cement substitution by blends of calcined clays and limestone, Ph. D. Thesis École Polytechnique Fédérale De Lausanne, Suisse.

ASTM C1152 (2013) Standard test method for acid soluble chlorides in mortar and concrete, Annual book of ASTM standards, West Conshohocken, PA, USA.

ASTM C1202 (2010) Standard test method for electrical indication of concrete's ability to resist chloride penetration, Annual book of ASTM standards, West Conshohocken, PA, USA.

ASTM C1218 (1999) Standard test method for water-soluble chlorides in mortar and concrete, Annual book of ASTM standards, West Conshohocken, PA, USA.

ASTM C125 (2003) Standard terminology relating to concrete and concrete aggregates, Annual book of ASTM standards, West Conshohocken, PA, USA.

ASTM C138 (2001) Standard test method for density (unit weight), yield, and air content (gravimetric) of concrete, Annual book of ASTM standards, West Conshohocken, PA, USA.

ASTM C143 (2000) Standard test method for slump of hydraulic-cement concrete, Annual book of ASTM standards, West Conshohocken, PA, USA.

ASTM C1556 (2003) Standard test method for determining the apparent chloride diffusion coefficient of cementitious mixtures by bulk diffusion, Annual book of ASTM standards, West Conshohocken, PA, USA.

ASTM C1585 (2013) Standard test method for measurement of rate of absorption of water by hydraulic-cement concretes, Annual book of ASTM standards, West Conshohocken, PA, USA.

ASTM C204 (2011) Standard test methods for fineness of hydraulic cement by air permeability apparatus, American Society for Testing and Materials, West Conshohocken, PA, USA.

ASTM C231 (1997) Standard test method for air content of freshly mixed concrete by pressure method, Annual book of ASTM standards, West Conshohocken, PA, USA.

ASTM D 4643 (2008) Standard test method for determination of water (moisture) content of soil by microwave oven heating, American Society for Testing and Materials, West Conshohocken, PA, USA.

ASTM G 57 (2012) Standard test method for field measurement of soil resistivity using the Wenner Four-Electrode method, Annual book of ASTM standards, West Conshohocken, PA, USA.

Atis, C.D. (2003) Accelerated carbonation and testing of concretes made with fly ash, *Construction and Building Materials*, **17 (3)**, 147 - 152.

Baroghel-Bouney, V. (2004) Which tool kit for durability evaluation as regards chloride ingress into concrete? Part – II Development of a performance approach based on durability indicators and monitoring parameters, Proceedings of *the Third International RILEM workshop on Testing and Modelling the Chloride Ingress into Concrete,* Madrid, September, 65-76.

Baroghel-Bouny, V, K. Kinomura, M. Thiery, and S. Moscardelli (2011) Easy assessment of durability indicators for service life prediction or quality control of concretes with high volumes of supplementary cementitious materials, *Cement and Concrete Composites*, **33**,832-847.

Baroghel-Bouny, V., T.Q. Nguyen, and P. Dangla (2009) Assessment and prediction of RC structure service life by means of durability indicators and physical/chemical models, *Cement and Concrete Composites*, **31**, 522-534.

Baroghel-Bouny, V., T.Q. Nguyen, M. Thiery, P. Dangla, and P. Belin (2006) Evaluation and prediction of reinforced concrete durability by means of durability indicators. Part II: multi-level predictive modelling, pp. 270 – 280. *In*: Kovler, K. (eds.), ConcreteLife'06 - International RILEM-JCI Seminar on Concrete Durability and Service Life Planning: Curing, Crack Control, Performance in Harsh Environments, RILEM Publications

Basheer, L., J. Kropp, and D. J. Cleland (2001) Assessment of the durability of concrete from its permeation properties: a review, *Construction and Building Materials*, **15**, 93-103.

Basheer, L., P.A.M. Basheer, and A.E. Long (2005) Influence of coarse aggregate on the permeation, durability and the microstructure characteristics of ordinary Portland cement concrete, *Construction and Building Materials*, **19**, 682-690.

Basheer, P. A. M. *Permeation analysis.* pp. 658 -737 *In* **V. S. Ramachandran, and J. J. Beaudoin** (eds.) Handbook of analytical techniques in concrete science and technology Principles, Techniques, and Applications, Noyes Publications, Park Ridge, New Jersey, USA, .2001

Basheer, P. A. M., S.E. Chidiac, and A.E. Long (1996) Predictive models for deterioration of concrete structures, *Construction and Building Materials*, **10**, 27-37.

Beaudoin, J.J., V.S. Ramachandran and R. F. Feldman (1990) Interaction of chloride and C-S-H, *Cement and Concrete Research*, **20**, 875 -883.

Bertos, M.F., S.J.R. Simons, C.D. Hills, and P.J. Carey (2004) A review of accelerated carbonation technology in the treatment of cement-based materials and sequestration of CO_2, *Journal of hazardous materials,* B112, 193 -205.

Beushausen, M. G. (2008) The South African durability index tests in an international comparison, *Journal of the South African Methods for Concrete*, **50**, 25-31.

Bickley, J., R. D. Hooton, and K.C. Hover (2006) Report of Preparation of a performance based specification for cast-in-place concrete. RMC research foundation (http://www.rmc-foundation.org/images/Phase%20I%20Report %20Final%20January%202006.pdf last accessed on 15/05/2015)

Bijen, J. (1996) Benefits of slag and fly ash, *Construction and Building Materials*, 10, 309 -314.

Bilodeau, A., and V.M. Malhotra (2000) High-volume fly ash system: Concrete solution for sustainable development, *ACI Material Journal*, **97**, 41-48.

Bouikni, A., R.N. Swamy, and A. Bali (2009) Durability properties of concrete containing 50% and 65% slag, *Construction and Building Materials*, **23**, 2836-2845.

Brown, P. W., and Badger, S. (2000) The distributions of bound sulfates and chlorides in concrete subjected to mixed NaCl, $MgSO_4$, Na_2SO_4 attack, *Cement and Concrete Research*, 1535–1542.

BS 6349 -1: 2000 Maritime structures – Part 1: Code of practice for general criteria, British Standards, London.

BS 8500 – 1:2006, Concrete – Complementary British Standard to BS EN 206 -1- Part 1: Method of specifying and guidance for the specifier, British Standards, London.

Buenfeld, N.R., M-T. Shurafa-Daoudi, and I.M. M^{c}Loughlin (1995) Chloride transport due to wick action in concrete, *1st RILEM workshop on Chloride Penetration into Concrete*, St. Rémy lès Chevreuse, France, October, 315-324.

Burden, D.(2006) The durability of concrete containing high levels of fly ash, Portland cement association, Research and development information, PCD R&D Serial No. 2989.

Castellote, M., and C. Andrade (2008) Modelling the carbonation of cementitious matrixes by means of the unreacted-core model, UR-CORE, *Cement and Concrete Research,* **38**, 1374-1384.

Castellote, M., L. Fernandez, C. Andrade, and C. Alonso (2009) Chemical changes and phase analysis of OPC pastes carbonated at different CO2 concentrations, *Materials and Structures*, **42**, 515-525.

Cheewaket, T., C. Jaturapitakkul and W. Chalee (2010) Long term performance of chloride binding capacity in fly ash concrete in a marine environment, *Construction and Building Materials*, **24**, 1352-1357.

Chen, J.J., J.J. Thomas, H.W.F. Taylor, and H.M. Jennings (2004) Solubility and structure of calcium silicate hydrate, *Cement and Concrete Research*, **34**, 1499 - 521.

Cheng, A., R. Huang, J. K. Wu, and C. H. Chen (2005) Influence of GGBS on durability and corrosion behaviour of reinforced concrete, *Materials Chemistry and Physics*, **93**, 404-411.

Chindaprasirt, P., C. Chotithanorm, H. T. Cao, and V. Sirivivatnanon (2007) Influence of fly ash fineness on the chloride penetration of concrete, *Construction and Building Materials*, **21**, 356-361.

Curtil, L., J. Gielly, and M. Murat (1993) The polarization microscope: A tool of interest for investigation on concrete: application to carbonation, *Cement and Concrete Research*, **23**, 329-334.

Deschner, F., F. Winnefeld, B. Lothenbach, S. Seufert, P. Schwesig, S. Dittrich, F. Goetz-Neunhoeffer, and J. Neubauer (2012) Hydration of Portland cement with high replacement by siliceous fly ash, *Cement and Concrete Research*, **42,** 1389-1400.

Dhanya, B.S. and M. Santhanam (2013) Performance specification for concrete construction in India: Are we ready?, *The Indian Concrete Journal,* **87**, 36-43.

Dhir, R. K., M.A.K. El-Mohr, and T.D. Dyer (1996) Chloride binding in GGBS concrete, *Cement and Concrete Research*, **26**, 1767-1773.

Dhir, R. K., M.A.K. El-Mohr, and T.D. Dyer (1997) Developing chloride resisting concrete using PFA, *Cement and Concrete Research,* **27 (11)**, 1633-1639.

DIN 1048 part 5 (1991) Testing of concrete, Testing of hardened concrete (Specimens prepared in mould), German standards.

du Preez A. A. and M. G. Alexander (2004) A site study of durability indexes for concrete in marine conditions, *Materials and Structures,* **37**,146-154.

Durability Index Testing Procedure Manual (2009), Concrete durability index testing, South Africa.

DuraCrete Final Technical Report (2000) General guidelines for durability design and redesign, The EU - Brite EURam III (Project BE95-1347), Probabilistic performance based durability design of concrete.

Ebensperger, L. and R. Torrent (2010) Concrete air permeability in situ test: status quo *Revista Ingeniería de Construcción*, **25 (3)** www.ing.puc.cl/ric

EN 206-1:2000, Concrete - Part 1: Specification, performance, production and conformity, (inclusive of amendments A1:2004 and A2:2005) European Standard, European committee for standardization, Rue De Stassart, 36 B-1050 Brussels.

Feldman, R. F., G. W. Chan, R. J. Brousseau, and P. J. Tumidajski (1994) Investigation of the rapid chloride permeability test, *ACI Materials Journal*, **91**, 246 - 255

Fraj, A., S. Bonnet, and A. Khelidj (2012) New approach for coupled chloride/moisture transport in non-saturated concrete with and without slag, *Construction and Building Materials*, **35**, 761-771.

Galan, I. and C. Andrade (2009) Comparison of Carbonation Models., *3rd International RILEM Ph.D. student workshop on modelling the durability of reinforced concrete,* University of Minho, Portugal.

Gonen, T. and S. Yazicioglu (2007) The influence of compaction pores on sorptivity and carbonation of concrete, *Construction and Building Materials*, **21**, 1040-1045.

Gopalan, M. K. (1996) Sorptivity of fly ash concretes, *Cement and Concrete Research*, **26**, 1189-1197.

Gulikers, J. Practical implications of performance specifications for durability design of reinforced concrete structure, pp. 341-350. *In* F. Dehn, and H. Beushausen (eds.) Proceedings of the *Workshop on Performance-based specifications of concrete*, Leipzig, Germany, 2011.

Gummerson, R. J., C. Hall and W. D. Hoff (1980) Water movement in porous building materials--lI. Hydraulic suction and sorptivity of brick and other masonry materials, *Building and Environment*, **15**, 101-108.

Gummerson, R. J., C. Hall, and W. D. Hoff (1981) Water movement in porous building materials--III. A sorptivity test procedure for chemical injection damp-proofing, *Building and Environment*, **16,** 193-199.

Gutteridge, W. A., and J. A. Dalziel (1990) Filler cement: The effect of secondary component on the hydration of Portland cement Part 2: Fine hydraulic binders, *Cement and Concrete Research*, **20**, 853 - 861.

Hall, C. (1977) Water movements in porous building materials - 1 unsaturated flow theory and its applications, *Building and Environment*, **12**, 117-125.

Hall, C. (1981) Water movement in porous building materials—IV The initial surface absorption and the sorptivity, *Building and Environment,* **16**, 201-207.

Hall, C. (1989) Water sorptivity of mortars and concrete – a review, *Magazine of Concrete Research*, **41**, 147, 51 – 61.

Hall, C., and A. N. Kalimeris (1982) Water movement in porous building materials--V. Absorption and shedding of rain by building surfaces, *Building and Environment,* **17**, 257-262.

Hall, C., and Kam-Ming Tse, T. (1986) Water movement in porous building materials – VII. The sorptivity of mortars, *Building and Environment*, **21 (2)**, 113-118.

Hall, C., W.D. Hoff, S.C. Taylor, M.A. Wilson , Yoon, Beom-Gi, H.W. Reinhardt, M. Sosoro, P. Meredith and A.M. Donald (1995) Water anomaly in capillary liquid absorption by cement-based materials, *Journal of Material Science Letters*, **14**, 1178-1181.

Hedegaard, S. E., and T. C. Hansen (1992) Water permeability of fly ash concretes, *Materials and Structures*, **25**, 381 – 387.

Higgins R.A. (1994), Properties of Engineering Materials, Industrial Press.

High performance concrete structural designers' guide (2005) FHWA Publication No. FHWA-RCBAL-05-007, Federal Highway Administration, U.S. Department of Transportation.

http://ciks.cbt.nist.gov/poresolncalc.html access verified April 2015 (Estimation of Pore Solution Conductivity)

http://people.hofstra.edu/j_b_bennington/121notes/pdfs/Porosity_Perm_Darcy.pd , access verified May 2015 (Article on Porosity, permeability and Darcy's law)

http://www.cement.org/for-concrete-books-learning/concrete-technology/durability/corrosion-of-embedded-materials, access verified May 2015 (site hosted by Portland Cement Association,)

Imamoto, K. and A. Tanaka *Evaluation of carbonation progress of existing concrete structure based on air permeability of concrete cover — a case study in Japan* pp. 309-314 *In* M.G. Alexander, H. D. Beushausen, F. Dehn and P. Moyo (eds), *Concrete Repair, Rehabiilitation and Retrofitting II*, Taylor & Francis Group, London, 2012.

IS:1727-1967 (2004) Indian Standard methods of test for pozzolanic materials, Bureau of Indian Standards, New Delhi, India (reaffirmed 2004).

IS:456-2000 (2000) Indian Standard for Plain and Reinforced Concrete –Code of Practice, Bureau of Indian Standards, New Delhi.

IS:516-1959 (2004) Indian standard methods of tests for strength of concrete, Bureau of Indian Standards, New Delhi. (reaffirmed 2004).

Jia, Y., B. Aruhan, and P. Yan (2012) Natural and accelerated carbonation of concrete containing fly ash and GGBS after different initial curing period, *Magazine of Concrete Research*, **64**, 143-150.

Julio-Betancourt, G. A., and R. D. Hooton (2004) Study of the Joule effect on rapid chloride permeability values and evaluation of related electrical properties of concretes, *Cement and Concrete Research*, **34,** 1007–1015.

Kropp J. and M. Alexander, Transport mechanisms and reference tests, *In*: **Torrent, R., and L. F. Luco**, Non-Destructive Evaluation of the Penetrability and Thickness of the Concrete Cover - State-of-the-Art Report of RILEM Technical Committee 189-NEC, RILEM publications, 2007

Kropp, J. (1999) Concrete durability – an approach towards performance testing, *Materials and Structures*, **32**, 163 – 173.

Kulkarni, V.R. (2009) Exposure classes for designing durable concrete, *The Indian Concrete Journal*, 23-43.

Lagerblad, B. (2005) Carbon dioxide uptake during concrete life cycle – State of the art, Swedish Cement and Concrete Research Institute, CBI , Nordic Innovation Centre, Norway.

Lamond, J. F. and J. H. Pielert, Significance of tests and properties of concrete and concrete making materials., ASTM International, West Conshohocken, PA, USA, 2006.

Lane, D. S., R. J. Detwiler, and D. Hooton (2010) Testing Transport Properties in Concrete: Assessing key indicators of durability, *Concrete International*, 33-40.

LIFE 365 (2012) Service life prediction model and computer program for predicting the service life and life-cycle cost of reinforced concrete exposed to chlorides,
URL: http://www.life-365.org/; Last accessed on 09/07/2014.

Lo, Y., and H.M. Lee (2002) Curing effects on carbonation of concrete using a phenolphthalein indicator and Fourier-transform infrared spectroscopy, *Building and Environment,* **37,** 507-514.

Lothenbach, B., K. Scrivener, and R.D. Hooton (2011) Supplementary cementitious materials, *Cement and Concrete Research*, **41**, 1244-1256.

Lu, S., E. N. Lardis, and D. T. Keane (2006) X-ray microtomographic studies of pore structure and permeability in portland cement concrete, *Materials and Structures*, **39**, 611-620.

Luo, R., Y. Cai, C. Wang, and X. Huang (2003) Study of chloride binding and diffusion in GGBS concrete, *Cement and Concrete Research*, 33, 1-7.

Luping, T. and H. Sørensen, Evaluation of the rapid test methods for measuring the chloride diffusion coefficients of concrete, NORDTEST Project No. 1388-98, Swedish National Testing and Research Institute, SP Report 1998:42, 1998.

Mackechnie J. R., Predictions of reinforced concrete durability in the marine environment, Research monograph No. 1, Departments of Civil Engineering, University of Cape Town and University of Witwatersrand, South Africa, 2001.

Mackechnie, J. R. and M. G. Alexander (2002) Durability predictions using early age durability index testing, Proceedings of the *9th Durability and Building Materials Conference*, Australian Corrosion Association, Brisbane.

Malhotra, V. M., M-H Zhang, P. H. Read, and J. Ryell (2000) Long-Term Mechanical Properties and Durability Characteristics of High-Strength / High-Performance Concrete Incorporating Supplementary Cementing Materials under Outdoor Exposure Conditions, *ACI Materials Journal*, **97 (5),** 518 -525.

Marriaga, J. M. R. L. (2009) Transport properties and multi-species modelling of slag based concretes, Ph.D. Thesis, Coventry University, UK.

Marsh, B. K. and R. L. Day (1988) Pozzolanic and cementitious reactions of fly ash in blended cement pastes, *Cement and concrete research*, **18**, 301 – 310.

Martys N. S.(1995) Survey of concrete transport properties and their measurements, U.S. Department of Commerce, Technology administration, National Institute of Standards and Technology, Galthersburg, MD.

McGrath, P. F. and R. D. Hooton (1999) Re-evaluation of the AASHTO T 259 90-day salt ponding test, *Cement and Concrete Research*, **29**, 1239-1248.

McPolin, D. O., P. A. M. Basheer, A. E. Long, K. T. V. Grattan, and T. Sun (2007) New test method to obtain pH profiles due to carbonation of concretes containing supplementary cementitious materials, *Journal of Materials In Civil Engineering ASCE*, **19 (11)**, 936-946.

Mehta, P. K. and P. J. M. Monteiro, *Concrete Microstructure, properties, and materials*, The McGraw-Hill Companies, USA., 2006.

Mehta, P. K., and R. W. Burrows (2001) Building durable structures in the 21st century, *The Indian Concrete Journal*, 437-443.

Morandeau, A., M. Thiéry, and P. Dangla (2014) Investigation of the carbonation mechanism of CH and C-S-H in terms of kinetics, microstructure changes and moisture properties, *Cement and Concrete Research*, **56**, 153-170.

Nanga, G. W. (2011) Practical implementation of the durability index-based performance approach, M. S. Thesis, University of Cape Town, South Africa.

NT BUILD 492 (1999) Concrete,Mortar and Cement-based repair materials: Chloride migration coefficient from non-steady-state migration experiments, Nordic Council of ministers, Finland.

Odriozola, M. A. B., and P. A.Gutierrez (2008) Comparative study of different test methods for reinforced concrete durability assessment in marine environment, *Materials and Structures*, **41**, 527–541.

Oh, B. H., S.Y. Jang, and Y.S. Shin (2003) Experimental investigation of the threshold chloride concentration for corrosion initiation in reinforced concrete structures, *Magazine of Concrete Research*, **55**, 117–124.

Osborne, G. L (1999) Durability of Portland blast-furnace slag cement concrete, *Cement and Concrete Composites*, **21**, 11-21.

Oslakovic, I. S., D. Bjegovic, and D. Mikulic (2010) Evaluation of service life design models on concrete structures exposed to marine environment, *Materials and Structures*, **43**, 1397–1412.

Papadakis V.G., C.G. Vayenas and M.N. Fardis (1992) Hydration and carbonation of pozzolanic cements, *ACI Materials Journal*, **89**, 119–130.

Papadakis V.G., C. G. Vayenas, and M. N. Fardis (1991a) Experimental investigation and mathematical modeling of the concrete carbonation problem, *Chemical Engineering Science*, **46**, 1333–1338.

Papadakis V. G., C. G. Vayenas, and M. N. Fardis (1991b) Physical and chemical characteristics affecting the durability of concrete, *ACI Materials Journal*, **8 (2)**, 186–196.

Papadakis, V. G. (2000) Effect of supplementary cementing materials on concrete resistance against carbonation and chloride ingress, *Cement and Concrete Research*, **30**, 291-299.

Parrot (1994) Design for avoiding damage due to carbonation induced corrosion**,** *ACI SP 145-15***,** American Concrete Institute, 283-298.

Permea-TORR User Manual v3.0 (2010), Measures the Air-Permeability of the Cover Concrete and other Porous Materials Swiss Standard Method SIA 262/1-E, Materials Advanced Services Ltd., 1425 Buenos Aires, Argentina.

Pfeifer, D. W., D. B. McDonald, and P. D. Krauss (1994) The rapid chloride permeability test and its correlation to the 90 – day chloride ponding tests, *PCI Journal*, **39 (1)**, 38 – 47.

Polder, R. (2000) Test methods for on-site measurement of resistivity of concrete RILEM TC 154-EMC: Electrochemical techniques for measuring metallic corrosion, *Materials and Structures*, **33**, 603 – 611.

Poulsen, E. and L. Mejlbro *Diffusion of chloride in concrete Theory and Application*, Taylor & Francis, Milton Park, Oxon, UK, 2006

Rabehi, M., B. Mezghiche, and S. Guettala (2013) Correlation between initial absorption of the cover concrete, the compressive strength and carbonation depth, *Construction and Building Materials*, **45**, 123-129.

Richardson, M. G. *Fundamentals of durable reinforced concrete*, Spon Press, London, 2002.

RILEM TC 116-PCD (1999) Recommendations of TC 116-PCD: Permeability of Concrete as a Criterion of its Durability, Tests for gas permeability of concrete. A.

Preconditioning of concrete test permeability specimens for the measurement of gas and capillary absorption of water, B. Measurement of the gas permeability of concrete by the RILEM - CEMBUREAU method, C. Determination of the capillary absorption of water of hardened concrete, *Materials and Structures*, **32**, 174-179.

RILEM TC 154 - EMC (2004) Recommendations of TC 154-EMC: Electrochemical Techniques for Measuring Metallic Corrosion, Test methods for on-site corrosion rate measurement of steel reinforcement in concrete by means of the polarization resistance method, *Materials and Structures*, **37**, 623-643.

RILEM TC 189 - NEC- (2007) Non-destructive evaluation of the penetrability and thickness of the concrete cover, State of the art report prepared by RILEM technical committee TC189 - NEC, **Torrent, R., and L. F. Luco** (Eds.), RILEM Publications.

RILEM TC 189 – NEC, and M. Romer (2005) Recommendation of RILEM TC 189-NEC Non-destructive evaluation of the concrete cover: Comparative test-Part I: Comparative test of 'penetrability' methods, *Materials and Structures*, **38**, 895 – 906

RILEM TC 211 PAE (2013) Performance of cement-based materials in aggressive aqueous environments, State of the art report prepared by RILEM technical committee TC 211 - PAE, **Alexander, M., A. Bertron, N. De Belie** (Eds.), Springer.

RILEM TC 230-PSC report, Draft (2015) Performance-based specification and control of concrete durability, State of the art report prepared by RILEM technical committee TC 230 - PSC, , **H. Beushausen** (eds.), RILEM

RILEM TC 56 – MHM (1988)**,** CPC-18 Measurement of hardened concrete carbonation depth, *Materials and structures*, **21**, 453 – 455.

Russell, **H. G.,** Measuring chloride penetration resistance, concrete products, 2001.

Safiuddin, M. and N. Hearn (2005) Comparison of ASTM saturation techniques for measuring the permeable porosity of concrete, *Cement and Concrete Research*, **35**, 1008-1013.

Salvoldi, B. G. (2010) Modelling the carbonation of concrete using early age oxygen permeability index tests, Concrete materials and structural integrity research unit, Department of Civil Engineering, University of Cape Town, South Africa.

Sanjuán, M. A., C. Andrade, M. Cheyrezy (2003) Concrete carbonation tests in natural and accelerated conditions, *Advances in Cement Research*, **15**, 171-180.

Saraswathy, V., and H. W. Song (2006) Electrochemical studies on the corrosion performance of steel embedded in activated fly ash blended concrete, *Electrochimica Acta*, **51**, 4601-4611.

Saravanan, R., and M. Santhanam (2012) Environmental exposure classification for concrete construction A relook, *The Indian Concrete Journal*, **86**, 18-28.

Sauman, Z. (1971) Carbonation of porous concrete and its main binding components,*Cement and Concrete Research*, 645–662.

Scanlon, J. M and M. R. Sherman (1996) Fly ash concrete: An evaluation of chloride penetration testing methods, *Concrete International*, 57 -62.

Schiessl, P., and Lay, S. (2005). Influence of concrete composition. pp. 91-134 *In* **Böhni, H.** (Ed.), Corrosion in reinforced concrete structures, Cambridge, England: Woodhead.

Schmitt, G. (2009) Global needs for knowledge dissemination, research, and development in materials deterioration and corrosion control, The world corrosion organization. (http://www.corrosion.org/wco_media/whitepaper.pdf, last accessed May 2015)

Schubert (1987) Carbonation behaviour of mortars and concretes made with fly ash, ACI SP 100 – 99, American Concrete Institute, 1945 – 1962.

Sengul, O., and O. E. Gjorv (2008) Electrical resistivity measurements for quality control during concrete construction, *ACI Materials Journal*, **105**, 541 – 547.

Shi, X., N. Xie, K. Fortune, and J. Gong (2012) Durability of steel reinforced concrete in chloride environments: An overview, *Construction and Building Materials*, **30**, 125-138.

SIA 262/1 (2003) Norme Suisse: "Construction en béton – Spécifications complémentaires, Annexe E: Perméabilité à l'air dans les Structures, 30-31 (in German and French)

Stanish, K. D., R. D. Hooton, and M. D. A. Thomas (1997) Testing the chloride penetration resistance of concrete: A literature review, FHWA Contract DTFH61-97-R-00022 Prediction of chloride penetration in concrete.

Steinar, H. Personal communication , 2014

Streicher, P. E., and M. G. Alexander (1995), A chloride conduction test for concrete. *Cement and Concrete Research*, **25 (6)**, 1284-1294.

Sulapha, P., S. F. Wong, T. H. Wee, and S. Swaddiwudhipong (2003), Carbonation of concrete containing mineral admixtures, *Journal of Materials in Civil Engineering ASCE*, **15(2),**134-143.

Suryavanshi, A. K., J. D Scantleybury, and S. B. Lyon (1996) Mechanism of Friedel's salt formation in cements rich in tri-calcium aluminate, *Cement and Concrete Research*, **26(5)**, 717-727.

Swamy, R. N. (2003) Holistic design: Key to sustainability in concrete construction, *The Indian Concrete Journal*, **77 (9)**, 1291-1299.

Swamy, R. N. (2008) Sustainable concrete for the 21st century concept of strength through durability, Japan Society of Civil Engineers Concrete Committee Newsletter.
(http://www.jsce.or.jp/committee/concrete/e/newsletter/newsletter13/Paper1.pdf)

Tang, L. (2008) Engineering expression of the ClinConc model for prediction of free and total chloride ingress in submerged marine concrete, *Cement and Concrete Research*, **38**, 1092-1097.

Tang, L. and L-O. Nilsson (1992) Rapid determination of the chloride diffusivity in concrete by applying an electrical field, *ACI Materials Journal*, **89 (1)**, 49-53.

Tang, L. and L-O. Nilsson (1993) Chloride binding capacity and binding isotherms of OPC pastes and mortars, *Cement and Concrete Research*, **23**, 247 – 253.

The Concrete Society (1988) Permeability Testing of Site Concrete—A Review of Methods and Experience, *Report of a Concrete Society Working Party,* Concrete Society Technical Report No. 31, p. 95, London

Thomas M. D. A. (2013) *Supplementary Cementing Materials in concrete*, CRC Press, Francis & Taylor Group, Florida, USA, 2013.

Thomas M. D. A. (2011) The effect of supplementary cementing materials on alkali silica reaction: a review, Cement and Concrete Research, 41, 1224 – 1231

Thomas, M. (1996) Chloride threshold in marine concrete, *Cement and Concrete Research*, **26**, 513–519.

Thomas, M. D. A. and J. D. Matthews (1992) The permeability of fly ash concrete, *Materials and Structures*, **25**, 388 – 396.

Thomas, M. D. A., and B. Bamforth (1999) Modelling chloride diffusion in concrete Effect of fly ash and slag, *Cement and Concrete Research*, **29**, 487-495.

Thomas, M. D. A., J. D. Matthews and C. A. Haynes (2000), Carbonation of fly ash concrete, In Proceedings of *the 4th ACI/CANMET International conference on the durability of concrete*, **Malhotra, V. M**. (eds.) ACI SP 192-33, **1**, 539 – 556.

Thomas, M. D. A., R. D. Hooton, A. Scott, and H. Zibara (2012) The effect of supplementary cementitious materials on chloride binding in hardened cement paste, *Cement and Concrete Research*, **42**, 1-7.

Torgal, F. P., S. Miraldo, J. A. Labrincha, and J. D. Brito (2012) An overview on concrete carbonation in the context of eco-efficient construction : Evaluation , Use of SCMs and / or RAC, *Construction and Building Materials*, **36,** 141-150.

Torrent, R. and G. Frenzer (1995) A method for the rapid determination of the coefficient of permeability of the 'covercrete', International Symposium on Non-Destructive Testing in Civil Engineering Berlin, Germany, 985 – 992.

Torrent, R., and L. F. Luco (2007) Non-Destructive Evaluation of the Penetrability and Thickness of the Concrete Cover - State-of-the-Art Report of RILEM Technical Committee 189-NEC, RILEM publications.

Torrent, R. J. (1992) A two-chamber vacuum cell for measuring the coefficient of permeability to air of the concrete cover on site, *Materials and Structures*, **25**, 358 - 365.

Tuutti, K. (1982) Corrosion of steel in concrete, Ph. D. Thesis, Swedish Cement and Concrete Research Institute, ISSN 0346-6906, Royal Institute of Technology, Stockholm.

Visser, J. H. M., Personal Communication (2014)

Vivas, E., A. J. Boyd and H. R. Hamilton (2007) Permeability of concrete - Comparison of diffusion and conductivity methods, Florida Department of Transportation, Research Management Center, FL 32301-8064

Wang, X. , M. Nguyen, M.G. Stewart, M. Syme, and A. Leitch (2010) Analysis of climate change impacts on the deterioration of concrete infrastructure - Part 1: Mechanisms, practices, modelling and simulations - A review, , Published by CSIRO, Canberra. ISBN 97804310365 8

Wee, T. H., A. K. Suryavanshi, and S. S. Tin (1999) Influence of aggregate fraction in the mix on the reliability of the rapid chloride permeability test, *Cement and Concrete Composites*, **21**, 59-72.

Wee, T. H., A. K. Suryavanshi, and S. S. Tin (2001) Evaluation of rapid chloride permeability test (RCPT) Results for concrete containing mineral admixtures, *ACI Materials Journal*, 221-232.

Whiting, D (1981) Rapid determination of the chloride permeability of concrete, Report No. FHWA/RD-81/119, Federal Highway Administration, Washington, D.C.

Wowra, O. (2002) Effects of carbonation to microstructure and pore solution. *In*: Proceedings of the RILEM Workshop on Frost Resistance of Concrete, Essen, Germany, RILEM Publications, 61–68.

Yuan, Q., C. Shi, G. D. Schutter, K. Audenaert, and D. Deng (2009) Chloride binding of cement-based materials subjected to external chloride environment – A review, *Construction and Building Materials*, **23,** 1-13.

LIST OF PAPERS ON THE BASIS OF THIS THESIS

REFEREED JOURNALS

1. **B. S. Dhanya and Manu Santhanam** (2013) Performance specification for concrete construction in India: Are we ready?, *The Indian Concrete Journal*, **87 (9**), 36-43.
2. **Santhosh George Cheriyan, B. S. Dhanya, and Manu Santhanam (**2014), Durability indices for concretes with different dosages of mineral admixtures, *The Indian Concrete Journal*, **88 (3)**, 60-68.

PRESENTATIONS IN INTERNATIONAL CONFERENCES

1. **B. S. Dhanya, M. Santhanam, R. G. Pillai and R. Gettu** (2014) Evaluation of various electrical methods used to assess chloride transport in concrete", Proceedings of *The fourth fib congress (Improving performance of concrete structures)*, Mumbai.
2. **Gettu, R., R. G. Pillai, M. Santhanam, and B. S. Dhanya** (2013) Ways of improving the sustainability of concrete technology through the effective use of admixtures, *Creative Concrete Technologies for sustainable Future*, Korea Concrete Institute, December, 107 – 126.
3. **B. S. Dhanya and M. Santhanam** (2014), Use of combined durability parameters for different exposure conditions, Proceedings of the *RILEM International Workshop on performance-based specification and control of concrete durability*, Croatia, June, 101-108.
4. **B. S. Dhanya and M. Santhanam** (2014) Influence of mineral admixtures on the durability parameters of concrete", Proceedings of *the 10th fib international Ph. D. Symposium in Civil Engineering,* Canada, July, 131-136.
5. **B. S. Dhanya, M. Santhanam and B. N. B. Kumar** (2014) Durability performance of slag as a supplementary cementitious material", Second International conference on durability of concrete, ICDC – 2014, December 2014.

PRESENTATIONS IN NATIONAL CONFERENCES

1. **Manu Santhanam and B. S. Dhanya**, Durability and performance specifications, One Day National Colloquium on Concrete Construction for Coastal Conditions - Causes, Concerns & Challenges (7-Cs), Cochin, December, 2012

DOCTORAL COMMITTEE

CHAIR PERSON	Dr. A. Meher Prasad Professor and Head Department of Civil Engineering
GUIDE	Dr. Manu Santhanam Professor Department of Civil Engineering
MEMBERS	Dr. Ravindra Gettu Professor Department of Civil Engineering
	Dr. Radhakrishna G. Pillai Assistant Professor Department of Civil Engineering
	Dr. B. S. Murthy Professor Department of Metallurgical and Materials Engineering
	Dr. Krishnan Balasubramanian Professor Department of Mechanical Engineering

CURRICULUM VITAE

Name : Dhanya B. S.

Date of birth : 28 - 04 - 1981

Educational qualification

2002 : **Bachelor of Technology (B. Tech.)**

Institution : T.K.M College of Engineering, Kollam, Kerala

University : University of Kerala

Specialization : Civil Engineering

2004 : **Master of Technology (M. Tech.)**

Institution : T.K.M College of Engineering, Kollam, Kerala

University : University of Kerala

Specialization : Structural Engineering and Construction Management

2015 : **Doctor of Philosophy (Ph. D.)**

Institution : Indian Institute of Technology, Madras, Chennai, India

Specialization : Building Technology and Construction Management (Construction Materials and Concrete Technology)

Registration date : 18/07/2011

Career details

2006 – Till date : Assistant Professor in Civil Engineering,
Rajiv Gandhi Institute of Technology,
Government Engineering College, Kottayam, Kerala
(Department of Technical Education,
Government of Kerala)

2011 – 2014 : On deputation to do Ph. D. at IIT Madras, Chennai.